

# *NOELINS* IN NEURAL DEVELOPMENT

Thesis by

Tanya Munnecke Moreno

In Partial Fulfillment of the Requirements

for the Degree of

Doctor of Philosophy

California Institute of Technology

Pasadena, California

2002

(Defended December 21, 2001)

©2002

Tanya Munnecke Moreno

All Rights Reserved

**DEDICATION**

This thesis is dedicated to my Dear Ones:

Ella Cheryl Moreno and Sophia Raquel Moreno, my beautiful daughters, I love you more than the whale loves his spout

My loving husband William Moreno III, whose endless encouragement, support and love through these years have kept me going and made all things possible

My sister Alyssa Vesta Hoeben, who inspires me and who loves me in spite of myself

Tom and Cheryl Munnecke, my parents, my first loves, who taught me that life is what I make it, who taught me to be my best, who set the best example

My grandparents Don and Elaine Munnecke, and Connie and Dolores Leverton, who loved me, encouraged me, and gave me home away from home

In memory of my grandmother Dolores

## ACKNOWLEDGEMENTS

There are many people to whom I owe my thanks for their roles in this work:

First, to my parents, who have given me so much encouragement and support all of my life, and now through graduate school. I could not have made it without them, financially or mentally. They have always been there for me, and are now there for my growing family. I deeply appreciate their efforts and support of my choices.

My husband and daughters have provided me with a reason for everything that I do; they are the lights of my life. Their patience and encouragement have made all the difference.

Lab members past and present have given me technical support, advice, and most importantly, friendship during these years of graduate school. Brad Martinsen encouraged me to join the lab when I thought my options had run out, and became a good friend. Sung Hee Kil was my pal and my partner in complaining about everything! Clare Baker, dancing partner, social director, and the best critiquer around, made life as a graduate student fun, and had every reference under the sun. Carole LaBonne took me in hand and got me on the right track more than once, and also got pregnant with me both times so that I wouldn't be alone in that endeavor. Sara Ahlgren, my new officemate, got margaritas and Mexican food with me when it was necessary; Anne Knecht was always ready for a Buffy night and Chinese food and trudging through my manuscripts; Laura Gammill solved all of my PCR problems and showed me the "right way" to format a paper; Kristie Artinger, Meyer Barembaum, Martin Basch, Sujata Bhattacharyya, Martin Garcia Castro, Andy Groves, Cathy Krull, Christophe Marcelle, Daniel Meulemans, Ben Murray, Seth Ruffins, Jack Sechrist, and Mike Stark were post-docs and grad students who were members of the lab and helped me in innumerable ways, from advice, to lunches out, to partners in late nights in the lab. Lab Mom Mary Flowers and Guru Gary Belford were indispensable and helped me with every problem from computers to rush orders for obscure reagents.

My committee members Scott Fraser, Bruce Hay, Paul Sternberg and Kai Zinn have my heartfelt thanks for guiding me through this project with encouragement and optimism.

Last, but not least, my advisor Marianne Bronner-Fraser helped me through difficult times in my thesis work, taught me who Superwoman really is (she is!), and made being a graduate student a stimulating, enlightening, interesting, fun and happy experience. She took me into the lab when I thought there was nowhere else for me to go, and has always encouraged and supported me. My experience with her has given me a solid love of science and experimentation. I could have had no better advisor, mentor, and friend than Marianne.

**ABSTRACT**

The nervous system arises from embryonic tissues beginning with neural induction, when signals from the mesoderm induce the overlying ectoderm to form neural precursors. During neurogenesis, neurons are selected to differentiate from the induced neural precursors. Here, I describe the isolation and characterization of the *Xenopus Noelins*, a family of gene isoforms that may play roles in both of these processes. Noelin proteins are alternatively spliced isoforms and are all secreted proteins. Biochemically, Noelin-1 and Noelin-4 interact; moreover, Noelin-4 interacts with BMP-4, a molecule that is implicated in the process of neural induction.

*Noelin* transcripts are detected beginning at late gastrulation stages. Later, transcripts are observed in post-mitotic neural tissues of the central and peripheral nervous systems, from the neural tube closure stage and continuing through swimming tadpole stage. In avian embryos, *Noelins* are expressed in the early neural plate and neural crest, and over-expression of *Noelin-1* and -2 leads to excess and prolonged neural crest emigration from the cranial neural tube. The *Xenopus Noelin* homologs do not appear to affect neural crest induction or migration; however, *Noelin-1* is shown to have a role in promoting neuronal differentiation in neural tissue. Furthermore, the secretion of *Noelin-1* is important for its ability to induce certain neural markers to be expressed. Remarkably, *Noelin-4* causes neural induction when over-expressed in naïve tissue; in whole embryos, it causes expansion and ectopic production of neural tissue and cement gland by conversion of ectoderm.

*Noelins* may also modulate each others' functions: *Noelin-1* activity is increased in the presence of *Noelin-4*, and surprisingly, *Noelin-4* is negatively affected by the presence of *Noelin-1*. Since Noelin-4 can act as a neural inducer and can interact with BMP-4, a model for this gene's activity is proposed for modulation of BMP signaling. The function of Noelin-1 in modulating Noelin-4 activity may be mediated through competition for binding to BMP proteins. I further show that Morpholino antisense oligonucleotides that target all four *Noelin* isoforms cause a severe neural phenotype: the forebrain, cement gland and cranial ganglia are severely reduced or missing in injected embryos. These results indicate that Noelin proteins may be essential for normal development of anterior neural tissues. Thus, *Noelin* isoforms represent novel secreted factors involved in nervous system development, from neural induction to neurogenesis.

# TABLE OF CONTENTS

<b>CHAPTER 1:</b> .....	<b>1</b>
<b>INTRODUCTION TO NEURAL DEVELOPMENT: PRECURSORS TO THE CENTRAL AND PERIPHERAL NERVOUS SYSTEM</b> .....	<b>1</b>
I. INTRODUCTION TO NEURAL DEVELOPMENT .....	2
<i>Developmental biology</i> .....	2
<i>Origin and development of neural tissue in Xenopus</i> .....	4
<i>Neural induction</i> .....	4
<i>Patterning the neural plate</i> .....	11
<i>Neurogenesis</i> .....	12
II. PRECURSORS TO THE PERIPHERAL NERVOUS SYSTEM .....	13
<i>The peripheral nervous system is formed by neural crest and placodes</i> .....	13
<i>Origin and induction of the neural crest</i> .....	15
<i>Neural crest stem cells</i> .....	30
<i>Lineage and cell fate decisions in the neural crest</i> .....	32
<i>Theme of the thesis</i> .....	37
<i>Acknowledgements</i> .....	38
 <b>CHAPTER 2:</b> .....	 <b>46</b>
<b>THE SECRETED GLYCOPROTEIN NOELIN-1 PROMOTES NEUROGENESIS IN XENOPUS ....</b>	<b>46</b>
ABSTRACT .....	47
INTRODUCTION .....	48
METHODS .....	51
<i>Library screening and cDNA isolation</i> .....	51
<i>Xenopus laevis fertilizations, dissections and collection of oocytes</i> .....	52
<i>Microinjections and transfection</i> .....	52
<i>Immunoprecipitation</i> .....	54
<i>Xenopus Noelin constructs</i> .....	55
<i>Dil injections</i> .....	56
<i>In situ hybridization and immunohistochemistry</i> .....	57
<i>RT-PCR analysis</i> .....	58
RESULTS .....	60

<i>Noelin-1 and -2 sequence and structure</i> .....	60
<i>Noelin-1 is a secreted glycoprotein</i> .....	61
<i>Expression pattern of Xenopus Noelin-1 and -2</i> .....	65
Cranial expression of Noelin.....	66
Trunk expression of Noelin-1 and -2.....	67
<i>Origin of Noelin-positive cells in the cranial ganglia</i> .....	69
<i>Noelin-1 and -2 are up-regulated by neurogenic genes</i> .....	70
<i>Noelin-1 promotes neurogenesis in a neural context</i> .....	72
<i>Noelin-1 induces sensory neural markers and early differentiation</i> .....	74
DISCUSSION.....	77
<i>Noelin-1 promotes neurogenesis in Xenopus</i> .....	77
<i>Developmental role of Noelin-1</i> .....	77
<i>Olfactomedin and related genes</i> .....	78
<i>Comparison of Noelin expression patterns</i> .....	79
The search for Xenopus Noelin-related genes.....	81
<i>Xenopus Noelin expression in cranial ganglia</i> .....	82
<i>Regulation of Noelin</i> .....	83
<i>Function of Noelin</i> .....	85
ACKNOWLEDGEMENTS.....	89

## **CHAPTER 3..... 105**

### **NOELIN-4: A NOVEL SECRETED PROTEIN THAT ACTS AS A NEURAL INDUCER AND BINDS TO BMP-4..... 105**

INTRODUCTION.....	106
METHODS.....	108
<i>Library screening and cDNA isolation</i> .....	108
<i>Xenopus laevis embryo and oocyte manipulations</i> .....	109
<i>Microinjections</i> .....	110
<i>Immunoprecipitations</i> .....	112
<i>In vitro translation (IVT) inhibition with Morpholino oligonucleotides</i> .....	113
<i>In situ hybridization and immunohistochemistry</i> .....	113
<i>RT-PCR analysis</i> .....	115
RESULTS.....	117
<i>Noelin-3 and -4 sequence and structure</i> .....	117
<i>Noelin-4 is a secreted protein</i> .....	119
<i>Noelin-4 binds Noelin-1</i> .....	120

<i>Noelins are expressed early in development</i> .....	121
<i>Noelin-3 and -4 are expressed in post-mitotic neural tissues</i> .....	123
<i>Noelin-4 is induced by neurogenic genes</i> .....	124
<i>Noelin-4 over-expression causes neural expansion in embryos</i> .....	126
Table 1: <i>Noelin-4 over-expression phenotypes-low and high doses</i> .....	126
<i>High dose Noelin-4 over-expression causes ectopic neural development</i> .....	129
Anterior neural phenotype: eye and cement gland.....	129
Trunk over-expression phenotype: ectopic neural structures.....	131
Epidermal defects.....	132
Localization of mRNA determines the type of phenotype.....	134
<i>Mechanism of Noelin-4-induced expansion is not increased proliferation</i> .....	135
<i>Noelin-4 causes expansion of neural tissue by conversion of ectoderm</i> .....	136
<i>Noelin-4 acts as a neural inducer</i> .....	137
<i>Noelin-4 and Noelin-1 functionally interact</i> .....	139
<i>Noelin-3 behaves similarly to Noelin-4 in over-expression experiments</i> .....	142
<i>Morpholino knock-down of Noelin expression</i> .....	143
<i>MO effects in whole embryos</i> .....	144
<i>Targeted MO injections</i> .....	146
<i>Noelin-4 interacts with BMP-4 in oocytes</i> .....	148
DISCUSSION .....	149
<i>Noelin isoforms are induced by the neurogenic cascade</i> .....	150
<i>Noelin-4 over-expression induces neural expansion</i> .....	151
<i>Noelin-4 acts as a neural inducer</i> .....	153
<i>Noelin-4 interacts with BMP-4</i> .....	155
<i>Morphant phenotype</i> .....	155
<i>Spatiotemporal expression and function of Noelin isoforms</i> .....	157
<i>Noelin proteins interact</i> .....	158
<i>Noelins modulate the function of other Noelins</i> .....	159
<i>Noelin-4 binding partners</i> .....	160
<i>Neural inducers also function after neural induction</i> .....	161
<i>Acknowledgements</i> .....	162

## CHAPTER 4..... 187

### MOUSE *NOELIN-1/2* EXPRESSION PATTERN AND COMPARISON WITH *NOELIN* HOMOLOGS IN OTHER VERTEBRATES ..... 187

INTRODUCTION .....	188
METHODS .....	190
<i>Cloning and sequencing a partial mouse Noelin-1</i> .....	190
<i>Embryo collection and whole mount in situ hybridization</i> .....	191
RESULTS AND DISCUSSION .....	192
<i>Cloning of mouse Noelin</i> .....	192
<i>Phylogeny of Noelin genes</i> .....	192
<i>Mouse Noelin is expressed in neural plate and neural crest</i> .....	193
<i>Noelin genes are expressed divergently in vertebrate species</i> .....	195
<b>CONCLUDING REMARKS .....</b>	<b>208</b>
NON-CONSERVED EXPRESSION OF NOELINS IN VERTEBRATES.....	209
NOELIN FUNCTIONS VARY AMONG SPECIES.....	209
NOELINS INTERACT FUNCTIONALLY .....	211
CONCLUSION .....	214
<b>APPENDIX CHAPTER 1:.....</b>	<b>216</b>
<b>NOELIN-1 IS A SECRETED GLYCOPROTEIN INVOLVED IN GENERATION OF THE NEURAL CREST .....</b>	<b>217</b>
<b>APPENDIX CHAPTER 2.....</b>	<b>224</b>
<b><i>XENOPUS RING3R</i>, A HOMOLOG OF <i>DROSOPHILA</i> FEMALE STERILE HOMEOTIC PROTEIN .....</b>	<b>224</b>
INTRODUCTION .....	225
<i>Drosophila female sterile homeotic protein</i> .....	225
<i>History of Ring3</i> .....	226
<i>Function of Ring3</i> .....	227
<i>Ring3 protein domains</i> .....	228
<i>Xenopus Ring3</i> .....	229
METHODS .....	229
<i>Library screening and cDNA isolation</i> .....	229
<i>Collection of embryos for in situ hybridization:</i> .....	230
<i>Xenopus laevis</i> fertilizations and collection of embryos .....	230

Chick embryo isolation .....	230
<i>Whole mount in situ hybridization and sectioning</i> .....	231
RESULTS AND DISCUSSION .....	231
<i>Sequence and structure information for Xenopus Ring3r</i> .....	231
<i>Expression pattern of Xenopus Ring3r</i> .....	233
<i>Pattern of Ring3r hybridization in chick embryos</i> .....	234
<i>Discussion</i> .....	235
ACKNOWLEDGEMENTS .....	237
<b>APPENDIX CHAPTER 3</b> .....	<b>242</b>
<b>METHODS AND MISCELLANEOUS INFORMATION</b> .....	<b>242</b>
APPENDIX 3.1: .....	243
<i>Table of clones sequenced in low-stringency screen for Noelin homologs</i> .....	243
APPENDIX 3.2: .....	244
<i>Protocols for in situ hybridization</i> .....	244
Xenopus whole mount <i>in situ</i> hybridization protocol .....	244
Xenopus <i>in situ</i> protocol solutions .....	246
Chick and mouse whole mount <i>in situ</i> hybridization protocol.....	248
Henrique <i>in situ</i> Protocol Recipes .....	249
Dil neural crest-labeling injections .....	250
APPENDIX 3.3: .....	251
<i>X-Gal Histochemistry</i> .....	251
APPENDIX 3.4: .....	253
<i>Cell transfections</i> .....	253
COS-7 cell lipofection protocol .....	253
APPENDIX 3.5: .....	254
<i>Protein methods:</i> .....	254
Immunoprecipitation .....	254
Deglycosylation of glycoproteins.....	255
Morpholino (MO) translation inhibition .....	256
Preparation and storage of Morpholino oligos .....	256
For Morpholino oligo injections into embryos .....	257
SDS-Polyacrylamide gel electrophoresis .....	257
SDS-PAGE Recipes .....	258
APPENDIX 3.6 .....	259
<i>RT-PCR</i> .....	259
Optimization of primer sets.....	259

Normalization of cDNA amounts .....	259
Isolation of RNA from animal caps and whole embryos .....	260
cDNA synthesis .....	260
PCR reactions .....	261
PCR gel recipes .....	261
PCR primer sets .....	262
APPENDIX 3.7 .....	263
<i>Antibodies</i> .....	263
<i>Secondary antibodies</i> .....	266
<i>Immunohistochemistry</i> .....	266
For sectioned samples .....	266
For whole mounts .....	267
APPENDIX 3.8: .....	268
<i>Expression constructs, Noelin subclones and in situ probes</i> .....	268
<b>APPENDIX CHAPTER 4: CITED LITERATURE.....</b>	<b>272</b>
REFERENCES .....	273

## LIST OF TABLES AND FIGURES

### CHAPTER 1: INTRODUCTION

Figure 1: <i>Xenopus</i> developmental stages .....	39
Figure 2: Anatomy of <i>Xenopus</i> development .....	40
Figure 3: From neural induction to neurogenesis .....	41
Figure 4: Neural induction in <i>Xenopus</i> .....	42
Figure 5: Neural crest migration in avians .....	43
Figure 6: <i>Slug</i> expression in <i>Xenopus</i> and chick embryos .....	44

### CHAPTER 2: NOELIN-1 PROMOTES NEUROGENESIS IN XENOPUS EMBRYOS

Figure 1: <i>Noelin-1</i> and <i>-2</i> sequence and structure .....	90
Figure 2: Subcellular localization of <i>Noelin-1</i> .....	92
Figure 3: Oocyte secretion assay .....	93
Figure 4: <i>Noelin-1</i> expression pattern .....	94
Figure 5: <i>Noelin-1</i> expression in early cranial ganglia and spinal cord .....	95

Figure 6: Rostral <i>Noelin</i> expression in stage 25 embryos .....	96
Figure 7: Cranial <i>Noelin</i> expression at stage 35 .....	97
Figure 8: Caudal expression of <i>Noelin-1</i> at pre-tailbud stages .....	98
Figure 9: Neuronal expression of <i>Noelin-1</i> and <i>-2</i> .....	99
Figure 10: DiI labeling of pre-migratory neural crest cells .....	100
Figure 11: <i>Noelins</i> are induced by <i>neurogenin</i> overexpression .....	101
Figure 12: <i>Noelin-1</i> promotes neuronal differentiation .....	102
Figure 13: <i>Noelin-1</i> induces sensory and differentiation markers .....	103

### CHAPTER 3: NOELIN-4 ACTS AS A NEURAL INDUCER AND BINDS TO BMP-4

Table 1: <i>Noelin-4</i> overexpression phenotypes-low and high dose .....	126
Figure 1: Sequence and structure information for <i>Noelin-4</i> .....	164
Figure 2: <i>Noelin-4</i> secretion and binding .....	165
Figure 3: Developmental series of <i>Noelin</i> expression .....	166
Figure 4: <i>Noelin</i> Y isoform expression .....	167
Figure 5: <i>Neurogenin</i> induces <i>Noelin-3</i> and <i>-4</i> .....	168
Figure 6: Neural plate expansion by overexpression of <i>Noelin-4</i> .....	169
Figure 7: Enlarged retina from <i>Noelin-4</i> overexpression .....	170
Figure 8: Retina expansion by overexpression of <i>Noelin-4</i> .....	171
Figure 9: High dose overexpression of <i>Noelin-4</i> .....	172
Figure 10: <i>Noelin-4</i> overexpression causes ectoderm conversion .....	174
Figure 11: Extra proliferation is not the expansion mechanism .....	175
Figure 12: Neural crest formation is perturbed by <i>Noelin-4</i> .....	176
Figure 13: <i>Noelin-4</i> induces cement glands .....	177
Figure 14: Neural induction by <i>Noelin-4</i> .....	178
Figure 15: <i>Noelin</i> isoforms modulate each others' functions .....	180
Figure 16: <i>Noelin-3</i> behaves like <i>Noelin-4</i> .....	181
Figure 17: Morpholinos inhibit translation of <i>Noelin</i> isoforms .....	182
Figure 18: Morpholino injections perturb neural development .....	183
Figure 19: Targeted A + B Morpholino injections .....	185
Figure 20: <i>Noelin-4</i> interacts with BMP-4 in oocytes .....	186

## CHAPTER 4: MOUSE *NOELIN-1/2* EXPRESSION PATTERN AND COMPARISON TO OTHER VERTEBRATE *NOELINS*

Figure 1: Noelin homologs sequence alignment.....	199
Figure 2: Sequence relationships between <i>Noelin</i> homologs.....	200
Figure 3: <i>Noelin</i> is expressed in early neural ectoderm.....	201
Figure 4: Mouse <i>Noelin</i> at E8.....	202
Figure 5: Mouse <i>Noelin</i> at E8.5.....	203
Figure 6: <i>Noelin</i> expression at E10.....	204
Figure 7: <i>Noelin</i> expression in cross-section at E10.....	205
Figure 8: Cross-species comparison of <i>Noelin-1</i> expression pattern.....	206

## APPENDIX CHAPTER 1: NOELIN-1 IS A SECRETED GLYCOPROTEIN INVOLVED IN GENERATION OF THE NEURAL CREST

Figure 1: Expression of avian <i>Noelin-1</i> .....	217
Figure 2: Late avian <i>Noelin-1</i> expression.....	218
Figure 3: Molecular characteristics of <i>Noelin-1</i> .....	219
Figure 4: Effects of <i>Noelin-1</i> overexpression on neural crest cells.....	220
Figure 5: <i>Noelin-1</i> increases neural crest production at r3.....	220
Figure 6: Effects of <i>Noelin-1</i> overexpression on neural tube.....	221
Figure 7: <i>Noelin-1</i> prolongs neural crest regeneration.....	221
Figure 8: <i>Noelin-1</i> overexpression up-regulates <i>Slug</i> expression.....	222

## APPENDIX CHAPTER 2: *XENOPUS RING3R*, A HOMOLOG OF *DROSOPHILA* FEMALE STERILE HOMEOTIC PROTEIN

Figure 1: <i>Xenopus Ring3r</i> sequence.....	237
Figure 2: <i>Ring3</i> and related genes.....	239
Figure 3: <i>Xenopus Ring3r</i> expression pattern.....	240
Figure 4: Chick embryos stained with <i>Xenopus Ring3r</i> .....	241

## APPENDIX CHAPTER 3: METHODS AND MISCELLANEOUS INFORMATION

Table 1: Clones sequenced in a screen for <i>Noelin</i> homologs.....	243
Table 2: SDS-Page recipes.....	258
Table 3: PCR gel recipes.....	261
Table 4: PCR primer sets.....	262

Table 5: Primary antibodies.....	263
Table 6: Secondary antibodies.....	266
Table 7: Expression constructs, <i>Noelin</i> subclones and <i>in situ</i> probes.....	268

## ABBREVIATIONS IN USE

Abbreviation	Definition
'	minutes
"	seconds
a/p	antero-posterior axis
AMY	<i>Noelin-4</i>
AMZ	<i>Noelin-2</i>
BMP	bone morphogenetic protein
BMY	<i>Noelin-3</i>
BMZ	<i>Noelin-1</i>
chd	<i>chordin</i>
Co-IP	co-immunoprecipitation
ER	endoplasmic reticulum
γ	micrograms
h	hours
IP	immunoprecipitation
IX	petrosal ganglion
λ	microliters
μg	micrograms
mg	milligrams
microns	micrometers
min	minutes
μl	microliters
ml	milliliters
mm	micrometers
M	molarity
MO	morpholino oligo
ng	nanograms
nl	nanoliters
nog	<i>noggin</i>
Ntub	<i>N-tubulin</i>
olf	olfactory placode/ pit
orig	trigeminal ganglion
pg	picograms
pl	picoliters
r/c	rostral-caudal axis
RT-PCR	reverse-transcriptase polymerase chain reaction
sec	seconds
SybII	<i>synaptobrevin II</i>
TGFb	<i>transforming growth factor b</i>
V	trigeminal ganglion
VII	geniculate ganglion
VIII	acoustic ganglion
X	nodose ganglion
X-ngnr-1	<i>Xenopus neurogenin</i>

## **Chapter 1:**

# **Introduction to neural development: precursors to the central and peripheral nervous system**

Tanya A. Moreno and Marianne Bronner-Fraser (2001)

Portions of this chapter were originally published as  
PNS Precursor Cells, in *Stem Cells and CNS Development* (ed. M. S. Rao),  
pp. 153-177. Totowa: Humana Press.

# I. INTRODUCTION TO NEURAL DEVELOPMENT

## **Developmental Biology**

The adult animal develops from a single fertilized egg containing one set of information that will direct the egg to form progressively more complex structures. The central question developmental biologists seek to answer is how a primitive cell reads out the information in its chromosomes and cytoplasm, and how a seemingly uniform cell can later become asymmetrical and form differentiated structures in a complex organism composed of billions of specialized cells.

Early embryologists observed the development of many different species on a morphological level. They described the ontogeny of structures based on microscopic observation, and their observations are the basis for continuing studies on development and evolution today. Early grafting experiments showed that regional cues located in particular tissues could instruct development of surrounding tissues, a process known as induction. Remarkably, when the inducing tissues were grafted heterotopically, these cues induce other tissues to adopt new fates that would not otherwise occur in that region. One such discovery was the finding that a region known as the dorsal lip of the amphibian embryo (now known as the organizer) could “organize” a second anterior-posterior axis if transplanted to the opposite side of the embryo. Hilde Mangold and Hans Spemann performed these experiments in the 1920s and opened up a field of research that has inspired the interest of hundreds of researchers in successive generations, all hoping to uncover and understand the

molecular basis for this process. In the last twenty years, with the advent of molecular biology, some of the most important discoveries about gene and chromatin function have been made, with the elucidation of many of the controls of gene expression and complex genetic interactions that lead to development of an egg into an embryo, and finally into a functioning adult organism. However, much remains to be explored to elucidate the mechanisms of neural development.

Many different organisms are used as model systems for studying development, each for different reasons. The frog, *Xenopus laevis*, has embryos that are large, external, and rapidly developing, thus making them ideal for experimental manipulation and observation. They develop from a fertilized egg into a neurulating embryo within twenty-four hours (see Figure 1). *Xenopus laevis* is a long-studied species that has provided a great deal of information regarding early development, from fertilization through neurogenesis.

This thesis examines a family of gene isoforms, the *Noelins*, that play multiple roles in nervous system development from neural induction through neurogenesis. *Noelin* family members have many interesting features that make them an important part of normal nervous system development. This chapter begins with an introduction to the embryonic development of the nervous system, from early induction when prospective neural tissue is specified, through neurogenesis, when neurons begin to differentiate. In Part II, I describe the origin and induction of the neural crest, an important embryonic neural tissue that gives rise to the peripheral nervous system.

## **Origin and development of neural tissue in *Xenopus***

Many of the important morphological changes in embryonic development occur during gastrulation. During this process in amphibian embryos, the mesoderm (specified as a ring around the margin of the blastula embryo) involutes through the lip of the blastopore and migrates internally along the ectoderm, creating a multi-layered embryo. Dorsal mesoderm signals and dorsalizes nearby ectoderm to a neural fate; thus ventral ectoderm develops into epidermis while dorsal ectoderm forms the nervous system, which is initially established as the neural plate. The first mesoderm to involute, the organizer tissue, eventually underlies the entire neural plate, and thus passes along underneath all of the prospective neural ectoderm (see Figure 2).

### **Neural induction**

#### *The “default model” of neural induction*

Our views of how neural induction takes place in the ectoderm have changed radically over the past 75 years. Initially, neural induction was thought to occur by an instructive signal from the organizer. Grafting experiments in amphibians had shown that a ventrally-transplanted dorsal blastopore lip (see Figure 2) could organize a second antero-posterior axis, with host tissues recruited to form the neural tube, while donor tissue contributed to mesodermal derivatives (Spemann and Mangold, 1924). These results demonstrated that the dorsal blastopore lip, or “organizer,” was sufficient to cause neural induction. In the normal embryo, the ectoderm overlying the organizer as gastrulation

proceeds forms the neural plate, while the ectoderm lying further from this mesoderm (ventral ectoderm) forms epidermis. In the grafted embryos, this ventral ectoderm was respecified to form neural tissue. Thus it was thought that epidermis was the default state for ectoderm, and that neural fate was induced. A long and fruitless search for the neural inducer ensued.

Sixty-five years later, it was shown that ectodermal explants (animal caps) isolated from pre-gastrula embryos could be neuralized by dissociation. The animal cap normally forms epidermis when isolated; when combined with grafted organizer tissue, it forms neural tissue (reviewed by Chang and Hemmati-Brivanlou, 1998a). However, when animal caps were dissociated and cultured alone, the cells began to express neural markers (Godsave and Slack, 1989; Grunz and Tacke, 1989; Sato and Sargent, 1989), demonstrating that neural induction does not require a signal from the organizer. The hypothesis proposed later for this result was that dissociation caused dilution of an inhibitory factor, uncovering another state of ectoderm fate. These results opened up a new range of possible mechanisms for neural induction; although their significance was not understood until much later when the first direct neural inducer was characterized (Hemmati-Brivanlou, and Melton, 1994; and see Weinstein and Hemmati-Brivanlou, 1997; Chang and Hemmati-Brivanlou, 1998a; Weinstein and Hemmati-Brivanlou, 1999 for review).

### BMP molecules induce epidermis

Molecules in the TGF $\beta$  (transforming growth factor  $\beta$ ) family of secreted growth factors are implicated in the fate choice between neural and non-neural ectoderm. Family members BMP-2, -4 and -7 (bone morphogenetic proteins) are

potent epidermal inducers in dissociated animal caps (Suzuki *et al.*, 1997; Wilson and Hemmati-Brivanlou, 1995). They are all expressed in the gastrula ectoderm, thus they are present at the right time and place to be involved in ectodermal patterning *in vivo* (Hawley *et al.*, 1995; Hemmati-Brivanlou and Thomsen, 1995). Activated downstream components of the BMP signal transduction pathway also induce epidermis in dissociated cells (Massagué *et al.*, 1997; Suzuki *et al.*, 1997). These results indicate that BMP signaling plays an important role in the cell fate decision between neural and non-neural ectoderm.

### BMP antagonism neuralizes ectoderm

BMPs rescue epidermal differentiation in dissociated animal caps. On the other hand, inhibition of BMP signaling by over-expression of dominant inhibitory mutants in BMP ligands, receptors, or in downstream effectors of BMP signaling (see Figure 3), then intact animal caps are neuralized (Hemmati-Brivanlou and Melton, 1994; Hawley *et al.*, 1995; Sasai *et al.*, 1995; Xu *et al.*, 1995). Together, these data suggest that BMP inhibition is sufficient to mediate neural induction. However, the mechanism of neural induction through BMP inhibition was unknown, until the discovery that several molecules expressed in the organizer actually functioned by inhibiting BMP signaling (Lamb *et al.*, 1993; Sasai *et al.*, 1995).

### BMP antagonists are neural inducers

Noggin, chordin, follistatin, Xnr3 (nodal-related), and Cerberus all act as neural inducers. Importantly, they are all expressed in the organizer and are all secreted factors. Noggin, chordin, and follistatin bind directly to BMPs and

inhibit them from subsequently binding to their receptors, thereby inhibiting the activity of the epidermis-inducing signal transduction cascade (Piccolo *et al.*, 1996; Zimmerman *et al.*, 1996; Fainsod *et al.*, 1997). Cerberus has been shown to physically interact with BMPs but has not been shown to prevent BMP binding to its receptor (Hsu *et al.*, 1998; Piccolo *et al.*, 1999), and Xnr3, another TGF $\beta$  family member like the BMPs, may compete with BMPs for receptor binding (Hansen *et al.*, 1997). Thus, these results support the model whereby neural induction is in fact a relief of neural inhibition by BMP molecules (see Figure 4).

Although it has not been directly shown that these factors neutralize by BMP antagonism and not some other mechanism, several experiments indicate that the former is true. For example, an antibody that prevents noggin from binding to BMP molecules also abrogates noggin's neuralizing activity (Zimmerman *et al.*, 1996); furthermore, experimental inhibition of any of the downstream effectors of BMP signaling results in phenotypes similar to the over-expression phenotypes of the BMP antagonists described here.

### *Neural induction in amniotes*

#### Evidence against the default model

All of the data described above are from the *Xenopus* system. Results in zebrafish also support similar mechanisms for neural induction (Kishimoto *et al.*, 1997; Schulte-Merker *et al.*, 1997); however, the model of neural induction that is well-characterized and consistent in amphibians does not entirely hold in amniotes. For example, while a grafted node (the amniote equivalent of the

dorsal lip of the blastopore) can induce a complete secondary axis in avian embryos (Gallera and Nicolet, 1969), mis-expression of *chordin* in the extra-embryonic or non-neural ectoderm cannot induce ectopic neural plate or expression of neural markers (Streit *et al.*, 1998). Dissociation of ectodermal cells from primitive-streak stage chick embryos (equivalent to dorsal lip stage in amphibians) does not cause neuralization (George-Weinstein *et al.*, 1996). Furthermore, BMP molecules are not expressed in a pattern analogous to those in *Xenopus*, where BMPs are expressed in the ectoderm before gastrulation and then restricted from the neural plate during gastrulation. Chick *BMP-2*, *-4*, and *-7* are not expressed in the primitive-streak stage ectoderm when neural induction is thought to begin (reviewed in Streit and Stern, 1999). In addition, the temporal patterns of *noggin* and *chordin* expression in the chick do not correlate with the neural-inducing capacity of the node (Connolly *et al.*, 1997; Streit *et al.*, 1998).

Mouse loss-of-function mutants in BMPs, their receptors, or the candidate neuralizers *noggin* and *follistatin* have been uninformative because their phenotypes are either weak in neural perturbation (*noggin*, McMahon *et al.*, 1998), or show no early neural phenotype (*BMP-2*, Dudley *et al.*, 1995; *follistatin*, Matzuk *et al.*, 1995; *BMP-2*, Zhang and Bradley, 1996). *BMP-4* null mutants have defects in posterior mesoderm, showing that *BMP-4* is essential for that tissue; however there were no reports of defects in the ectoderm (Winnier *et al.*, 1995). Furthermore, mutation in mouse BMP type I receptor causes very early embryo lethality and is thus also uninformative (Mishina *et al.*, 1995). These data do not argue against the default model, but they do not support it either (reviewed in Streit and Stern, 1999).

### Evidence in favor of the default model

However, there is also evidence to support the default model in amniotes. In mammalian cell lines (P19 cells) that can be induced to form neurons by addition of retinoic acid, co-exposure of the cells with retinoic acid and BMP-4 prevents this neuralization (Hoodless and Hemmati-Brivanlou, 1997). Furthermore, transfection of the uninduced cells with *follistatin* can induce neural differentiation (Fainsod *et al.*, 1997). These experiments show that mammalian cells can respond in a similar manner to *Xenopus* cells in neural induction assays. Furthermore, in the chick, ectopically-expressed *BMP-4* at the border of the neural plate and non-neural ectoderm can generate epidermis at the expense of neural plate (Pera *et al.*, 1999). These lines of evidence suggest that, at least in principle, the model of neural induction proposed in *Xenopus* may function to some degree in amniote vertebrates as well, though perhaps involving more complex interactions than previously described in *Xenopus*.

In support of the applicability of the neural induction default model in amniotes, recent work by Wilson *et al.* (2000) has demonstrated that indeed neural induction in chick epiblast can occur by antagonism of BMP signaling. Treatment of explants from pre-primitive streak-stage embryos with noggin or chordin caused the expression of neural markers in the tissue; furthermore, BMPs were found to be expressed in this tissue, and extinction of their expression correlated with establishment of neural fate. These workers showed that neural induction could occur much earlier *in vivo* than previously thought, well before the establishment of the node (Wilson *et al.*, 2000). These experiments were done at a much earlier developmental stage than those described in Streit *et*

*al.* (1998), which were done at primitive streak stages. The implications for the node as the *in vivo* neural inducer are unclear; however, these results clearly show that amniotes may have an analogous pathway for neural induction in which BMP antagonism causes the establishment of neural fate, but that perhaps earlier signals are required.

Still, because of the many contradictions with the default model in other species, much work must be done to clarify the exact mechanisms that operate in each species. Streit and Stern (1999) have proposed that animal caps used for neural induction assays in *Xenopus* are already induced and patterned to some degree, since by some fate maps, the blastula animal pole contains the future cement gland, which is at the border between neural and non-neural ectoderm and is considered to be the most anterior ectodermal fate. In chicks, this border region is the only area that is sensitive to manipulation of the BMP signaling pathway at the primitive streak stage (reviewed in Streit and Stern, 1999). In response, Harland (2000) has proposed that other BMPs not inhibited by noggin and chordin may exist in the chick embryo, and the mechanism of neural induction there may be conserved in principle, if not in detail. The new data from Wilson *et al.* (2000) indicate that the default model may indeed function in chick, but that the actual induction is not as closely linked to activity from Hensen's Node as has been traditionally thought. Thus, although the precise details of the signaling pathways that effect particular fate choices in one species may not operate exactly the same way in another species, the overall results are functionally conserved, in that neural induction can occur by antagonism of BMP signaling in the ectoderm. In amniotes, BMP antagonism is important but may

not be sufficient for neural induction; however, in *Xenopus* BMP antagonism is sufficient to cause neural induction.

### **Patterning the neural plate**

The positional character of the neural plate is established during or soon after neural induction occurs. A widely accepted theory for how this occurs is the Activation-Transformation model (Nieuwkoop, 1952a; Nieuwkoop, 1952b; reviewed by Chang and Hemmati-Brivanlou, 1998a). In this model, the organizer activates neural fate, which by default is an anterior state. Tissues in different antero-posterior levels are then modified to a more posterior fate by other inducers from the mesoderm that by themselves cannot cause neural induction.

In *Xenopus*, there are two main experimental paradigms in support of the activation-transformation model: first, neural inducers like noggin and chordin induce only anterior neural tissue. Second, molecules that posteriorize induced neural tissue generally do not themselves directly induce neural fate, although this is debatable in the case of FGF (reviewed in Harland, 2000). Candidate caudalizing factors are fibroblast growth factors (FGF), retinoic acid (ra), and some Wnt signaling pathway genes (reviewed in Chang and Hemmati-Brivanlou, 1998a). Each of these is able to posteriorize neuralized animal caps, and they are all expressed in posterior regions of the embryo.

### **Neurogenesis**

Once the neural tissue has been induced and the initial pattern has been established, the further development of the nervous system begins. The next

step is the selection of specific neurogenic regions from the neural field. This is accomplished by a cascade of neurogenic basic helix-loop-helix (bHLH) transcription factors that activate neuronal differentiation programs. Proneural bHLH genes activate determination genes like *NeuroD* (Lee *et al.*, 1995; Ma *et al.*, 1996), and also lateral inhibition genes to narrow the field of differentiating neurons (Chitnis *et al.*, 1995; reviewed in Chitnis, 1999).

The bHLH genes *neurogenin* (atonal class) and *Xash-3* (achaete-scute class) are expressed from neural plate stages onward. These proneural genes cause neuronal differentiation to occur in the epidermis when ectopically expressed, bypassing neural induction (Ferreiro *et al.*, 1994; Ma *et al.*, 1996; Zimmerman *et al.*, 1993). *Neurogenin* also induces the expression of *Delta*, the inhibitory *Notch* ligand that selects which of the *neurogenin*-positive cells will later differentiate (Chitnis *et al.*, 1995). This neurogenic and lateral inhibitory process serves to refine and maintain the neuronal differentiation program (see Chitnis, 1999). The immediate result in *Xenopus* is a primary nervous system consisting (in the spinal cord) of three stripes of neurons along the antero-posterior axis: lateral (sensory neurons), medial (interneurons) and ventral (motor neurons), which are used for feeding and swimming in early larval life; later development of the more complex adult nervous system begins during tadpole stages. This basic model of neurogenesis in the simplified *Xenopus* primary nervous system has yet to be verified in other vertebrates, although it is likely that the molecular pathways operate similarly in those more complex environments.

The preceding sections have addressed the initial steps of neuralization and later neurogenesis in central nervous system precursors. However, the fate

choices for ectoderm are more complex than simply neural or non-neural. Embryonic cell populations at the border of the neural plate and the non-neural ectoderm give rise to neural tissues of other types: the neural crest and placodes. The neural crest is a migratory population of multipotent cells (reviewed in Moreno and Bronner-Fraser, 2001) and the ectodermal placodes are thickened regions of multipotent cranial ectoderm (reviewed in Baker and Bronner-Fraser, 2001). Together these give rise to the peripheral nervous system. Differential levels of BMP signaling have been implicated in the induction of these border region fates in *Xenopus*, which is discussed in detail in Part II of this chapter. The following section discusses the origin, induction, and development of the neural crest.

## II. PRECURSORS TO THE PERIPHERAL NERVOUS SYSTEM

### **The peripheral nervous system is formed by neural crest and placodes**

The peripheral nervous system (PNS) is comprised of groups of neurons and support cells whose cell bodies lie outside the spinal cord and brain. These peripheral ganglia relay sensory input back to the central nervous system (CNS), where the information is processed and physical responses are generated. The PNS is primarily derived from a population of precursor cells called neural crest cells that arise within the developing CNS but subsequently migrate to the

periphery and are highly versatile with respect to the types of derivatives that they form.

The neural crest is one of the defining features of vertebrates. Neural crest cells originate in the ectoderm of the early embryo and develop as a ridge of cells flanking the rostrocaudal length of the open neural tube, resembling a "crest." Initially, these cells appear to be multipotent and subsequently give rise to both neuronal and non-neuronal derivatives, including neurons and support cells of the peripheral nervous system, pigment cells, smooth muscle cells, and cartilage and bone of the face and skull (Le Douarin, 1982; Hall and Hörstadius, 1988). More recently, it has been shown that some neural crest cells are stem cells that self-renew *in vivo* and can contribute to at least some of the derivatives generated by the neural crest (Morrison *et al.*, 1999).

Interest in the mechanisms of induction, migration and differentiation of neural crest cells has occupied developmental biologists for more than 130 years (His, 1868; Landacre, 1921; Stone, 1922; Harrison, 1938; Hörstadius, 1950, reprinted in Hall and Hörstadius, 1988). Much is known about the later steps of neural crest development such as migration pathways and cell fate decisions (Le Douarin, 1982; Bronner-Fraser, 1993; Erickson and Perris, 1993; Stemple and Anderson, 1993; Selleck and Bronner-Fraser, 1995). However, molecular aspects of these processes have only begun to be uncovered within the last two decades. This review will summarize recent findings regarding neural crest induction and the isolation and characterization of neural crest stem cells.

## Origin and Induction of the Neural Crest

### *Neural Crest Origin*

The ectoderm is the source of the tissues that eventually form the epidermis, CNS and PNS of all vertebrates. It is initially patterned into neural and non-neural ectoderm by signals emanating from a mesodermal organizing center during gastrulation which establishes the region where the neural plate will form (see Part I of this chapter). The ectoderm outside of the neural plate will give rise to the epidermis, and in the head region, placodes. Placodes are regional thickenings of the ectoderm which will contribute to the cranial sensory ganglia and the sense organs of the head such as the eyes, ears and nose (Le Douarin *et al.*, 1986; Webb and Noden, 1993; Baker and Bronner-Fraser, 2001). They form the remainder of the PNS that is not generated by the neural crest.

Induction of the neural crest occurs at the border region between the future epidermis and the neural plate (reviewed in Baker and Bronner-Fraser, 1997; LaBonne and Bronner-Fraser, 1999). As development proceeds, the neural plate begins to roll into a tube, causing its lateral edges to form folds that eventually approximate at the dorsal midline of the embryo. The neural folds typically contain the premigratory neural crest cells, although there are some exceptions. For example, in *Xenopus*, the cranial neural crest is not incorporated into the neural tube, but remains as a separate condensed mass of cells in the border region. Thus, neural crest cells delaminate from the neuroepithelium and begin to migrate before neural tube closure in some species (e.g., mouse, *Xenopus*) (Hall and Hörstadius, 1988; Olsson and Hanken, 1996; Bartelmez, 1922;

Holmdahl, 1928; Verwoerd and van Oostrom, 1979; Nichols, 1981), whereas in other species (e.g., chicken), they migrate only after apposition of the neural folds (Bronner-Fraser, 1986). Thus, the CNS is formed from the rolled-up neural plate, and the PNS is formed from the ectodermal placodes and the neural crest cells residing in and around the dorsal neural tube, which delaminate from the neural epithelium and migrate throughout the embryo (see Figure 5).

It was originally thought that the neural crest was a segregated population of cells, largely based on the fact that these cells appear morphologically distinct from neural tube cells in some species (e.g., axolotl and zebrafish). In other species, however, presumptive neural crest cells are not readily distinguishable from dorsal neural tube cells. Moreover, single cell lineage analyses of the dorsal neural tube have shown that individual precursors in the neural tube can form both neural crest and neural tube derivatives in chick (Bronner-Fraser and Fraser, 1988; Bronner-Fraser and Fraser, 1989), frog (Collazo *et al.*, 1993), and mouse (Serbedzija *et al.*, 1992; Serbedzija *et al.*, 1994). Even more strikingly, prior to neural tube closure, the neural folds can give rise to all three ectodermal derivatives: epidermis, neural tube and neural crest (Selleck and Bronner-Fraser, 1995). Recently, genetic screens in zebrafish have identified a mutation called narrowminded, which supports a shared lineage between CNS and PNS cells. This mutant lacks both early neural crest cells (PNS) and sensory neurons in the neural tube (CNS) (Artinger *et al.*, 1999). Further evidence for a common neural progenitor comes from isolation of stem cells from the spinal cord neuroepithelium (NEP) cells that can form both CNS and PNS derivatives (Mujtaba *et al.*, 1998).

Not only has it been shown the neural tube/neural crest lineage is shared, but it has also been demonstrated that these cells are not irreversibly committed to either fate until relatively late in development. The ability of the neural tube to produce neural crest cells may persist for long periods of time. Sharma *et al.* (1995) identified a late-emigrating population of neural tube cells that form neural crest-like derivatives. When transplanted into neural crest migratory pathways of younger embryos, these cells can migrate and differentiate into neural crest derivatives (Korade and Frank, 1996). Conversely, it has been shown that early-migrating neural crest cells can reincorporate into the ventral neural tube and express markers characteristic of floor plate cells when challenged by transplantation (Ruffins *et al.*, 1998).

### *Neural Crest Induction*

#### Cell-Cell Interaction at the Neural Plate Border

Several theories of neural crest induction exist (reviewed in Baker and Bronner-Fraser, 1997). Both the mesoderm and the epidermal ectoderm have been shown to have the ability to induce neural crest. (This section will discuss the evidence for ectodermal interactions; see later for a discussion of mesoderm.) The best-supported model for neural crest induction is one in which cell-cell interaction at the border between neural and non-neural ectoderm is responsible for inducing the neural crest. *In vivo* grafting experiments suggest that interactions between presumptive epidermis and neural plate can form neural crest cells. In amphibians, epidermis grafted into the neural plate generates

neural crest cells (Rollhäuser-ter Horst, 1980; Moury and Jacobson, 1990). In avians and frogs, neural plate tissue grafted into the epidermal ectoderm results in the production of migratory cells expressing neural crest cell markers (Dickinson *et al.*, 1995; Selleck and Bronner-Fraser, 1995; Mancilla and Mayor, 1996). *In vitro* co-culture experiments have similarly provided evidence for the sufficiency of the neural plate/epidermal ectoderm interaction to generate neural crest cells (Dickinson *et al.*, 1995; Selleck and Bronner-Fraser, 1995; Mancilla and Mayor, 1996). Interestingly, both the epidermis and the neural plate cells contributed to the neural crest cell population (Moury and Jacobson, 1990; Selleck and Bronner-Fraser, 1995).

The potential for more ventral neural tube cells to generate neural crest was examined in ablation experiments in which the dorsal region of the neural folds containing the presumptive neural crest cells is removed, thus bringing more ventral regions of the tube into contact with epidermal ectoderm. In this situation, neural crest cells are regenerated at the zone of contact (Scherson *et al.*, 1993; Sechrist *et al.*, 1995; Hunt *et al.*, 1995; Suzuki and Kirby, 1997; but also see Couly *et al.*, 1996), for a limited period of time. These data show that a very important mechanism of neural crest induction is mediated through cell-cell interactions at the border between the epidermal ectoderm and the neural plate.

### The Role of BMPs in Neural Crest Induction: Setting up the Neural Plate Border Region

There is growing evidence, particularly from the *Xenopus* system, that members of the TGF $\beta$  superfamily of signaling molecules play an integral role in

setting up the border between neural and non-neural ectoderm. Given that neural crest cells arise at this border, it is likely that these cells are an important target of this signaling process.

Several lines of evidence support the idea that BMP molecules play a role in neural induction (for review, see Weinstein and Hemmati-Brivanlou, 1997; Wilson and Hemmati-Brivanlou, 1997). *Xenopus BMP-4* is expressed throughout the ectoderm prior to neural induction, then is lost from regions fated to become the neural plate (Dale *et al.*, 1992; Fainsod *et al.*, 1994; Hemmati-Brivanlou and Thomsen, 1995). The secreted BMP antagonists *noggin* (Lamb *et al.*, 1993; Zimmerman *et al.*, 1996), *chordin* (Sasai *et al.*, 1994; Piccolo *et al.*, 1996), and *follistatin* (Hemmati-Brivanlou *et al.*, 1994; Fainsod *et al.*, 1997) all are expressed in Spemann's organizer, the tissue responsible for patterning the ectoderm. Thus, the neural plate forms adjacent to the organizer, the source of BMP inhibition, whereas the non-neural ectoderm lies distal to the organizer (see Figure 4).

One possibility is that inhibition of BMP signaling is sufficient to generate both the neural plate and the neural crest, with high levels of inhibition yielding neural tissue and intermediate levels yielding neural crest. The idea that a diffusible morphogen could act to instruct the ectoderm to assume the various available fates was first proposed by Raven and Kloos (1945), who hypothesized that an 'evocator' present in a graded fashion could generate neural crest at low levels and neural plate and neural crest at high levels, (reviewed in Baker and Bronner-Fraser, 1997). In *Xenopus* ectodermal explants (animal caps), varying the level of BMP activity leads to varying fates of ectoderm (Knecht *et al.*, 1995; Wilson *et al.*, 1997). Over-expression of a dominant-negative BMP receptor

(Marchant *et al.*, 1998) or of the BMP antagonist chordin (LaBonne and Bronner-Fraser, 1998b) in *Xenopus* ectodermal explants causes neural crest marker expression, and in whole embryos enhances the neural crest domain in a dose-dependent fashion (LaBonne and Bronner-Fraser, 1998b). In contrast, the reciprocal experiment of over-expressing *BMP-4* itself in intact embryos does not influence the size of the neural crest domain. Instead, the size of the neural plate decreases in a dose-dependent fashion, thus moving the location, but not the extent, of the presumptive neural crest (LaBonne and Bronner-Fraser, 1998b). Furthermore, chordin by itself cannot induce robust expression of neural crest markers in *Xenopus* animal caps (LaBonne and Bronner-Fraser, 1998b). Taken together, these results indicate that inhibition of BMP signaling alone is not sufficient to induce neural crest formation.

#### Genetic Evidence for the Involvement of TGF $\beta$ Family Members in Neural Crest Induction

Genetic evidence in the zebrafish supports a role for TGF $\beta$  family molecules influencing the fate of the ectoderm. Nguyen *et al.* (1998) have investigated *swirl* (Hammerschmidt *et al.*, 1996; Kishimoto *et al.*, 1997), a mutation in the zebrafish *BMP-2* gene. *Swirl* mutants display a loss of neural crest progenitors, while mutations in genes downstream of *Bmp-2b* such as *somitabin* (mutation in *Smad5*, a BMP signal transducer) expand the neural crest domain (Nguyen *et al.*, 1998). The zebrafish mutant *radar*, which affects a *dpp-Vg1*-related molecule distinct from the BMP-2/4 and BMP-5/8 subgroups (Delot *et al.*, 1999; and see Hogan 1996 for review of TGF $\beta$  family relationships), results in the loss of the neural crest marker *msxC* and selected neural crest derivatives.

Conversely, over-expression of the radar gene causes upregulation of *msxC* expression, but only in areas contiguous with the endogenous *msxC* domain (Delot *et al.*, 1999). In these mutants, however, the mesoderm underlying the neural crest is also affected, allowing for the possibility that the strength of the phenotype is not solely due to changes in BMP signaling in the ectoderm. This suggests that the activity of TGF $\beta$  family members contributes to the patterning of the ectoderm. However, only certain regions are competent to respond to these molecules suggesting that other gene activities may be required for the establishment of the neural crest.

Transgenic mice bearing null mutations in *BMP-4* (Winnier *et al.*, 1995), *follistatin* (Matzuk *et al.*, 1995) or *noggin* (McMahon *et al.*, 1998) do not display the neural defects that would be expected by extrapolation from the experiments in *Xenopus* described above. It has been suggested that redundancy between different BMP family members, the antagonizing molecules, or other developmental defects may obscure the phenotype (reviewed in Lee and Jessell, 1999). Alternatively, there may be interesting species differences in the process of neural induction and neural crest formation. Indeed, many studies in the chick embryo have added to the interspecific discrepancies that are found upon investigation of the role of TGF $\beta$  signaling as a mechanism for neural induction and neural crest formation.

### BMPs Can Induce Neural Crest in Culture

In the chick embryo, *BMP-4* and *BMP-7* are expressed in the epidermal ectoderm that contacts the neural tube (Liem *et al.*, 1995; Schultheiss *et al.*, 1997). As development proceeds, however, expression is lost in the epidermal ectoderm

but *BMP-4* is expressed in the neural folds and dorsal neural tube (Watanabe and Le Douarin, 1996), along with another TGF $\beta$  family member, *dorsalin-1*, which is up-regulated after neural tube closure (Basler *et al.*, 1993; Liem *et al.*, 1995). When added to isolated intermediate neural plates in tissue culture, both BMP-4 and -7 have been shown to induce neural crest markers and migratory cells (Liem *et al.*, 1995). This seemingly contrasts with the results in *Xenopus* where inhibition of BMP signaling yield neural fates. However, the paradigm for neural induction by BMP repression in the neural plate does not appear to function in the chick embryo at the time of neural crest/neural plate border formation (see Part I of this chapter). *Chordin*, which inhibits BMP activity, is expressed in the avian organizer (Hensen's node) but alone cannot neuralize ectoderm (Streit *et al.*, 1998). Additionally, neither *BMP-4* nor -7 is sufficient to repress neural induction in the neural plate when ectopically expressed (Streit *et al.*, 1998).

Furthermore, by implanting noggin-producing cells into the neural tube or under the neural fold regions, it has been shown that BMP signaling is required in the chick neural tube for expression of neural crest markers, but not at the stage at which BMP is expressed in the ectoderm (Selleck *et al.*, 1998). Pera *et al.* (1999) found that ectopic expression of *BMP-2* or -4 under the neural/non-neural border region distorts the neural plate and causes epidermal ectoderm marker expression in areas which would normally give rise to neural plate. Taken together, these results seem to indicate that BMP signaling plays several important roles in neural crest development, beginning with the positioning of the neural plate border and continuing with the maintenance of neural crest induction. Importantly, it is likely that other molecules are involved in the

initiation of neural crest induction. Later, BMPs in the dorsal neural tube induce roof plate cells and sensory neurons (Liem *et al.*, 1997). Still later, BMPs are involved in the differentiation of sympathoadrenal precursors from neural crest cells (Anderson, 1993; Varley *et al.*, 1998; Schneider *et al.*, 1999).

There is no direct evidence that either BMP-4 or -7 is the molecule that diffuses from the epidermal ectoderm to induce crest cells (Liem *et al.*, 1995). Indeed, it was shown that BMP-4 induces epidermis at the expense of neural tissue (Wilson and Hemmati-Brivanlou, 1995). The ability of BMP-4 and-7 to induce neural crest from neural plate cultures (Liem *et al.*, 1995; Liem *et al.*, 1997) may be a reflection of the molecule having first induced epidermis which in turn interacted with the neural plate to induce neural crest. Another possibility is that exogenous BMP bypasses an epidermal signaling event and mimics a later action of endogenous BMP signaling in the dorsal neural tube which is sufficient to generate neural crest cells. This possibility is supported by the later neural tube requirement for BMP signaling to produce neural crest cells as demonstrated by Selleck *et al.* (1998). Thus, the action of BMPs may be required within the responding tissues to maintain crest production, rather than being a property of the initial induction (reviewed in LaBonne and Bronner-Fraser, 1999).

It is important to bear in mind that although many experimental differences between species are reported in the literature, these are most likely to be a result of the rather striking differences among the organisms that are used for study. Differences in morphology and timing of development must require differences in gene expression to achieve the overall goal of properly forming the animal. For example, the frog embryo begins as a hollow ball of cells whereas

the chick embryo begins as a flat sheet of cells. In the frog embryo, development relies for a period of time on maternal stores of messenger RNAs, which contrasts with the chick embryo. Moreover, the distances between signaling centers and their responding tissues may require different mechanisms in order to effect induction of neural tissue and other developmental events. Although there are many apparent species differences, these may reflect variations in the finer details that accommodate spatial and temporal variations amongst organisms, whereas the general mechanisms are likely to be common for all vertebrates (LaBonne and Bronner-Fraser, 1999).

#### *Other Sources of Neural Crest-Inducing Signals:*

##### The Mesoderm

It would be overly simplistic to assume that a single signaling event within the ectoderm is sufficient to account for induction of the neural crest. There are many lines of evidence to suggest that the non-axial mesoderm is also involved in inducing the neural crest. Although conjugating epidermis and neural plate *in vitro* is sufficient to induce neural crest markers in the absence of mesoderm (Moury and Jacobson, 1990; Dickinson *et al.*, 1995; Selleck and Bronner-Fraser, 1995; Mancilla and Mayor, 1996), mesoderm could represent an important modifier. Mesoderm/neural plate conjugates do not induce early neural crest markers (Mitani and Okamoto, 1991; Selleck and Bronner-Fraser, 1995). However, it was demonstrated that paraxial mesoderm conjugated with neural plate could induce the formation of melanocytes, a late neural crest

derivative (Selleck and Bronner-Fraser, 1995). Similarly, non-axial mesoderm from both chick and frog can induce neural crest markers in neural plate co-culture experiments (Bang *et al.*, 1997; Bonstein *et al.*, 1998; Marchant *et al.*, 1998) and removal of the non-axial mesoderm before neural induction is complete results in a failure of the ectoderm to express neural crest markers (Bonstein *et al.*, 1998; Marchant *et al.*, 1998). The evidence that mesoderm can influence neural crest formation suggests that there may be other molecules involved in the early steps of neural crest induction.

### Wnt Family Members

As discussed above, it seems likely that inhibition of BMP alone cannot account for neural crest induction, making it probable that other signaling systems are involved. Possible candidates for involvement in this process are secreted molecules expressed in both mesoderm and ectoderm, and that have been implicated in patterning the neural tube. These include members of the wingless/int family known in vertebrates as Wnts (see Wodarz and Nusse, 1998) and the fibroblast growth factor (FGF) family (see Seiber-Blum, 1998; Vaccarino *et al.*, 1999). In *Xenopus* ectodermal explants (animal caps), Wnt1 and Wnt3a (Saint-Jeannet *et al.*, 1997b), Wnt7b (Chang and Hemmati-Brivanlou, 1998b) and Wnt8 (LaBonne and Bronner-Fraser, 1998b), in conjunction with inhibition of BMP signaling (i.e., neural induction) can induce the expression of neural crest markers. Furthermore, over-expression of  $\beta$ -catenin (a downstream component of the Wnt signaling pathway) expands the neural crest domain, whereas

expression of a dominant-negative Wnt ligand eliminates the neural crest domain in *Xenopus* embryos (LaBonne and Bronner-Fraser, 1998b).

One of the earliest neural crest markers in *Xenopus* is the zinc finger transcription factor, *Slug* (Mayor *et al.*, 1995, and see Figure 6). When animal caps over-expressing *Slug* are juxtaposed to *Wnt8*-expressing explants, neural crest markers are induced, thus bypassing the requirement for inhibition of BMP signaling (LaBonne and Bronner-Fraser, 1998b). In contrast, *Slug* alone cannot induce neural crest (LaBonne and Bronner-Fraser, 1998b). *Slug*, in turn, can expand its own expression domain when over-expressed in the whole embryo (LaBonne and Bronner-Fraser, 1998b). These results suggest that a two-signal model may account for the events underlying neural crest formation, such that Wnt signaling together with inhibition of BMP signaling induces the neural crest marker, *Slug*, with *Slug* expression abrogating further need for BMP inhibition (LaBonne and Bronner-Fraser, 1998b).

Many Wnt molecules are expressed in spatiotemporal patterns appropriate for involvement in various aspects of neural crest development. *Xenopus Wnt8* is expressed in the ventrolateral mesoderm (Christian *et al.*, 1991), a tissue that has been shown to be a neural crest inducer when conjugated with neural plate *in vitro* (Bang *et al.*, 1997; Bonstein *et al.*, 1998; Marchant *et al.*, 1998) and avian *Wnt-8C* is similarly expressed in the non-axial mesoderm (Hume and Dodd, 1993). *Xenopus Wnt7b* is expressed throughout the ectoderm at gastrulation (Chang and Hemmati-Brivanlou, 1998b) and other Wnts may well be expressed in the ectoderm.

In chick (Dickinson *et al.*, 1995; Hollyday *et al.*, 1995), frog (Wolda *et al.*, 1993; McGrew *et al.*, 1997) and mouse embryos (Roelink and Nusse, 1991; Parr *et al.*, 1993), *Wnt1* and *Wnt3a* are expressed in the dorsal neural tube well after the initial expression of neural crest markers, although *Xenopus Wnt3a* is also expressed before neural tube closure at the edges of the neural plate (McGrew *et al.*, 1997). Furthermore, avian neural crest can be induced in conjugates of epidermis and neural plate without the concomitant expression of either *Wnt1* or *Wnt3a* (Dickinson *et al.*, 1995). This suggests that *Wnt-1* and *-3a* are not involved in the initial induction of neural crest. However, *Wnt1/3a* double knock-out mice have a reduction in neurogenic and gliogenic neural crest derivatives, suggesting that fewer neural crest cells emerge in embryos lacking both genes (Ikeya *et al.*, 1997). Not all neural crest derivatives are affected, with ventral-most derivatives such as sympathetic ganglia demonstrating normal morphology while dorsal root ganglia are markedly reduced. This is consistent with the possibility that these Wnts play a later maintenance role in neural crest production by the neural tube. Wnts may be involved in the expansion of neural crest progenitors, most likely by regulating the proliferation of the cells after induction has occurred, but prior to commencement of emigration (Ikeya *et al.*, 1997).

Wnt family members may also be able to control some aspects of neural crest cell fate. In zebrafish experiments, single neural crest cells overexpressing molecules of the Wnt signaling pathway form pigment cells at the expense of neurons or glia. Conversely, over-expressing inhibitors of the pathway biases the neural crest cells to form neurons at the expense of pigment cells (Dorsky *et al.*, 1998).

Recent work by Baker *et al.* (1999) has put forward a novel model for Wnt function. They demonstrate that expression of *Xenopus Wnt8*, mouse *Wnt8* and downstream Wnt targets in frog ectodermal explants can induce expression of the early pan-neural marker *NCAM*, without neural induction by BMP antagonists. Additionally, they demonstrate that Wnt signaling components suppress *BMP-4* expression in ectoderm explants as assayed by *in situ* hybridization. In fact, *Wnt8*, and not the BMP antagonist *noggin*, seems to be capable of blocking *BMP-4* expression in the neural plate throughout gastrula stages, suggesting that an early Wnt signal and not a direct BMP antagonist is responsible for the early inhibition of *BMP-4* expression in the neural plate. Finally, the authors suggest that there may be parallel pathways for the effects of Wnt signaling in neural induction since inhibition of *Wnt8*-mediated activation of the neural inducers *Xnr3* and *siamois* did not abrogate *Wnt8*'s ability to itself promote neural induction. These results suggest that Wnt signaling may be involved in multiple inductive events in early development. The ramifications of these data for the role of Wnt signaling in neural crest induction are unclear, as these investigators did not explore the effects of the perturbations on neural crest markers. Previous results showing that Wnts could not induce neural crest without a co-expressed neural inducer (Saint-Jeannet *et al.*, 1997; Chang and Hemmati-Brivanlou, 1998b; LaBonne and Bronner-Fraser, 1998b) taken together with the results of Baker *et al.* (1999) may indicate that the precise levels of Wnt signaling are critical. Further investigation will be required to determine exactly what role Wnts play during neural crest development.

## Fibroblast Growth Factors

Other molecules expressed in the mesoderm have been shown to have neural crest inducing activities. FGF signaling can induce neural crest markers in frog ectodermal explants when in the presence of BMP antagonists (Mayor *et al.*, 1997; LaBonne and Bronner-Fraser, 1998b; Kengaku and Okamoto, 1993). Over-expression of a dominant-negative FGF receptor can inhibit the expression of the early neural crest marker *XSlug* in whole embryos (Mayor *et al.*, 1997). Other investigators have demonstrated that FGF signaling has a posteriorizing effect on neural tissue (Kengaku and Okamoto, 1993; Cox and Hemmati-Brivanlou, 1995; Lamb and Harland, 1995; Launay *et al.*, 1996; Xu *et al.*, 1997). Indeed, members of the FGF family are spatiotemporally expressed in a way that is consistent with their playing roles in the process of neural and/or neural crest induction (Tannahill *et al.*, 1992; Isaacs *et al.*, 1992; Mahmood *et al.*, 1995; Riese *et al.*, 1995; Bueno *et al.*, 1996; Storey *et al.*, 1998). The results indicate that FGFs may be able to generate both posterior and lateral (i.e., neural crest) fates in the CNS and PNS. The role of FGFs becomes complicated in light of evidence from transgenic frog experiments, however, in which frog embryos expressing a dominant-negative FGF receptor have normally-developing posterior neural tissue and border regions including the neural crest, although the investigators did not test a full range of neural crest markers (Kroll and Amaya, 1996). Moreover, FGF-treated neural plate explants do not form neural crest tissue (Mayor *et al.*, 1997). Finally, neural crest induction by FGF may be a secondary result of its ability to induce a member of the Wnt family (LaBonne and Bronner-Fraser, 1998b). Thus,

FGF signaling is not required for neural crest induction, and the demonstrated effects may be indirect.

## Neural Crest Stem Cells

In the past decade, work by several investigators has led to the identification and purification of neural crest stem cells—cells with the potential to self-renew and also to give rise to the diverse population of derivatives that are generated by the neural crest. The first neural crest stem cells were isolated *in vitro* by clonal analysis of cells that were fractionated from rat neural crest cultures by cell sorting based on expression of a cell-surface epitope (Stemple and Anderson, 1992). These cells can be replated to form new stem cells and also can give rise to "blast" cells that are partially restricted to form neurons or glia. These include the sympathoadrenal sublineage, which includes precursors to sympathetic neurons and adrenomedullary cells (Doupe *et al.*, 1985a; Doupe *et al.*, 1985b), that, in the embryo, appear specified by the time that neural crest-derived cells reach their sites of localization around the dorsal aorta.

Specific molecules can instruct neural crest stem cells to adopt specific fates; for example, glial growth factor (neuregulin) causes the development of glia (Schwann cells), BMP-2 biases clones to develop into neurons (and a small number of smooth muscle cells), and TGF $\beta$ 1 promotes development of smooth muscle cells (Shah *et al.*, 1994; Shah *et al.*, 1996; Shah and Anderson, 1997). Thus it is interesting to note that members of the TGF $\beta$  superfamily are not only involved in induction of the neural crest but are also implicated in subsequent cell fate decisions.

Although the neural crest stem cells are very useful in testing the ability of factors to promote certain cell fate decisions, there are possible caveats; for example, the stem-cell qualities of the purified cells may have been acquired *in vitro* and may not reflect an actual state that is present in the embryo. The findings of Frank and colleagues (Sharma *et al.*, 1995; Korade and Frank, 1996) that neural tubes can give rise to neural crest-like cells that emigrate long after the normal period of neural crest formation suggests that neural crest stem cells may persist within the spinal cord and other sites for long periods of time. Consistent with this possibility, Morrison *et al.* (1999) have recently isolated neural crest stem cells from embryonic rat peripheral nerve. The cells were isolated by fluorescence-activated cell sorting using cell surface epitopes p75 and P0. Under proper culture conditions, these cells self-renew and can differentiate into neurons, glia, and smooth muscle cells within single colonies. The cells are also instructively promoted to form neurons or glia by exposure to either BMP-2 or glial growth factor, respectively, in clonal cultures. An important test of the qualities of these neural crest stem cells is to determine whether newly-isolated cells are multipotent when transplanted into an embryo. Indeed, freshly isolated cells that were p75+/P0- have stem cell properties and can be back-transplanted into chick embryos, giving rise to both neurons and glia as assayed by differential marker expression (Morrison *et al.*, 1999). By labeling actively dividing cells in embryos with the thymidine analog, BrdU, it was shown that endogenous neural crest stem cells persist in the embryo by self-renewing (Morrison *et al.*, 1999).

## Lineage and Cell Fate Decisions in the Neural Crest

The existence of neural crest stem cells in the embryo supports the idea that the fate of neural crest cells *in vivo* is primarily determined by their environment (Le Douarin, 1986). Neural crest cell fate decisions and their relationships to cell lineage have been debated for many years. While it has been accepted that at least some, if not most neural crest cells are multipotent, some evidence indicates that other neural crest cells have restricted fates *in vivo* (Bronner-Fraser and Fraser, 1988; Bronner-Fraser and Fraser, 1989; Frank and Sanes, 1991). However, in these experiments, the potential of the cells has not actually been tested by challenging the cells with all possible factors that might influence cell fate choice. It is obviously difficult to quantify and compare the environment of one cell with another, beginning from their origins in the neural tube and following their migration trajectories through the periphery. In these lineage experiments, single dye-labeled or retrovirally-tagged cells often gave rise to clones of progeny with multiple derivatives, but sometimes gave rise to clones of only one cell type, suggesting an earlier specification for that progenitor cell. Thus, alternate methods of marking and challenging neural crest cells will be necessary in order to define the state of multipotency at the single cell level. This is an area where the neural crest stem cells and their blast cells promise to provide new and important information.

### *Mechanisms of Neural Crest Diversification*

If neural crest cells are truly multipotent and only receive instructions for differentiation when migrating to or reaching their final destinations, then it is

interesting to consider how cells are instructed to take on different fates. For example, neural crest cells in the dorsal root ganglia differentiate into both sensory neurons and glia. An asymmetric cell division could produce a blast cell of each type, which could in turn replicate. Alternatively, the progenitor may replicate itself and produce a more restricted daughter cell which then goes on to form the final derivatives. The latter seems more likely given the ability of neural crest stem cells to self renew.

### Environmental Cues versus Timing of Emigration

Both the environment and the timing of emigration from the neural tube have been proposed to affect the cell fate decisions of the neural crest. A restriction in available cell fate accompanies the time of emigration from the neural tube: the latest migrating cells only populate the dorsal root ganglia as neurons and form melanocytes in the skin and feathers (Sharma *et al.*, 1995; Serbedzija *et al.*, 1989). However, when transplanted into earlier embryos, neural crest-like cells derived from much older spinal cords were able to migrate more ventrally and make sympathetic and peripheral neurons (Weston and Butler, 1966; Korade and Frank, 1996). Similarly, in the head, late-migrating cells only formed dorsal derivatives because of the presence, ventrally, of earlier-migrating cells; however, they are not restricted in potential (Baker *et al.*, 1997). Furthermore, the latest-migrating cells of the main wave of crest emigration make melanocytes in the skin, but skin-culture experiments show that they have the potential to form neurons (Richardson and Sieber-Blum, 1993). This suggests that the restriction in available fates in these cases is made by the environment

that the cells occupy rather than the time that they emerge from the neural tube (see Figure 5).

Additional evidence for the influence of environment on neural crest cell fate comes from neural crest stem cells, in which single progenitor cells can generate smooth muscle cells when exposed to TGF $\beta$  molecules. However, a community effect takes place when more dense cultures are exposed to TGF $\beta$  molecules, such that either neurons form or cell death occurs, rather than differentiation of smooth muscle cells (Hagedorn *et al.*, 1999). These data suggest that cell fate in the embryo could also be determined by community effects in which cells respond differently to the same factors depending on the density of neighboring cells (Hagedorn *et al.*, 1999). Other interesting studies on neural crest stem cells reveal that they can integrate multiple instructive cues and are biased to certain levels of responsiveness based on the growth factors to which they are exposed. If cultures of neural crest stem cells are exposed to saturating levels of both BMP2 and glial growth factor (neuregulin), BMP-2 appears dominant and neurons differentiate. However, BMP-2 and TGF $\beta$ 1 seem to be co-dominant (Shah and Anderson, 1997).

There is evidence, however, that some neural crest cell populations may undergo early fate restrictions. By culturing "early-migrating" and "late-migrating" trunk neural crest cells, Artinger and Bronner-Fraser (1992) found that the latter are more restricted in their developmental potential than the former; although they can form pigment cells and sensory-like neurons, they fail to form sympathetic neurons. Additionally, late-migrating cells transplanted into an earlier environment could colonize the sympathetic ganglia but failed to

form adrenergic cells (Artinger and Bronner-Fraser, 1992). Thus, the time that a precursor leaves the neural tube may contribute to its potency. Perez *et al.* (1999) have provided evidence for early specification of sensory neurons by the basic helix-loop-helix transcription factors neurogenins 1 and 2. These molecules are expressed early in a subset of neural crest cells, and ectopic expression of the molecules biases migrating neural crest cells to localize in the sensory ganglia and express sensory neuron markers.

Another way to account for the process of promoting two different cell fates from one precursor population within a single tissue is the proposal that temporal changes in the target environment bias the cell fate decision (Frank and Sanes, 1991). This is supported by the fact that first neurons, then glia are born in the dorsal root ganglia (e.g., Carr and Simpson, 1978). The target environment could be influenced to change by early-differentiating neural crest cells themselves; for example, some neurons produce glial-promoting factors (Marchionni *et al.*, 1993; Orr-Urtreger *et al.*, 1993; Meyer and Birchmeier, 1995; Lemke, 1996; Meyer *et al.*, 1997). Also, the loss of certain inhibitory glycoconjugates from the extracellular matrix in the dorsolateral migration pathway has been linked to the migration of late-emigrating neural crest cells along this pathway (Oakley *et al.*, 1994), where they are exposed to melanogenic factors and hence adopt a melanocyte fate (Perris *et al.*, 1988). Thus, there is evidence for the influence of both the timing of emigration and environmental cues in determining neural crest fates.

### Progressive Lineage Restriction

It has been proposed that neural crest cells adopt specific fates by progressive lineage restrictions (see Anderson, 1993; Stemple and Anderson, 1993; Anderson, 1999). One way to explain the intermingling of clonally related neurons and glia is that the choice is made stochastically, such that each cell has the capacity to adopt either fate, and environmental factors act by influencing the probability of a fate choice rather than imposing strict commitments (Frank and Sanes, 1991). Support for the idea of progressive fate restriction comes from the neuroepithelial stem cell (NEP) which can give rise to both CNS and PNS-type stem cells. PNS stem cells (indistinguishable from neural crest stem cells as described by Stemple & Anderson, 1992) are formed on addition of BMP-2/-4 to the NEP cell cultures (Mujtaba *et al.*, 1998). BMP-2, a molecule that is known to instruct neural crest stem cells toward an adrenergic neuronal fate, is expressed in the dorsal aorta, near where sympathetic ganglia form (Bitgood and McMahon, 1995; Lyons *et al.*, 1995; Shah *et al.*, 1996). Thus, there is evidence that environmental cues may be able to promote progressive restriction of neural crest cell fates. Many factors act selectively by affecting the proliferation or survival of neural crest derivatives, while others act instructively on multipotent progenitors to promote one fate over another. Further work will be required to answer the complex question of how individual cells within the same environment can adopt different fates. The evidence in support of both multipotentiality and lineage restriction may imply that neural crest cells take cues both from the timing of emigration from the neural tube and the environments to which they are exposed in cell lineage decisions. For more

discussion on the topic of neural crest diversification, the reader is referred to several recent reviews (Ito and Sieber-Blum, 1993; LaBonne and Bronner-Fraser, 1998a; Groves and Bronner-Fraser, 1999).

### **Theme of the thesis**

The demonstration that multiple molecules from different gene families have the inductive capacities implies that the mechanism of neural and neural crest induction involves complex and perhaps parallel pathways. Although great strides have been made towards understanding the induction of neural cell fate decisions, many mysteries remain. In this thesis, I investigate the role of a family of gene isoforms, the *Noelins*, during amphibian neural and neural crest development. *Noelins* were first described as brain-specific genes in neonatal rats. *Noelin* genes are alternatively spliced isoforms derived from two different promoters; all share a common central region and two different upstream and downstream regions. Intriguingly, during embryonic avian development, *Noelins* are expressed in a pattern initially corresponding to tissues that have the potential to form neural crest; later, expression is found in pre-migratory and migrating neural crest cells, and later in many derivatives of the peripheral and central nervous system.

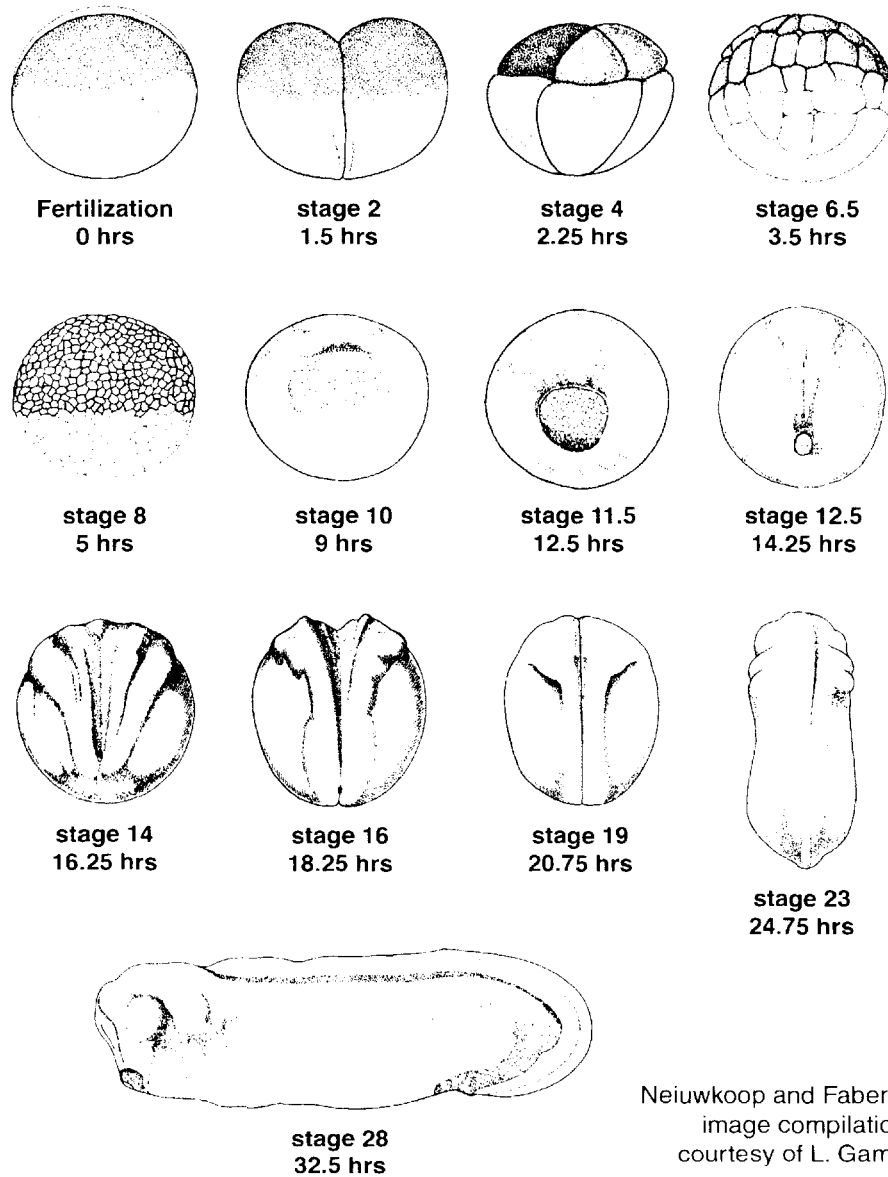
Using amphibian embryos, I show that *Noelin* genes have a different expression pattern, in which the later CNS and PNS expression is conserved, but the early expression in future neural crest cells is not, although the isoforms are detected at early neural stages by more sensitive methods. In addition, I demonstrate that functionally, *Noelin-4* acts as a neural inducer and promotes

neural fate, while Noelin-1 can promote neuronal differentiation but does not act as a neural inducer. Biochemical characterization of the proteins shows that they are secreted, and that they may interact *in vivo* by forming complexes. Noelin-4 also may interact with BMP-4 *in vivo*, suggesting that it could function by modulating BMP signaling in some aspect. Furthermore, *Noelin* genes may modulate each other's activities in neural development: *Noelins* may serve as a regulatory co-factors for other *Noelins*; in co-expression experiments, I show that Noelin-4 is less active in the presence of Noelin-1, while the activity of Noelin-1 is increased in the presence of Noelin-4. Finally, an evolutionary comparison of *Noelin* genes in frog, chick and mouse is made, showing that the highly conserved sequence of the genes may indicate conserved functions, although the expression pattern of the homologs in each species are somewhat divergent. Thus these genes may represent important regulators of neural induction and neurogenesis.

## **Acknowledgements**

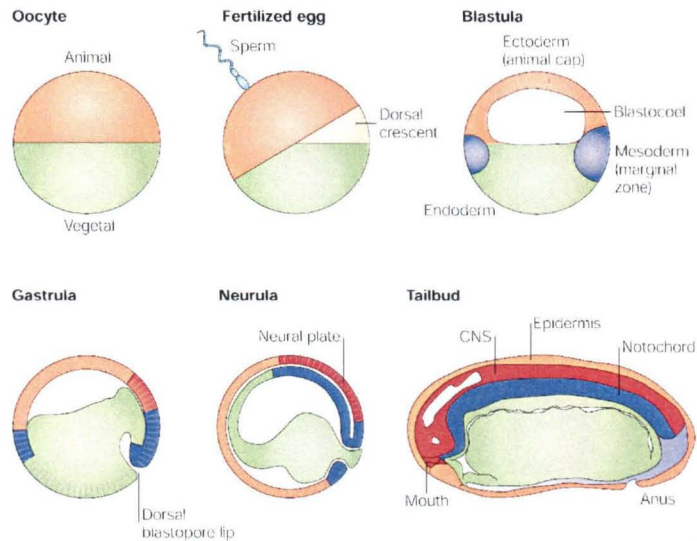
I am indebted to Clare Baker and Anne Knecht for critical reading of the manuscript prior to publication and after modifications of this chapter in preparation for the thesis.

## Figure 1: *Xenopus* developmental stages



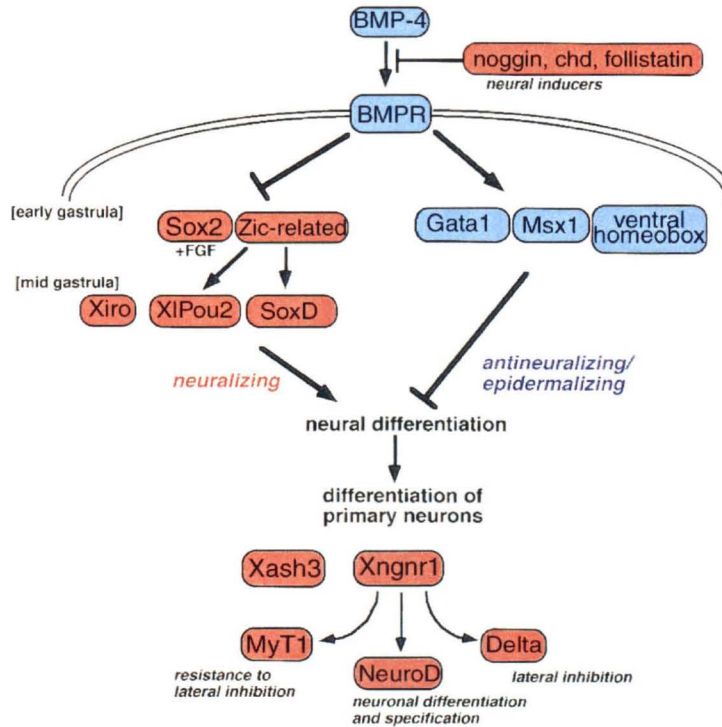
Nieuwkoop and Faber (1967) schematic drawings of *Xenopus* embryos from fertilization through tailbud stages. Approximate time of development is given below the stage numbers. Embryos through stage 8 are side views with animal pole up; stages 10-12.5 are posterior/dorsal views; stages 14-23 are dorsal views; stage 28 is a side view.

## Figure 2: Anatomy of *Xenopus* development



The anatomy of *Xenopus* development. The oocyte is radially symmetrical and is divided into an animal and a vegetal domain. One hour after fertilization, an unpigmented dorsal crescent is formed in the fertilized egg opposite the sperm entry point. As the embryo rapidly divides into smaller and smaller cells without intervening growth (cleavage stages), a cavity called the blastocoel is formed, which defines the blastula stage. By the late blastula stage (stage 9), the three germ layers become defined. The ectoderm (animal cap) forms the roof of the blastocoel. The mesoderm is formed in a ring of cells in the marginal zone, located between the ectoderm and endoderm. At the gastrula stage (stage 10), involution of the mesoderm towards the inside of the embryo starts at the dorsal blastopore lip. The morphogenetic movements of gastrulation lead to the formation of the vertebrate body plan, patterning the ectoderm, mesoderm and endoderm. At the neurula stage (stage 14), the neural plate, or future central nervous system (CNS), becomes visible in dorsal ectoderm. By the tailbud stage (stage 26-42), a larva with a neural tube located between the epidermis and the notochord has formed. The blastopore gives rise to the anus, and the mouth is generated by secondary perforation. (Modified from DeRobertis et al., 2000)

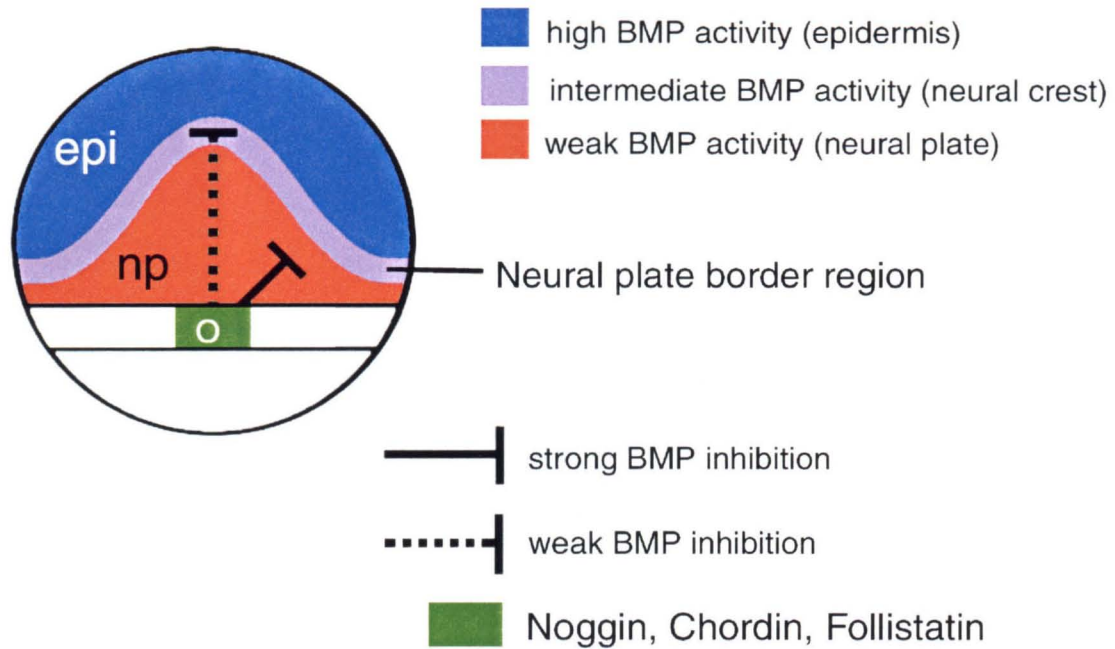
**Figure 3: From neural induction to neurogenesis**



A model for the regulatory genes involved during early neural differentiation is shown within the context of a possible cascade of genetic interactions. Positive and negative regulators of neurogenesis are boxed in red and blue, respectively. BMP-4 binds to its receptor and activates epidermal induction through *Gata1*, *Msx1* and ventral homeobox genes. *Noggin*, *chd* (*chordin*) and *follistatin* are neural inducers that inhibit epidermal induction by preventing BMP-4 binding to its receptor. Inhibition of expression of *Sox2* and *Zic-related* genes is relieved by early gastrula stages, and subsequent neural markers are expressed at midgastrula. Neuralization activates neurogenic genes, with *Xash3* and *Xngnr1* being the first known proneural genes expressed. *Xngnr1* activates downstream determination genes and lateral inhibition machinery (*Delta*), resulting in neuronal differentiation.

(Modified from Sasai, 1998)

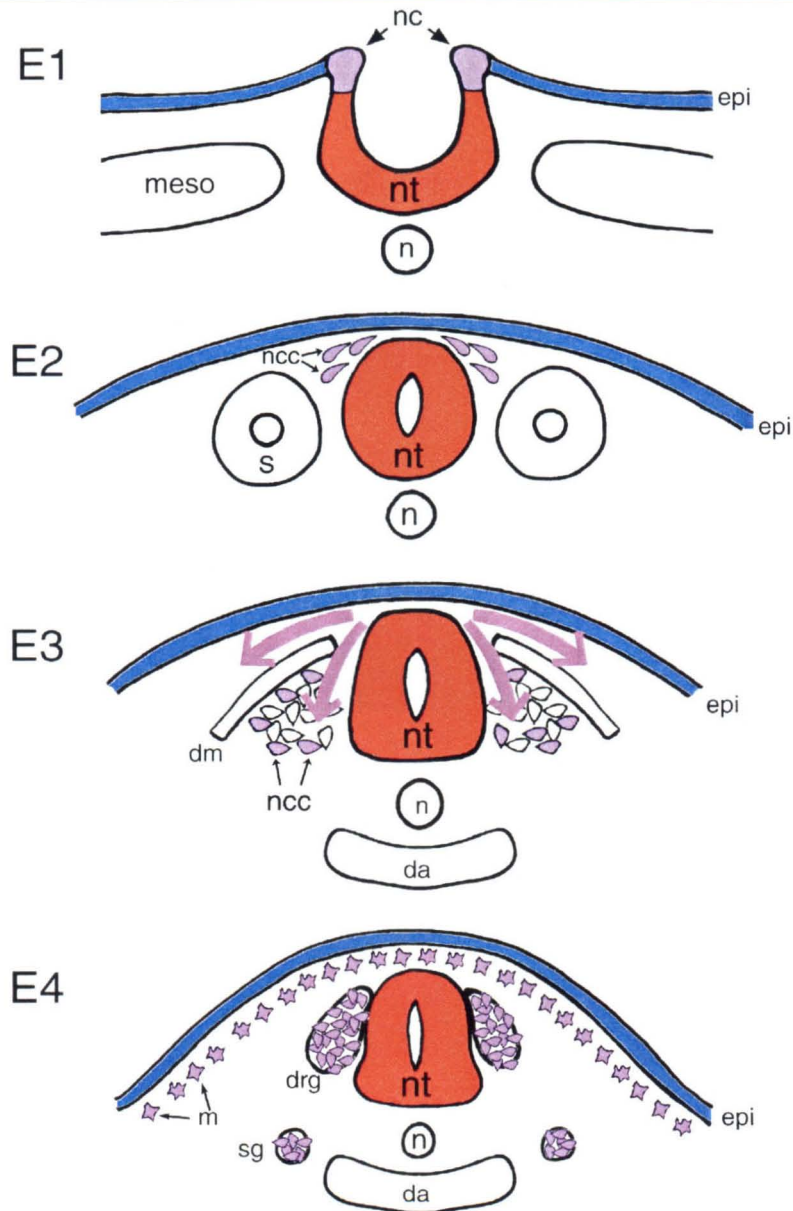
**Figure 4:** Neural induction in *Xenopus*



Schematic diagram of the *Xenopus* model of neural induction. The BMP antagonists *noggin*, *chordin* and *follistatin* are secreted from Spemann's Organizer (green box) to modulate BMP activity in the ectoderm (colors represent prospective ectodermal fate). The activity of BMP molecules establishes three fates of ectoderm: lowest activity = neural plate; intermediate activity = neural crest; highest activity = epidermis. This simplistic model does not include the evidence for the involvement of other molecules in neural and neural crest induction, but is intended as a simplified model of neural induction. e, epidermis (blue); np, neural plate (red); O, organizer (green); neural crest and placode-forming region (purple).

(Modified from LaBonne and Bronner-Fraser, 1999)

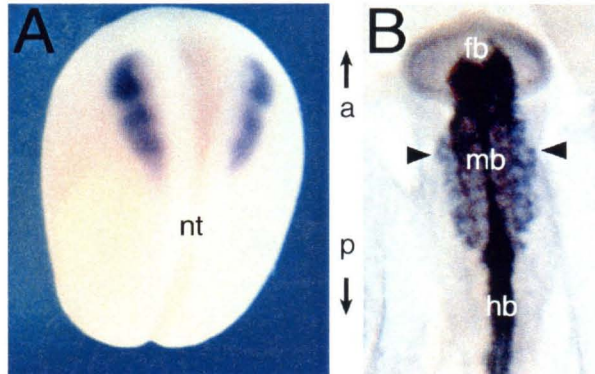
## Figure 5: Neural crest migration in avians



Cross-sectional schematic views of neural crest-forming regions and migration pathways in avians. **E1:** (Embryonic day 1) Thickened epithelium at the midline begins to fold into a tube. The border of the neural and non-neural ectoderm is the site of neural crest formation. **E2:** Neural crest cells delaminate from the dorsal neural tube and begin to migrate. **E3:** Two migration pathways are shown in the trunk: the dorsolateral pathway passes between the dermomyotome and epidermis, and the ventral pathway that passes through the sclerotome of the somites. **E4:** Neural crest cells in the trunk populate the dorsal root ganglia, sympathetic ganglia, and form melanocytes in the skin. da, dorsal aorta; dm, dermomyotome; drg, dorsal root ganglion; epi, epidermis; m, melanocyte; meso, non-axial mesoderm; ncc, neural crest; nt, neural tube; s, somite; sg, sympathetic ganglion.

**Figure 6:** *Slug* expression in *Xenopus* and chick embryos

---



---

The zinc-finger transcription factor *Slug* is an early marker for the neural crest in *Xenopus* and chick. Anterior is up. **A:** a late-neurula *Xenopus* embryo with *Slug* mRNA expression in the cranial neural crest on both sides of the closing neural tube. The groove down the central portion of the embryo is the forming neural tube. **B:** an E1.5 (10-somite stage) chick embryo with *Slug* mRNA marking the early-migrating neural crest in the head (arrowheads) and pre-migratory neural crest at more posterior levels of the neural tube.



## **Chapter 2:**

# **The secreted glycoprotein Noelin-1 promotes neurogenesis in *Xenopus***

Tanya A. Moreno and Marianne Bronner-Fraser (2001)

Portions of this chapter were originally published in

*Developmental Biology* **240**, 340-360.

Reprinted with permission from Academic Press.

**ABSTRACT**

Neurogenesis in *Xenopus* neural ectoderm involves multiple gene families, including basic helix-loop-helix transcription factors, which initiate and control primary neurogenesis. Equally important, though less well understood, are the downstream effectors of the activity of these transcription factors. I have investigated the role of a candidate downstream effector, *Noelin-1*, during *Xenopus* development. *Noelin-1* is a secreted glycoprotein that likely forms large multi-unit complexes. In avians, over-expression of *Noelin-1* causes prolonged and excessive neural crest migration. My studies in *Xenopus* reveal that this gene, while highly conserved in sequence, has a divergent function in primary neurogenesis. *Xenopus Noelin-1* is expressed mainly by post-mitotic neurogenic tissues in the developing central and peripheral nervous systems, first appearing after neural tube closure. Its expression is upregulated in ectopic locations upon over-expression of the neurogenic genes *X-ngnr-1* and *XNeuroD*. *Noelin-1* expression in animal caps induces expression of neural markers *XBrn-3d* and *XNeuroD*, and co-expression of secreted *Noelin-1* with *noggin* amplifies *noggin*-induced expression of *XBrn-3d* and *XNeuroD*. Furthermore, in animal caps neuralized by expression of *noggin*, co-expression of *Noelin-1* causes expression of neuronal differentiation markers several stages before neurogenesis normally occurs in this tissue. Finally, only secreted forms of the protein can activate sensory marker expression, while all forms of the protein can induce early neurogenesis. This suggests that the cellular localization of *Noelin-1* may be important to its function. Thus, *Noelin-1* represents a novel secreted factor involved in neurogenesis.

## INTRODUCTION

During nervous system development, a variety of cellular interactions influence cell fate decisions. Neural induction begins during gastrulation, when a region of mesodermal tissue in amphibians called the Spemann Organizer involutes and comes to underlie the ectoderm, signaling it to become neural (Spemann and Mangold, 1924; and see Lee and Jessell, 1999; Weinstein and Hemmati-Brivanlou, 1999; and Harland, 2000 for review). Antagonism of BMP signaling by secreted factors such as Noggin, Chordin and Follistatin plays a major role in allowing the ectoderm to form neural tissue instead of epidermis (Lamb *et al.*, 1993; Hemmati-Brivanlou *et al.*, 1994; Sasai *et al.*, 1994; Piccolo *et al.*, 1996; Zimmerman *et al.*, 1996; Fainsod *et al.*, 1997).

Following initial induction, a neurogenic cascade of transcription factors is activated which results in differentiation of neurons within the neural field, and ultimately in the formation of the nervous system (reviewed in Anderson, 1995; Chitnis, 1999). Basic helix-loop-helix (bHLH) transcription factors of the *achaete-scute* and *atonal* families play an important role in this process. The proneural bHLH genes *XASH-3* and *X-ngnr-1* are expressed in the neural plate shortly after gastrulation (Ferreiro *et al.*, 1994; Ma *et al.*, 1996). Moreover, some bHLH genes have further roles in neuronal development. For example, neurogenins have been shown to have distinct neuronal cell-type inducing properties in the cranial ganglia in addition to their roles in initiating neurogenesis (Ma *et al.*, 1996; Fode *et al.*, 1998; Ma *et al.*, 1998; Perez *et al.*, 1999). In *Xenopus*, over-expression of *X-ngnr-1* induces neurons of sensory character in the non-neural ectoderm, while in the eye it promotes development of specific subtypes of retinal neurons

(Olson *et al.*, 1998; Perron *et al.*, 1999). In addition to the bHLH transcription factors, genes of the Zinc finger and paired-domain families also are involved in initiation of neurogenesis. The zinc finger transcription factor NKL can promote neurogenesis in amphibian and chick embryos (Lamar *et al.*, 2001) and the paired-domain transcription factor Pax-6 can direct neurogenesis of ectopic retina (Chow *et al.*, 1999).

While many types of transcription factors are known to activate the programs of cell fate decisions in neural development, the downstream effectors are complex and poorly understood. Such genes exert their activities in a specific context and are unable to initiate neurogenesis alone. An example of such a molecule is Noelin-1, a secreted glycoprotein expressed in the early neural plate of the chick embryo (Barembaum *et al.*, 2000).

*Noelin* isoforms were first identified in a screen of randomly selected clones from a rat brain cDNA library (Danielson *et al.*, 1994). The protein sequences of Noelin-1 and -2 show similarity to that of Olfactomedin, an extracellular matrix molecule thought to be involved in facilitating or mediating odorant recognition (Snyder *et al.*, 1991; Bal and Anholt, 1993; Yokoe and Anholt, 1993). Four structurally distinct messenger RNAs are spliced from the *Noelin* gene, each sharing a common central exon (M), with two different 5' exons (A or B) added by differential promoter utilization, and two different 3' exons (Y or Z) added by alternative splicing, making up the four isoforms, BMZ, AMZ, BMY, and AMY (Danielson *et al.*, 1994), termed *Noelin-1* through -4 respectively (Barembaum *et al.*, 2000). In mouse and rat, the four *Noelin* isoforms are expressed at varying levels in the postnatal cortex (Danielson *et al.*, 1994; Nagano *et al.*, 1998). Differential expression of the four isoforms is found also in the chick,

where *Noelin-1* and *-2* are expressed during neurula stages but *Noelin-3* and *-4* are not expressed until later embryonic stages (Barembaum *et al.*, 2000).

Previous studies from my lab have shown that avian *Noelin-1* is involved in the generation of neural crest cells (Barembaum *et al.*, 2000). To my knowledge, *Noelin-1* is the earliest marker of neural crest potential in the chick, preceding the expression of other established neural crest markers such as *Slug* (Nieto *et al.*, 1994), *AP-2* (Shen *et al.*, 1997) and *Id2* (Martinsen and Bronner-Fraser, 1998). Avian *Noelin-1* is expressed from early stages in the neural plate and then is subsequently limited to the neural folds and adjacent ectoderm, both tissues that have the potential to form neural crest cells. Furthermore, retroviral over-expression of *Noelin-1* in avian embryos causes excessive and prolonged cranial neural crest emigration, suggesting a role for *Noelin-1* in neural crest formation. *Noelin-1* expression persists into later stages and is observed in migrating neural crest cells and their derivatives including cranial ganglia. It is also expressed in neurons in the brain and spinal cord. This suggests that *Noelin-1* protein could also function in later steps of neural development in addition to its earlier role in neural crest formation.

Here, I characterize the function of *Noelin-1* in *Xenopus* embryos. I describe the *Xenopus* homologs of *Noelin-1* and *-2* and examine their roles during early nervous system development. Interestingly, my studies reveal temporal differences in expression of these transcripts between species that result in striking variations in their utilization. Although chick *Noelin-1* is involved in neural crest generation, *Xenopus Noelin-1* appears to be involved in promoting neuronal differentiation, suggesting that *Noelin* isoforms may have been co-opted for different functions in different vertebrates.

## METHODS

### Library screening and cDNA isolation

A stage 28 phage cDNA library in Lambda ZapII made from head tissues was kindly provided by Dr. R. Harland (Hemmati-Brivanlou *et al.*, 1991).  $1 \times 10^6$  plaque-forming units were screened with chick *Noelin-1* and a PCR fragment of the mouse Z exon. The mouse subclone was generated by RT-PCR using upstream primer 5'-CAG AAG GTG ATA ACC GG-3' and downstream primer 5'-CAG CGC GCG GTC TTT AG-3' to amplify a 616 base pair (bp) fragment of the Z exon from embryonic day 10 cDNA. Total RNA was isolated using RNazol B (Tel-Test, Inc.) according to manufacturer's instructions. cDNA was synthesized using MMLV Reverse Transcriptase (Roche). A stage 15 (neural plate stage) cDNA library kindly provided by M. King was screened at low stringency with the *Xenopus Noelin* Olfactomedin domain in a search for *Noelin*-related genes.

Full-length clones of *Noelin-1*, -2 and -4 were obtained after low-stringency screening. Sequencing was done by PCR using dye-terminators and run on an ABI Prism automated sequencer. Sequences were compiled and edited using the DNASTar programs. Sequences were compared to others in GenBank using BLAST (Altschul *et al.*, 1990).

The largest open reading frame of the *Noelin-1* cDNA (2885 bp full length) is 1455 bp, running from nucleotide #348-1805 and predicting a 485 amino acids (aa) protein with a molecular mass of approximately 56 kD. *Noelin-2* (2961 bp) coding sequence is located between nucleotides #443-1819, predicting a 458 aa

protein with a molecular mass of approximately 53 kD. GenBank accession numbers: *Noelin-1* (AF416483) and *Noelin-2* (AF416482).

### ***Xenopus laevis* fertilizations, dissections and collection of oocytes**

*Xenopus* embryos were obtained by *in vitro* fertilization using eggs from pigmented and albino females and testis from pigmented males, according to established methods (Sive *et al.*, 2000). Embryos were staged according to the normal tables of Nieuwkoop and Faber (1967).

Animal caps were manually isolated from stage 8-9 blastulae and cultured in 3/4 X NAM (Slack and Forman, 1980) until siblings reached stage 24 or 27 when they were fixed in MEMFA for 1 hour and then stored in 100% ethanol or processed for RT-PCR.

*Xenopus* ovaries were dissected from sexually mature females through an abdominal incision after anesthetizing in Finquel's solution (Tricaine, Argent Chemical Laboratory). Ovaries were rinsed in OR2 medium (Sive *et al.*, 2000) and then stored at 14°C in OR2 for up to 4 days. Stage VI oocytes were manually defolliculated in OR2 with fine forceps and allowed to recover for 1 day before injection. Oocytes that were in any way damaged by nicking or tearing were discarded.

### **Microinjections and transfection**

For oocyte microinjections: Capped messenger RNA was transcribed *in vitro* (Sive *et al.*, 2000) and 2 ng was injected per oocyte in a volume of up to 20 nl.

Oocytes were allowed to recover for 4 hours before injection of 4  $\mu$ Ci of  $^{35}$ S-methionine (Express Protein Labeling Mix, NEN) in a volume that did not exceed 40 nl total. Injected oocytes were cultured for 24 hours in 96-well plates filled with 200  $\mu$ l of OR2 per 5 oocytes. All samples were run in duplicate for each experiment.

For embryo microinjections: Capped messenger mRNA was transcribed as above, or by using the mMessage mMachine SP6 kit (Ambion). Varying concentrations were injected in volumes ranging from 5-10 nl at the two-cell stage, into both blastomeres for animal cap experiments or into one cell of two for whole embryo experiments. *X-ngr-1* was injected at 100 pg per embryo, *XNeuroD* was injected at 500 pg per embryo. *Noelin-1* or *-2* were injected at a range from 50 pg-1.5 ng or as indicated in the text. *Noggin* was injected at a range of 50-100pg per embryo. Embryos were cultured until the indicated stage in 0.1 X MMR and fixed for 1 hour in MEMFA, then stored in 100% ethanol until further use.

For COS-cell transfections: Cells were grown to 50-80% confluence before transfecting. DNA and Lipofectamine (Gibco) were prepared:

8  $\lambda$  Lipofectamine

92  $\lambda$  OptiMem (Gibco) in a sterile tube per sample to be transfected

1-2  $\gamma$  DNA in 100  $\lambda$  OptiMem (total volume)

DNA and Lipofectamine were mixed and incubated at room temperature for 15 to 45 minutes to form liposomes. Cells were rinsed with 2 ml OptiMem solution (serum free). DNA + Lipofectamine mix was added to 800  $\lambda$  OptiMem and this lipofection mixture was added to the cells and incubated at 37°C with 5% CO<sub>2</sub> for

approximately 5 hours. After the transfection incubation period, 1 ml DMEM with double strength serum (20% for COS-7) was added and the cells were incubated at 37°C with 5% CO<sub>2</sub> for 24 hours and then processed for staining with anti-*flag* M2 antibody (Sigma).

DNA constructs used were: *Noelin-1-flag* (as described in Barembaum *et al.*, 2000) or  $\beta$ -*galactosidase* subcloned into the pCI-neo expression vector (Invitrogen).

## **Immunoprecipitation**

Oocyte and supernatant fractions were collected separately. The oocytes were rinsed with 200  $\mu$ l of OR2 to remove any secreted material that might have adhered to the cell surface; this wash was added to the supernatant fraction. Samples were quick-frozen at -80°C until further processing. *In vitro* translated protein was synthesized using the same capped mRNAs in Nuclease-treated Rabbit Reticulocyte Lysate (Promega) according to the manufacturer's instructions.

The oocyte fraction was prepared for immunoprecipitation by pipet trituration of 5 oocytes in 300  $\mu$ l PBS + 1% NP40 + inhibitors (PBSNI; inhibitors: Aprotinin, Leupeptin, Pepstatin; Sigma), centrifugation and then collection of the aqueous phase, which was brought up to 750  $\mu$ l with PBSNI. The supernatant fraction was prepared for immunoprecipitation by bringing up to 750  $\mu$ l with PBSNI. Anti-*myc* antibody (mouse monoclonal antibody 9E10, Santa Cruz Biotechnology) was used at 1:500 for 2 hours at 4°C. Protein A Sepharose (Sigma) was incubated with the antibody-treated samples for 1 hour at 4°C with

rocking; the sepharose beads were then washed three times in PBSNI and resuspended in SDS loading buffer. Samples were boiled for 5 minutes before loading on 8-12% SDS-polyacrylamide gels (Laemmli, 1970). Gels were fixed, amplified with 1M Na-Salicylate (Sigma), dried and exposed overnight at  $-80^{\circ}\text{C}$  with an intensifying screen.

Deglycosylation was performed with Peptide-N-Glycosidase (Promega) according to the manufacturer's instructions. The enzyme is active in SDS sample buffer, so the reactions were done on samples that were already prepared for loading.

### ***Xenopus Noelin* Constructs**

The coding region of *Noelin-1* was amplified using the following PCR primers: upstream primer 5'-CCA TCG ATC CAA GCA AAC ATG TCT GTG CC-3'; downstream primer 5'-GCG GAT ATC AAT TCA TCG GAT CG-3'. *Pwo* polymerase (Roche) and low cycle number (10 cycles of  $94^{\circ}\text{C}$  for 1 minute,  $55^{\circ}\text{C}$  for 45 seconds,  $72^{\circ}\text{C}$  for 45 seconds) were used to minimize error introduction during amplification. Restriction sites embedded in the primers were used to subclone the 1.5 kb PCR product into the pCS2-mt expression vector (Rupp *et al.*, 1994; Turner and Weintraub, 1994) in which five of the 6 *myc* tags were removed by the digestion with *Cla* I and *Nco* I. In some constructs, I found that including six *myc* tags prevented the protein from being secreted. The constructs were verified to be in frame and without PCR-induced mutation by sequencing.

In order to subclone sequences encoding the amino acids SDEL or KDEL at the amino terminus of these constructs, oligonucleotides flanked by *Xho* I sites

were synthesized (Integrated DNA Technologies) and treated with Polynucleotide Kinase (Roche) to add 5' phosphate groups. Duplex oligonucleotides were then prepared by mixing at a 1:1 ratio of top and bottom strand oligos, denaturing at 95°C and cooling slowly to room temperature. Annealed oligo duplexes were then ligated into the *Xho* I site in pCS2+*Noelin-1*-mt that occurs just after the *myc* tag. Oligo sequences were: SDEL top strand: 5'-TCG AGT CAG ATG AAC TGT AGC-3'; SDEL bottom strand: 5'-TCG AGC TAC AGT TCA TCT GAC-3'; KDEL top strand: 5'-TCG AGA AAG ATG AAC TGT AGC-3'; KDEL bottom strand: 5'-TCG AGC TAC AGT TCA TCT TTC-3'. Subclones were verified to be in frame with the preceding *Noelin-1-myc* region by sequencing.

## **DiI injections**

Vitelline membranes of early neurula embryos (stages 13-15) were removed and embryos were allowed to recover in 1 X MMR before injection at stage 17 with Cell Tracker CM DiI (Molecular Probes). CM DiI was prepared by dissolving one tube in 10 µl of 100% ethanol, to which 90 µl of fresh 10% sucrose was then added. The mixture was centrifuged prior to loading in the needle to minimize clogging. Less than 3 nl was injected into several positions along the neural folds, usually in three locations on each side of the embryo. Embryos were cultured until approximately stage 33 in 0.1 X MMR. Embryos were fixed in MEMPFA (fresh paraformaldehyde improved DiI fixation) for 3-4 hours to ensure that the DiI was well fixed. This resulted in lower signal for *in situ*

hybridization, but fix time could be reduced although with some loss of DiI signal.

### ***In situ* Hybridization and Immunohistochemistry**

*In situ* hybridization was performed as described in (Knecht *et al.*, 1995), except that only embryos hybridized to *N-tubulin* were treated with RNaseA and T1 to eliminate signal in ciliated epidermal cells. For sectioning, embryos were embedded in wax: embryos were dehydrated to 100% ethanol, then washed 2 X 20 minutes in HistoSol (National Diagnostics), 1 X 1 hour Paraplast Plus wax (Oxford) at 60°C, followed by an overnight incubation in wax. Embryos were embedded in fresh wax and sectioned on a Leitz microtome at 10 µm. Sections to be immunostained were dewaxed and rehydrated, then stained with 1:500 anti-*myc* antibody (IgG; 9E10, Santa Cruz Biotechnology) or 1:1 HNK-1 supernatant (IgM; American Type Culture Collection). The primary antibodies were detected with Alexa 488 goat anti-mouse IgG or IgM (Molecular Probes) as appropriate at 1:1000. Transfected COS-7 cells were fixed for 20 minutes in 4% paraformaldehyde in PBS and the stained with anti-*flag* M2 antibody (Sigma) at 10 g/ml and detected with goat-anti-mouse IgG Hi-FITC secondary antibody (Antibodies, Inc.) at 1:300 dilution. Fluorescence and bright field images were visualized on a Zeiss Axiophot and images were captured on an Apogee digital camera.

## RT-PCR Analysis

Pools of total RNA from 2 embryos or 10 animal caps were isolated by Proteinase K treatment (ICN Pharmaceuticals; 250 µg/ml in 20mM Tris, 100mM NaCl, 30mM EDTA, 1% SDS) for 1 hour at 37°C. DNA was removed by treatment with RNase-free DNase I (Roche) for 1 hour at 37°C. First strand cDNA was synthesized on RNA from 5 animal cap equivalents using Superscript II Reverse Transcriptase (Life Technologies) with random hexamers according to manufacturer's instructions. The amount of cDNA synthesized in experimental samples was normalized for EF1α using a PhosphorImager and ImageQuant software (Molecular Dynamics). All RNA samples were tested for genomic DNA contamination in minus-reverse transcriptase reactions. The linear ranges of amplification for each primer set was determined using cDNA representing 0.005 of a whole embryo for each reaction (roughly equivalent to 0.25 of 1 animal cap explant), at the stage for which the animal caps were to be analyzed. PCR reactions were performed in 1 X PCR buffer: 10mM Tris-HCl pH 8.3, 1.5mM MgCl<sub>2</sub>, 50mM KCl; with 0.5µCi [ $\alpha$ -<sup>32</sup>P]-dCTP, 100µM each nucleotide, 0.8µM each primer and 1.5 units Taq polymerase. Cycle conditions used were: (30 seconds at 94°C, 1 minute at 55°C, 1 minute at 72°C) for the cycle number indicated below; preceded by a 5 minute denaturation at 94°C and followed by a 6 minute extension at 72°C. One-third of each reaction was run on a 5% polyacrylamide gel and analyzed autoradiographically and on the PhosphorImager. PCR primer sets and the cycle numbers used for each are listed below:

*EF1α*: (Agiuset al., 2000); 221 nt; 20 cycles  
U: 5'-CCT GAA CCA CCC AGG CCA GAT TGG TG-3'  
D: 5'-GAG GGT AGT CAG AGA AGC TCT CCA CG-3'

*Muscle actin*: (Hemmati-Brivanlou and Melton, 1994); 222 nt; 23 cycles

U: 5'-GCT GAC AGA ATG CAG AAG-3'

D: 5'-TTG CTT GGA GGA GTG TGT-3'

*NCAM*: (Hemmati-Brivanlou and Melton, 1994); 342 nt; 26 cycles

U: 5'-CAC AGT TCC ACC AAA TGC-3'

D: 5'-GGA ATC AAG CGG TAC AGA-3'

*Otx2*: (Sasai *et al.*, 1995); 315 nt; 28 cycles

U: 5'-GGA TGG ATT TGT TGC ACC AGT C-3'

D: 5'-CAC TCT CCG AGC TCA CTT CTC-3'

*En2*: (Hemmati-Brivanlou and Melton, 1994); 302 nt; 28 cycles

U: 5'-CGG AAT TCA TCA GGT CCG AGA TC-3'

D: 5'-GCG GAT CCT TTG AAG TGG TCG CG-3'

*Krox20*: (Mariani and Harland, 1998); 323 nt; 30 cycles

U: 5'-ATT CAG ATG AGC GGA GTG-3'

D: 5'-ATG TGC TCC AGG TCA CTT-3'

*HoxB9*: (Hemmati-Brivanlou and Melton, 1994); 217; 28 cycles

U: 5'-TAC TTA CGG GGC TTG GCT GGA-3'

D: 5'-AGC GTG TAA CCA GTT GGC TG-3'

*Synaptobrevin II*: (Knecht *et al.*, 1995); 307 nt; 30 cycles

U: 5'-ATT TGT CTG TGC GCA GGT-3'

D: 5'-TTT AAG CCA CTC CCT GCT-3'

*NeuroD*: (Lallier and DeSimone, 2000); 238 nt; 30 cycles

U: 5'-GTG AAA TCC CAA TAG ACA CC-3'

D: 5'-TTC CCC ATA TCT AAA GGC AG-3'

Primer set designed for this study:

*XBrn3d*: 277 nt; 28 cycles

U: 5'-CAT CAC CCT TCT GTT TTA-3'

D: 5'-GGG TCT GTT TCA CTT TCA-3'

## RESULTS

### ***Noelin-1* and -2 sequence and structure**

*Xenopus Noelin-1* and -2 were cloned from a tailbud stage (stage 28, Nieuwkoop and Faber, 1967) head cDNA library. These isoforms vary only in their differential usage of upstream promoters, synthesizing BMZ (*Noelin-1*) or

AMZ (*Noelin-2*) (see Fig. 1A, boxed upper right for splicing schematic of the four *Noelin* isoforms). The nucleotide and predicted protein sequences are shown in Fig. 1A. *Noelin-1* and *-2* both contain predicted signal peptides (red underlines), several N-linked glycosylation sites (black arrowheads), potential hyaluronate binding sites (black underlines), and a glycosaminoglycan initiation site (gray underline). *Noelin-1* and *-2* proteins are approximately 92% identical to the chick counterparts; the proteins are also globally similar to Olfactomedin, with *Noelin-2* being slightly more related overall because of a shorter 5' exon region that requires fewer gap insertions on the alignment. *Noelin-1* and *-2* share approximately 29% overall identity (44% similarity) to Olfactomedin.

Furthermore, the *Noelin* Z region contains an Olfactomedin domain (yellow underline). Several important structural features are conserved between *Noelin* and Olfactomedin in this domain, including three glycosylation sites (arrowheads, Fig. 1A) and three spatially conserved cysteine residues, one within the Olfactomedin domain and two that lie outside of the Olfactomedin domain (green asterisks in Figs. 1A and B). In Olfactomedin, these latter two residues may form intermolecular disulfide bonds that create oligomers in the extracellular matrix (Yokoe and Anholt, 1993).

The Olfactomedin-related family includes *Noelin* homologues, MYOC/TIGR (Stone *et al.*, 1997), and the  $\alpha$ -Latrotoxin receptor (Davletov *et al.*, 1996); all are more highly conserved in the Olfactomedin domain, and share 42-48% identity to *Xenopus* *Noelin* (Fig. 1B). Olfactomedin has 32% identity within the Olfactomedin domain (51% similarity) to *Xenopus* *Noelin*. An alignment of the *Noelin* Olfactomedin domain with that of Olfactomedin and related proteins is shown in Fig. 1B. The presence of the Olfactomedin domain and other regions

of homology between *Noelin* and Olfactomedin suggest that the two may share some features, such as extracellular location, glycosylation, and polymerization.

### **Noelin-1 is a secreted glycoprotein**

The A and B regions of the Noelin isoforms contain hydrophobic sequences at their amino termini (see Fig. 1A, red underline). Such sequences can mediate either localization in the cell membrane or secretion, depending upon whether the signal is cleavable. A computer modeling method (<http://www.cbs.dtu.dk/services/SignalP>; Nielsen *et al.*, 1997) predicts the translated sequences to be cleaved: in the A region after residue #16 in the sequence TMA-MI; and in the B region after residue #26 in the sequence VLP-TN (see red arrowheads, Fig. 1A).

In order to examine the subcellular localization of *Noelin-1*, a *flag*-tagged quail *Noelin-1* construct (described in (Barembaum *et al.*, 2000) was transfected into COS cells. Transfected cells were stained with anti-*flag* antibody and Noelin-1-*flag* protein was found in the endoplasmic reticulum (ER, Fig. 2B). The protein was not observed in the nucleus or the cell wall. This was similar to results that had been previously described for rat and mouse *Noelin-1* (Danielson *et al.*, 1994; Nagano *et al.*, 1998). However, one group described Noelins as restricted to the ER and not in the Golgi apparatus (Nagano *et al.*, 1998). I observed Noelin-1-Flag protein in a matrix of fibrous and punctate material throughout cultured cells, suggesting that both ER and Golgi contained Noelin-1-*flag*.

The carboxy terminus for Noelin-1 and -2 (Z region) encodes the sequence Ser-Asp-Glu-Leu (SDEL) that is similar but not identical to the consensus

sequence Lys-Asp-Glu-Leu (KDEL), the consensus sequence for protein retention in the endoplasmic reticulum (ER) of vertebrate, *Drosophila*, *C. elegans* and plant cells (Munro and Pelham, 1987). Proteins containing the retention signal at their carboxy termini are selectively retrieved from post-ER compartments so that they permanently reside in the ER instead of being secreted along with proteins that do not contain the signal. Previous authors have described Noelins as ER-localized proteins based on sequence interpretation and observation of immunostained cells (Danielson *et al.*, 1994; Nagano *et al.*, 1998).

To determine whether the *Xenopus Noelin-1* putative signal peptide is cleavable *in vivo* and whether the protein would be retained in the ER, I performed *in vivo* secretion assays by expressing *Noelin-1* mRNA in *Xenopus* oocytes. Three different single-*myc* tagged constructs of *Noelin-1* were prepared (see Fig. 3A schematic). *Noelin-1-myc* includes a *myc* epitope at the carboxy terminus which blocks the endogenous Noelin SDEL sequence from any receptors. *Noelin-1-myc-SDEL* contains the natural Noelin-1 carboxyl terminal sequence subcloned after the *myc* tag, since any ER retention signal must be available at the extreme carboxyl terminus for binding to the retrieval receptors (Munro and Pelham, 1987). *Noelin-1-myc-KDEL* includes the consensus ER localization sequence after the *myc* tag. All three constructs were synthesized using only a single *myc* tag as it was found that including six *myc* tags inhibited the secretion of Noelin-1 (data not shown).

The *Noelin-1* constructs were microinjected into oocytes with <sup>35</sup>S-methionine and the oocyte and culture supernatant were analyzed by immunoprecipitation. After expression in *Xenopus* oocytes, Noelin-1-*myc* protein was robustly secreted. The secreted form of the protein appeared as a high

molecular weight complex (Fig. 3B, lane 3 arrowhead, compare to core size *in vitro*-translated (IVT) in lane 1). This species, along with a smaller, specifically immunoprecipitated band, was recognized in oocyte fractions of Noelin-1-myc injections (arrow, lane 2). I next tested whether the sizes of the proteins in the oocyte and supernatant fractions were larger than core size due to glycosylation, by treatment of the samples with a deglycosylating enzyme. All specifically immunoprecipitated proteins in the oocytes and supernatant (lanes 2 and 3) were reduced to a core size (lanes 4 and 5) equivalent to that of *in vitro*-translated protein (IVT, lane 1), demonstrating that Noelin-1-myc was glycosylated.

Noelin-1-myc-SDEL, which mimics the natural carboxy terminal sequence of Noelin-1, was secreted but to a lesser degree than Noelin-1-myc (Fig. 3C, arrowhead, lane 3). This suggests that the endogenous SDEL sequence may act as a suboptimal retrieval signal, allowing some of the protein to be secreted but retaining a significant proportion within the cell. As with Noelin-1-myc, the higher molecular weight species was present in both the oocytes and the supernatant of the Noelin-1-myc-SDEL construct (lanes 2 and 3, arrowhead), while the intermediate form of the protein was present only in the oocytes (lane 2, arrow). Additionally, upon deglycosylation, the proteins collapsed to the predicted core size (lanes 4 and 5; IVT in lane 1).

As expected, the control construct Noelin-1-myc-KDEL was not secreted (Fig. 3D), indicating that the oocytes recognized the retention signal and properly retained this protein. Importantly, oocytes expressing this construct did not exhibit the higher molecular weight band that is characteristic of the secreted constructs (see Fig. 3D lanes 2 and 3), but only contained the intermediate-size protein (arrow, lane 2). This implies that the protein did not

move far enough through the Golgi apparatus to become as highly glycosylated as the secreted constructs did, and provides additional confirmation that the KDEL sequence caused all of the protein to be retrieved to the ER while the SDEL sequence did not. Deglycosylation of this sample collapsed the band down to the core size (lane 4 compared to IVT in lane 1). A secretion control sample using *myc*-tagged Noggin showed that oocytes secreted and glycosylated this construct as expected (Fig. 3F). The data show that the Noelin-1 protein is glycosylated, contains a cleavable signal sequence, and that the putative ER localization signal is not sufficient to retain all of the protein within the ER.

In order to determine whether Noelin-1 protein could form large complexes similar to those described for Olfactomedin, immunoprecipitated oocyte and supernatant samples were run under non-reducing conditions. This allows intra- and intermolecular disulfide bridges to remain intact and reveals whether protein complexes have formed. The complexes formed by Noelin-1 in cultured oocytes and supernatant were so large that they did not run through a 9% resolving gel, but rather remained at the top, larger than the 200kD molecular weight marker, indicating the presence of high molecular weight complexes (Fig. 3E, oocytes in lane 2, supernatant lane 3; compare to IVT in lane 1). No proteins were specifically immunoprecipitated in uninjected control oocytes or supernatant (Fig. 3G). It is possible that the protein homopolymerizes by intermolecular disulfide bonding or that it forms complexes with other proteins. Similar multimerization has been observed for Olfactomedin in the extracellular matrix (Yokoe and Anholt, 1993), suggesting this may be a conserved feature of the two proteins. Thus, Noelin-1 is a secreted glycoprotein that forms high molecular weight complexes in *Xenopus* oocytes.

## Expression pattern of *Xenopus Noelin-1* and *-2*

*Xenopus Noelin* isoforms 1 and 2 were present in a stage 28 library from which they were isolated; expressed sequence tags containing the Z exon have also been found in a *Xenopus* oocyte cDNA library (GenBank accession numbers AW199780 and AW199284). In order to characterize the expression of *Noelin-1* and *-2* in greater detail, *in situ* hybridization using the A, B and Z exons was performed (see Fig. 1A box for isoform schematic). Signals from the A exon alone (found in *Noelin-2* and *-4*), or the B exon alone (found in *Noelin-1* and *-3*) were always present wherever Z expression was found, suggesting that *Noelin-1* and *-2* have identical expression patterns. Therefore, I used the Z exon to represent the expression patterns of both *Noelin-1* and *-2*. Expression of the Y isoforms *Noelin-3* and *-4* will be reported elsewhere.

*Noelin-1* and *-2* expression was predominantly observed in neurogenic tissues (Fig. 4). The earliest transcript expression was seen just after neural tube closure at approximately stage 21. Positive cells were located in the spinal cord and in the olfactory placode and profundal-trigeminal regions of the developing cranial sensory ganglia (V, Fig. 4A). The neural tube did not express the Z exon in brain regions, but signal was visible posteriorly as two punctate stripes of positive cells along each side of the spinal cord (Fig. 4A and E) that appears to correlate with the segmental development of neurons (see Hartenstein, 1993). At stage 27, the olfactory placode, V<sup>th</sup> (trigeminal) and VII<sup>th</sup> (facial nerve and geniculate) ganglia, the pineal gland, and cells of the spinal cord expressed the Z exon (Fig. 4B). By stage 33, intense signal was found in these regions and in the brain (Fig. 4C). By stage 35, the IX<sup>th</sup> and X<sup>th</sup> ganglia also expressed *Noelin-1* and

-2 (Fig. 4D). Also at stage 35, a few cells expressed *Noelin-1* and -2 in the branchial arches that may be of neural crest origin (arrowhead, Fig. 4D). Within the developing brain, Z exon transcripts were not detected until stage 25 in a small number of medially-located cells that are likely to be interneurons (data not shown). With increasing age, the signal in the brain became more widespread and intense rostrally. No signal was observed in the brain at stage 22 (Fig. 4E); however, staining extended into the midbrain by stage 27 (Fig. 4F) and through the forebrain by stage 33 (Fig. 4G).

### *Cranial expression of Noelin*

I next examined the cranial expression of *Noelin-1* and -2 in cross-sections. At stage 21, the Z exon was observed in the trigeminal ganglion maxillary and mandibular components (Fig. 5A and B, arrowheads) and in the olfactory placode (data not shown), but not in the eye, cranial neural tube, or other cranial ganglia. At stage 25, expression was observed in the olfactory placodes (arrowheads, Fig. 6B) trigeminal ganglia (V<sup>th</sup>, arrows in Fig. 6C and D) and in a few cells in the midbrain adjacent to the mandibular trigeminal lobe (Fig. 6D). In the hindbrain region, *Noelin-1* and -2 were expressed in the geniculate ganglion (VII<sup>th</sup>, arrow in Fig. 6E) and in the marginal zone of the hindbrain near the geniculate ganglion.

At stage 35, more neurogenic tissues were positive for *Noelin-1* and -2. Some but not all cells in the pineal gland expressed *Noelin-1* and -2, with more than half of pineal cells positive in some regions (Fig. 7A). In the PNS, the trigeminal ganglia and olfactory placodes were the first structures to express the Z exon at stage 21. At stage 35, all of the cranial sensory ganglia expressed

*Noelin-1* and *-2*: V<sup>th</sup> and VII<sup>th</sup> (trigeminal and facial nerve/geniculate ganglion, Fig. 7C), VIII<sup>th</sup> (facial-acoustic, Fig. 7B), IX<sup>th</sup> (glossopharyngeal, Fig. 7B, E) and X<sup>th</sup> (vagal, see Fig. 4D). In addition, cells in the retinal ganglion and inner nuclear layers of the developing eye were stained (Fig. 7D).

Cranial sensory ganglia are peripheral nervous system (PNS) structures, many of which are comprised of both epidermal placode- and cranial neural crest-derived cells. Neurogenic placodes develop from the early ectoderm as regional thickenings and contribute many neurons to the cranial sensory ganglia (see Baker and Bronner-Fraser, 2001 for review). *Noelin-1* and *-2* did not mark the cranial placodes themselves but only the ganglia that are derived from them. It is difficult to discern whether *Noelin-1* and *-2* were expressed in lateral line ganglia in the head; in *Xenopus* these ganglia are fused with the branchiomic nerves (see Schlosser and Northcutt, 2000).

#### *Trunk expression of Noelin-1 and -2*

To determine precisely which cells in the spinal cord express *Noelin-1* and *-2*, I examined transverse sections of various embryonic stages. *Xenopus* embryos develop a simple primary nervous system before metamorphosis that directs motor responses to sensory input. Three stripes of primary neurons are found on each side of the neural plate and later within the neural tube corresponding to motor (ventral), inter-(medial) and sensory (dorsal) neurons (reviewed in Chitnis, 1999). Within the spinal cord, the *Noelin*-positive cells were found in the marginal zone where neurons are beginning to differentiate and not in the ventricular zone where undifferentiated neuroblasts divide.

The earliest *Noelin-1* and *-2*-positive cells found in the spinal cord at stage 21 were in the proper position to form interneurons and motor neurons, since Rohon-Beard cells (sensory neurons) are located more dorsally than the cells that contained *Noelin* transcripts (arrows, Fig. 5C). By stage 25, more populations of cells were positive for the Z exon at different levels of the spinal cord; some sections revealed dorsal and intermediate cells to be positive, while others showed intermediate and ventral positive cells (Fig. 8B-E).

Embryos at stage 28 exhibited similar staining for *Noelin* Z exon in the spinal cord (arrowheads, Fig. 9A and C). The carbohydrate epitope antibody HNK-1 recognizes neurons in amphibian spinal cord (Nordlander, 1989); immunostaining with this antibody showed co-localization of mRNA for the Z exon and the antibody signal in these sections (arrowheads, Fig. 9B and D). HNK-1 staining was generally found in wider regions than *Noelin-1* and *-2* transcripts, indicating that *Noelin-1* and *-2* were not expressed by all developing neurons at these stages. At stage 33, most cells in the marginal zone of the ventral spinal cord were positive for *Noelin* (Fig. 9E). Furthermore, at stage 35, a gradation of signal from dorsal to ventral was observed, with dorsal expression being the strongest. Interestingly, neural crest cells migrating into the fin were also found to express *Noelin-1* and *-2* beginning at stage 35 (arrow, Fig. 9F).

In contrast to the distribution pattern of the homologous chick *Noelin* isoforms (Barembaum *et al.*, 2000), *Xenopus Noelin-1* and *-2* were not found in neural plate stages, premigratory or migratory neural crest cells (except at fairly late stages in the fin mesenchyme). Thus, the *Xenopus Noelin-1* and *-2* expression pattern is similar to the later chick distribution, but *Xenopus* lacks the corresponding early expression in neural tissues.

## Origin of *Noelin*-positive cells in the cranial ganglia

I next examined the population of cells in the cranial sensory ganglia that express *Noelin-1* and -2. Most of the cranial sensory ganglia are made up of both placodal and neural crest cells. *Xenopus* embryos contain two main bodies of cranial neural crest cells, lateral and medial (see Sadaghiani and Thiebaud, 1987). The lateral neural crest forms in large masses outside the boundary of the neural plate, very close to the placodal ectoderm (see schematic, pink region in Fig. 10A). These cells generally migrate as a group, mainly contributing to distal derivatives in the branchial arches (A. Collazo, C. LaBonne, M. B.-F. and S. Fraser, in preparation). A smaller medial cranial neural crest population exists as part of the neural folds relatively distant from the placodes (red dots in Fig. 10A) and migrates slightly later than the lateral crest cells, also contributing to the cranial ganglia and other head structures.

To address whether the *Noelin-1* and -2-expressing cells in the cranial ganglia are derived from medial neural crest cells, premigratory medial neural crest cells were labeled by focal injection with DiI at stage 17, and the embryos were allowed to develop to stage 33 when they were fixed and processed for *in situ* hybridization with the Z exon. DiI-positive cells were found in the neural tube, epidermal ectoderm and migrating neural crest cells. Neural crest cells containing DiI were found in the head mesenchyme, branchial arches and in the regions surrounding cranial ganglia V, VII, VIII and IX (see Fig. 10). DiI-positive cells were found closely approximating the cranial ganglia, but not mixed within the ganglia except in sections that passed through their margins (data not shown). To control for the possibility that placodal ectoderm was inadvertently

labeled, some embryos were fixed after a short recovery period and processed for *in situ* hybridization against *Xenopus Brn-3r*, a gene which is expressed in placodes and sensory neurons of the cranial ganglia but not in neural crest cells (O. Akin, M. B.-F. and C. LaBonne, in preparation), and which has the same expression pattern as the closely-related gene *XBrn-3d* (Hutcheson and Vetter, 2001). *XBrn-3r* expression did not overlap with DiI signal, showing that the placodes were not labeled in these experiments (data not shown).

Transverse sections of DiI-labeled embryos hybridized to the Z exon showed that the main bodies of the cranial ganglia are strongly positive for *Noelin-1* and *-2* (Fig. 10B, D). However, no DiI positive neural crest cells were found within this population (Fig. 10B-C, D-F). Instead, the DiI-positive neural crest cells surrounded the ganglia and failed to express *Noelin-1* and *-2*. While I cannot exclude the possibility that the earlier-migrating lateral neural crest contributed cells to the ganglia which then later expressed the Z exon, my data suggest that the later-migrating medial neural crest cells probably contribute a greater amount of the neural crest proportion of the cranial ganglia. These data indicate that later migrating medial neural crest cells do not express *Noelin-1* and *-2* or enter the ganglia at least before stage 33/34, and that *Noelin-1* and *-2* expression at earlier stages is in placode-derived ganglion cells.

### ***Noelin-1* and *-2* are up-regulated by neurogenic genes**

Since the expression of *Xenopus Noelin-1* and *-2* isoforms commences well after the time of neural induction and since its distribution correlates with neuronal differentiation, I examined whether *Noelin-1* and *-2* could be

downstream of the neurogenic cascade. The proneural gene *X-ngnr-1* (Ma *et al.*, 1996) and the neural determination gene *XNeuroD* (Lee *et al.*, 1995) cause ectopic neurogenesis in the non-neural ectoderm of embryos when they are over-expressed. This ectopic neurogenesis induces *N-tubulin* expression, among other neural and neuronal markers (Lee *et al.*, 1995; Ma *et al.*, 1996).

To test whether *Noelin-1* and *-2* were downstream of these neurogenic genes, I over-expressed *XNeuroD* or *X-ngnr-1* and then looked for effects on *Noelin-1* and *-2* expression by *in situ* hybridization. *Noelin-1* and *-2* were dramatically up-regulated in the ectopic neurons that were induced in the skin of embryos expressing these genes (*X-ngnr-1* effects shown in Fig. 11A, B). It is interesting to note that in these experiments, sibling embryos expressing either neurogenic gene appeared to have a greater number of ectopic *N-tubulin*-positive cells than *Noelin-1* or *-2* positive cells, suggesting that *Noelin-1* and *-2* mark a subset of the neurons induced by these neurogenic genes (compare Fig. 11C with A and B).

Over-expression of *X-ngnr-1* or *XNeuroD* also causes an excess of neural tissue to form in the head. This tissue is thought to differentiate early, thus bypassing normal patterning in the region of ectopic expression. For example, embryos over-expressing *XNeuroD* fail to form eyes in many cases and do not express *Pax-6* in the affected tissue (Hirsch and Harris, 1997); while in sibling embryos, *N-tubulin* is highly expressed. Upon examination with a probe to the Z exon, I found that *Noelin-1* and *-2* were up-regulated in regions of this extra tissue as well, further supporting a role for this gene in neuronal differentiation (Fig. 11A).

I next examined whether *Noelin-1* and -2 could be directly activated by the neurogenic genes in the absence of other tissue interactions by performing animal cap explant experiments. Animal caps from late blastula stage embryos are considered to be relatively naïve ectoderm that will differentiate into epidermis if cultured alone. I isolated animal cap ectoderm from blastula-stage embryos over-expressing either *X-ngnr-1* or *XNeuroD*, cultured the caps to tailbud stages and then looked for expression of *Noelin-1* and -2. It was previously shown that *X-ngnr-1* and *XNeuroD* induce neurogenesis directly (without mesoderm induction) in animal caps; *X-ngnr-1* causes induction of *N-tubulin* expression (Ma *et al.*, 1996) and *XNeuroD* causes induction of NCAM (Lee *et al.*, 1995). In my experiments, *X-ngnr-1* and *XNeuroD* induced *Noelin-1* and -2 expression (Fig. 11D), but the response was quite weak compared to the more robust induction that is seen for *N-tubulin* in the animal cap explants (Fig. 11E) or for *Noelin-1* and -2 and *N-tubulin* in whole embryos expressing *X-ngnr-1* (Fig. 11A, B). Animal caps injected with  $\beta$ -galactosidase did not express *Noelin-1* and -2 (Fig. 11F) or *N-tubulin* (Fig. 11G). Thus, *Noelin-1* and -2 are responsive to neurogenic signals but probably require input from other genes or inducers to be highly expressed.

### ***Noelin-1* promotes neurogenesis in a neural context**

I next examined the function of *Noelin-1* and -2 by over-expression, alone and in combination with other neuralizing factors. Over-expression of either *Noelin-1* or -2 alone had no obvious phenotype. Embryos injected with varying doses in various locations did not display any overt morphological

perturbations. The size and location of the major central nervous system structures such as brain, eye, and spinal cord, appeared normal. Neural crest-derived branchial arches and melanocytes also appeared normal in size, position and number. To show that the injected mRNA produced protein that persisted to tailbud stages, I performed immunohistochemistry for the *myc* epitope in *Noelin-1-myc*-injected embryos and found that the protein was expressed at least until stage 25 (data not shown). *In situ* hybridization analysis with a panel of neural and neural crest markers did not reveal any effects on marker gene expression patterns for: 1) the pan-neural marker *Sox-2* (Mizuseki *et al.*, 1998); 2) the neuronal differentiation marker *N-tubulin* (Oschwald *et al.*, 1991); 3) the early neural crest marker *XSlug* (Mayor *et al.*, 1995); 4) later neural crest marker *XTwist* (Hopwood *et al.*, 1989); 5) the sensory neuron marker for spinal cord and cranial ganglia *XBrn-3r* (O. Akin, M. B.-F. and C. LaBonne, in preparation); 6) the interneuron marker *Pax-2* (Heller and Brandli, 1997) or 7) *Noelin-1* and *-2* (data not shown).

I next tested whether *Noelin-1* might function synergistically with neuralizing factors. When exposed to the BMP antagonist Noggin either by addition of protein or by expression of *noggin* mRNA, animal caps are induced to express the general neural marker *NCAM* and make tissue characteristic of forebrain, expressing the marker *Otx2* (Lamb *et al.*, 1993). However, these explants do not express general neuronal differentiation markers such as *N-tubulin* or *SynaptobrevinII* until late tailbud/early tadpole stages, reflecting the timing of neuronal differentiation in normal embryos in which forebrain becomes positive for these differentiation markers at around stage 33 (Lamb *et*

*al.*, 1993; Ferreiro *et al.*, 1994; Knecht *et al.*, 1995; Papalopulu and Kintner, 1996; Messenger *et al.*, 1999; Lallier and DeSimone, 2000).

Animal caps co-expressing both the neural inducer *noggin* and *Noelin-1* were cultured to stages 24 and 27. In whole mount *in situ* hybridization assays, *N-tubulin* expression was activated by stage 24 in animal caps that were expressing both *noggin* and *Noelin-1*, but not in explants expressing either gene alone as shown in Figs. 12A and 12B. Neurons differentiated in a scattered manner in the *Noelin-1 + noggin* animal caps, rather than converting the entire explant into a neuronal domain (Fig. 12C). This effect was reproduced in three separate experiments, with as few as 50% of explants expressing *N-tubulin* (3/6 at stage 24) and up to 14/17 (82%) of explants expressing *N-tubulin* at stage 27 (shown in Fig. 12). Thus, although *Noelin-1* over-expression alone has no apparent phenotype, *Noelin-1* promotes early neurogenesis in animal cap tissue that has been neuralized by *noggin*.

### ***Noelin-1* induces sensory neural markers and early differentiation**

To further investigate the role of *Noelin-1* during neuronal development, I examined relative levels of gene expression in animal cap explants that were injected with *Noelin-1*, *noggin*, or both, by performing reverse-transcriptase polymerase chain reaction (RT-PCR) assays on the explants. *Noelin-1 + noggin* induced the neuronal differentiation marker *SynaptobrevinII* (*SybII*, Knecht *et al.*, 1995) by stage 24 (Fig. 13A). This is consistent with our findings of early neuronal differentiation based on *in situ* hybridization results on whole animal caps with the *N-tubulin* marker. *Noelin-1 + noggin* did not induce expression of

more posterior neural markers such as *En-2* (expressed in the midbrain-hindbrain border, Hemmati-Brivanlou *et al.*, 1991), *Krox-20* (hindbrain marker, Bradley *et al.*, 1993), or *HoxB9* (spinal cord marker previously known as *XlhBox6*, Wright *et al.*, 1990) in the explants. In contrast, *Noelin-1* alone could induce *Krox-20* and very low levels of *HoxB9* and the forebrain marker, *Otx2* (Blitz and Cho, 1995), whereas it was not sufficient to induce the general early neural marker NCAM (Kintner and Melton, 1987), or *En-2* expression. Therefore, the early neuronal differentiation observed in *Noelin-1 + noggin* animal caps was not due to posteriorization of the forebrain-character neural tissue that was induced by *noggin*, although alone *Noelin-1* expression of some posterior markers.

I next wished to determine whether secretion of Noelin-1 was required for its function in promotion of neuronal differentiation. Our *in vivo* secretion assay showed that the endogenous form of Noelin-1 protein was secreted, although a significant portion of the synthesized protein remained within the oocyte fraction, probably inside the ER. I expressed *Noelin-1-myc* (a robustly secreted form), or *Noelin-1-myc-KDEL* (exclusively ER-localized form), or the endogenous form of *Noelin-1*, with or without *noggin*, to compare their activities in our animal cap assay. Induction of early neuronal differentiation was seen at stage 24 by activation of *SybII* expression from all three constructs (Fig. 13B, *SybII* row, lanes 4, 6, 8); however, the robustly secreted *Noelin-1-myc* caused the greatest induction of *SybII*. Quantitation of *SybII* data in Fig. 13B revealed that *Noelin-1 + noggin* or *Noelin-1-myc-KDEL + noggin* both caused a 2.4-fold induction of *SybII* expression over *noggin* alone, and *Noelin-1-myc + noggin* caused a 3.3-fold induction over *noggin* alone. Thus the highly secreted construct of *Noelin-1* was able to induce the highest levels of *SybII* expression in the explants, though this

induction was only slightly greater than that produced by the endogenous or non-secreted forms of *Noelin-1*.

In contrast, the secreted forms (endogenous *Noelin-1* and *Noelin-1-myc*) both caused an upregulation of *XBrn-3d* in the explants co-expressing *noggin*, while the non-secreted form did not (Fig. 13B, *XBrn-3d* row, lanes 4 and 6). *Noggin* alone induced *XBrn-3d* to some degree (0.7 fold greater than in control-injected animal caps; lanes 2 and 3), while *Noelin-1* + *noggin* (lane 4) caused a 2.7-fold upregulation of *XBrn-3d* over *noggin* alone, and *Noelin-1-myc* + *noggin* (lane 6) caused a 3.4-fold upregulation. *Noelin-1-myc-KDEL* + *noggin* and *Noelin-1-myc-KDEL* did not induce *XBrn-3d* expression as compared to *noggin* alone (compare lane 3 with 8 and 9). The secreted *Noelin-1* constructs, when expressed alone, induced *XBrn-3d* expression at levels comparable to that of *noggin* alone (lanes 5 and 7).

Interestingly, the well-secreted *Noelin-1-myc* induced strong *XNeuroD* expression in the absence of neuralization by *noggin*, while neither the endogenous *Noelin-1* nor the ER-localized form caused this response (lane 7). I also found that expression of *Noelin-1* alone, in any form, was sufficient to activate robust expression of *Krox-20* (Fig. 13A and B, *Krox-20* row lanes 5, 7, 9), with the secreted form being the best inducer of this marker (lane 7). The ER-localized construct did not have any activity that was not also present in the secreted constructs. Furthermore, forced secretion or ER localization of *Noelin-1* did not change the anterior/posterior character of *noggin*-induced neural tissue. *Noelin-1*, whether retained within the ER or secreted from the cell, promoted the early differentiation of neurons and induce *Krox-20* expression, but only the secreted forms could induce the sensory marker *XBrn-3d* and *XNeuroD*. Thus

the secreted forms of Noelin-1 have added activities that the ER-localized form does not, suggesting that endogenously, the localization of Noelin-1 may be an important determinant of its function.

## DISCUSSION

### ***Noelin-1* promotes neurogenesis in *Xenopus***

My findings suggest that *Xenopus Noelin-1* is involved in neurogenesis. Noelin-1 is a secreted glycoprotein that is first expressed in developing neurons just after neural tube closure, and activated by the neurogenic genes *X-ngnr-1* and *XNeuroD*. *Noelin-1* itself has limited abilities to induce certain neural markers, and in neuralized animal cap explants, *Noelin-1* induces the expression of differentiated neuronal markers much earlier than in the embryo or in animal caps neuralized by *noggin* alone. These results suggest a role for Noelin-1 in promotion of neurogenesis.

### **Developmental role of *Noelin-1***

Chick *Noelin-1* has a striking expression pattern that correlates with the potential of ectodermal cells to later form the neural crest (Barembaum *et al.*, 2000). The correlation of *Noelin-1* expression with the potential to form neural crest and its ability to prolong neural crest emigration *in vivo* are novel and intriguing properties of the protein. Since *Xenopus* embryos are more easily manipulated for functional studies of genes, I investigated the possibility that

*Noelin-1* and -2 were conserved in *Xenopus* and examined their roles in development. My results reveal some interesting similarities and differences in both expression pattern and function. Its secretion and general structure appear very similar in both species. However, while *Noelin-1* appears to function in promoting neural development in both species, it is expressed later in *Xenopus* and, in fact, too late to respond to neural crest induction as in the chick. Instead, it seems to be expressed in response to neurogenic gene activation, and appears to promote a neuronal differentiation program.

### **Olfactomedin and related genes**

*Noelin* sequence is highly conserved among species, with 92% identity to its chick counterpart. Moreover, in the "Olfactomedin domain" which is found in the carboxy-terminal half of the Z region (Barembaum *et al.*, 2000; Kulkarni *et al.*, 2000), *Noelin -1* and -2 proteins exhibit approximately 51% similarity at the amino acid level to Olfactomedin, a protein thought to be involved in facilitating or mediating odorant recognition (Snyder *et al.*, 1991). The tertiary structure of Olfactomedin is predicted to be a polymer of ordered Olfactomedin units that are covalently linked by inter- and intramolecular disulfide bonds (Yokoe and Anholt, 1993). In this model, the N-linked glycosylation sites are apposed to form a network of extracellular matrix material. *Noelin-1* and -2 homologs contain residues in similar positions for disulfide bond formation and glycosylation, suggesting that the tertiary structure could be similar to Olfactomedin in this domain (Karavanich and Anholt, 1998). Additionally, it is likely that *in vivo*, like Olfactomedin, the proteins associate into large, high

molecular-weight complexes based upon the large size of the recombinant proteins under non-denaturing SDS-PAGE conditions. These observations, along with the suggestive conservation of the Olfactomedin domain and disulfide-bridge-forming cysteine residues, imply that the native protein may form a part of the extracellular matrix of cells in which it is made. Its role in promoting neurogenesis may indicate that it acts as an extracellular signal.

In addition to the similarity to Olfactomedin, Noelin-1 and -2 also exhibit sequence similarity to several other recently discovered proteins of diverse function and structure such as the open angle glaucoma locus GLC1A (Stone *et al.*, 1997) also called TIGR by Nguyen *et al.*, (1998) or Myocilin by Kubota *et al.*, (1997) and now designated MYOC; and the black widow spider venom ( $\alpha$  - latrotoxin) receptor protein Latrophilin (Davletov *et al.*, 1996) or CIRL (calcium-independent receptor of  $\alpha$ -latrotoxin, Krasnoperov *et al.*, 1997). These proteins also contain the Olfactomedin domain, as do several unidentified EST sequences (Kulkarni *et al.*, 2000). Currently, there are no data on the function of the Olfactomedin domain.

### **Comparison of *Noelin* Expression Patterns**

In early chick embryos, *Noelin-1* mRNA is distributed throughout the neural plate but is excluded from the midline. At later stages of development, it becomes progressively restricted to the tissues that are capable of giving rise to neural crest cells: the neural folds, the dorsal neural tube, and finally the premigratory and migratory crest. Chick *Noelin-1* mRNA is also found in the cranial placodes, cells of the spinal cord and brain, and anterior regions of the

limb bud. This expression pattern is due to two separate isoforms of *Noelin*, with one differentially expressed isoform (*Noelin-1*) found in the neural crest at early stages and the other (*Noelin-2*) found in the early placodal ectoderm; later in development their expression patterns overlap (Barenbaum *et al.*, 2000). Although homologues of *Noelin* have also been isolated from rat (Danielson *et al.*, 1994) and mouse (Nagano *et al.*, 1998), their early embryonic expression in these species was not documented.

In contrast to the chick, *Xenopus Noelin-1* and *-2* have a later onset of expression correlating with early neurogenesis in the cranial ganglia, eye, brain, and neurons of the spinal cord. Expression is also found in the pineal gland. In the cranial ganglia and spinal cord, the onset of *Noelin-1* and *-2* expression parallels other signs of neuronal differentiation such as axon extension. Onset of *Noelin-1* and *-2* expression in the cranial ganglia correlates with the timing of the first detectable differentiation of neurons in these regions (see Schlosser and Northcutt, 2000). Migrating ganglion cells can be identified just preceding the onset of *Noelin* expression in the VII<sup>th</sup>, IX<sup>th</sup> and X<sup>th</sup> (epibranchial) ganglia, and neurite extension occurs when *Noelin* is highly expressed in these regions. In contrast, expression in the V<sup>th</sup> ganglion (trigeminal) is concurrent with the first appearance of ganglionic cells. Since the time of origin and the location of the profundal-trigeminal placode is separate from that of the epibranchial placodes (termed the dorsolateral placode area by Schlosser and Northcutt), it is likely that the difference in timing of *Noelin-1* and *-2* expression among these ganglia reflects differences innate to the early placodal domains.

*Xenopus Noelin-1* and *-2* are not expressed in early neural tissues, or in premigratory or migrating neural crest (at least until late stages in the fin). The

later expression pattern of avian *Noelins* corresponds to the *Xenopus* pattern, with the exception of the migrating neural crest cells that are positive in the chick. Additionally, in *Xenopus*, neither *Noelin-1* nor *Noelin-2* marks placodal ectoderm as is the case in the chick, nor do they display distinct distribution in placodal versus neural crest cell types. These differences in *Noelin* isoform expression between two species may indicate that the role of *Noelin-1* is not to promote neural crest or neural development in particular, but to participate in neuronal differentiation in general during nervous system development. Alternatively, the varying expression patterns and functions of *Noelin-1* could indicate that the same isoform has different developmental roles in different species, or that avian embryos may have an added function in neural crest generation. Whether avian *Noelin-1* can promote neurogenesis as the *Xenopus* homolog does has not yet been characterized.

#### *The search for Xenopus Noelin-related genes*

In addition to isolating the *Xenopus Noelin* homologs, I also searched for genes related to *Noelin*. This was important because none of the frog *Noelin* isoforms appear to be expressed in the neural crest and since chick *Noelin-1* appears to play an important role in neural crest formation, it was possible that another gene may act as the functional equivalent of chick *Noelin-1* in *Xenopus*. I reasoned that the Olfactomedin domain would make a good probe for this purpose, since it is conserved in many proteins among the vertebrate genomes, and since it could be an important structural domain for the proteins that contain it.

To this end, I screened two cDNA libraries (a neural plate stage and a tailbud stage) and performed Northern blots on a developmental series of RNA from stages 12-31. I used low stringency conditions with a *Xenopus Noelin* Olfactomedin-domain probe to try to pick up any related genes. In all of these screens, the only genes I found to be closely related were the *Noelin* genes themselves (summary of genes clones given in Appendix 1.1). This suggests that the *Noelin* genes are either divergent in function, with the frog gene playing a role in neurogenesis, and the chick gene playing a role in neural crest induction, or that the chick co-opted *Noelin-1* for the neural crest function as a separate mode of operation.

### ***Xenopus Noelin* expression in cranial ganglia**

*Xenopus* cranial neural crest consists of two physically separate populations of cells; the early migrating cranial masses (lateral neural crest) that generally underlie the placodal ectoderm, and a later-migrating population of neural crest cells in the neural folds (medial neural crest; see Sadaghiani and Thiebaud, 1987; Schlosser and Northcutt, 2000). In amniotes, the cranial sensory ganglia consist of proximal and distal lobes, with neural crest cells making up the proximal ganglia and placode cells making up the distal (Baker and Bronner-Fraser, 2001). In contrast, in *Xenopus* embryos, proximal and distal regions of the cranial ganglia are fused (Schlosser and Northcutt, 2000). Thus, it is not possible to describe ganglion cells as crest- or placode-derived based on their positions in the *Xenopus* embryo. Therefore, I labeled premigratory medial

neural crest cells to determine whether they contributed to the *Noelin-1* and -2-expressing cells in the ganglia.

DiI labeling experiments show that *Noelin-1* and -2 are not expressed by the late (medial) neural crest in the cranial ganglia. Medial neural crest cells migrate to the areas surrounding the cranial ganglia but do not enter; rather they remain in proximity and are distinguishable by their positions approximating the ganglia. These later-migrating neural crest cells do not express *Noelin-1* and -2, and do not appear to enter the cranial ganglia until after stage 33/34. Since *Noelin-1* and -2 expression in the cranial ganglia appears fairly uniform at all stages including stages after those that were addressed in the DiI labeling experiments, it is likely that neural crest cells entering the ganglia up-regulate *Noelin-1* and -2 expression once they reach their destination, and that the ganglion cells expressing *Noelin-1* and -2 are placode-derived. Perhaps an autoregulatory loop exists in which neural crest cells that enter the ganglia and contact *Noelin-1* and -2-positive cells (ganglion cells) are induced to begin transcribing the gene themselves and begin neuronal differentiation. Although *Noelin-1* was not able to induce its own expression in whole embryos, it is possible that in the correct context (e.g., presence or balance of cofactors) this mechanism could operate. This idea is supported by the extracellular localization of *Noelin* isoforms, which could allow for cell contact-mediated signaling to occur.

### **Regulation of *Noelin***

Over-expression of *X-ngnr-1* and *XNeuroD* causes premature and ectopic neuronal differentiation (Lee *et al.*, 1995; Ma *et al.*, 1996). These genes also

activate *Noelin-1* and -2 expression. In whole embryos, both isoforms are induced in ectopic neurons induced by expression of these genes. It has been shown that the character of neurons induced by *X-ngnr-1* is sensory in nature (Olson *et al.*, 1998; Perron *et al.*, 1999); accordingly, neurons induced by *X-ngnr-1* do not express the interneuron marker *Pax-2* (Heller and Brandli, 1997). It is likely that *Noelin-1* and -2 expression in these ectopic neurons represents a subclass of sensory type, perhaps similar neurons generated in the cranial ganglia. Additionally, regions of the increased neural tissue in the head induced by *X-ngnr-1* and *XNeuroD* also express *Noelin-1* and -2. *N-tubulin*, among many other markers of neuronal differentiation, is induced in the head regions of embryos injected with these genes. However, the transcription factor *Pax-6* is down-regulated in tissues that would normally express it (Hirsch and Harris, 1997). Thus, genes that may be responsible for patterning neural tissue are down-regulated in favor of neuronal differentiation markers. Since *Noelin-1* and -2 expression is induced in the tissue regions and cells that are undergoing differentiation, a role in neuronal differentiation is further supported.

*Noelin-1* is weakly induced in a more direct test of the effect of neurogenic genes in animal cap explants. *XNeuroD* and *X-ngnr-1* also promote neuronal differentiation in animal caps, in the absence of mesodermally-mediated neural induction. Since *Noelin-1* and -2 up-regulation in whole embryos expressing the same neurogenic genes is much more robust, it seems likely that the expression of *Noelin-1* and -2 requires other signals, either as a result of neural induction or from surrounding tissues that may supply necessary cofactors for their expression.

## Function of *Noelin*

Experiments designed to test the functional capabilities of *Noelin-1* in the chick show that it can affect neural crest development. Alone, neither *Xenopus Noelin-1* nor *-2* detectably affected neural or neural crest development when over-expressed in whole embryos. This lack of effect was not due to protein degradation, since the *myc*-tagged protein, which was assumed to correlate with exogenous *Noelin-1* expression, persisted at least through stage 25 as assessed by *myc*-immunoreactivity. It is possible that cells possess regulatory factors that control the response to exogenous *Noelin-1* and *-2*. Alternatively, it is also possible that increasing *Noelin-1* and *-2* expression has no effect unless levels of another cofactor are also increased. Since any partners to *Noelin-1* and *-2* are as yet unknown, this is a speculation that must be explored. Cofactor requirements have been shown for other genes; for example the proneural gene *XASH-3* promotes neurogenesis much more efficiently in the presence of its binding partner *XE12*. Further, *XASH-3* plus *XE12* activate stable neurogenesis only when expressed in Noggin-treated tissue; otherwise, the effect is transient (Ferreiro *et al.*, 1994).

In neuralized animal cap explants, *Noelin-1* promotes neurogenesis, causing neuronal differentiation markers to be expressed earlier than in neuralized caps alone. By RT-PCR and *in situ* hybridization, *SybII* and *N-tubulin* are induced by stage 24 in animal cap explants co-injected with *Noelin-1* and *noggin*, while in *noggin*-injected animal caps, these markers are not expressed until around stage 33. One way to explain the early differentiation in the explants is that the tissue could have been posteriorized, since neuronal

differentiation occurs much earlier in more caudal regions of the embryo. My results show that posteriorization was not the mechanism for inducing early differentiation, since *Noelin-1*+ *noggin* did not activate the more posterior neural markers *En-2*, *Krox-20*, or *HoxB9*. Further, the induced neurons in *Noelin-1* + *noggin* injected animal caps are likely to be of sensory character, since *XBrn-3d* was upregulated. Accordingly, it seems likely that endogenously *Noelin-1* plays a role in promoting neuronal fate, since in whole embryos it is expressed in developing neurons and it can accelerate neurogenesis in neuralized animal caps.

In addition to promoting neuronal differentiation in neuralized animal caps, my results show that *Noelin-1* itself has limited neural inducing properties. *Noelin-1* expression alone induced *XBrn-3d*, *Krox-20* and *XNeuroD*, without inducing *NCAM* expression. Interestingly, it appears that the secreted form of the protein is required for induction of the sensory marker *XBrn-3d* and *XNeuroD*, while both secreted and ER-localized forms could induce early differentiation (*SybII*) and expression of *Krox-20*. This indicates that the protein may have different functions depending on whether it is outside or inside the cell; inside the cell it functioned to promote general differentiation, when it was secreted it could also direct upregulation of subtype-specific neural markers that in the embryo are expressed before differentiation. The induction of *Krox-20* by all three *Noelin-1* constructs suggests that it is activated by an intracellular *Noelin-1*, since my oocyte secretion assay showed that the secreted forms also are abundantly present inside the cell. Thus cellular localization may play an important role in determining the capability of *Noelin-1* to promote differentiation or fate choices in developing neurons.

Interestingly, in whole animal caps, *N-tubulin* activation in *noggin* + *Noelin-1* samples was not found throughout the explants; rather it was confined to small areas with scattered cells. A similar pattern of neurogenesis was found in animal caps expressing *noggin* + Noradrenaline, where this neurotransmitter caused induction of neuronal differentiation in neuralized animal caps (Messenger *et al.*, 1999). This could be due to mosaic inheritance or uneven distribution of the injected mRNAs. Alternatively, the effect could be reminiscent of a pre-existing pattern of gene expression in non-neural ectoderm tissue. The formation of ciliated epidermal cells in *Xenopus* is regulated by the *Notch-Delta* lateral inhibition pathway in which certain cells take up the fate of ciliated epidermis, thereby preventing neighboring cells from acquiring that fate (Deblandre *et al.*, 1999). Activation of *N-tubulin* expression in this punctate manner could reflect this pre-existing expression of lateral inhibition machinery in the ectoderm, such that *Noelin-1* could prompt cells expressing these genes (that are also involved in neuronal selection) to be more receptive to become neurons and thus make a fate decision and express *N-tubulin*.

Together, these results suggest that although *Noelin-1* expression is not sufficient to cause general neural induction as indicated by induction of *NCAM*, perhaps it may participate in a signaling pathway as a factor to promote or maintain a neuronal differentiation program. This is suggested by its ability to induce expression of later neural markers such as *XBrn-3d*, *XNeuroD* and *Krox-20*, and by its failure to posteriorize *noggin*-induced neural tissue. Alternatively, it could be that the differentiation-promoting property of *Noelin-1* in *noggin*-treated explants is separate from its ability to induce *Krox-20* on its own, as the ability of *noggin* to induce neural tissue of forebrain character could not be

altered to a more posterior fate (to express *Krox-20*) by *Noelin-1*; in fact, *noggin* co-expression repressed the *Noelin-1*-mediated induction of *Krox-20* in explants. My results in *Xenopus* explants may also indicate that *Noelin-1* has divergent or added functions in neural development among vertebrate species, since avian *Noelin-1* affects neural crest development while *Xenopus Noelin-1* did not. However, the possible role of *Noelin-1* in avian neurogenesis has not yet been tested.

In conclusion, I find that *Xenopus Noelin-1* is an evolutionarily conserved protein by sequence and protein structure, but that its expression pattern and function are considerably different in *Xenopus* and avian embryos during early development. Its differing roles in neural crest formation in the chick and neurogenesis in *Xenopus*, and the dependence of its inductive abilities on its localization, may indicate that it functions in multiple mechanisms of neural development. Future work will address how *Noelin-1* exerts its neural effects, whether other *Noelin* isoforms in *Xenopus* have been co-opted for a function similar to that in chick, and with what partners *Noelin* may interact in the developing embryo.

## ACKNOWLEDGEMENTS

I gratefully acknowledge Drs. A. Knecht, L. Gammill and C. Baker for critical reading of the manuscript; C. Baker, L. Gammill, A. Knecht, members of the laboratory and especially C. LaBonne for support, valuable insights and discussion. C. LaBonne kindly assisted with oocyte labeling experiments. The authors thank the following for their kind gifts of reagents: Drs. R. Harland and M. King for the *Xenopus* cDNA libraries; D. Anderson, *X-ngnr-1*; A. Brändli, *Pax-2*; K. Cho, *6-myc-Noggin*; C. LaBonne, *XBrn-3r*; C. Kintner, *N-tubulin*; J. Lee, *XNeuroD*; R. Mayor, *XSlug* and the anonymous reviewers for helpful comments. T.A.M. is a Fellow of the ARCS Foundation. This work was supported by USPHS grants NS36585 and NS41070.



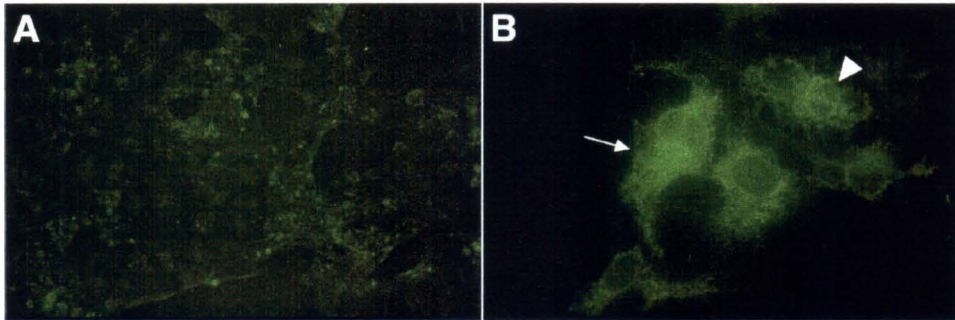
## Figure 1: Sequence and Structure of *Xenopus Noelin-1* and -2

---

**A:** Upper right corner box shows a schematic diagram for splice variants. The A (green) and B (blue) exons are added by differential promoter utilization, M (yellow) is common to all four isoforms, Y (orange) and Z (red) are added by alternative splicing. In the sequence portion of the figure, the A and B sequences are shown separately from the M-Z region which is shown as spliced. The deduced amino acid sequences of the *Noelin* exons are shown below nucleotide sequences. Both A and B regions encode putative signal peptides (red underlines; predicted cleavage site depicted with a red arrow). *Noelin* isoforms contain several potential sites for N-linked glycosylation throughout the sequences (6 sites for *Noelin-2*, and 7 for *Noelin-1*; arrowheads), two potential hyaluronate binding sites in the common M region (black underline), a glycosaminoglycan initiation site (gray underline) and three cysteine residues that are conserved between Olfactomedin and *Noelin* in the M and Z regions (green asterisks). The Olfactomedin domain is indicated with a yellow underline. **B:** *Xenopus Noelin* Olfactomedin domain is compared to four other Olfactomedin-related proteins and to Olfactomedin itself. Residues shaded in black are identical to Olfactomedin; residues shaded in yellow denote sequences conserved between all other family members but not Olfactomedin. Red underlines denote regions of grouped identities; green asterisk marks conserved cysteine residue. Chick *Noelin-1* (Barembaum *et al.*, 2000), a human *Noelin*-related gene (GenBank accession #AF131839), MYOC/TIGR (Nguyen *et al.*, 1998), the  $\alpha$ -latrotoxin receptor Latrophilin (Krasnoperov *et al.*, 1997) all share varying degrees of identity to Olfactomedin, and a higher degree of similarity to each other than to Olfactomedin. In the Olfactomedin domain, *Noelin* shares between 42-48% identity to these proteins (90.4% to chick *Noelin*).

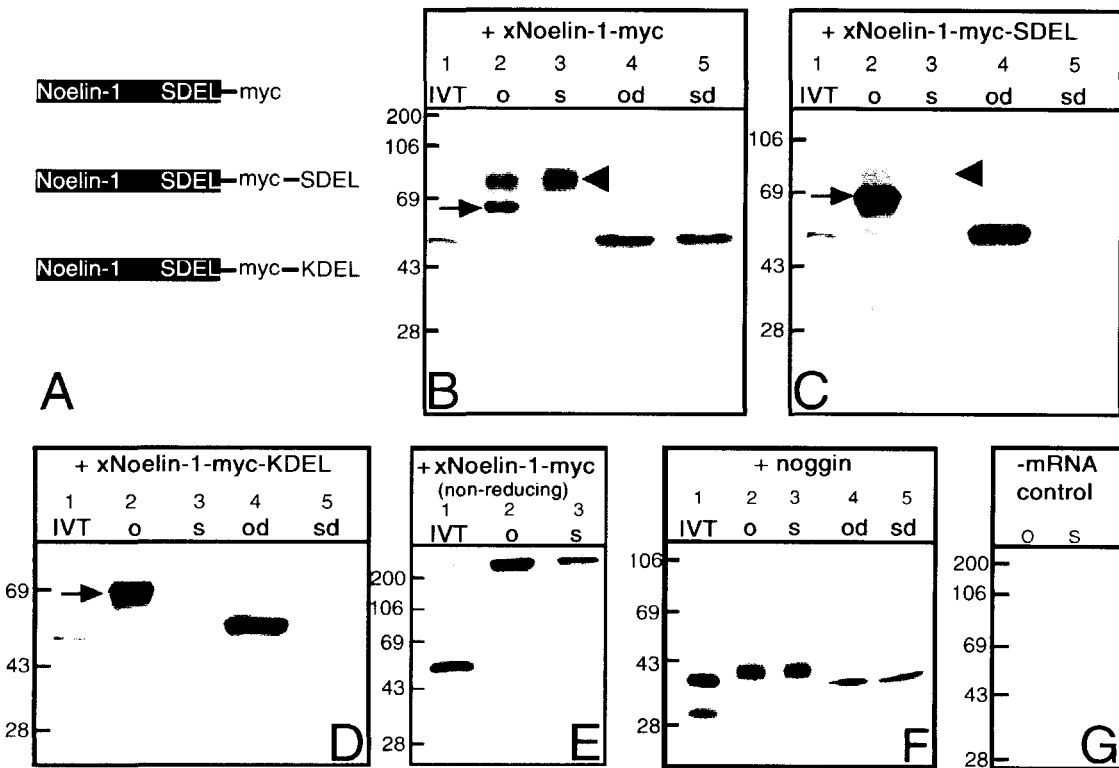
---

**Figure 2:** Subcellular localization of *Noelin-1*

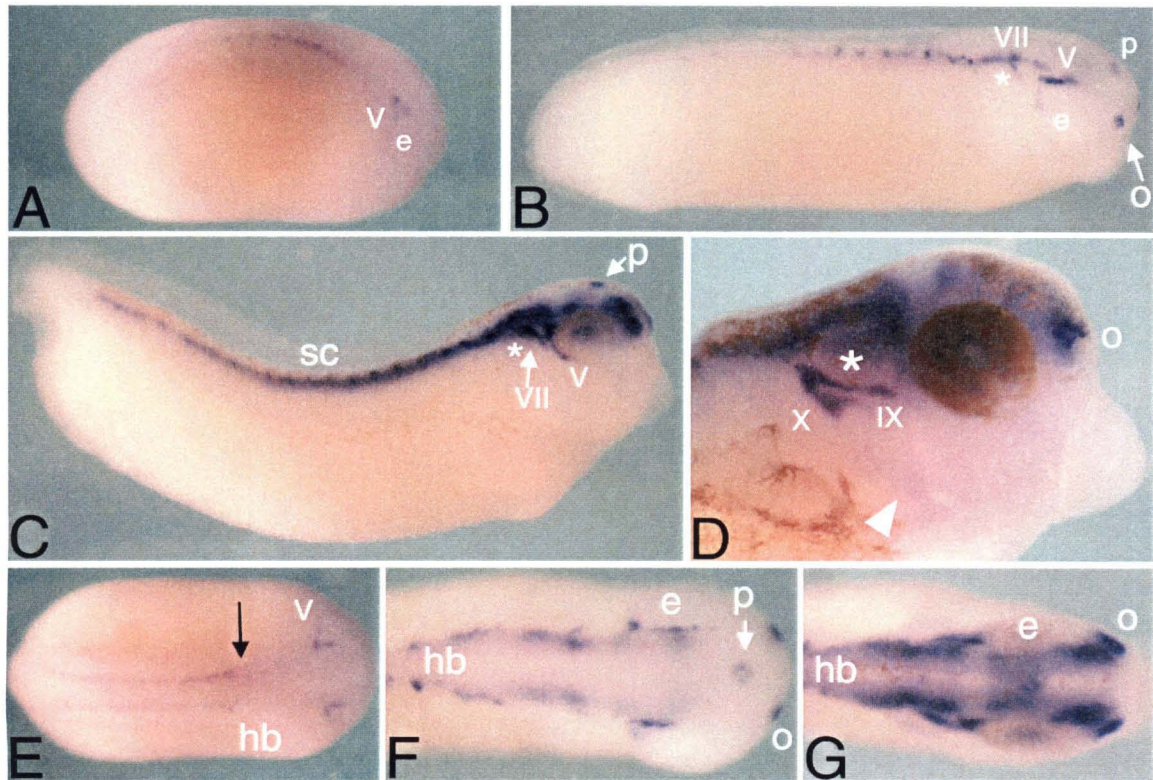


*Noelin-1* protein is found in the endoplasmic reticulum (secretory pathway) of cultured cells. COS-7 cells were transfected with *Noelin-1-flag* or  $\beta$ -*galactosidase*, cultured for 24 hours and then stained with the anti-*flag* antibody. **A:** Control transfections show no staining with the anti-*flag* antibody. Non-specific background is visible as scattered green regions. **B:** Cells transfected with *Noelin-1-flag* stain with the anti-*flag* antibody in the endoplasmic reticulum (arrow, fluorescent green stain). Nuclear border is visible surrounding the non-staining nucleus (arrowhead); the endoplasmic reticulum is visible as a fibrous network extending from the nucleus to the boundaries of the cells. Six stained cells are visible.

### Figure 3: Oocyte secretion assay

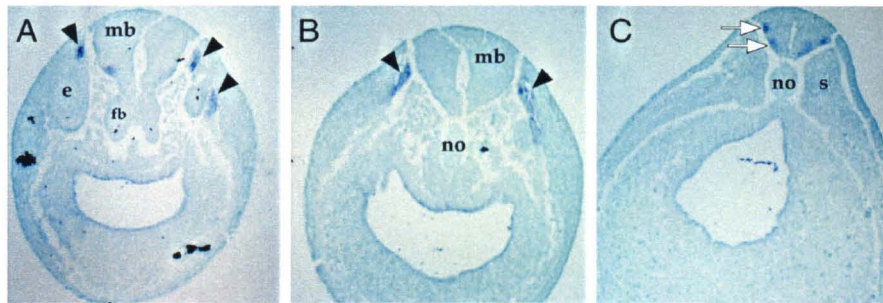


Noelin-1 is secreted into the supernatant when injected into oocytes. *Myc*-tagged constructs were co-injected along with  $^{35}\text{S}$ -methionine and oocyte and supernatant fractions were immunoprecipitated with anti-*myc* antibody. All gels were run under reducing conditions except for E. **A**: Schematic diagram showing constructs of *Noelin-1* used in injections. Natural carboxy terminal sequence is SDEL. This is part of all three constructs but is blocked by the *myc* tag; thus additional SDEL or KDEL-encoding oligonucleotide sequences were subcloned 3' to the *myc* tag. **B**: *Noelin-1-myc* is robustly secreted from the oocytes (lane 2), seen as the large band in the supernatant (lane 3). Oocytes contain an intermediate form of the protein that runs just smaller than the 69 kD marker (arrow in lane 2). *In vitro* translated (IVT) protein runs at approximately 56 kD, the size predicted from the amino acid sequence (lane 1). The proteins made in the oocyte fraction and the secreted species are glycosylated, as treatment with peptide-N-glycosidase (PNGase) reduces the bands down to the core size comparable to the IVT sample (deglycosylated samples shown in lanes 4 (oocytes) and 5 (supernatant)). **C**: Oocytes secrete *Noelin-1-myc-SDEL*, in which the endogenous carboxy terminal sequence SDEL is subcloned after the *myc* tag, but at a lower level than *Noelin-1-myc*. Oocytes also contain the intermediate protein species (arrow, lane 2). As with the gel in (A), only the largest species of protein in the oocytes is secreted into the supernatant (arrowhead, lane 3). The proteins are highly glycosylated and treatment with PNGase reduces all species to the core protein size (lanes 4 and 5). **D**: A *Noelin-1* construct containing the consensus ER retention signal at the carboxy terminal was tested to verify proper protein sorting by oocytes. *Noelin-1-myc-KDEL* is not secreted and does not form the higher molecular weight species found in the secretable constructs. Arrow in lane 2 marks the intermediate size protein found in all *Noelin-1*-injected oocytes. This intermediate-size protein is glycosylated as in the *Noelin-1-myc* and *Noelin-1-myc-SDEL* constructs, deglycosylated sample is shown in lane 4. **E**: *Noelin-1-myc* protein forms high molecular weight complexes that do not run into a 9% resolving gel under non-reducing conditions. The species present in these samples are larger than 200kD. **F**: XNoggin-6myc is secreted as expected and is mildly glycosylated. **G**: Uninjected oocyte controls contain no specifically immunoprecipitated protein from oocytes or supernatant. Numbers and bands drawn at the left of each gel correspond the positions of molecular weight markers of the indicated size. IVT, *in vitro* translated protein; o, oocyte fraction; s, supernatant fraction; od, deglycosylated oocyte fraction; sd, deglycosylated supernatant fraction.

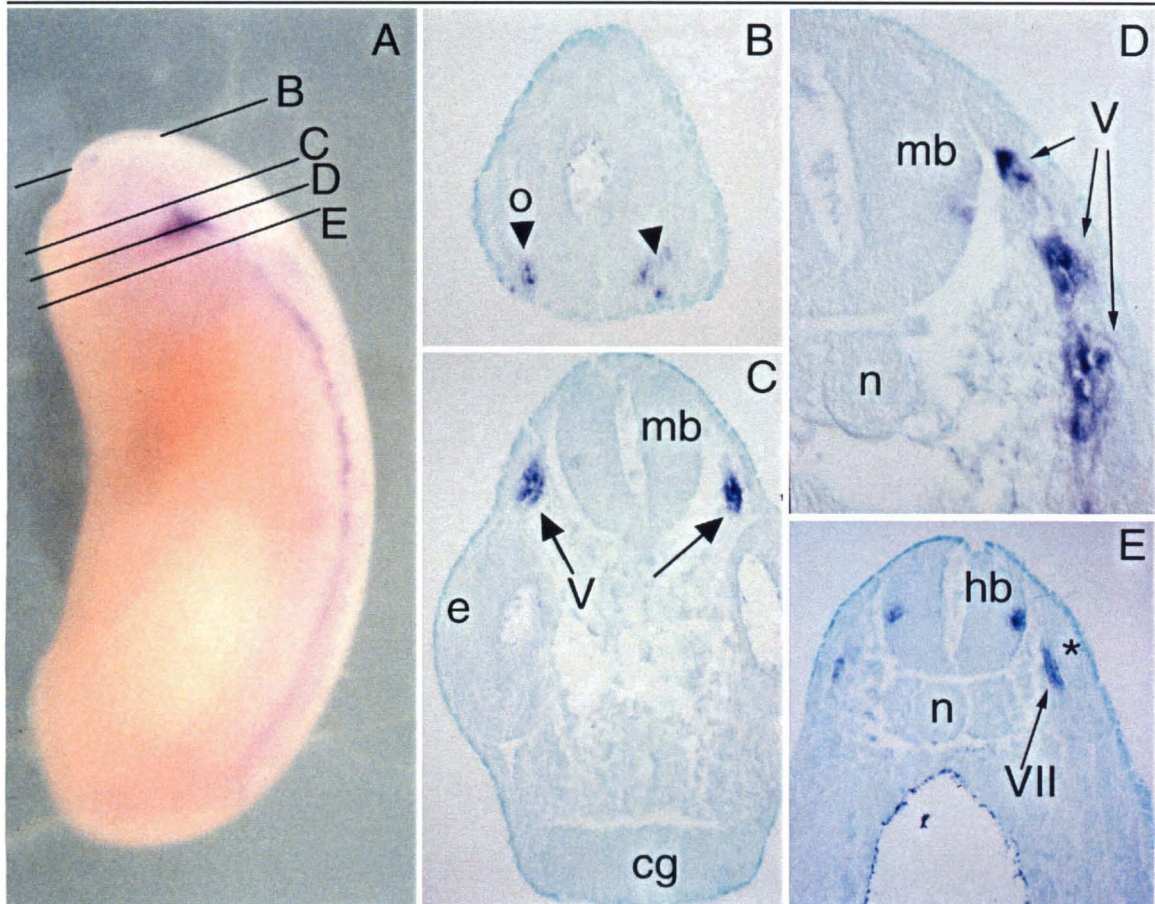
**Figure 4: *Noelin-1* expression pattern**

Whole mount *in situ* hybridization with a probe to the Z exon reveals the distribution of *Noelin-1* and *Noelin-2* transcripts in the neural tube and cranial ganglia. All embryos are oriented with anterior to the right. **A:** Earliest expression is seen after neural tube closure in the spinal cord and trigeminal ganglia at stage 22. **B:** By stage 27 cells in the olfactory placodes and in the trigeminal (V) and geniculate (VII) ganglia are strongly reactive. Punctate staining is visible in the pineal gland and spinal cord. **C:** A stage 33 embryo shows increasing signal in the Vth and VIIIth ganglia, olfactory pits, pineal gland and spinal cord. A population of cells in the retina is also positive for *Noelin-1* and *-2*. **D:** By stage 35/36 the IXth and Xth ganglia are also positive for the transcripts. A small number of cells in the branchial arches express the Z exon (arrowhead). **E-G:** Dorsal views of embryos in A-C. **E:** Stage 22 embryo shows staining in the Vth ganglia and in the spinal cord. Transcripts are not detected in the brain at this stage. The black arrow marks the anterior extent of *Noelin-1* and *-2* signal in the neural tube. **F:** By stage 27, spinal cord staining extends into the brain and up to the level of the midbrain. The pineal gland and olfactory placodes are visible. **G:** At stage 33 the signal is increasingly intense in the cranial ganglia, spinal cord, and more rostrally into the forebrain. e, eye; hb, hindbrain; o, olfactory placode/pit; p, pineal gland; sc, spinal cord; V, trigeminal; VII, geniculate; IX, glossopharyngeal; X, vagal; asterisks mark the general position of otic vesicles. Brown color is due to melanocytes in the skin or retinal pigmented epithelium in the eye.

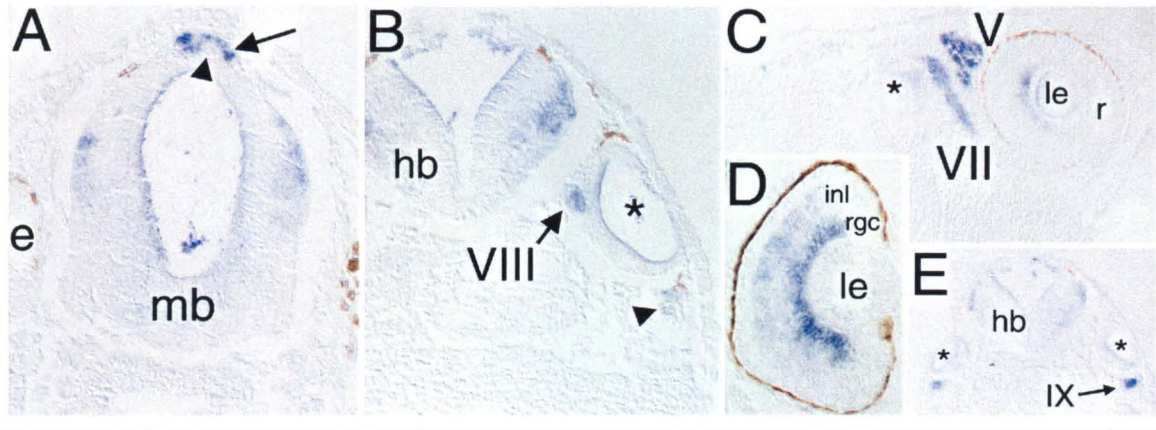
**Figure 5:** *Noelin-1* expression in early cranial ganglia and spinal cord



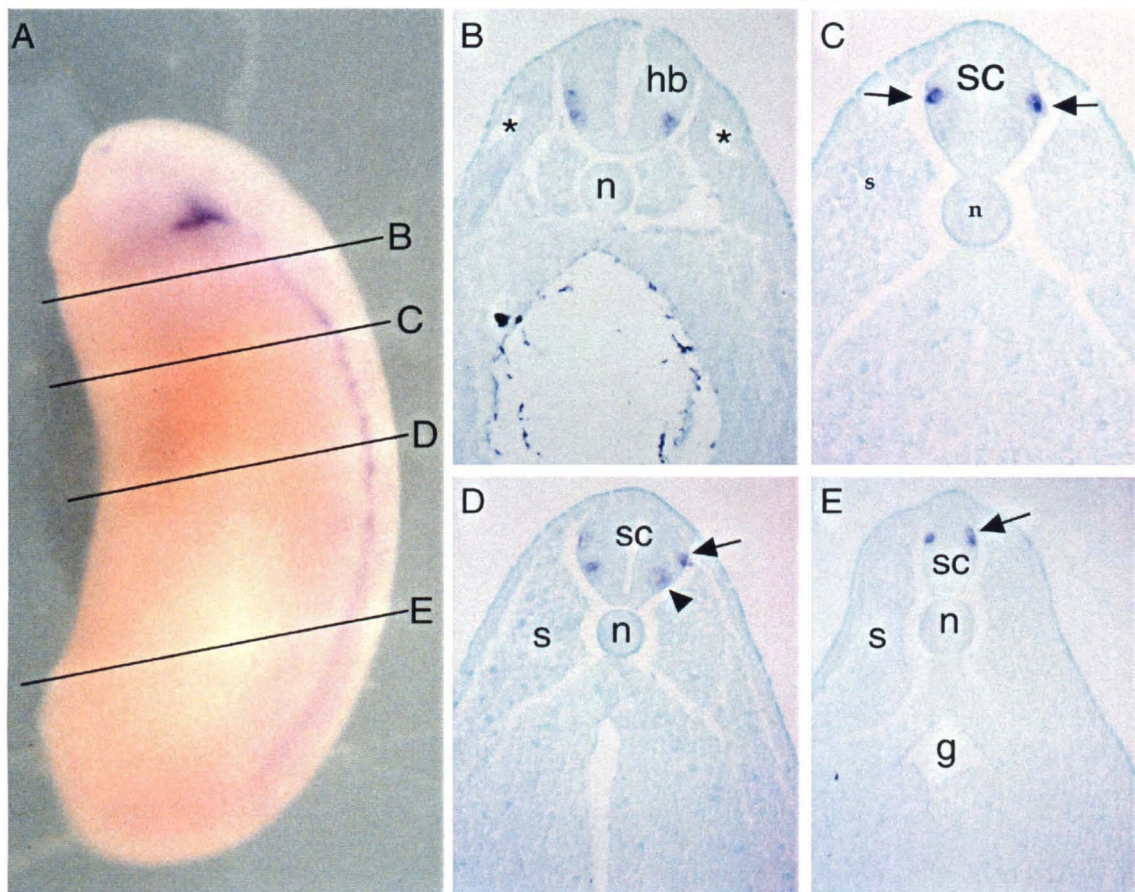
*Noelin-1* is expressed in the early cranial ganglia and spinal cord. Stage 21 embryo stained with a probe for the Z exon reveals *Noelin-1* and *-2* expression pattern. **A:** Cross-section through the cranial region shows staining in the developing trigeminal ganglia (arrowheads). The plane of section is through the midbrain and eye, with some forebrain visible as well. **B:** Caudal midbrain section reveals transcripts for the Z exon in the mandibular component of the trigeminal ganglion (arrowheads). **C:** In the spinal cord, *Noelin* transcripts are found in the interneurons and motor neurons (white arrows). Sections are 10 microns thick and counterstained with Light Green SF to visualize tissue morphology in unstained regions. e, eye; fb, forebrain; mb, midbrain; no, notochord; s, somite.

**Figure 6:** Rostral *Noelin* expression in stage 25 embryos

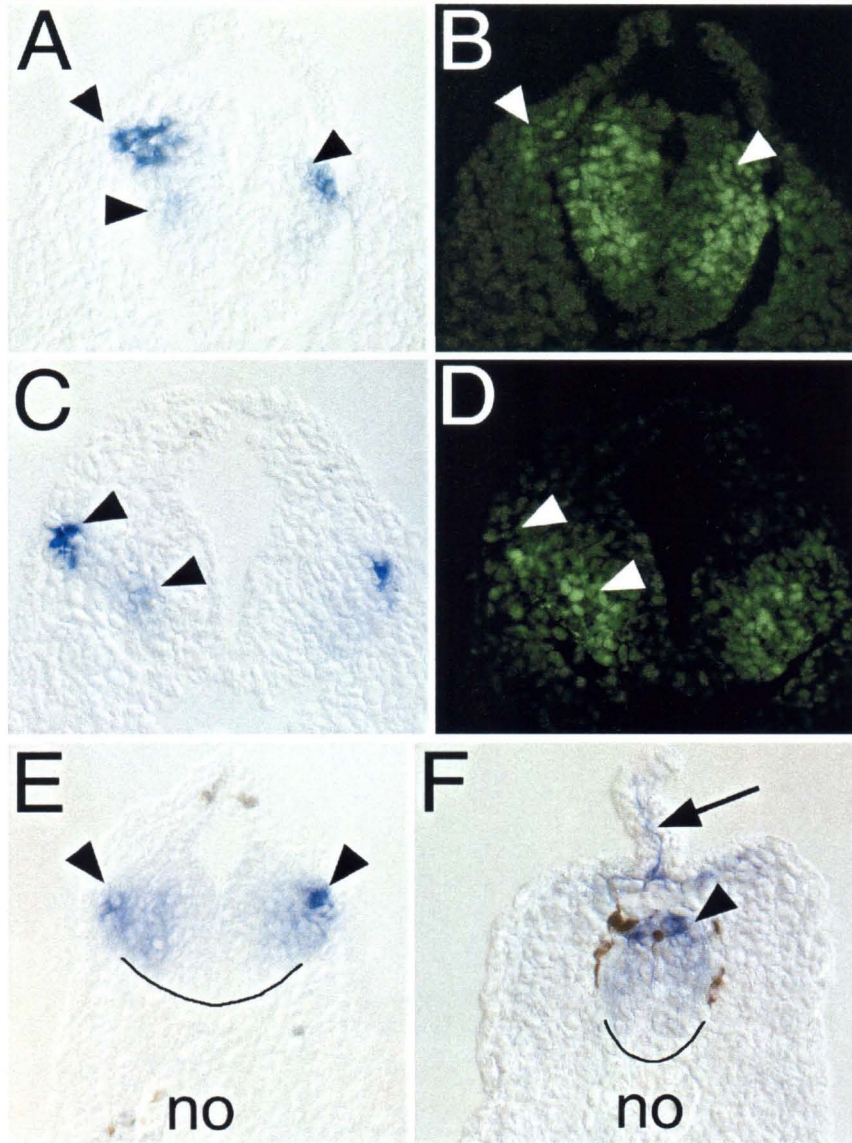
Rostral expression of *Noelin* Z transcripts increases with development. Whole mount embryo shown in A indicates levels of sections in B-E. Anterior is up in A. Sections in B-E are counterstained with Light Green SF in order to visualize tissue morphology. **A:** Lateral whole mount view; staining is visible in the trigeminal ganglion and spinal cord. **B:** Section through the forebrain and olfactory placodes (arrowheads). **C:** Maxillary component of the trigeminal ganglion (V, arrow) is visible above the optic vesicles (e). Cement gland is indicated (cg). **D:** Mandibular component of trigeminal (V) is visible in a section through the caudal midbrain. **E:** A section through the hindbrain reveals staining in the geniculate ganglia (VII, arrow) underneath the otic vesicle (asterisk). e, eye; cg, cement gland; hb, hindbrain; mb, midbrain; n, notochord; o, olfactory placode; V, trigeminal ganglion; VII, geniculate ganglion.

**Figure 7: Cranial *Noelin* expression at stage 35**

10  $\mu$ m sections through head regions of a stage 35 embryo similar to that in Fig. 4D, stained with a probe to the Z exon. **A:** A midbrain-region transverse section reveals *Noelin-1* and *-2*-positive cells in the pineal gland and brain. Arrow points to the body of the gland, arrowhead denotes cells that are not positive for *Noelin-1* or *-2*. **B:** A hindbrain section at the mid-otic vesicle level shows signal in the VIIIth ganglion (arrow) and faintly in the IXth ganglion (arrowhead) ventral to the otic vesicle. **C:** Parasagittal section through the eye, Vth and VIIth ganglia and the otic vesicle. The retinal ganglion cell layer also contains signal. **D:** A higher-power view of a transverse section through the eye reveals transcripts in the retinal ganglion cell layer and inner nuclear layer, but not in the pigmented epithelium, photoreceptor layer, ciliary marginal zone or lens. **E:** A hindbrain section showing signal in the IXth ganglion. e, eye; hb, hindbrain; inl, inner nuclear layer; le, lens; mb, midbrain; rgc, retinal ganglion cell layer; V, trigeminal; VII, facial nerve and geniculate; VIII, facial-acoustic; IX, glossopharyngeal; asterisks denote otic vesicle; brown pigment is seen in melanocytes and retinal pigmented epithelium.

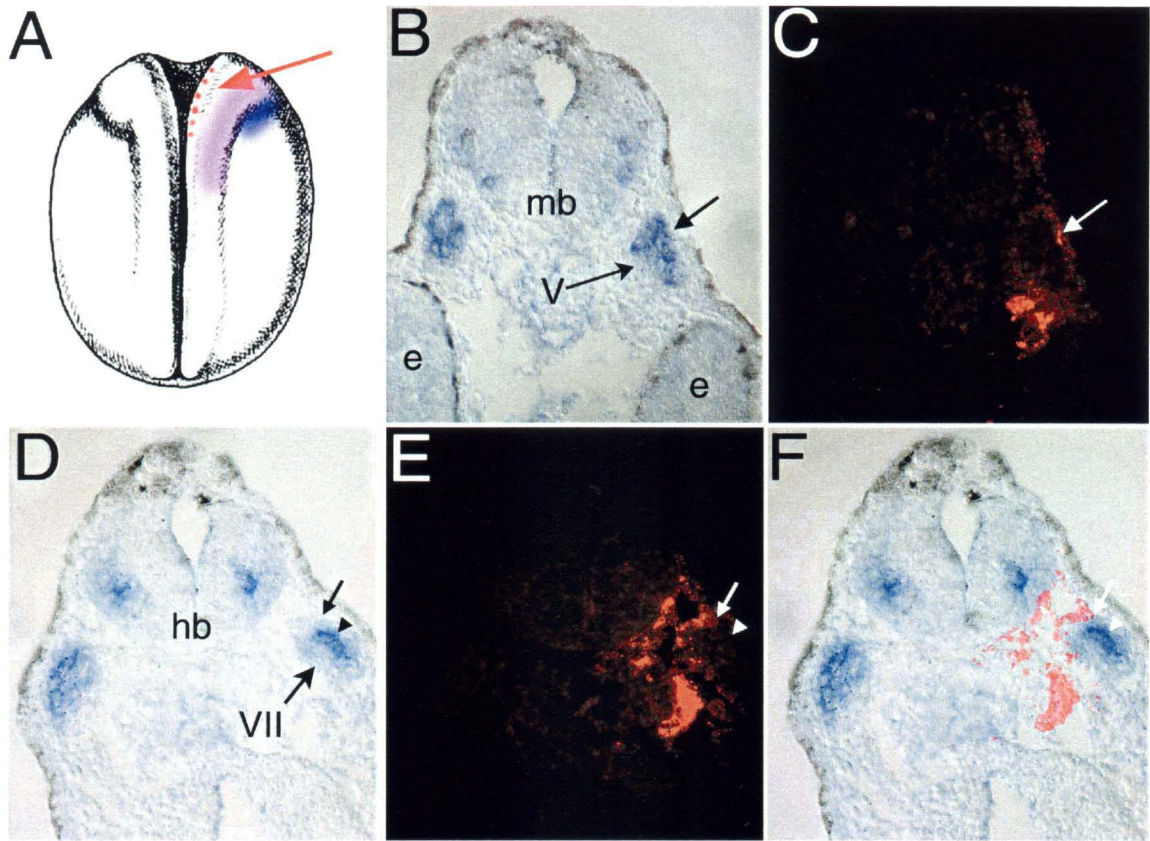
**Figure 8:** Caudal expression of *Noelin-1* at pre-tailbud stage

Caudal expression of *Noelin-1* and *-2* at pre-tailbud stages (stage 25) is in the marginal zone of the neural tube. Embryo in **A** (lateral view, anterior is up) shows level of sections in B-E; this is the same embryo as in Figure 6. Sections were cut at 10 micrometers and counterstained with Light Green SF. **B:** A section through the otic vesicles (asterisks) level shows neural tube staining in the ventral marginal zone in the hindbrain (arrowhead). **C:** Rostral trunk section shows neuronal populations in the spinal cord in the position of interneurons (arrows). **D:** Middle trunk section with staining in the same populations and in the more ventral motoneurons (arrowhead). **E:** Caudal trunk section shows staining in the dorsally located sensory neurons (Rohon-Beard cells, arrowheads). g, gut; hb, hindbrain; n, notochord; s, somite; sc, spinal cord.

**Figure 9:** Neuronal expression of *Noelin-1* and *-2*

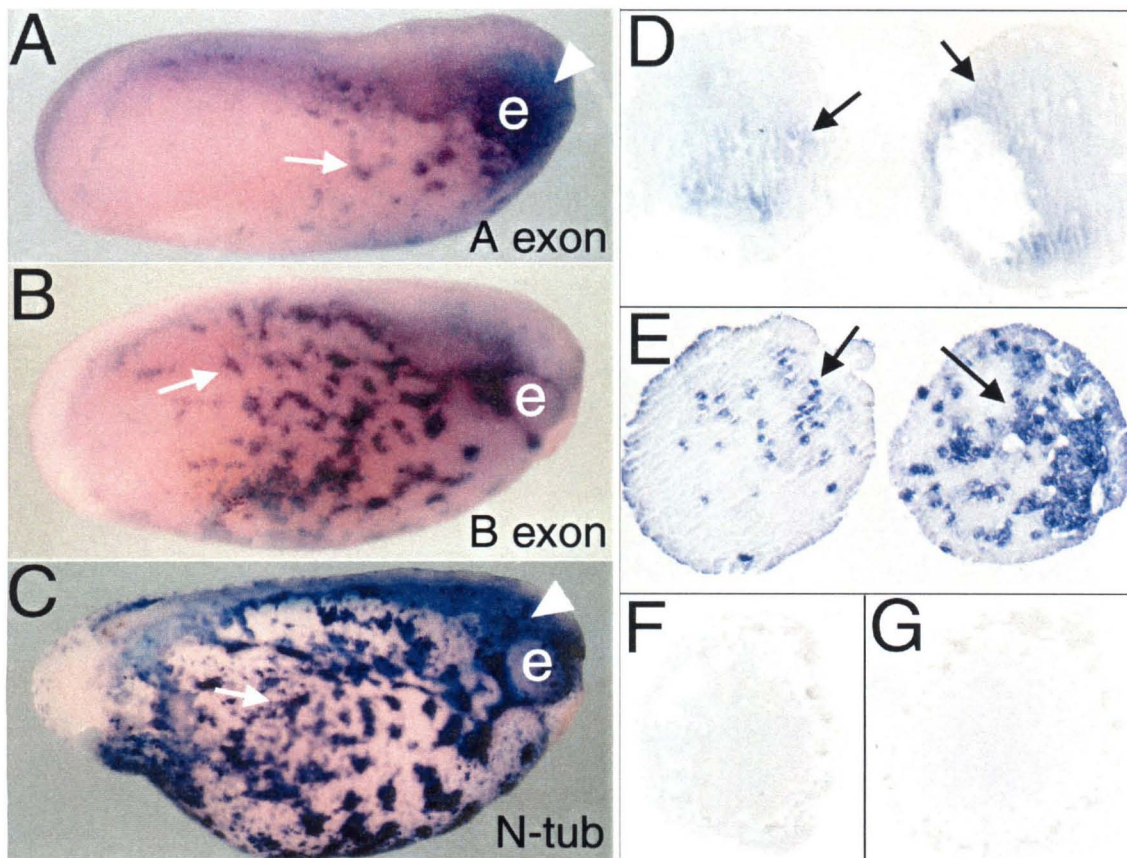
10  $\mu\text{m}$  sections through embryos stained with the Z exon. Arrowheads mark neuron populations in the spinal cord that express the gene. **A:** Stage 28 embryo with signal in Rohon-Beard cells and interneurons. **B:** The same section stained with *HNK-1* shows that *Noelin* marks only a subset of the neurons present. Some of the *HNK-1* signal is quenched by the in situ reaction product. **C:** Stage 28 embryo with signal in interneurons and motor neurons. **D:** *HNK-1* staining of the same section as in C. **E:** Stage 33 spinal cord illustrates expanding domain of *Noelin-1* and *-2* expression. **F:** Stage 35 spinal cord shows neural crest cells migrating into the fin (arrow) expressing *Noelin-1* and *-2*. In E and F, black line demarcates the ventral neural tube. Brown cells are pigmented neural crest cells (melanocytes). no, notochord.

## Figure 10: Dil labeling of pre-migratory neural crest cells



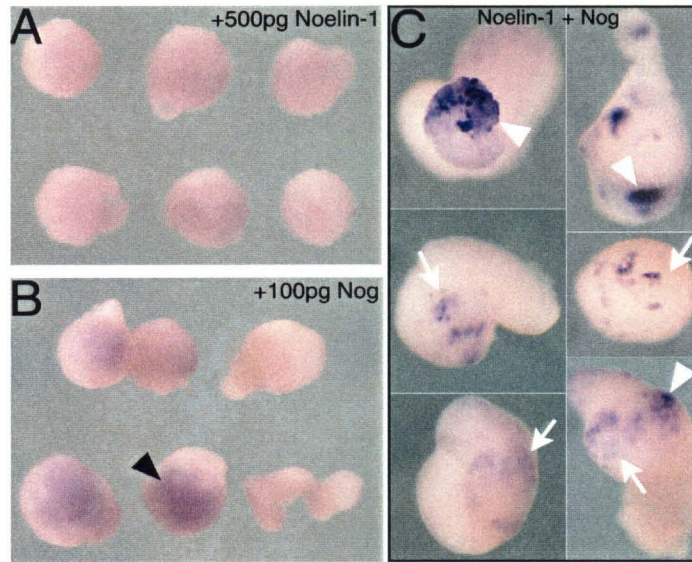
*Noelin-1* and *-2* are expressed in the cranial ganglia. Transverse section through stage 33 embryos with neural crest cells labeled by focal injections of Dil in the neural folds at stage 17. Whole mount *in situ* hybridization was performed against the Z exon. **A:** Schematic diagram of a stage 17 embryo illustrating relative locations of lateral neural crest (pink), placode domain (blue) and the medial neural crest which were labeled with Dil (red dots, arrow). **B:** Bright field view of a stage 33 embryo section at the caudal eye level, showing *Noelin-1* and *-2* expression in the Vth ganglion. The cells marked by the arrow are not *Noelin-1* or *-2*-positive. **C:** Fluorescent view of section in B, arrow marks Dil positive neural crest cells. **D:** Bright field view of a hindbrain level section including the VIIth ganglia. Ganglion cells express *Noelin-1* and *-2* (arrowhead), migrating neural crest cells do not (arrow). **E:** Fluorescent image of section in (D) shows Dil-positive cells surrounding, but not mixed within the ganglion. Arrow marks a cell that is Dil positive and *Noelin-1* and *-2* negative; arrowhead marks a cell that is *Noelin-1* and *-2* positive and Dil negative. **F:** Overlay of the fluorescent image shows non-overlapping Dil and *Noelin-1* and *-2* cells. In both embryos (B-C and D-F), Dil positive neural crest cells surround the condensing ganglia but do not appear to mix with the placodal cells at this stage. Analysis at later stages was not possible due to dilution of the Dil. e, eye; hb, hindbrain; mb, midbrain; V, Vth ganglion (trigeminal); VII, VIIth ganglion (facial nerve and geniculate ganglion).

**Figure 11:** *Noelins* are induced by *neurogenin* overexpression

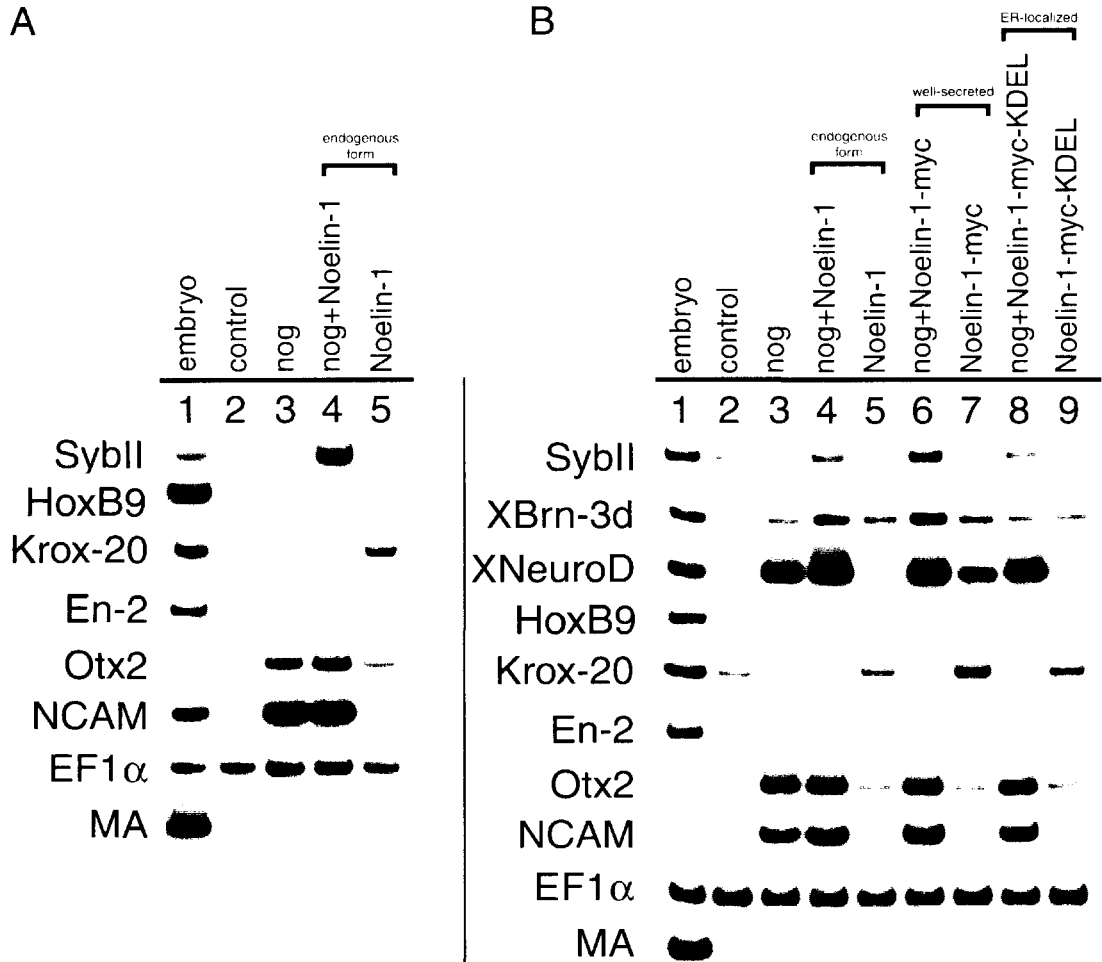


Embryos injected with 100pg *X-ngnr-1* make ectopic neurons in the epidermis. *Noelin-2* upregulation is represented by expression of the A exon and *Noelin-1* is represented by expression of the B exon. These *in situ* results are identical to those performed for the Z exon, and results are identical for *X-ngnr-1* and *XNeuroD*. Embryos shown are siblings from the same injection experiment, with anterior to the right. **A:** *Noelin-2* is upregulated robustly in *X-ngnr-1*-injected embryos. An embryo probed for the A exon shows induced *Noelin-2* expression in ectopic neurons (for example, see white arrow). Also note ectopic staining for the A exon in the head (arrowhead). **B:** Sibling injected embryo stained for the B exon. Ectopic neurons (arrow) express *Noelin-1*. **C:** Sibling embryo stained with *N-tubulin* shows massive ectopic induction of neurons in the epidermis (arrow). Note the extent of *N-tubulin* staining as compared to embryos in (A) and (B). Extra head tissue is positive for *N-tubulin* (arrowhead). **D-G:** Animal caps sectioned at 12 microns. Embryos were injected with *X-ngnr-1* or  $\beta$ -galactosidase (control) at the 2-cell stage, caps were collected at stage 9 and cultured to stage 24. *In situ* were performed for *N-tubulin* or the separate *Noelin* exons, the Z pattern is representative of *Noelin-1* and *-2*. **D:** *Noelin-1* and *-2* are upregulated weakly in animal caps as compared to the results in whole embryos (arrows). **E:** Animal caps stained with *N-tubulin* show robust activation of expression (arrows). **F:** Control animal cap stained with the Z exon shows no induction of *Noelin* expression in the absence of *X-ngnr-1*. **G:** Control animal cap stained with *N-tubulin* also fails to express this gene. e, shows region of eye, usually malformed or absent in injected embryos.

**Figure 12:** *Noelin* promotes neuronal differentiation



Animal caps were collected at stage 9 from embryos injected at the 2-cell stage with 100pg *noggin*, 500pg *Noelin-1*, or both. The explants were cultured to stage 27. Whole mount *in situ* hybridization was performed against *N-tubulin*. **A:** Animal caps injected with *Noelin-1* alone do not express *N-tubulin*. **B:** Animal caps injected with *noggin* do not express *N-tubulin*. (Diffuse purple color is due to trapping of reaction components inside animal cap cavities; see black arrowhead.) **C:** Animal caps co-injected with *noggin* and *Noelin-1* upregulate *N-tubulin* by stage 24 (caps shown in this figure were fixed at stage 27). At stage 24, a smaller proportion of the explants express *N-tubulin* (3/6, data not shown). In the representative experiment shown here, 14/17 explants express *N-tubulin* to varying degrees. In some cases, strongly positive *N-tubulin* regions were confined to small areas of the explant (arrowheads); the majority of explants with induced *N-tubulin* expression show positive cells scattered through regions of the explants (arrows).

**Figure 13: *Noelin-1* induces sensory and differentiation markers**

### Figure 13: *Noelin-1* induces neural marker expression

---

RT-PCR analysis shows *Noelin-1* induces expression of several neural markers. 2-cell stage embryos were injected with 500pg *Noelin-1* constructs, 100pg *noggin*, or both; control animal caps were injected with 600pg green fluorescent protein mRNA. Animal caps were dissected at stage 9 and cultured to stage 24. **A:** Lane 1: whole embryo control at stage 24; lane 2: St 24 control injected animal caps; lane 3: *noggin*-injected animal caps; lane 4: *noggin* + *Noelin-1* animal caps; lane 5: *Noelin-1* injected animal caps. Animal caps injected with both *noggin* and *Noelin-1* express *Sybl1* (*Sybl1* row, lane 4). *HoxB9* is very slightly induced by *Noelin-1* alone in this experiment. *Krox-20* is induced by *Noelin-1*, but not by *Noelin-1* + *noggin*. *En-2* is not induced by any of the injections. *Otx2* and *NCAM* are induced by explants injected with *noggin* (lanes 3 and 4), *Noelin-1* alone slightly induces *Otx2* (lane 5). *EF1 $\alpha$*  is a loading control. *Muscle actin (MA)* is a control for mesoderm contamination of animal cap explants. **B:** Secretion or ER localization of *Noelin-1* affects its inducing capabilities. Three different forms of *Noelin-1* were expressed either alone or in conjunction with *noggin*. *Noelin-1* is the endogenous form of the protein; *Noelin-1-myc* is a highly secreted form (see Fig. 2B); and *Noelin-1-myc-KDEL* is retained in the endoplasmic reticulum (ER, see Fig. 2D). Lane 1: st 24 whole embryo; lane 2: st 24 control injected animal caps; lane 3: *noggin* caps; lane 4: *noggin*+*Noelin-1*; lane 5: *Noelin-1*; lane 6: *noggin*+*Noelin-1-myc*; lane 7: *Noelin-1-myc*; lane 8: *noggin*+*Noelin-1-myc-KDEL*; lane 9: *Noelin-1-myc-KDEL*. *Sybl1* is upregulated in all samples with *Noelin* isoforms when explants are co-injected with *noggin* (lanes 4, 6, 8 of *Sybl1* row). Highly secreted form of *Noelin-1* caused greatest *Sybl1* expression (lane 6). *XBrn-3d* is induced by *noggin* and by *Noelin-1* (lanes 3-9 of *XBrn-3d* row). In conjunction with *noggin*, secreted forms of *Noelin-1* cause up to 3.4-fold induction of this gene over *noggin* alone (lanes 4 and 6). *XNeuroD* expression is activated by *noggin* and by *Noelin-1* co-expression (lanes 3, 4, 6 and 8 of *XNeuroD* row). *Noelin-1-myc* alone induces *XNeuroD* expression (lane 7). *HoxB9*, *En-2* and *NCAM* are not induced by *Noelin-1* (lanes 5, 7, 9 of appropriate rows). *Otx2* is upregulated by *Noelin-1* constructs by 2-fold over control animal caps (lane 2 vs lanes 5, 7 and 9); however, *noggin* is several times stronger an activator of *Otx2* than *Noelin-1*. *Krox-20* expression is induced by all three constructs of *Noelin-1* (lanes 5, 7 and 9 of *Krox-20* row); however, addition of *Noelin-1* is not sufficient to cause *noggin*-injected explants to express *Krox-20*. *EF1 $\alpha$*  and *MA* are controls as described above.

---

## **Chapter 3**

**Noelin-4: a novel secreted protein that acts as a neural inducer and binds to BMP-4**

## INTRODUCTION

Neural induction is a complicated process that requires the activities of many opposing and cooperative signaling pathways. The process begins during gastrulation when the dorsal mesoderm comes to underlie the ectoderm, signaling it to become neural. In *Xenopus*, noggin and chordin proteins are secreted from the early dorsal mesoderm (the Spemann Organizer) and neuralize the overlying ectoderm by inhibiting the BMP signaling pathway. BMP signaling in the ectoderm induces epidermis; when antagonized, this uncovers the “default” neural state, and allows neural development to proceed in the regions exposed to these factors (for review, see Sasai and De Robertis, 1997; Chang and Hemmati-Brivanlou, 1998; Weinstein and Hemmati-Brivanlou, 1999; Harland, 2000). A broad domain of neural fate characterized by expression of early response genes is established first (Ferreiro *et al.*, 1994; Turner and Weintraub, 1994; Kroll *et al.*, 1998; Mizuseki *et al.*, 1998a; Mizuseki *et al.*, 1998b). Neurogenesis is subsequently activated by a cascade of transcription factors, namely the proneural and neurogenic genes such *X-ngnr-1* and *XNeuroD* (Lee *et al.*, 1995; Ma *et al.*, 1996).

In addition to its role in neural induction during gastrulation, BMP signaling plays later roles during neural development. It has recently been shown that continued BMP repression is necessary for normal neural plate development after gastrulation, and that *BMP-4* and *-7* are expressed in the anterior mesendoderm, the tissue that underlies the anterior neural plate (Hartley *et al.*, 2001). Inhibition of BMP activity in *Xenopus* is important for establishing the neural plate border region from which the neural crest arises

(LaBonne and Bronner-Fraser, 1998; Marchant et al., 1998). Additionally, active BMP signaling is involved in dorsal interneuron differentiation, while limiting ventral fate in the spinal cord of other vertebrates (Dickinson et al., 1995; Liem et al., 1997; Liem et al., 1995; Nguyen et al., 2000) as well as in anterior neural tube regions where over-expression of *BMP-4* dorsalizes forebrain (Furuta et al., 1997; Golden et al., 1999). Recently it has been demonstrated that BMP signaling may be responsible for the differential timing of hindbrain neuron differentiation (Eickholt et al., 2001). Thus it appears that BMP signaling plays multiple, and seemingly, contradictory roles in neural development: first, its repression is required for neuralization to occur; second, later some signaling must occur for normal neural differentiation processes.

Together, these data suggest that mechanisms for regulating levels of BMP signaling at different times and locations during development are required for proper patterning of neural tissues after neural induction has occurred. Many molecules are known to interact with BMPs, and the diversity of tissues in which BMP signaling is involved in patterning or differentiation suggests that similar regulatory mechanisms may operate in different tissues, accomplished by different molecules.

I have isolated a *Xenopus* gene with neural-inducing properties that is expressed from neural plate stages, and is highly expressed in post-mitotic neural tissues after neural tube closure. *Noelin-4* is an isoform of a family of four secreted glycoproteins, and a member of the larger family of genes that contain the Olfactomedin domain (Barenbaum et al., 2000; Kulkarni et al., 2000), although *Noelin-4* itself does not contain an Olfactomedin domain. The *Noelin*

gene makes four isoforms by differential promoter usage and alternative splicing, synthesizing *Noelin-1* (BMZ), *Noelin-2* (AMZ), *Noelin-3* (BMY) and *Noelin-4* (AMY) from the four available exons, A, B, M, Y and Z (Danielson et al., 1994; Barembaum et al., 2000).

To date, no functional data for *Noelin-4* in other species have been published, although the expression patterns of *Noelin* isoforms have been described in mouse, rat, and chick (Barembaum et al., 2000; Kondo et al., 2000; Nagano et al., 2000; Nagano et al., 1998). Here, I present evidence for a unique function of *Noelin-4 in vivo*.

In whole embryos, *Xenopus Noelin-4* causes expansion of neural tissue by conversion of ectoderm into a neural fate. In animal caps, *Noelin-4* induces anterior neural fate. *Noelin-4* is a secreted protein and binds to another isoform, *Noelin-1*, in oocyte protein assays; in co-expression assays, *Noelin-4* and *Noelin-1* appear to cooperate to synergize induction of some neural marker genes, while *Noelin-4* activity is negatively affected by *Noelin-1*. Morpholino antisense oligos that target the four *Noelin* isoforms cause a reduction in dorsoanterior structures. Furthermore, in oocyte assays, *Noelin-4* appears to interact with BMP-4, suggesting that the mechanism of *Noelin-4* action might be to antagonize BMP signaling.

## METHODS

### Library screening and cDNA isolation

A stage 28 phage cDNA library in Lambda ZapII made from head tissues was kindly provided by Dr. R. Harland (Hemmati-Brivanlou et al., 1991).  $1 \times 10^6$

plaque-forming units were screened with chick *Noelin-1* and a PCR fragment of the mouse Z exon. The mouse subclone was generated by RT-PCR as described (Moreno and Bronner-Fraser, 2001; Chapter 4). Full-length clones of *Noelin-1*, -2 and -4 were obtained after low-stringency screening. Sequencing was done by PCR using dye-terminators and run on an ABI Prism automated sequencer. Sequences were compiled and edited using the DNASTar programs. Sequences were compared to others in GenBank using BLAST (Altschul et al., 1990). Signal peptide prediction was done by a computer modeling method on the server <http://www.cbs.dtu.dk/services/signalP> (Nielsen *et al.*, 1997).

*Noelin-3* (encoded by exons B-M-Y) was assembled from existing clones of *Noelin-1*. The B and M exons were amplified by PCR with the following oligos: upstream: 5'-CCA TCG ATC CAA GCA AAC ATG TCT GTG CC-3', and downstream: 5'-AGG CAG TTT AAG GGC TGA ATT CCG-3'. The oligos contain nested *Eco* RI (upstream) and *Cla* I (downstream) restriction sites for cloning into the same sites in pCS2+ (Rupp et al., 1994; Turner and Weintraub, 1994). The downstream oligo is complementary to the last 12 bases of the M exon, with an added glycine residue and stop codon (Y exon sequences) before the *Cla* I restriction site.

### ***Xenopus laevis* embryo and oocyte manipulations**

*Xenopus* embryos were obtained by *in vitro* fertilization using eggs from pigmented and albino females and testis from pigmented males, according to established methods (Sive et al., 2000). Embryos were staged according to the normal tables of Nieuwkoop and Faber (1967).

Animal caps were manually isolated from stage 8-9 blastulae and cultured in 3/4 X NAM (Slack and Forman, 1980) until siblings reached the stage indicated, when they were quick-frozen and stored at  $-80^{\circ}\text{C}$  until processing for RT-PCR.

*Xenopus* ovaries were dissected from sexually mature females through an abdominal incision after anesthetizing in Finquel's solution (Tricaine, Argent Chemical Laboratory). Ovaries were rinsed in OR2 medium (Sive et al., 2000) and then stored at  $14^{\circ}\text{C}$  in OR2 for up to 4 days. Stage VI oocytes were manually defolliculated in OR2 with fine forceps and allowed to recover for one day before injection. Oocytes that were in any way damaged by nicking or tearing were discarded.

## Microinjections

For oocytes: Capped messenger RNA was transcribed *in vitro* (Sive et al., 2000) and up to 2 ng was injected with a microinjection system (Medical Systems, Inc.) per oocyte in a volume of up to 20 nl. 5 injected oocytes per well of a 96-well dish were cultured in OR2 medium supplemented with 1 mg/ml of BSA (Sigma), Gentamycin and 10  $\mu\text{Ci}$  of [ $^{35}\text{S}$ ]-methionine (Express Protein Labeling Mix, NEN) in a total volume of 200  $\mu\text{l}$ . Injected oocytes were cultured for 24 hours. All samples were run in duplicate or triplicate for each experiment.

For embryos: Capped messenger mRNA was transcribed as above, or by using the mMessage mMachine SP6 kit (Ambion). Varying concentrations were injected in volumes ranging from 5-10 nl at the two-cell stage, into both blastomeres for animal cap experiments, into one cell of two for whole embryo

experiments, or 5 nl into 32-cell-stage blastomeres. *X-ngnr-1* was injected at 100 pg per embryo; *XNeuroD* was injected at 500 pg per embryo. *Noelin-3* or *-4* were injected at a range from 50 pg-1.5 ng or as indicated in the text. *noggin* was injected at a range of 50-100pg per embryo.

10 nl Morpholino Oligonucleotides (MOs, GeneTools LLC) were injected at a concentration range of 0.5  $\mu\text{g/ml}$  to 2  $\mu\text{g/ml}$  in water, with or without 80 pg  $\beta$ -galactosidase as a lineage tracer. Morpholinos were designed to complement the first 25 coding bases for the A or B exons:

AMO: 5'-TCA GCT TGC TTG GCG GTT GCT *Tca t-3'*

BMO: 5'-CAA TCT TGA GTA AAG GCA CAG *Aca t-3'*

(Underlined residue in BMO indicates a mismatch. This oligo was designed by M. Barembaum against the chick homolog; *Xenopus Noelin* B exon contains a T residue in that location. Lower-case, italicized residues indicate the initiation codon.)

Injected embryos were cultured until the indicated stage in 0.1 X MMR and fixed for 1 hour in MEMFA. After fixation, embryos were stored in 100% ethanol at  $-20^{\circ}\text{C}$  until further processing.

Embryos injected with  $\beta$ -galactosidase were stained with X-Gal (\*\*\*) or Magenta Gal (Biosynth): fixed embryos were rinsed 3 X 5 minutes in PBS, then 2 X 5 minutes in  $\beta$ -galactosidase Staining Buffer: (1 X PBS, 10mM Potassium Ferricyanate, 10mM potassium Ferrocyanate, 1mM  $\text{MgCl}_2$ ). X-Gal or Magenta Gal were added to the second wash at 1.5 mg/ml and staining was accomplished at  $37^{\circ}\text{C}$ . After staining was complete, embryos were rinsed twice in PBS and then stored in 100% ethanol until further use.

## Immunoprecipitations

Oocyte and supernatant fractions were collected separately. The oocytes were rinsed with 200  $\mu$ l of OR2 + BSA to remove any secreted material that might have adhered to the cell surface; this wash was added to the supernatant fraction. Samples were quick-frozen at  $-80^{\circ}\text{C}$  until further processing. *In vitro* translated protein was synthesized using the same capped mRNAs in Nuclease-treated Rabbit Reticulocyte Lysate (Promega) according to the manufacturer's instructions.

The oocyte fraction was prepared for immunoprecipitation by pipet trituration of 5 oocytes in 300  $\mu$ l PBS + 1% NP40 + inhibitors (PBSNI; inhibitors: Aprotinin, Leupeptin, Pepstatin; Sigma), centrifugation at  $4^{\circ}\text{C}$  for 3 minutes and then collection of the aqueous phase, which was brought up to 750  $\mu$ l with PBSNI. The supernatant fraction was prepared for immunoprecipitation by bringing up to 750  $\mu$ l with PBSNI. Anti-*myc* antibody (mouse monoclonal antibody 9E10, Santa Cruz Biotechnology) was used at 1:500 for 2 hours at  $4^{\circ}\text{C}$ . Anti-*flag* M2 antibody (mouse monoclonal, Sigma) was used at 10  $\mu\text{g}/\text{ml}$ . 15  $\mu$ l of settled bed volume Protein A Sepharose (Sigma) was incubated with the antibody-treated samples for 1 hour at  $4^{\circ}\text{C}$  with rocking; the sepharose beads were then washed three times in 1ml PBSNI and resuspended in SDS loading buffer. Samples were boiled for 5 minutes before loading on 8-14% SDS-polyacrylamide gels (Laemmli, 1970). Gels were fixed, amplified with 1M Na-Salicylate (Sigma), dried and exposed overnight to several days at  $-80^{\circ}\text{C}$  with an intensifying screen, or dried down directly and exposed to a Phosphor Storage

plate overnight, which was read on a PhosphorImager 445SI (Molecular Dynamics).

### ***In vitro* translation (IVT) inhibition with Morpholino oligonucleotides**

Roughly 500 ng each of *in vitro*-synthesized Noelin-1 and Noelin-4 mRNA (1  $\mu$ l) were pre-incubated with 2  $\mu$ l of MO (dissolved at 10 mg/ml or 1.1  $\mu$ M in sterile water) for 15 minutes at room temperature, along with 3  $\mu$ l reticulocyte lysate (nuclease-treated Rabbit Reticulocyte Lysate, Promega), 0.5  $\mu$ l amino acids minus methionine (Promega), and 0.5  $\mu$ l of RNase inhibitor (Promega). Following this incubation, the translation mix was added: 14  $\mu$ l of reticulocyte lysate, 1  $\mu$ l amino acids minus methionine, 1  $\mu$ l [ $^{35}$ S]-methionine (Express Protein Labeling Mix, NEN); this was incubated at 30°C for 90 minutes. IVT samples were stored at -80°C until further processing. Samples were run on SDS-PAGE gels with 14% acrylamide, and Benchmark Molecular Weight standards (Life Technologies) were used to determine approximate protein size.

### ***In situ* hybridization and immunohistochemistry**

*In situ* hybridization was performed as described (Knecht et al., 1995), except that only embryos hybridized to *N-tubulin* (Oschwald et al., 1991) were treated with RNases A and T1 to eliminate signal in ciliated epidermal cells. Probes were synthesized with digoxigenin-UTP (Roche) with the appropriate polymerase and purified by two ammonium acetate/ethanol precipitations, to avoid increased background due to free digoxigenin-UTP in the probe.

For immunohistochemistry, embryos were stored in ethanol, rehydrated to PBS and incubated in PBT (1XPBS, 1% Triton-X-100, 1 mg/ml BSA) for 15 minutes. Embryos were then blocked in PBT + 10% Goat serum (Life Technologies) for 1 hour at room temperature. Primary antibody incubation was overnight at 4°C with anti-phospho-histone H3 (rabbit IgG, Upstate Technologies) diluted 1:200 in PBT + 5 % goat serum, followed by 6 washes for 2 hours each in PBT. The primary antibody was detected with Horseradish Peroxidase-conjugated goat anti-rabbit IgG (Molecular Probes) at 1:400 in PBT + 5% goat serum, incubated overnight at 4°C. Secondary antibody was washed for 8 hours with several changes of PBT. Color detection reaction was carried out with 1 mg/ml 3', 3'-diaminobenzidine in PBS with H<sub>2</sub>O<sub>2</sub> at 1:1000. When staining was complete, embryos were rinsed several times in water, washed in PBS and photographed, then stored in ethanol at -20°C.

For sectioning, embryos were dehydrated to 100% ethanol, then washed 2 X 20 minutes in HistoSol (National Diagnostics), 1 X 1 hour Paraplast Plus wax (Oxford) at 60°C, followed by an overnight incubation in wax. Embryos were embedded in fresh wax and sectioned on a Leitz microtome at 10 µm. Sectioned whole mount *in situs* were counterstained in Light Green SF (Sigma): sections were de-waxed 3 X 5 minutes in HistoSol, 2 X 1 minute 100% ethanol, 1 minute 95% ethanol, 1 minute 90% ethanol, followed by 30 seconds to 2 minutes in 0.25% Light Green in 90% ethanol. Once sections were determined to be adequately stained, sections were rinsed in clear 90% ethanol and dehydrated back to HistoSol before cover-slipping with Permount (Sigma). Images were captured on a Zeiss Axiophot with an Apogee digital camera.

## RT-PCR Analysis

Pools of total RNA from 2 embryos or 10 animal caps were isolated beginning by Proteinase K treatment (ICN Pharmaceuticals; 250 µg/ml in 20mM Tris, 100mM NaCl, 30mM EDTA, 1% SDS) for 1 hour at 37°C. DNA was removed by treatment with RNase-free DNase I (Roche) for 1 hour at 37°C. First strand cDNA was synthesized on RNA from 5 animal cap equivalents using Superscript II Reverse Transcriptase (Life Technologies) with random hexamers (Life Technologies) according to manufacturer's instructions. The amount of cDNA synthesized in experimental samples was normalized for *EF1α* using a PhosphorImager 445SI and ImageQuant software (Molecular Dynamics). All RNA samples were tested for genomic DNA contamination in minus-reverse transcriptase reactions. The linear ranges of amplification for each primer set were determined using cDNA representing 0.005 of a whole embryo for each reaction (roughly equivalent to 0.25 of 1 animal cap explant), at the stage for which the animal caps were to be analyzed. PCR reactions were performed in 1 X PCR buffer: 10mM Tris-HCl pH 8.3, 1.5mM MgCl<sub>2</sub>, 50mM KCl; with 0.5µCi [ $\alpha$ -<sup>32</sup>P]-dCTP, 100µM each nucleotide, 0.8µM each primer and 1.5 units Taq polymerase. Cycle conditions used were: [30 seconds at 94°C, 1 minute at 55°C, 1 minute at 72°C] for the cycle number indicated below; preceded by a 5 minute denaturation at 94°C and followed by a 6 minute extension at 72°C. One-third of each reaction was run on a 5% polyacrylamide gel and analyzed autoradiographically and on the PhosphorImager. PCR primer sets and the cycle numbers used for each are listed below:

*EF1 $\alpha$* : (Agius et al., 2000); 221 nt; 20 cycles

U: 5'-CCT GAA CCA CCC AGG CCA GAT TGG TG-3'

D: 5'-GAG GGT AGT CAG AGA AGC TCT CCA CG-3'

*Muscle actin*: (Hemmati-Brivanlou and Melton, 1994); 222 nt; 23 cycles

U: 5'-GCT GAC AGA ATG CAG AAG-3'

D: 5'-TTG CTT GGA GGA GTG TGT-3'

*NCAM*: (Hemmati-Brivanlou and Melton, 1994); 342 nt; 26 cycles

U: 5'-CAC AGT TCC ACC AAA TGC-3'

D: 5'-GGA ATC AAG CGG TAC AGA-3'

*Otx-2*: (Sasai et al., 1995); 315 nt; 28 cycles

U: 5'-GGA TGG ATT TGT TGC ACC AGT C-3'

D: 5'-CAC TCT CCG AGC TCA CTT CTC-3'

*En2*: (Hemmati-Brivanlou and Melton, 1994); 302 nt; 28 cycles

U: 5'-CGG AAT TCA TCA GGT CCG AGA TC-3'

D: 5'-GCG GAT CCT TTG AAG TGG TCG CG-3'

*Krox20*: (Mariani and Harland, 1998); 323 nt; 30 cycles

U: 5'-ATT CAG ATG AGC GGA GTG-3'

D: 5'-ATG TGC TCC AGG TCA CTT-3'

*HoxB9*: (Hemmati-Brivanlou and Melton, 1994); 217 nt; 28 cycles

U: 5'-TAC TTA CGG GGC TTG GCT GGA-3'

D: 5'-AGC GTG TAA CCA GTT GGC TG-3'

*Synaptobrevin II*: (Knecht et al., 1995); 307 nt; 30 cycles

U: 5'-ATT TGT CTG TGC GCA GGT-3'

D: 5'-TTT AAG CCA CTC CCT GCT-3'

*XNeuroD*: (Lallier and DeSimone, 2000); 238 nt; 30 cycles

U: 5'-GTG AAA TCC CAA TAG ACA CC-3'

D: 5'-TTC CCC ATA TCT AAA GGC AG-3'

*XBru3d*: (Moreno and Bronner-Fraser, 2001); 277 nt; 28 cycles

U: 5'-CAT CAC CCT TCT GTT TTA-3'

D: 5'-GGG TCT GTT TCA CTT TCA-3'

*Pax-6*: (<http://www.lifesci.ucla.edu/hhmi/derobertis/index.html>); 232 nt, 26 cycles

U: 5'-CAG AAC ATC TTT TAC CCA GGA-3'

D: 5'-ACT ACT GCT AAT GGG AAT GTG-3'

*Slug*: (LaBonne and Bronner-Fraser, 1998); 26 cycles

U: 5'-CAA TGC AAG AAC TGT TCC-3'

D: 5'-TCT AGG CAA GAA TIG CTC-3'

*Sox-2*: (<http://www.lifesci.ucla.edu/hhmi/derobertis/index.html>); 214 nt, 25 cycles

U: 5'-GAG GAT GGA CAC TTA TGC CCA C-3'

D: 5'-GGA CAT GCT GTA GGT AGG CGA-3'

*Noelin* isoform primers: A+Y, A+Z, B+Y, B+Z; each product approx. 330 nt, 30 cycles

*Noelin A*: 5'-GCA AGC TGA TGA GTC TCT TC-3'

*Noelin B*: 5'-GGA ACC TTG GAT AGG AGC-3'

*Noelin Y*: 5'-TGC CTC TTC AGT CTT TGC-3'

*Noelin Z*: 5'-CAA CAC TGG TAT CAG AGG-3'

## RESULTS

### ***Noelin-3* and *-4* sequence and structure**

*Noelin-4* was previously isolated from rat (GenBank accession #I73636), mouse (pancortin-4, BAA28764), and human (JC5272), with shared identity of between 89-92% for these species. Although this protein is slightly related to *Olfactomedin*, the founding family member of the Olfactomedin-domain containing family (Kulkarni et al., 2000; Snyder et al., 1991), it lacks the Z region of *Noelin-1* and *-2* that contains this domain. Additionally, a region of *Noelin-4* (amino acids # 45-115) has approximately 56% similarity to a short domain of a myosin heavy chain protein found in *C. elegans* (GenBank accession # CAA95848) and 49% similarity in the same domain to an undescribed protein found in the *Drosophila melanogaster* genome (GenBank accession # AF49873).

*Xenopus Noelin-4* was isolated in a low-stringency screen for genes containing nucleotide sequences similar to the Olfactomedin domain and surrounding regions of *Noelin-1* (Moreno and Bronner-Fraser, 2001). A full-length clone (Fig. 1; 1227 base pairs, bp) of *Noelin-4* including 5' and 3' untranslated regions was cloned from a stage 28 head library (Hemmati-Brivanlou et al., 1991). This isoform contains the A, M, and Y exons, and is the smallest of the four *Noelin* splice variants. The longest open reading frame (381 bp) from the first start codon encodes a predicted 126 amino acid (aa) protein with a molecular weight of approximately 14.7 kilodaltons (kD).

*Noelin-4* has several conserved features including one N-linked glycosylation site (Fig. 1, black arrowhead) and two potential hyaluronate

binding sites (Fig. 1, yellow underlines). Furthermore, two cysteine residues are conserved in all Noelin isoforms (Fig. 1, green asterisks) and are spatially homologous to two cysteine residues that in Olfactomedin are thought to be responsible for intermolecular disulfide bonding (Yokoe and Anholt, 1993). As with Noelin-2, Noelin-4 has a hydrophobic leader sequence that is predicted to be cleaved after residue #26 in the sequence VLP –TN, which removes the entire A region. This leaves essentially the M region as the mature protein since the Y exon encodes one glycine residue and then a stop (Fig.1, signal sequence denoted by red residues). Together, the sequence results suggest that Noelin-4 may be a glycosylated and secreted protein.

*Noelin-3* was not isolated in the library screens, but due to its simple structure, the coding sequence of this isoform was assembled from existing clones. *Noelin-3* was synthesized by the removal of the Z exon from *Noelin-1* and the addition of the only coding sequence of the Y exon, a glycine residue followed by a stop codon (see Methods). Its sequence and structure are identical to the B and M regions of *Noelin-1* that are shown in detail in Moreno and Bronner-Fraser, 2001. It differs from *Noelin-4* in that the B region is longer than the A region, and it encodes a shorter signal peptide. After cleavage this leaves a greater number of residues in the mature protein than in *Noelin-4*. The deduced protein length is 156 aa, with a predicted molecular weight of 17.3 kD. *Noelin-3* contains an additional N-linked glycosylation site (see Chapter 1 and Moreno and Bronner-Fraser, 2001, Fig. 1A).

### **Noelin-4 is a secreted protein**

To determine whether Noelin-4 was a secreted protein, I performed oocyte secretion assays. Two different constructs of *Xenopus Noelin-4* (Fig. 2A) were expressed in oocytes, which were cultured in the presence of [<sup>35</sup>S]-methionine. Oocyte and supernatant fractions were immunoprecipitated with antibodies to the epitope tags subcloned into the constructs.

Full-length Noelin-4 with a carboxy-terminal *myc* tag was found in both the oocyte and supernatant fractions (Fig. 2B, lanes 1 and 2). Furthermore, the size of the oocyte-synthesized protein was larger than the *in vitro*-translated protein (lane 3), suggesting that the oocytes glycosylated Noelin-4. Thus the hydrophobic leader sequence was indeed cleaved *in vivo*, and the protein was robustly secreted from *Xenopus* oocytes.

Noelin-4 was more robustly secreted than Noelin-1 or -2 (compare to oocyte assays in Chapter 2, Fig. 3C), most likely because it does not contain the carboxy terminal sequence Ser-Asp-Glu-Leu (SDEL) that is found in the Z-containing isoforms. This sequence is similar but not identical to the consensus sequence Lys-Asp-Glu-Leu (KDEL), which is the consensus sequence for protein retention in the endoplasmic reticulum (ER) of vertebrate, *Drosophila*, *C. elegans* and plant cells (Munro and Pelham, 1987). The ER-like signal in Noelin-1 and -2 is likely responsible for less efficient secretion (Moreno and Bronner-Fraser, 2001).

To show that the A region was responsible for the secretion of Noelin-4, another construct was made in which the A region was removed (see Fig. 2A for schematic). Noelin-4ΔA-*myc* was synthesized in oocytes (Fig. 2C, lane 2) but was

not secreted (lane 3). In addition, the protein made from this construct was not glycosylated, since *in vitro* translated protein was the same size as *in vivo* synthesized protein (compare lanes 1 and 2). Glycosylation occurs as proteins move through the ER and Golgi apparatus; if they never enter (because they do not contain a signal peptide) then they will not be glycosylated. This shows that the A region is necessary for the secretion of Noelin-4 and confirms that the leader sequence functions as a signal peptide.

Noelin-3 was not directly tested in this assay; however, it is very likely that this protein is also secreted. Its amino-terminal leader sequence is the same as in Noelin-1 (B region), which was cleaved, allowing Noelin-1 to be secreted. Furthermore, Noelin-3 contains the Y region and not the Z region. Unlike the Z region, the Y region encodes no known signals for sorting mechanisms within the cell or for retention in the ER.

### **Noelin-4 binds Noelin-1**

My previous studies of Noelin-1 (Chapter 2) demonstrated that it may have binding partners either within the cell or in the extracellular environment. Under non-reducing gel conditions, Noelin-1 protein ran as a band larger than 205 kD, the largest size-marker used. I hypothesized that because of the similarities between Noelin-1 and Olfactomedin, a protein that forms multimers in the extracellular matrix, Noelin-1 may also form multimers with itself or other protein partners. Noelin-4 and Noelin-1 share the common M region that contains spatially conserved cysteine residues (see Fig. 1, green asterisks) that in

Olfactomedin are responsible for intermolecular disulfide bonds (Yokoe and Anholt, 1993).

To determine whether these protein isoforms could interact in my assay system, I co-expressed Noelin-4 and Noelin-1 and then immunoprecipitated with antibodies to the different epitope tags on each protein. The *Xenopus* Noelin-4 construct contains a carboxy terminal *myc* tag; this was co-expressed with a quail Noelin-1 construct bearing an internal *flag* epitope at a unique Bam HI site in the Z region. Quail Noelin-1 performed similarly to *Xenopus* Noelin-1 in secretion assays and is 93% identical in protein sequence (Barembaum et al., 2000; Moreno and Bronner-Fraser, 2001).

Co-injected oocytes made proteins of the expected sizes for both Noelin-4 and Noelin-1. In oocyte and supernatant fractions, the greatest portion of immunoprecipitated Noelin-4 migrated at approximately 22 kD, with a weaker band found at about 11 kD (Fig. 2D, lanes 3 and 4 Noelin-4 bands). Immunoprecipitated Noelin-1 ran at approximately 60 and 77 kD (cellular and secreted forms, respectively), and only the larger species was found to be secreted (Fig. 2D, lanes 5 and 6 Noelin-1 bands). Immunoprecipitation of Noelin-4-myc co-precipitated Noelin-1-flag (see Fig. 2D, lanes 3 and 4). The reciprocal was also true; Noelin-1-flag brought down Noelin-4-myc with the anti-*flag* antibody (see lane 5). Thus, co-expression of Noelin-4 with Noelin-1 in *Xenopus* oocytes reveals that the two proteins can form complexes *in vivo*.

### **Noelins are expressed early in development**

*Noelin-1* and *-2* are expressed from stage 20 in post-mitotic neural tissues (Moreno and Bronner-Fraser, 2001). In chick embryos, *Noelin* isoforms begin to

be expressed at neural plate stages (Barenbaum et al., 2000), much earlier than was observed in *Xenopus* (Moreno and Bronner-Fraser, 2001). Thus, to examine Noelin expression in earlier stages more closely, a developmental series of RT-PCR was performed. cDNA was made from total RNA isolated from stages ranging from late gastrulation (stage 12) through tailbud stages (stage 31 was the latest stage used). PCR oligonucleotides directed to regions flanking the common central M exon were designed in order to specifically amplify each of the four isoforms individually.

Figure 3 details the results of this experiment. Interestingly, the B-containing isoforms were amplified from stage 14 onward, with increasing expression as development proceeds (Fig. 3, lanes 2-6 in *Noelin-1* [BMZ] and *Noelin-3* [BMY] gels). Note that although the levels of expression appear different between *Noelin-1* and *Noelin-3* in these gels, they are not directly comparable since different primer sets have different efficiencies of amplification in PCR. This experiment simply detects the presence of transcripts in the samples, but relative abundance cannot be ascribed outside of each primer set. The A-containing isoforms *Noelin-2* and *Noelin-4* were present at very low levels through the same stages as the B-containing isoforms, and may be present at very low levels even earlier (Fig. 3, *Noelin-2* [AMZ] and *Noelin-4* [AMY] gels), and like the B isoforms, were also strongly expressed by stage 25 (lane 5). It is not known whether these low levels expressed in the neural plate stages are functionally significant. It is interesting to note that all four isoforms may be present beginning from earlier developmental stages than were detected by whole mount *in situ* hybridization (Moreno and Bronner-Fraser, 2001).

### ***Noelin-3* and *-4* are expressed in post-mitotic neural tissues**

To examine the spatial expression pattern of *Noelin-3* and *-4*, whole mount *in situ* hybridization was performed with several probes from different regions of the sequences of *Noelin-3* (BMY) and *Noelin-4* (AMY). Results with the Y exon probe are shown in Figure 4, and are equivalent to those obtained with the A and B exons (Moreno and Bronner-Fraser, 2001).

The expression pattern observed with the Y exon (*Noelin-3* and *-4*) is the same as for that of the Z exon (*Noelin-1* and *-2*; Moreno and Bronner-Fraser, 2001). *In situ* hybridization for the Y exon reveals the distribution pattern of the mRNAs in post-mitotic neural tissues in the brain, spinal cord and cranial ganglia beginning at stage 21 (see Fig. 4). Y-exon expression in the spinal cord, trigeminal (V<sup>th</sup>) ganglia and olfactory placodes at stage 21 is shown in Fig. 4A and B. Stronger expression in these tissues was observed at stage 26 (Fig. 4C and D), along with the onset of expression in the geniculate ganglion (VII<sup>th</sup>). By stage 28, expression was very strong in the spinal cord and cranial ganglia. At stage 42 (Fig. 4G), strong expression was noted in the eye (arrow) and cranial ganglia (arrowheads). Furthermore, expression was found in the neuromasts of the lateral lines, which are hair and support cells that are innervated by the lateral line ganglia (Fig. 4H).

Thus *Noelin* isoforms mark post-mitotic neural cells in both the peripheral nervous system (cranial ganglia and lateral lines) and the central nervous system (eye, brain, spinal cord). Furthermore, all *Xenopus Noelin* isoforms appear to be expressed with the same distribution patterns, at least as visualized by whole mount *in situ* hybridization.

### ***Noelin-4* is induced by neurogenic genes**

Neurogenesis is controlled by a neurogenic cascade of transcription factors that activate and promote neuronal differentiation. Ectopic expression of neurogenic genes causes neurons to develop in the epidermis. Since *Noelin* genes are expressed in post-mitotic neural tissues, and since *Noelin-1* and *-2* are induced by the neurogenic genes *Neurogenin* (*X-ngnr-1*) and *XNeuroD* (Moreno and Bronner-Fraser, 2001), I wished to confirm that *Noelin-3* and *-4* were also downstream of the neurogenic cascade.

As with *Noelin-1* and *-2* (Z exon representation), the Y exon was also expressed in the ectopic neurons induced by both *XNeuroD* and *X-ngnr-1*. Figure 5A shows an embryo injected with 100 pg *X-ngnr-1* mRNA and stained with the Y exon probe. Many ectopic neurons developing within the epidermis were also positive for *Noelin-3* and *-4* (arrows). The neuronal differentiation marker *N-tubulin* (Oschwald et al., 1991) was induced to a higher degree and in more cells as compared to *Noelin* induction (arrows, Fig. 5B; compare to 5A), as was observed for *Noelin-1* and *-2* (see Chapter 2). In general, every embryo injected with *X-ngnr-1* or *XNeuroD* displayed the ectopic neuron phenotype as assayed by *N-tubulin* or Y-exon induction in the epidermis (for one representative experiment: 96%, n = 25). In addition, *N-tubulin* appeared to mark a greater number of neurons than *Noelin* isoforms did. This suggests that *Noelin* isoforms mark a subset of neurons induced by neurogenic genes. The results were identical with *XNeuroD* injections (data not shown).

I next examined whether neurogenic genes could induce *Noelin-3* and *-4* expression in the absence of mesoderm signals, by using animal cap explants.

*Xenopus* animal caps normally differentiate into epidermis when cultured; however, when exposed to neuralizing signals, animal caps can be induced to express neural markers. This experiment is a more direct test of the ability of *Noelins* to be induced by neurogenic genes, since in the embryo, the neurogenic domain is established in the ectoderm where many neuralizing signals from the mesoderm have already been received; whereas animal caps have not been exposed to mesoderm and thus are considered to be more “naïve.” Thus, this is a more direct test of the ability of neurogenic genes to induce *Noelin* expression.

Embryos were injected in both blastomeres at the 2-cell stage with 100 pg *X-ngnr-1* mRNA; controls were injected with 100 pg of  $\beta$ -galactosidase mRNA. Animal caps were isolated at stage 8-9 and were cultured until sibling embryos reached stage 24, when they were fixed and processed for whole mount *in situ* hybridization against the Y exon or *N-tubulin*. *Noelin-3* and *-4* were induced weakly in animal caps expressing *X-ngnr-1* (Fig. 5C). *N-tubulin* was highly induced by *X-ngnr-1* (Fig. 5D). Control animal caps injected with  $\beta$ -galactosidase did not express the Y exon (Fig. 5E). The results obtained for *XNeuroD* injections were identical (data not shown).

Thus *Noelin-3* and *-4* are also induced by genes in the neurogenic cascade. Like *Noelin-1* and *-2*, they are induced to a higher degree in whole embryos, suggesting that further signals that are not present in animal caps are required for robust expression. Furthermore, these results show that both A and B promoters can be induced by over-expression of neurogenic transcription factors.

## ***Noelin-4* over-expression causes neural expansion in embryos**

I next wished to examine the function of *Noelin-4* by over-expression of the gene in whole embryos. *Xenopus* embryos divide into right and left halves with their first cleavage after fertilization. Injection of one of the cells at this stage gives a fairly reliable distinction between injected and uninjected halves in the left-right axis of the later embryo, in which the uninjected side can often be considered an internal control. At *Noelin-4* doses ranging from 500 pg to 1 ng, 85% of the injected embryos exhibited abnormal development of the nervous system. A summary of phenotypes that are described in the following sections is given in Table 1.

Table 1: *Noelin-4* over-expression phenotypes

Phenotype	Injection dose	%injected/ %control
Spina bifida	500 pg, 1 ng	41/2
Dorsalization	500 pg, 1 ng	50/2
Bifurcated tail	500 pg, 1 ng	18/0
Enlarged retina	500 pg, 1 ng	38/0
Enlarged neural tube	500 pg, 1 ng	33/0
Ectopic cement gland	1 ng	18/0
Ectopic pigment cells	1 ng	10/0
Retinal pigmented epithelium extending into midbrain	1 ng	15/2
Ectopic neural structures (e.g., partial duplicated axis, Fig. 9M)	1 ng	10/0
Tissue protrusions/bare mesoderm	1 ng	5/0
Disorganized/missing anterior neural structures (conglomeration)	1 ng	18/0
Normal phenotype	500 pg, 1 ng	15/94

Table 1: Over-expression phenotypes observed for *Noelin-4*. Two experiments were combined (injected embryos  $n = 100$ , control embryos  $n = 50$ ) and data were tabulated for both. Most embryos displayed multiple phenotypes, e.g., dorsalization was often accompanied by enlarged neural tissue; spina bifida was also found with enlarged retina. Most embryos with spina bifida were dorsalized. Cement glands, pigment cells, and retinal pigmented epithelium extension were scored by visual inspection of unstained whole mounts. Enlarged neural tube and retina, as well as ectopic neural structures, were scored by Sox-2 staining appearance.

When embryos were injected with 500 pg of *Noelin-4* mRNA in one blastomere at the 2-cell stage, I observed an expansion of neural tissue (numbers are given in Table 1). This phenotype was easily scored as an enlarged, asymmetrical neural plate developed. In one example shown in Figure 6, staining of an embryo with the pan-neural marker *Sox-2* at stage 16 showed that on the injected side, the neural plate had grown considerably larger than on the uninjected side (Fig. 6A). In cross-section, the neural plate was obviously wider on the injected side (Fig. 6B). Sibling embryos injected with *Noelin-2* (AMZ) or  $\beta$ -galactosidase did not exhibit an expansion of neural tissue either by overt morphology or by *Sox-2 in situ* hybridization (Fig. 6C and D).

Embryos that were allowed to develop to stage 24 also showed an expansion effect in the retina in addition to expanded neural tube (Fig. 7). At this stage, *Sox-2* staining demarcates the neural tube and the emerging optic vesicles. On the injected side of the embryo in Figure 7A the retinal staining of *Sox-2* showed an expanded eye. In cross-section, the expanded retina was observed to be much larger than on the control side. Figures 7B –D show that throughout the eye-region sections, the injected-side retina was enlarged in anterior-posterior length as well as in thickness of the retina. When the injection site was not localized to the eye but rather to more caudal regions of the neural tube, the result was an expansion of the neural tube (Fig. 7E), showing that the expansion effect was not restricted to retinal or strictly anterior cell types.

At later stages, the *Noelin-4*-induced expansion of retina was observed to cause further defects in development. At stage 29, the optic vesicle has begun to evaginate and form the optic cup. Embryos over-expressing *Noelin-4* often

displayed retinas that were delayed in evagination in addition to being enlarged. Figure 8 shows an example of this phenotype. On the control side, normal *Sox-2* staining was observed (Fig. 8A and C). On the injected side, the retina appeared much larger (Fig. 8B and C). In cross-section at the largest diameter of the uninjected eye, the retina had begun evagination (Fig. 8D). An image of the injected-side eye at the same magnification shows a greatly enlarged retina in both circumference and thickness, and also reveal that the retina did not evaginate (Fig. 8E). Evagination may not have occurred because of morphological problems due to the large retina size, or to a delay in its development by a molecular mechanism related to the over-expression of *Noelin-4*. This embryo also exhibited an expansion of the neural tube (Fig. 8F).

In addition to the neural expansion phenotype I have described in this section, I also observed a high percentage of injected embryos with mild dorsalization (reduction of tail structures, bent axis) and spina bifida (open spinal cord; see Table 1). These phenotypes can be seen as non-specific perturbations of development in a low percentage of untreated embryos; however, my results suggest that in the context of *Noelin-4* over-expression, these perturbations may be due to the dorsalization effects of *Noelin-4* in which ventral/posterior fates are lost and dorsal/anterior fates are increased (e.g., expansion of neural plate and subsequent structures).

### **High dose *Noelin-4* over-expression causes ectopic neural development**

I next examined whether the phenotype of *Noelin-4* over-expression was dose-dependent. I injected higher doses (1 ng mRNA) and followed with whole

mount *in situ* hybridization for several gene markers of different neural fates. It was immediately evident that higher doses increased the frequency and severity of the spina bifida phenotype. As many as 50% of embryos exhibited a failure of neural tube closure in five separate experiments (n = 185; see also Table 1). In some cases the neural tube was closed in the head but remained open in the trunk; in others the neural tube was open along the entire axis. In all spina bifida cases, most head structures developed (cement gland, eye, cranial ganglia) but on the injected side of the embryo, if the lineage tracer localized to the head region, the brain and eye were observed to be much larger than on the uninjected side. Embryos with naturally-occurring spina bifida most commonly developed symmetrically-shaped heads in the absence of *Noelin-4* over-expression (data not shown). Moreover, embryos injected with the same doses of *Noelin-2* did not exhibit this phenotype (data not shown), indicating that these results were specifically due to the over-expression of *Noelin-4*.

#### *Anterior neural phenotype: eye and cement gland*

Neural-specific perturbations were observed in anterior regions with high-dose *Noelin-4* over-expression. Additional morphological effects were observed in the head: phenotypes observed were an extension of the retinal pigmented epithelium (RPE) into the midbrain, ectopic *Sox-2*-positive regions, and ectopic pigmented cells that resembled RPE cells (see Table 1). These were in addition to expansion of the eye and brain similar to the lower dose over-expression phenotype.

In Figure 9, a sampling of the observed phenotypes is shown. A stage 35 embryo stained with *Sox-2* exhibited a normal uninjected side (Fig. 9A), but on

the injected side, a mass of tissue above the eye (arrowhead) was observed. In the whole mount view, pigmented cells were gathered on the ectopic mass, however the color is obscured by the staining for the lineage tracer and *Sox-2* hybridization (Fig. 9B). In cross-section, this mass can be seen as a round-shaped *Sox-2* positive region with a morphology and expression of *Sox-2* resembling an eye. Some pigmented cells are on the ectodermal side of the mass (arrowhead in Fig. 9C) indicating they may be of neural crest origin. The ectopic mass had a basement membrane as well, which is visible in the magnified view (Fig. 9D, arrow).

Another embryo displayed gross perturbations of anterior development (Fig. 9E-H). In this case, the injected-side eye was indistinguishable upon observation of the whole mount embryo (Fig. 9F). In cross-section, this embryo exhibited aberrant eye development, with a dorsally expanded retina (arrowhead, Fig. 9G). Ventrally the eye appeared to be relatively normal; its retina was partially evaginated and a lens had formed (compare stars in Figs. 9G and H). Interestingly, a group of pigmented cells grouped around the dorsal expansion of the retina (Fig. 9G, arrow). It is not clear whether these are melanocytes or retinal pigmented epithelium. Slightly more caudal to the section in Fig. 9G, the eye was found to be continuous with the midbrain (Fig. 9H, arrowhead), which is abnormal for this stage.

Several embryos displayed ectopic cement gland development (see Table 1). The cement gland is considered to be the most anterior ectodermal structure, and although it is not neural in nature, it is induced along with the neural ectoderm. Thus its ectopic presence can be considered a mark of neural

perturbation as well as cement gland induction. Cement glands were identified by cellular morphology and overall structural appearance (Fig. 9H, arrow). Ectopic cement glands were discontinuous with the endogenous ones (compare “cg” in Fig. 9F with arrow in 9F and 9H) and were always located on the head ectoderm, usually below the midlevel of the eye, often on top of the branchial arches.

*Trunk over-expression phenotype: ectopic neural structures*

Over-expression of *Noelin-4* at high doses also led to perturbed trunk development. Some embryos displayed ectopic *Sox-2* staining near the neural tube in the trunk, some developed ectopic vesicular structures, and some had aberrant epidermal development (see Table 1). Examination of posterior regions of the embryos also revealed that normal tail structures failed to form; often the embryos were mildly dorsalized with shortened tail structures.

A sample of some of the trunk phenotypes is given in Figures 9I-Q. A dorsalized embryo with the characteristic lack of tail structures is shown in Figure 9I. *Sox-2* staining revealed the location of the normal neural tissue as well as a stretch of ectopic neural development along the antero-posterior axis. In cross-section, this ectopic *Sox-2*-positive tissue contained a vesicle, similar to an otic vesicle (arrow, Fig. 9J). This vesicle formed considerably caudal to the normal otic vesicles, which formed at the hindbrain level (asterisk in Fig. 9I).

In addition to ectopic vesicle formation, another trunk phenotype observed was the development of neural tissue that resembled a partially duplicated axis. Stretches of bulging neural tissue (as characterized by *Sox-2* staining) were observed near the neural tube, and were connected with the

neural tube at their caudal extents (see Table 1). An example of this lower-frequency phenotype is shown in Fig. 9K-Q. On the injected side, the embryo exhibited several regions of ectopic *Sox-2*-positive cells, both in the head (arrows) and trunk levels (arrowhead, Fig. 9L). In a dorsal view, the ectopic *Sox-2* staining in the trunk is continuous with the neural tube at its posterior extent (Fig. 9M, black arrow for ectopic structure, white arrow for neural tube; and Fig. 9Q for cross-section). The embryo shown also developed an extra vesicle structure. A section through the otic vesicles at the hindbrain level is shown in Fig. 9O (asterisks mark vesicles). The ectopic vesicle developed posterior to the normal otic vesicles (arrow, Fig. 9P). In addition, the reduced tail structures phenotype is evident in this embryo.

### *Epidermal defects*

In addition to ectopic neural development near endogenous neural tissue, ectopic neural tissue formed in distal regions, concurrent with severe perturbations in epidermal development. Some embryos displayed tissue protrusions in the ectoderm covering the trunk, and in those cases, the epidermis appeared to have constricted into the protrusions and did not cover the mesoderm in that region. Also, some cells at the tips of the protrusions expressed *Sox-2* (see Table 1). An example of this phenotype is given in Figure 10. On the injected side, the embryo displayed ectopic regions of *Sox-2* staining (Fig. 10B), enlarged neural tissues (Fig. 10D) and a possible axial duplication (Fig. 10E). Tail structures in this embryo were reduced (asterisk, Fig. 10C).

In cross-section, this embryo displayed elements of the lower-dose phenotype in the expansion of the otic vesicle on the injected side. A section

through the hindbrain level revealed that the injected-side otic vesicle was at least twice the size of the control side (Fig. 10D, inset at same magnification). Panel E shows ectopic neural tissue that resulted from over-expression of Noelin-4. In this section a bulge of neural tissue (*Sox-2*-positive) was observed adjacent to the neural tube. It is unclear whether this tissue resulted from an incompletely duplicated axis, an increase in proliferation of earlier neural precursors, or conversion of other tissues into a neural fate.

In an example of what appears to be conversion of tissue to a neural fate, Figure 10F shows a cross-section through a tissue protrusion that formed in the ectoderm of this embryo. At the distal end of the protrusion, a small region of *Sox-2* stain was observed indicating the presence of neural tissue. The shape of the *Sox-2* stain suggested that a basement membrane had formed (arrow). Intriguingly, several pigment cells were observed at the junction of the *Sox-2*-positive tissue and the non-neural portion of the protrusion (arrowhead). It cannot be ruled out that the pigmented cells were endogenous melanocytes. However, in normal embryos, the trunk melanocytes generally lie closer to the neural tube; the path for a cell to move into the tip of the protrusion would be much further than a melanocyte would typically travel. Furthermore, the neural tube in this embryo was closed through the length of the tail, eliminating the possibility that somehow the tissue protrusions formed from cells that should have made up part of the neural tube. Neural crest cells are induced at the border between neural and non-neural ectoderm; this type of border could have occurred in the protrusion with the *Sox-2*-positive tissue representing the neural fate and adjacent epidermis representing the non-neural fate. Together, these

observations suggest a conversion of ectoderm into a neural fate, and that the melanocytes may have been induced to form inside the tissue protrusion.

*Localization of mRNA determines the type of phenotype*

A further interesting observation from the high-dose phenotype embryos is that lineage tracer-positive cells, which presumably indicate cells derived from the highest concentration of the injected mRNA (lineage tracer was injected at 1/5 – 1/10 of the concentration of *Noelin-4*), generally were found surrounding ectopic neural tissue. Expanded neural regions expressed the lineage tracer as well, but the most highly expressing cells were usually found adjacent to the ectopic *Sox-2* tissue (see Figs. 9C, D, G, H and 10D-F). However, when ectopic cement glands formed, the cells highly expressing the lineage tracer were part of the ectopic structure instead of adjacent to it. This may suggest that some of the effects of *Noelin-4* over-expression are non-cell-autonomous (ectopic neural tissue), while others may be cell-autonomous (ectopic cement glands).

In addition to neural tissues, mesoderm was also examined for perturbation. In all experiments described here, the injection was targeted to future ectoderm, thus mesoderm itself was not expected to express appreciable levels of *Noelin-4*, although it would be exposed to *Noelin-4* protein by secretion from the ectoderm. Examination of tissue cross-sections showed relatively normal organization of notochord and somites considering the degree of perturbation in the ectoderm. In examinations of cross-sectioned embryos with bulges of neural tissue similar to a duplicated axis, I did not observe ectopic notochord or segmentation of the mesoderm underlying the ectopic neural masses to indicate somites (e.g., see Fig. 9J, 9O, 10E, 11G, 11H).

### **Mechanism of *Noelin-4*-induced expansion is not increased proliferation**

I next wished to examine the mechanism of neural expansion by *Noelin-4* over-expression. It is possible that the enlarged neural tissue resulted from increased proliferation by *Noelin-4*-expressing cells; alternatively, the expansion of neural fate could be accomplished by conversion of other ectodermal cells (neural crest and epidermal ectoderm). To determine whether increased proliferation could be the cause of the expansion, I used the mitosis marker anti-phospho-histone H3 antibody, which marks cells in and shortly after metaphase. *Xenopus* cell division patterns have previously been characterized using this marker (Saka and Smith, 2001); thus for these studies it was a useful way to compare proliferation in normal *versus* *Noelin-4* overexpression contexts.

Figure 11 shows the results of these experiments. Embryos were injected with the lower dose of *Noelin-4* mRNA (500 pg) that caused the expansion phenotype, and examined for expression of phospho-histone H3. At stage 14, no evidence of increased cell division was observed (n = 4, Fig. 11A). In cross-section, the neural plate appeared expanded on the injected side (arrows, Fig. 10B), but no increase of cells in metaphase was observed (Fig. 11B). Also at stage 23, no increase in proliferation was observed (n = 4). Dorsal (Fig. 11C) and lateral (Fig. 11D) views of an embryo with a clear expansion of tissue in the injected region did not exhibit any extra mitotic cells. In cross-section, metaphase cells were observed (arrowheads, Fig. 11G); however, there was no difference between injected and uninjected sides, even in the strongly stained regions of lineage tracer (Fig. 11H). Thus it seems likely that *Noelin-4* does not induce neural expansion by increasing rates of proliferation in affected areas.

### ***Noelin-4* causes expansion of neural tissue by conversion of ectoderm**

To examine whether *Noelin-4*-induced neural expansion occurred at the expense of other ectodermal derivatives such as the neural crest and epidermis, I examined expression of the neural crest marker *XTwist* (Hopwood et al., 1989) in injected embryos. Neural crest formation and migration appeared normal in control embryos and on the uninjected side of *Noelin-4*-injected embryos. Some embryos exhibited reduced neural crest as judged by *XTwist* staining; others were missing some of the neural crest streams. In all cases, the neural crest was affected only when the lineage tracer localized to the neural crest-forming region (n= 14/17; controls n = 1/20).

An example of the phenotype is shown in Figure 12. All neural crest streams were present on the control side (Fig. 12A); however, on the injected side, a drastic reduction in neural crest was observed (Fig. 12B). The hyoid and branchial neural crest streams were missing, while the mandibular crest stream around the eye was still present but reduced in size. The bulk of the lineage-tracer-positive cells were located caudal to the mandibular stream, which may indicate that the caudal streams were exposed to a higher dose of *Noelin-4*. In cross-section, another embryo with a very similar phenotype exhibited an ectopic structure in the head region due to *Noelin-4* overexpression (arrowhead, Fig. 12D), but exhibited reduced *XTwist* staining in the neural crest (arrow on injected side, Fig. 12D). Furthermore, the ectopic structure, which is likely to be *Sox-2*-positive based on observations of dozens of other embryos with this morphological phenotype, was not *XTwist*-positive, suggesting that neural crest was not induced by *Noelin-4* over-expression.

These results suggest that expression of *Noelin-4* causes conversion of neural crest into neural fate. The hypothesis of conversion rather than proliferation is also supported by the development of ectopic neural structures in the high-dose phenotype (see Figs. 9 and 10) in which ectopic *Sox-2* positive regions were found in epidermis that normally would not develop into neural tissue fates. Thus, both neural crest and epidermis, tissues of ectodermal origin, can be converted to neural fate by ectopic expression of *Noelin-4*.

### **Noelin-4 acts as a neural inducer**

Since *Noelin-4* displayed an interesting over-expression phenotype in whole embryos, I next wished to determine whether *Noelin-4* had any direct neuralizing effects in animal cap explants. Unperturbed animal caps give rise to epidermis when cultured; however, neuralizing factors cause these explants to express an array of neural markers without a requirement for additional signals from the mesoderm. Neural inducers like *noggin* and *chordin* induce anterior neural tissue when overexpressed in animal caps (Lamb et al., 1993; Sasai et al., 1995). Anterior is considered to be the default state for neural tissue that has not received any posteriorizing signal such as FGFs or retinoic acid, neither of which is present in animal cap explants (see Weinstein and Hemmati-Brivanlou, 1999; Harland, 2000).

I injected varying doses of *Noelin-4*, *noggin*, or *noggin* + *Noelin-4* into both blastomeres of 2-cell-stage embryos and explanted animal caps at stage 8-9. The animal caps were cultured until sibling embryos reached either stage 17 or stage 25 when they were collected for analysis by RT-PCR. Visual inspection of animal

caps at stage 25 revealed that the lowest dose injection of *Noelin-4* had induced cement glands to form (Fig. 13A) while animal caps from the higher-dose injections appeared to be typical epidermal explants without cement glands (Fig. 13B and C). Cement gland formation in animal caps is often an indicator of neural induction since anterior neural development, which is initiated by neural inducers like *noggin* and *chordin*, also initiates cement gland formation (Lamb et al., 1993; Sive and Bradley, 1996).

The animal caps were then examined by RT-PCR for expression of a range of neural markers (Fig. 14). Animal caps isolated from embryos injected with the low dose (250 pg) of *Noelin-4* expressed a range of neural markers. These included the early neural markers like *NCAM* (Kintner and Melton, 1987), anterior markers like *Otx-2* (Blitz and Cho, 1995) and *Pax-6* (Hirsch and Harris, 1997), at both stages 17 and 25. *XNeuroD* (Lee et al., 1995) was induced at stage 25 only. Interestingly, low dose (250 pg) *Noelin-4* acted very similarly to *noggin* in animal caps, except that *Noelin-4* did not induce *XBrn-3d* expression as well as *noggin* did. Otherwise, *Noelin-4* acted as a neural inducer at low doses in animal caps.

In contrast, the higher doses of *Noelin-4* (500 pg and 1 ng) did not induce the range of neural markers that the 250 pg dose did, although at stage 25, animal caps injected with 500 pg *Noelin-4* did express low levels of *XNeuroD*. At no concentration did *Noelin-4* animal caps express the more posterior neural markers *En-2* (expressed in the midbrain-hindbrain border, Hemmati-Brivanlou et al., 1991), *Krox-20* (hindbrain marker, Bradley et al., 1993), *HoxB9* (spinal cord marker previously known as *XlhBox6*, Wright et al., 1990), or the differentiation

marker *Synaptobrevin II* (*SybII*, Knecht *et al.*, 1995, Moreno and Bronner-Fraser, 2001). Also not induced was the neural crest marker *Slug* (Mayor *et al.*, 1995); however, it is interesting to note that the background level of *Slug* expression in non-induced animal caps was eliminated by low dose expression of *Noelin-4*, just as it is by expression of *noggin*.

In addition, I examined whether *Noelin-4* could modulate *noggin*-mediated neural induction by co-expressing the two together in animal caps. I found that there were no genes induced by *noggin* that were not induced by the combination as well. *XBrn-3d*, *XNeuroD*, *Pax-6*, *Otx-2* and *NCAM* were all induced by *noggin* alone and by *noggin* + *Noelin-4*. This assay also shows that *Noelin-4* acts differently from *Noelin-1*. *Noelin-1* induced early differentiation as marked by *SybII* when expressed together with *noggin*. However, *Noelin-4* did not induce *SybII* expression in conjunction with *noggin*. These results show that *Noelin-4* acts as a neural inducer in animal caps, and that it does not have differentiation-promoting activity like *Noelin-1*.

### ***Noelin-4* and *Noelin-1* functionally interact**

Since *Noelin-4* has neural inducing properties, and I had previously shown that *Noelin-1* induced early differentiation in *noggin*-neutralized animal caps, I wished to determine whether *Noelin-4* and *Noelin-1* together could cooperate or antagonize the other's function in this assay system. In order to take into account the different sizes of the transcripts, molar ratios of mRNA were co-injected into both blastomeres of 2-cell-stage embryos at either high/high, high/low, or low/high doses (1 : 1, 1 : 0.25, or 0.25 : 1) for *Noelin-1* : *Noelin-4*.

RT-PCR analysis of animal caps expressing these genes at stage 21 is shown in Figure 15. The hindbrain marker *Krox-20* was induced by *Noelin-1*<sup>high</sup> as expected, and quantification of results from co-expression of *Noelin-1*<sup>high</sup> with *Noelin-4*<sup>high</sup> or *Noelin-4*<sup>low</sup> revealed that this induction increased by 2-fold over *Noelin-1*<sup>high</sup> alone (Fig. 15, *Krox-20* gel, lanes 3 and 4, compare with lane 7). *Noelin-4*<sup>high</sup> alone did not induce *Krox-20*, and *Noelin-1*<sup>low</sup>/*Noelin-4*<sup>high</sup> very weakly induced *Krox-20* expression (lanes 5 and 6). Thus, *Noelin-4* may synergize with *Noelin-1* to promote *Krox-20* expression.

Two other neural markers were induced to greater levels when *Noelin-1* and *Noelin-4* were co-expressed. The sensory neural marker *XBrn-3d* was induced by *Noelin-1*<sup>high</sup> as expected (Fig. 15, *XBrn-3d* gel lane 7), and this induction was increased by co-expression with *Noelin-4*<sup>high</sup> (lane 3), but not by co-expression with *Noelin-4*<sup>low</sup> (lane 4). *XBrn-3d* was also not greatly induced in animal caps expressing *Noelin-1*<sup>low</sup> + *Noelin-4*<sup>high</sup> (lane 5). Thus *Noelin-4* could not simply additively substitute for *Noelin-1*. The neuronal determination marker *XNeuroD* was induced by high/high and high/low dose of *Noelin-1*/*Noelin-4*, and very weakly induced by *Noelin-1*<sup>low</sup> / *Noelin-4*<sup>high</sup>, and by each alone (Fig. 15, *XNeuroD* gel lanes 3-7). These animal caps were collected at an earlier stage than those shown in Figure 14, which could account for the lower levels of *XNeuroD* induction seen here. Results with *Sybil* were not consistent and are not presented here; no conclusions could be drawn regarding *Noelin* interactions promoting differentiation-marker expression.

By contrast, it appeared that *Noelin-1* may interfere with the ability of *Noelin-4* to induce expression of the anterior neural marker *Pax-6*. *Pax-6* was

induced by *Noelin-4*<sup>high</sup> alone, and by co-expression with *Noelin-1*<sup>low</sup> and *Noelin-1*<sup>high</sup> doses (Fig. 15, *Pax-6* gel, lanes 3, 4 and 6). Quantification of the data shown in this gel revealed that *Noelin-4*<sup>high</sup> induced *Pax-6* expression 5-fold over control injections; but when *Noelin-1*<sup>high</sup> was co-injected with either *Noelin-4*<sup>high</sup> *Noelin-4*<sup>low</sup>, this induction was reduced by about half: 3-fold over control for *Noelin-1*<sup>high</sup>/*Noelin-4*<sup>high</sup> and 2-fold for *Noelin-1*<sup>high</sup>/*Noelin-4*<sup>low</sup>. It is interesting to note that *Pax-6* was not induced by *Noelin-4*<sup>high</sup> plus *Noelin-1*<sup>low</sup> (lane 5). This was unexpected since *Noelin-4*<sup>high</sup> induced *Pax-6* (lane 6). *Noelin-1*<sup>high</sup> alone also did not induce *Pax-6* expression (lane 7). Thus in the case of *Pax-6* expression, *Noelin-1* decreased the *Noelin-4*-mediated induction.

These results suggest that *in vivo*, *Noelin-1* and *Noelin-4* may modulate each other's functions. The two isoforms synergized to cause greater induction of the neural markers *Krox-20*, *XBrn-3d* and *XNeuroD*. These genes are all induced by *Noelin-1* alone to some degree, but co-expression of *Noelin-4* resulted in an increase in their levels of induction. Furthermore, this was not simply an additive effect, since *Noelin-4*<sup>high</sup> could not compensate for low doses of *Noelin-1* in inducing *Krox-20* or *XBrn-3d*. In addition, *Noelin-1* appeared to negatively affect *Noelin-4* activity. *Noelin-4*<sup>high</sup> induced *Pax-6* 5-fold over controls, but when *Noelin-1* was co-expressed, this induction was reduced by half.

These results demonstrate that the two isoforms possess differing activities: *Noelin-4* can cause expression of anterior neural markers, while *Noelin-1* activates expression of sensory and neuronal determination markers. In light of the biochemical results showing that *Noelin-1* and *Noelin-4* can bind in oocyte assays, this suggests that they may modulate each other's functions *in vivo* as

binding partners. These results indicate that *in vivo* *Noelins* may produce a complex set of effects, whereby *Noelin-4* positively affects *Noelin-1* activity, while *Noelin-4* itself is negatively affected by *Noelin-1*.

### ***Noelin-3* behaves similarly to *Noelin-4* in over-expression experiments**

I hypothesized that because *Noelin-3* and *-4* share most of their biochemical features, they may act similarly in my assay systems. *Noelin-3* contains 30 amino acids more at the amino terminal, but otherwise shares the same structural features found in the M region, including the conserved cysteine residues and hyaluronate binding sites (see Fig. 1). I tested the effects of *Noelin-3* over-expression in whole embryos and in animal caps.

Preliminary experiments have shown that *Noelin-3* has a similar over-expression phenotype in whole embryos to *Noelin-4*. 500 pg of *Noelin-3* mRNA was microinjected into one blastomere at the 2-cell stage and the embryos were allowed to develop to stage 24 when they were assayed for *Sox-2* expression by whole mount *in situ* hybridization. Embryos exhibited a characteristic expansion of neural tissue that was seen for *Noelin-4*. Over-expression of *Noelin-3* in the anterior neural tube regions resulted in an expanded *Sox-2*-positive domain on the injected side (e.g., Figs. 16C and D, arrows). When the injection localized to the eye, this caused enlarged retina (Fig. 16E-G). These results suggest that *Noelin-3* and *Noelin-4* act similarly in whole mount over-expression experiments. *Noelin-3* was also tested in animal cap induction experiments at a range of doses from 250 pg to 1 ng, and was found to cause neural induction similarly to *Noelin-4* (data not shown).

## **Morpholino knock-down of *Noelin* expression**

*Noelin* genes have an interesting array of neural phenotypes upon over-expression in embryos and in animal cap induction assays. However, a better gauge of the function of a gene is given by its loss-of-function phenotype, to determine what processes it may be necessary for. A new approach for “knock-down” of gene expression is provided by Morphant technology. Morpholino antisense oligos (MOs) have an altered chemical structure that is not metabolized by the cell and is non-toxic, thus allowing such oligos to persist for long periods within embryos without causing cell death, which had been a problem with traditional antisense oligo experiments. The MO binds at or near the translation initiation site on an mRNA transcript by duplexing complementary sequences, thus preventing ribosomal entry on the transcript and blocking translation (Ekker and Larson, 2001; Heasman et al., 2000; Summerton and Weller, 1997).

Since *Noelin* isoforms appear to have redundant functions in sufficiency experiments [*Noelin-1* and *-2* have apparently similar function (Moreno and Bronner-Fraser, 2001), as do *Noelin-3* and *-4* (this chapter)], it is important to be able to knock-down the expression of all four isoforms. *Noelin-1* and *-3* would be affected by a MO against the B exon, and *Noelin-2* and *-4* would be affected by a MO against the A exon. The result is that a MO against the B exon leaves the AMZ and AMY isoforms unaffected, which will likely be able to compensate for any reduction in BMZ or BMY. In order to perform loss-of-function experiments, I designed MOs against the A and B exons of *Noelin* genes.

I first confirmed the binding of the MOs to mRNA for *Noelin-1* and *Noelin-4* in *in vitro* translation experiments. These experiments were performed based upon experiments by Summerton *et al.*, (1997) with several modifications (see Methods). Both *Noelin* isoforms were *myc*-tagged to allow for purification of the translation products by immunoprecipitation.

Figure 17 shows the results of the MO-mediated *in vitro* translation inhibition. mRNAs for *Noelin-1-myc* and *Noelin-4-myc* were combined in each sample to show that an MO against each isoform were specific. A control MO was also used to show that the effects were sequence-specific. The control MO did not have any effect on translation of *Noelin-1* or *Noelin-4* (Fig. 16, lane 1). However, when the A or B exon MOs were added, a loss of translation of either *Noelin-4* or *Noelin-1* was observed (lanes 2 and 3). When A and B were added together to *Noelin-1* and *Noelin-4*, nearly all translation of both isoforms was inhibited. Furthermore, none of the MOs, the *Noelin*-specific MOs or the control MO, had any effect on translation of *noggin*, an unrelated control mRNA (lanes 5-7). These results show that the MOs could specifically reduce translation from the transcripts of *Noelin* genes.

### **MO effects in whole embryos**

Preliminary studies to examine the phenotype of MO knock-down of *Noelin* genes in embryos indicate that *Noelins* may be important mediators of neural development. I first injected a range of B-exon MO doses from 5-40 ng of oligo into both blastomeres at the 2-cell stage. Fluoresceinated MOs allowed the cells in which they were present to be visualized (Fig. 18A and B). I observed

mild toxicity only at the highest doses. I examined a range of neural markers in MO-injected embryos by *in situ* hybridization.

MO injection had no apparent effect on expression of the neural crest marker *Slug*. Embryos injected with 20 ng control MO or 20 ng B exon MO appeared normal at stage 17 (Fig. 18C and D). Embryos that were allowed to develop to stage 24 showed perturbations in the expression of the differentiation marker N-tubulin. In control-injected embryos, the trigeminal ganglia appeared normal (Fig. 18E, F). However in B-exon MO-injected embryos, cells expressing N-tubulin appeared outside of the ganglia, at the surface ectoderm instead of in the neural tube or in the ganglia. This effect could be accounted for by placode cells that differentiated *in situ* instead of migrating into the ganglia, or by a conversion of ectodermal cells into neuronal-like cells. This effect was seen in several embryos injected with the B-exon MO (6/8, 3 shown in Fig. 18 G-J), and not in controls in this experiment (8/8, Fig. 18 E, F). However, this effect occurs naturally, though rarely, in control embryos, where in some batches it can be seen at a low frequency in uninjected or in control-MO-injected embryos.

In addition, the olfactory placodes occasionally appeared to be perturbed in their expression of *N-tubulin*. This phenotype is difficult to score, however, because the olfactory placodes commonly diverge in size and appearance between embryos, within limits. For example, the control MO-injected embryo in Fig. 18F has asymmetric olfactory placodes. The effect is amplified in the B-exon MO injected embryo shown in Figure 18I and J, in which *N-tubulin* staining is missing from one of the placodes.

When 10 ng of B-exon MO was injected in one of two blastomeres at the 2-cell stage, more severe phenotypes were occasionally observed (2/7 reduced eye phenotype). An embryo allowed to develop to stage 29 and stained for the pan-neural marker *Sox-2* demonstrated a reduced eye size on the injected side (Fig. 18K-M). The control side appeared normal; however, the embryo lacked characteristic placodal staining of *Sox-2* on the injected side (compare arrows in Figs. 18K and L) and had a small eye as well (Fig. 18L and M).

These results suggest that *Noelin* genes may play a role in neural plate formation, and additionally in placode and ganglion development. However, it is important to demonstrate the effects more specifically. Because of the later onset of expression and the early time of injection, higher doses or doses injected into later blastomeres may give a better result in knocking down gene expression from endogenous *Noelin* transcripts.

### **Targeted MO injections**

In order to better target and deliver high doses of MOs at the stages of interest, I injected the A and B exon MOs together into A and B-tier cells at the 32-cell stage. *Xenopus* embryos have been extensively fate mapped (Dale and Slack, 1987; Moody, 1987), and cells in these tiers are known to give rise to ectodermal derivatives (neural plate, neural crest, and epidermis). By targeting the MO injections to A and B-tier cells, it effectively raises the local concentration of the oligos in regions that will later express the *Noelin* isoforms, thereby reducing the level of MO dilution that must necessarily occur when they are injected into a 2-cell-stage embryo.

Embryos were injected with 5 ng A+B MO in two cells at the 32-cell stage and were allowed to develop until stage 27 when they were assayed by whole mount *in situ* hybridization with the neuronal marker *N-tubulin* and the pan-neural marker *Sox-2*. Control MO-injected embryos generally appeared normal; however, there was more toxicity with these injections than there had been for the 2-cell-stage injections, and there was a 20% frequency of spina bifida among all injected embryos. Figure 19 shows examples of the phenotypes observed for the injections. Morphologically, the A + B exon MO injections caused a reduction in head structures. The forebrain was often missing and the cement gland formed much more dorsally than is normal. By *N-tubulin* staining (Figs. 19A-C), the trigeminal and geniculate ganglia, and the olfactory placodes were absent or reduced (e.g., Fig. 19C arrow). By *Sox-2* staining, eye size and brain structures were reduced (Figs. 19D-F). Otic vesicle staining was sometimes absent (Fig. 19E). The frequency of this phenotype for A + B MO injection was 21/28 embryos; in control MO injections this phenotype was observed at lesser severity, with a frequency of 5/21 embryos.

The specificity of this phenotype must be confirmed by rescue experiments to show that over-expression of *Noelins* can overcome the depletion of endogenous proteins by the MOs. It is also important to show directly the reduction of translated *Noelin* isoforms. In any case, these results suggest that *Noelin* genes may play an important early role in neural development.

### **Noelin-4 interacts with BMP-4 in oocytes**

Several lines of data indicate that *Noelin-4* could participate in neural induction. Its over-expression phenotype causes expansion of neural tissue,

conversion of ectoderm and neural crest into a neural fate, and induction of neural fate in animal caps. MO knock-down also suggests a role in anterior neural development. Furthermore, as a secreted factor, it may act non-cell-autonomously. Because of these data, I hypothesized that Noelin-4 may exert its effects by interacting with the molecules that are known to play a role in neural ectoderm induction in *Xenopus*, namely the BMP signaling pathway. *noggin* and *chordin* exert their neuralizing effects by binding directly to BMPs to inhibit their binding and activating the BMP receptor. This relieves BMP inhibition in the ectoderm and causes neuralization. To determine whether Noelin-4 could also interact with BMPs, I co-injected *Noelin-4* and *BMP-4* mRNAs into oocytes, immunoprecipitated with epitope tags to each of the proteins, and looked for a co-precipitation of the other protein. Noelin-4 was *myc*-tagged at the carboxy terminal, while BMP-4 had an internal *flag* epitope that would be found in the pre-protein and the cleaved pro-domain, but not in the mature protein (Hawley *et al.*, 1995)

Anti-*myc* antibody specifically immunoprecipitated Noelin-4-*myc* from oocytes that were injected with that construct (Fig. 20, lane 1). Uninjected control oocytes did not contain proteins that were specifically immunoprecipitated with anti-*myc* (Fig. 20, lane 2). When Noelin-4-*myc* was co-expressed with BMP-4-*flag*, followed by immunoprecipitation with the *myc* antibody, a protein the size of Noelin-4 was found, as well as a larger protein corresponding to the size of BMP-4 (Fig. 20, asterisk lane 3, compare with BMP-4-*flag* alone in lane 6). In the reciprocal experiment, anti-*flag* immunoprecipitation for the BMP-4-*flag* protein also brought down a protein corresponding to the size of Noelin-4 (Fig. 20, lane

5, asterisk for Noelin-4). In a positive control, Noggin-6-myc co-immunoprecipitated a BMP-4-flag-size protein with the anti-*myc* antibody (Fig. 20 lane 4, noggin =open arrowhead, BMP-4 = asterisk). Each protein immunoprecipitated from oocytes corresponded to the expected size, roughly equivalent to the *in vitro* translated protein made from the same transcripts as were injected into the oocytes (Fig. 20, lanes 7-9).

These results indicate that Noelin-4 may have the ability to bind to the uncleaved BMP-4 protein *in vivo*. These experiments do not reveal whether Noelin-4 binds to the mature BMP-4 protein; however, these results do offer a possible mechanism for the over-expression phenotype of this gene, whereby maturation of BMP-4 could be prevented by Noelin-4 binding to it, thus inhibiting downstream signaling events.

## DISCUSSION

My findings suggest that *Noelin-4* is involved in neurogenesis from early stages of neural development. It is a secreted, glycosylated protein that is expressed from neural plate stages onward. By whole mount *in situ* hybridization, it is expressed in developing neurons; however, transcripts for the gene are detected at earlier stages by RT-PCR. Its expression is induced by the neurogenic genes *X-ngnr-1* and *XNeuroD*. Over-expression of Noelin-4 causes expansion of neural tube and retina and a general dorsalization phenotype at lower doses, and ectopic development of neural tissue and cement gland at higher doses. In animal caps, *Noelin-4* acts as a neural inducer. Morpholino antisense oligonucleotide knock-down of *Noelin-4* expression results in a

phenotype of reduced head structures, with loss of anterior neural structures such as eye and cranial ganglia. Biochemically, Noelin-4 interacts with Noelin-1 and the two isoforms may cooperate in function during embryogenesis. Finally, Noelin-4 interacts with BMP-4 in oocyte injection assays, suggesting that *Noelin-4*, like noggin, may mediate neural induction by inhibition of BMP signaling.

### ***Noelin* isoforms are induced by the neurogenic cascade**

Both *X-ngnr-1* and *XNeuroD* induced expression of all *Noelin* isoforms. The data shown here were for the Y exon; however, the A, B, and Z exons also were induced (Moreno and Bronner-Fraser, 2001 and data not shown). Since *Noelin-1* (BMZ) and -3 (BMY) share the B exon and its promoter, as *Noelin-2* (AMZ) and -4 (AMY) share corresponding A regions, it is expected that all isoforms are transcribed if the A and B exons are both expressed. The importance in showing separate expression data for the Y and Z exons, when A and B exon expression indicate *Noelins* are induced, is that differential regulation of the Y isoforms from the Z isoforms has been suggested in the avian system. In chick embryos, the Y variants are expressed later than Z variants. This may be due to RNA degradation of Y isoforms or other splicing or post-transcriptional regulation. However, in my neurogenesis experiments, I show that at least in *Xenopus*, the four *Noelin* isoforms are all induced by the same signal, and that their transcripts are made and persist long enough to be visualized by *in situ* hybridization.

Furthermore, expression of neurogenic genes is activated at late gastrula/early neural plate stages of neural development: *X-ngnr-1* is expressed

in post-mitotic neurons by stage 12, and *XNeuroD* is expressed by stage 13. Although *Noelin* expression is not detectable by *in situ* hybridization at these stages, RT-PCR results showed that transcripts for the B-containing isoforms *Noelin-1* and *-3* are present by stage 14, and the A-containing isoforms may also be present as early as late gastrulation (stage 12). The ability of neurogenic genes to induce expression of *Noelins* and their inherent neural-inducing properties suggest a possible endogenous function for the *Noelin* isoforms in early neural development.

### ***Noelin-4* over-expression induces neural expansion**

*Noelin-4* over-expression caused expansion of neural tissue at the expense of other ectodermal derivatives. Phenotypes observed were enlarged neural structures such as retina and neural tube; ectopic neural tissue suggesting partial axis duplication and ectopic otic-like vesicles; dorsalization and spina bifida; and conversion of epidermal ectoderm into tissue protrusions expressing neural markers. Most neural expansion was of proliferative neural precursors as scored by *Sox-2* staining (marker of proliferative neural tissue, Mizuseki *et al.*, 1998a), although some ectopic differentiating cells were also observed by *N-tubulin* staining.

The mechanism of expansion was shown to not be increased proliferation, as antibody staining with the mitosis marker anti-phospho-histone H3 was not found in increased numbers of cells on the injected side of embryos with the expanded neural phenotype. Cranial neural crest was reduced in areas of *Noelin-*

4 overexpression, while ectopic neural structures formed in its place. These results all point to a neural expansion by a conversion mechanism.

The *Noelin-4* over-expression phenotype shares some characteristics with those of the transcription factors *Pax-6*, *XBF-1 (FoxG1)* and *Otx-2*. *Pax-6* is a paired domain transcription factor that is important for eye and lens development (Altmann et al., 1997; Chow et al., 1999; Hirsch and Harris, 1997). When over-expressed, it causes expanded retina, ectopic lens development, and when injected at the 32-cell stage, it causes ectopic eye development (Altmann et al., 1997; Chow et al., 1999). Other phenotypes include mild dorsalization and spina bifida (Hirsch and Harris, 1997). This range of morphological perturbation is echoed by the *Noelin-4* over-expression profile.

The winged helix/forkhead related transcription factor *XBF-1(FoxG1)* has an interesting array of phenotypes; at low doses it causes neural expansion, and at high doses it causes increased proliferation and conversion of ectoderm to neural fate (Bourguignon et al., 1998; Hardcastle and Papalopulu, 2000). Embryos over-expressing *XBF-1* also make tissue protrusions similar to those found in *Noelin-4* embryos (Hardcastle and Papalopulu, 2000).

*Noelin-4* also acts similarly to *Otx-2*, a homeobox gene related to *Drosophila Orthodenticle*, in the induction of ectopic cement glands and partially duplicated anteroposterior axes. Pannese *et al.* (1995) found that more ventral sites of *Otx-2* over-expression resulted in ectopic cement gland formation, while dorsal region over-expression resulted in partial axis duplication (Pannese et al., 1995). These phenotypes are similar to that of *Noelin-4* over-expression, in which cement glands formed when the injection site was on the ventral half of the anterior

ectoderm, and ectopic neural structures that were continuous with the neural tube occurred with injections that localized to dorsal ectoderm.

The genes described above participate in patterning the anterior neural plate and positioning specific neural regions. Their expression is triggered in response to neuralization through BMP antagonism. *Pax-6* and *Otx-2* themselves are induced by *Noelin-4* over-expression in animal caps. The similarities between the over-expression phenotype of *Noelin-4* and these very different transcription factors may indicate that *Noelin-4* interacts in the pathways of action for each of these genes, or alternatively, that *Noelin-4* exerts this function at an earlier step of neural induction, and then has downstream effects that are similar to the described transcription factors.

### ***Noelin-4* acts as a neural inducer**

In animal cap assays, *Noelin-4* acted as a neural inducer. It induced expression of the general neural marker *NCAM*, and anterior neural markers *Otx-2* and *Pax-6*. It also activated expression of *XNeuroD*. However, many molecules can cause neuralization without functioning endogenously as neural inducers. For example, the BMP-interacting molecule Gremlin acts as a neural inducer, but its expression does not commence until well after neural induction is over (Hsu *et al.*, 1998). If neural-inducing genes are not normally expressed at the right time or location, then neural-inducing activity may be irrelevant in the embryo, and their true function during development could be entirely separate from the ability to activate neural gene expression.

Many molecules are known to act as neural inducers as gauged by induction of pan-neural markers in isolated animal cap ectoderm. Some function by directly activating expression of neural gene expression pathways, and are usually transcription factors. For example, *Otx-2* can activate expression of the neural marker *NCAM* in animal caps (Blitz and Cho, 1995; Gammill and Sive, 2001). Other molecules such as Activin act as secondary neural inducers, by first inducing mesoderm formation, which in turn induces neural fate (Gurdon et al., 1994; Hemmati-Brivanlou et al., 1994; Hemmati-Brivanlou and Melton, 1994; Smith et al., 1990).

Direct neural inducers act by antagonizing BMP signaling, which relieves the BMP-mediated inhibition of neural fate and allows neuralization to occur. *noggin*, *chordin*, and *follistatin* all bind to and antagonize BMP signaling in the neural plate by preventing BMP binding to its receptor (Lamb et al., 1993; Hemmati-Brivanlou et al., 1994; Sasai et al., 1994; Piccolo et al., 1996; Zimmerman et al., 1996; Fainsod et al., 1997). Another way to inhibit BMP signaling is through inhibition of the downstream effectors of BMP signals. For example, the antagonistic Smad6 protein interacts with activated type I BMP receptor and prevents it from phosphorylating R-Smads (proteins that help translocate the BMP signal to the nucleus to affect transcription), or by competing for binding sites with signaling Smads (Smad4) (Hata et al., 1998; Nakayama et al., 1998). Thus, there are many possible pathways that can activate neural induction. Noelin-4 may function through one of these, determined by its biochemistry and extracellular localization.

### **Noelin-4 interacts with BMP-4**

The possible mechanisms for the neuralizing activity of *Noelin-4* are limited by its structure and biochemistry. The gene does not have any domains to suggest that it acts as a transcription factor, and furthermore, it is a secreted protein. It does not induce mesoderm in animal caps, suggesting that it cannot act as a secondary inducer. This implies that any function in neural induction is through antagonism of BMP signaling at the extracellular level, which could occur by inhibiting the binding of BMP molecules to their receptors, or by inhibiting activation of the receptor upon BMP binding, or by interacting with other cofactors that affect BMP receptor activity.

In order to test this hypothesis, I performed co-immunoprecipitation experiments with BMP-4 and Noelin-4 expressed in oocytes. When I immunoprecipitated with anti-*myc* (on Noelin-4-*myc*), a band of the same size as BMP-4-*flag* was also brought down. The reciprocal experiment was also true; when I immunoprecipitated BMP-4-*flag* with anti-*flag* antibody, a protein the size of Noelin-4-*myc* co-immunoprecipitated. These results suggest that Noelin-4 can bind to BMP-4, and may exert its neuralizing activity in animal caps by inhibiting BMP signaling.

### **Morphant phenotype**

In further confirmation of the data showing that *Noelin-4* acts as a neural inducer by inhibiting the BMP signaling pathway, Morpholino antisense experiments revealed a reduction in head structures of embryos injected with MOs targeted against all four isoforms. Embryos displayed reduced head size,

reduced or missing eyes, reduced forebrain and cement gland, and missing cranial ganglia at high local concentrations (injected at the 32-cell stage), and ectopic *N-tubulin*-positive cells near the ganglia at low local dose (2-cell-stage injections).

This last seemingly contradictory result may in fact be due to the perturbation of *Noelin* Z isoform expression (*Noelin-1* and *-2*). One hypothesis is that the Z isoforms, which promote neurogenesis in neuralized animal caps, are involved *in vivo* in the development of the cranial placodes (they are expressed in the ganglia). Neither one alone is sufficient to cause neurogenesis or to affect ganglion development, but perhaps the loss of their expression uncovers a role for their function, in which proper expression of the Z isoforms could be necessary for the placode cells to ingress into the ganglia, where they would normally differentiate (express *N-tubulin*). When Z isoform expression was reduced, the placode cells remained at superficial levels and differentiated into neurons (expressed *N-tubulin*) in improper locations.

Regardless, these results complement the gain-of-function data and suggest that *Noelin* genes may play an important role in neural development, specifically in neural induction and cranial ganglia formation. In order to address this more stringently, further studies must be done. First, a rescue of the phenotype must be performed to show that the MO phenotype is due to loss of *Noelin* expression; second, protein levels must be shown to be reduced in MO-injected embryos. Currently there exists no antibody to *Noelin* isoforms in *Xenopus*, thus co-expression of a construct of the stable *green fluorescent protein*

(*gfp*) with translational start sequences from the Noelin genes may give a better indication of *in vivo* inhibition of translation from the MO injections.

### **Spatiotemporal expression and function of *Noelin* isoforms**

*Noelin* isoforms are expressed from neural plate stages as assayed by RT-PCR. Later in development, all isoforms are expressed in post-mitotic neural tissues in the brain, spinal cord and cranial ganglia. The low levels of expression that are undetectable by *in situ* hybridization may have important functions early in development. It is important that the isoforms are expressed early in the context of the gain-of-function phenotype of *Noelin-3* and *-4*, since a neural-inducing effect is not meaningful for a molecule that is not expressed at times when neural induction processes occur.

My results suggest that two separate functional domains reside in the Noelin proteins: a neuralizing activity that is found in the M region, and a differentiation function that resides in the Z region. All Noelin isoforms contain the M region but differ in their upstream and downstream exons. The longer, Z-region-containing isoforms Noelin-1 and *-2* are involved in neurogenesis, but do not themselves act as neural inducers. The Y-containing isoforms Noelin-3 and *-4* act as neural inducers but do not promote neuronal differentiation. Due to the Y exon encoding only a glycine residue and then a stop, these isoforms are comprised essentially of the M region only. The Z region, which is large (329 aa) and has five glycosylation sites (Barembaum *et al.*, 2000; Moreno and Bronner-Fraser, 2001), may act to block or sterically hinder the M region on the same

molecule. This could also explain why the Z isoforms do not act as neural inducers even though they contain the M region, as all *Noelin* isoforms do.

The matter is further complicated by the fact that the two Z-containing isoforms (*Noelin-1* and *-2*) are made by two different promoters, as are the two Y-containing isoforms (*Noelin-3* and *-4*); in other words, a Y- and a Z-containing isoform are both transcribed from the same promoter. Thus, whenever a cell makes *Noelin-1* (BMZ), it also transcribes *Noelin-3* (BMY). Further levels of regulation by splicing mechanisms or mRNA stability probably play an important role in regulating levels of expression of each isoform. Evidence for this hypothesis comes from the chick system, where the Y-containing isoforms are expressed later than the Z-containing isoforms (Barembaum et al., 2000). This implies a level of splicing regulation that I have not observed in *Xenopus*; however, it also suggests that a mechanism may be in place for specific regulation of splice forms that has not been uncovered in the frog.

Furthermore, the endogenous co-expression of the isoforms suggests that they could function together. Biochemically, the isoforms *Noelin-1* (BMZ) and *Noelin-4* (AMY) interact in oocyte assays, suggesting that the M region containing the conserved cysteine residues could be responsible for disulfide bonding between isoforms. This interaction and implications from the data regarding the different functional domains of *Noelin* isoforms suggest that the *Noelin* isoforms may act as cofactors.

## **Noelin proteins interact**

There are several possible hypothetical scenarios for this interaction. The large, Z-containing isoforms, which are known to be less well-secreted (Moreno and Bronner-Fraser, 2001), could act to restrict secretion of the Y-containing isoforms by binding them in the endoplasmic reticulum and then preventing their exit from the cell at the higher levels to which they would normally be secreted. This could regulate neutralizing effects of these isoforms (see Figure 15).

Alternatively, the Z-containing isoforms, which are highly glycosylated, could act as anchors in the extracellular matrix for the smaller Y-containing isoforms, to maintain them in a local area instead of allowing them to disperse. This could provide a local concentration of the Y isoforms to exert their effects. Moreover, these two proposed mechanisms could perform in concert, with the Z isoforms slowing the secretion of the Y isoforms, and then maintaining them all in a local area for further activity. These hypotheses must be tested in order to determine whether they may describe the cooperation between *Noelins in vivo*.

## ***Noelins* modulate the function of other *Noelins***

The above-described hypotheses seem possible; moreover, it has not been shown that any isoform absolutely requires another for its gain-of-function phenotype. While *Noelin-1* had no apparent effect in over-expression experiments and its neurogenesis-promoting ability occurred only in neuralized animal caps (Moreno and Bronner-Fraser, 2001), *Noelin-4* functioned alone to cause neural induction in animal caps and expansion of neural tissue in whole embryos.

I have also shown that some synergy of induction occurs when *Noelin-1* and *Noelin-4* are co-expressed in animal caps. *Krox-20*, *XBrn-3d*, and *XNeuroD* were induced to a higher degree by co-expression of both isoforms together, but after single injections, they were induced by *Noelin-1* and only weakly (or not at all) by *Noelin-4*. Thus, *Noelin-4* synergized the inducing capability of *Noelin-1*, but was not sufficient to activate the genes to the same level when expressed alone.

It is interesting to note that synergy of induction only occurred for genes induced by *Noelin-1*. *Noelin-4* co-expression up-regulated the induction of *Krox-20* and *XBrn-3d* by *Noelin-1*, but *Noelin-1* did not up-regulate *Noelin-4*-mediated induction of *Pax-6*. In fact, *Noelin-1* appeared to negatively affect the *Pax-6*-inducing ability of *Noelin-4*. These results suggest that *Noelins* may have complex cooperative and antagonistic functions in addition to the separate activities they display in neural induction and promotion of neurogenesis.

### **Noelin-4 binding partners**

Noelin-4 co-immunoprecipitated both with Noelin-1 and with BMP-4 in oocyte injection assays. These results suggest some interesting hypotheses for the mode of action of the *Noelin* genes. Noelin-4 apparently binds with greater affinity to Noelin-1, since immunoprecipitations with antibodies to epitopes on either Noelin protein brought down greater relative amounts of the other protein than the co-immunoprecipitation of Noelin-4 with BMP-4 did. What is the significance of these interactions? Two possibilities are: 1) Noelin-4 could be presented by Noelin-1 to its surroundings more efficiently than when unbound

or alone; or 2) Noelin-4 binding to Noelin-1 sequesters it from binding to other molecules (e.g., BMPs), thus accounting for its reduced activity in the presence of Noelin-1. Preliminary data demonstrating that Noelin-1 antagonizes Noelin-4 activity support the latter postulate. However, the story is more complicated than a simple inhibitory interaction, since Noelin-4 apparently makes Noelin-1 a stronger inducer of the neural markers that it can up-regulate on its own. The mystery of *Noelin* cross-regulation remains to be elucidated with more experiments to directly test their cooperative and antagonistic activities.

### **Neural inducers also function after neural induction**

What is the importance of a neural inducer expressed after neural induction has begun or finished? Recently, Hartley *et al.* (2001) have shown that continued repression of BMP signaling is required for normal anterior neural development. They showed that BMPs are expressed in the anterior mesendoderm, which underlies the anterior neural plate. When they ectopically expressed *BMP-4* in the anterior neural plate in transgenic frogs with the *Pax-6* promoter driving *BMP-4* expression, they found that a range of anterior neural markers were lost. In light of these new results, a role for a later-expressed neural inducer is proposed.

BMP signaling regulation is also important at later stages in the hindbrain, where neurons differentiate at different times depending on their location. Projection interneurons and motor neurons differentiate later in odd-numbered rhombomeres than in even-numbered ones. *BMP-4* is expressed in the odd-numbered rhombomeres, and is proposed to be the factor that controls the later

time of differentiation of the neurons therein. When *chordin*-expressing cells were implanted next to the odd-numbered rhombomeres, the timing of neuronal differentiation matched that of the even-numbered rhombomeres (Eickholt et al., 2001). Thus, even at later stages, regulation of BMP signaling pathway activity is important for proper neural development. In both of these cases, a molecule that inhibits BMP signaling in the extracellular environment could provide the mechanism to explain the data.

In conclusion, I have described here the functional characterization of *Xenopus Noelin-4*. It is expressed from early neural plate stages and later is found in post-mitotic neurogenic tissue in the PNS and CNS. Upon over-expression, it acts as a neural inducer and causes expansion of neural tissue at the expense of neural crest and epidermis. Noelin-4 protein binds both to Noelin-1 and to BMP-4 in oocyte assays. Moreover, *Noelins* may have complex positive and negative regulatory interactions for some of their activities. The neuralizing activity of *Noelin-4* may be attributable to inhibition of BMP signaling through its interaction with BMP-4. Future studies will be necessary to complete the loss-of-function MO experiments and to determine the specific interaction between Noelin-4 and BMP-4 proteins.

**Acknowledgements**

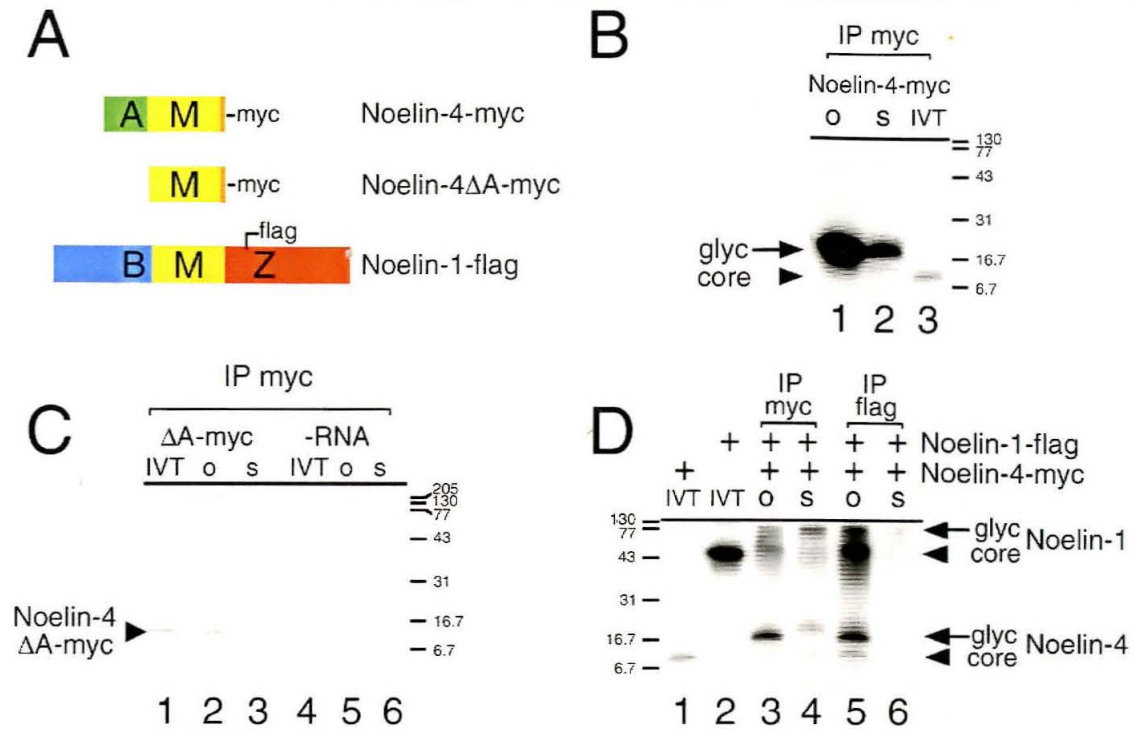
I am grateful to Clare Baker, Laura Gammill and Anne Knecht for critical reading of the manuscript, and Laura Gammill, Anne Knecht and Carole LaBonne for extremely helpful discussions and advice during the course of this work. cDNA libraries used were kind gifts of R. Harland and M. King. T.A.M. is a fellow of the ARCS foundation

**Figure 1:** *Noelin-4* sequence and structure information

CCGAGAGAATCAGTCCCTCTGAGATACAATTGTGGTACCTTTTTGCAAGCTGCATCCCTGCTAACCCT  
 GCTTTTTTTCCTCCCTCTGTCCCTGCCCTTCTTTTCAAGGCAAACCTTTGGCAAAGGCAGCACTGTCA  
 TCCTCTGCTCCGTTGAGTTTCTCTTTTATTTATTTACATTTTTTCTCCCCTTTTTGTGCAAATGCCTT  
 TCAATCAAGGAAGCCATTAAAAGAAAAGAAGCAGCAGCAACAGAGAGGGAAGAGAGGATCGGGACAGA  
 GTAAATATGCAAAGTGAGCACTTTACAAACCAGACTCCTTGCTTGCTCCTAGGGCTGCCTAAAAGC  
 CGCCACCACCGTTACATAGGGAAGAATCACGGACCGGAGTCTGGAATAGAAATTGAAGAAAAAAGCA  
 CACTGAAAAGAAGGCCAAAACACACACATAAAAAAGAGGAGGAGAAGAAAAAATCTGGGGGTCTTGAC  
 TGAAGCTGAGATGAAGCAACCGCCAAGCAAGCTGATGAGTCTCTTCCCTTCTCATCTTGATGGGCACCG  
 M K Q P P S K L M S L F L L I L M G T E  
 AACTCACCCAACTTTTGCACCAACCCAGAAGAGAGCTGGCAAGTGTACAGCTCTGCCCAGGACAGC  
 L T Q V L P T N P E E S W Q V Y S S A Q D S  
 GAAGGGCGGTGTATATGCACAGTGGTGGCACCTCAACAGACAATGTGCTCACGGGATGCCAGGACAAA  
 E G R C I C T V V A P Q Q T M C S R D A R T K  
 ACAGCTCAGGCAGCTATTAGAAAAGGTGCAAAACATGTCTCAGTCAATAGAAGTATTGGACAGGCGGA  
 Q L R Q L L E K V Q N M S Q S I E V L D R R T  
 CCCAGCGGGACCTGCAATACGTAGAGAGAATGGAAAACCAAATGAAGGGCCTGGAATCTAAGTTCAA  
 Q R D L Q Y V E R M E N Q M K G L E S K F K  
 CAAGTGAAGAAACACATAGGCAACACCAAGCCAGGCAGTTTAAAGGGCTAACTTAAGTTGCAAAGACT  
 Q V E E T H R Q H Q A R Q F K G ★  
 GAAGAGGCAGTTTACTCCCATGTTCCCATGAAAGAGAGACACACAGCATTTTTTGGGCACCAATCATA  
 TTTTTAAAAACCTTTATTCTCCCAATTAGCGCGTTATCACTAAGGAACCCTGATCACCTTTGCGCTCA  
 AATCTTCATTTGCATGCAACTGTAGCTGCATTCCATGAAGACAATTTTTAACCTTTGTCAATGCATA  
 TATATATCTCTATTTTTTTCTTTTCTAAAGGAAGAACTCTTTGTGTATGTGTTTTAAAGCATGTAACC  
 ATAAAGATGTTGCATTTGAAAACAAAATGACTAATAAAGACCTTTCCCAAAAAAAAAAAGAAAAA  
 AA

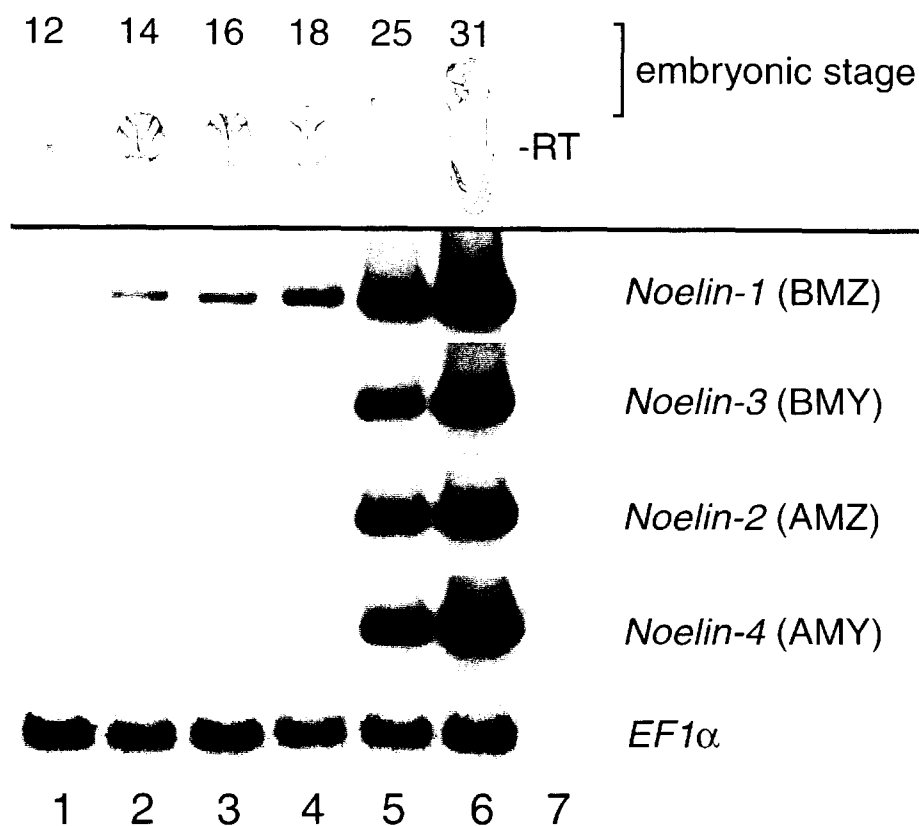
The 1227 base-pair clone contains both 5' and 3' untranslated regions (nucleotide sequences are in black). Deduced amino acid sequence (126 aa) is shown beneath coding residues in blue (mature protein sequence) and red (predicted cleaved signal peptide); the translational start and stop sites are also denoted with red markings. Exon boundaries are denoted with a vertical line separating A/M and M/Y regions. Conserved cysteine residues are marked with green asterisks; N-linked glycosylation site is denoted with a black arrowhead; and two potential hyaluronate binding site sequences are marked with yellow underlines. The polyadenylation signal is boxed.

## Figure 2: Noelin-4 secretion and binding

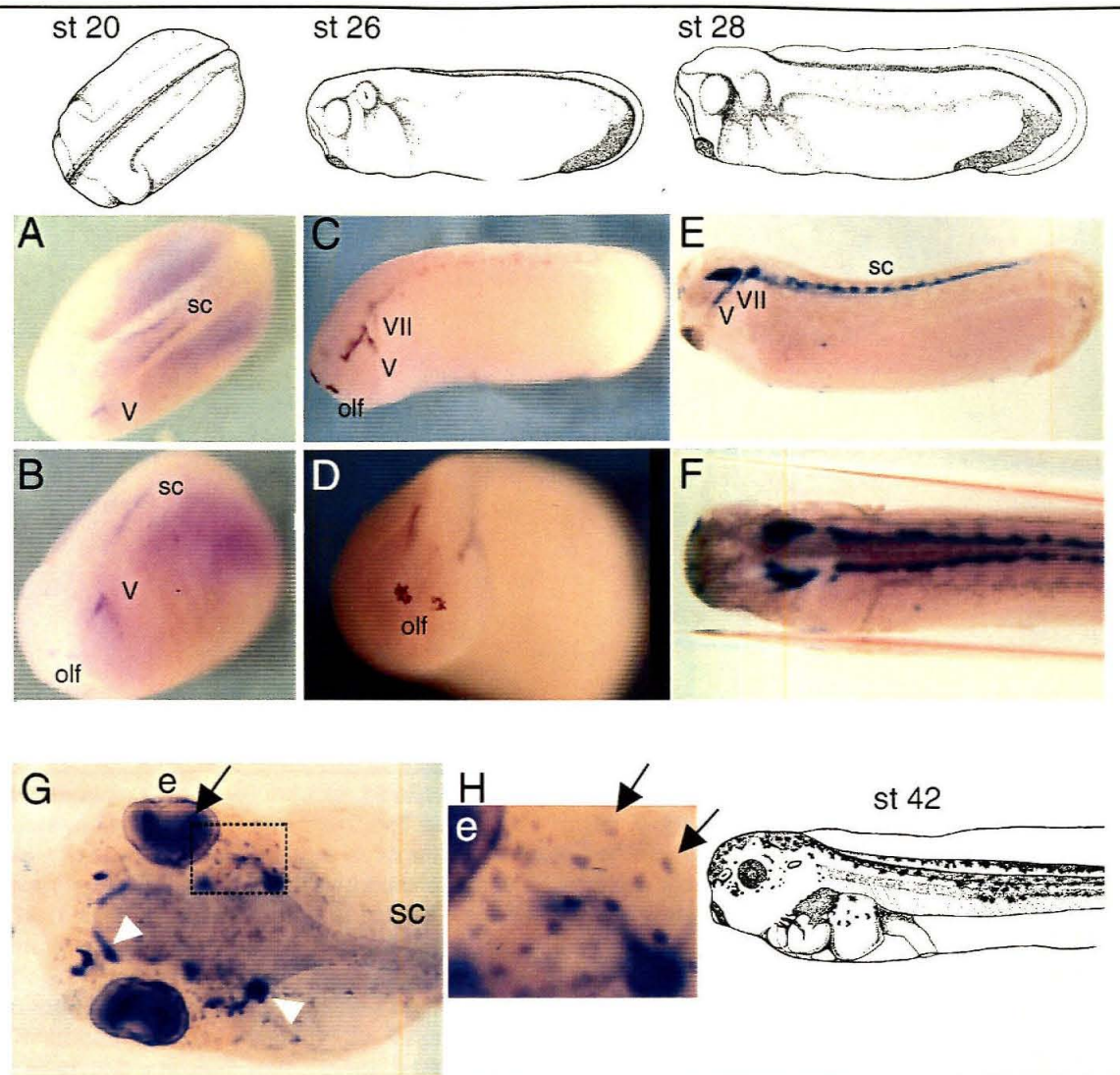


Noelin-4 protein is secreted into the media of cultured oocytes. Oocytes were injected with tagged constructs and cultured in the presence of  $^{35}\text{S}$ -methionine, followed by immunoprecipitation as indicated and electrophoresis on 14% SDS-polyacrylamide gels. **A:** *Noelin* constructs used in this assay were epitope-tagged with either a single *myc* tag at the carboxy terminus, or with an internal *flag* epitope. Schematic diagrams show position of tags relative to *Noelin* coding sequences. Noelin-4 constructs are *Xenopus* clones, Noelin-1-flag is a quail homolog that is 93% identical to *Xenopus* Noelin-1 and behaves similarly in oocyte secretion assays. The *flag* tag is subcloned into a unique *Bam* HI site in the Z region. **B:** Noelin-4-myc is secreted into the medium. Samples were immunoprecipitated with an anti-*myc* antibody. Lane 1: oocyte fraction; lane 2: supernatant fraction; lane 3: *in vitro* translated protein from the same mRNA that was injected into the oocytes. Oocyte and supernatant-derived Noelin-4-myc is larger than the core *in vitro* translated protein suggesting that the protein is glycosylated. **C:** Noelin-4ΔA-myc is a construct in which the A exon (containing the putative signal peptide) has been removed. Samples were immunoprecipitated with anti-*myc*. Lane 1: *in vitro* translated protein; lane 2: oocyte fraction; lane 3: supernatant fraction. Noelin-4ΔA-myc is not secreted, and its size in the oocyte fraction suggests that it is unglycosylated. Lane 4: negative control, *in vitro* translation without RNA, immunoprecipitated with anti-*myc*; lane 5: negative control, oocyte fraction; lane 6: negative control, supernatant fraction. No proteins are immunoprecipitated with the antibody under these conditions. **D:** Noelin-4 forms complexes with Noelin-1 in the oocyte system. Lane 1: *in vitro* translated Noelin-4-myc; lane 2: *in vitro* translated Noelin-1-flag; lanes 3 and 4: oocyte and supernatant fractions expressing both Noelin-4-myc and Noelin-1-flag and immunoprecipitated with anti-*myc*; lanes 5 and 6: oocyte and supernatant fractions immunoprecipitated with anti-*flag*. Lanes 3-6 were successively immunoprecipitated, thus less protein was found in lane 6 than in lane 4. Noelin-4 co-immunoprecipitates Noelin-1, and vice versa, suggesting that these proteins associate in complexes in the oocytes. IVT, *in vitro* translated protein; o, oocyte fraction; s, supernatant fraction. Glycosylated protein sizes are denoted with arrows; core protein sizes are denoted with arrowheads.

**Figure 3:** Developmental series of *Noelin* expression

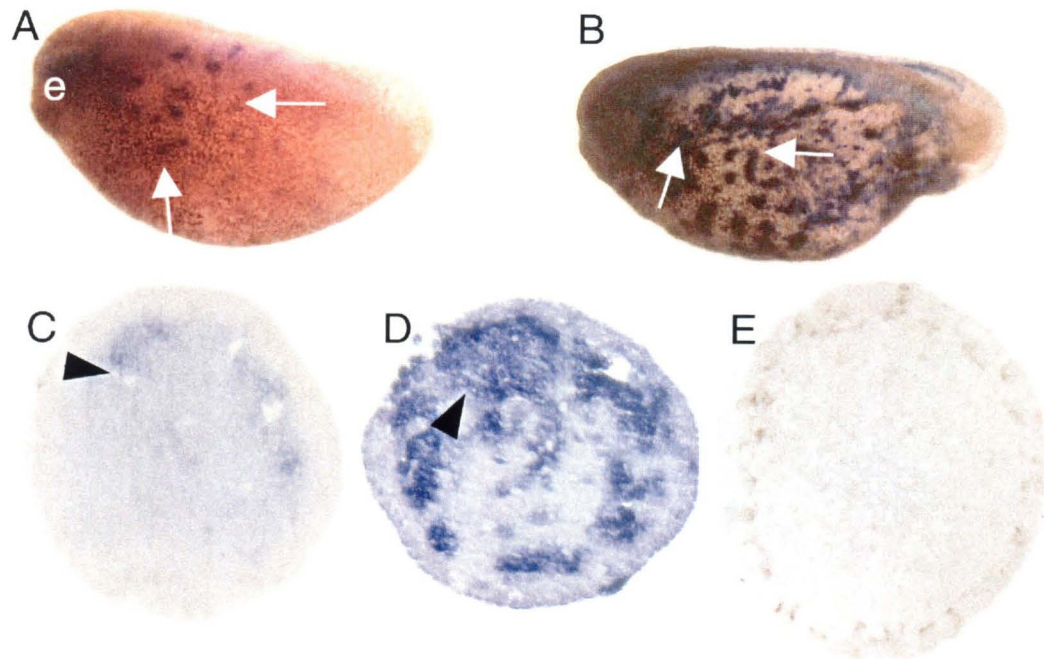


*Noelin* expression from late gastrulation through tailbud stages. *Noelin* isoforms were detected by RT-PCR using pairs of oligonucleotides designed against the A, B, Y or Z exons, in order to amplify each isoform specifically. Numerical developmental stages are given for each lane, with schematic drawings for each stage below (stages and drawings from Nieuwkoop and Faber, 1967). **Lane 1**, stage 12, late gastrulation; **lane 2**, stage 14, early neural plate; **lane 3**, stage 16, mid-neurula; **lane 4**, stage 18, closing neural tube; **lane 5**, stage 25 pre-tailbud; **lane 6**, stage 31, tailbud; **lane 7**, -RT control. The B-containing isoforms *Noelin-1* and *-3* are amplified beginning at the neural plate stage 14 (lane 2), with greatly increasing expression after neural tube closure (lane 5, neural tube is considered closed at stage 21). A-containing isoforms *Noelin-2* and *Noelin-4* are detected at very low levels from stage 12 onward, with much higher levels of expression beginning after neural tube closure (lane 5).

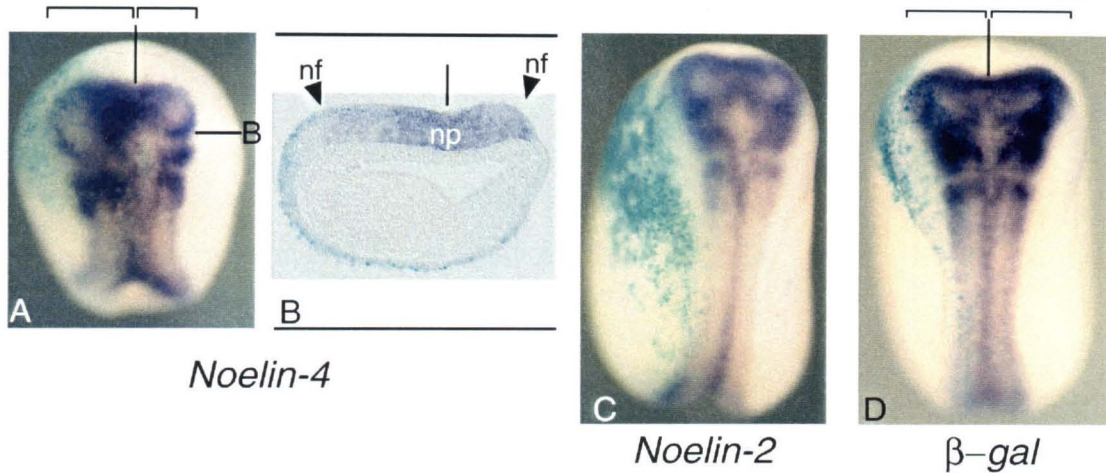
**Figure 4:** *Noelin* Y isoform expression pattern

Expression pattern of *Noelin-3* and *-4*. Expression is detected in neural tissues after neural tube closure by whole mount *in situ* hybridization. Nieuwkoop and Faber (1967) schematic drawings of embryonic stages shown are given above photographs of embryos shown in A-F, and to the right of G and H. All embryos are oriented with anterior to the left. **A**: dorsal view of a stage 20 embryo showing Y exon expression in cells of the spinal cord and trigeminal ganglion. **B**: dorso-lateral view of the same embryo showing *Noelin* expression in spinal cord, trigeminal ganglia and olfactory placodes. Diffuse purple staining in A and B is due to probe trapping, not specifically stained tissue. **C**: lateral view of a stage 26 embryo with *Noelin* expression in the trigeminal (V) and geniculate (VII) ganglia and olfactory placodes. **D**: the same embryo from the anterior. **E**: lateral view of a stage 28 embryo showing intense staining in cranial ganglia V and VII and cells of the spinal cord. **F**: dorsal view of the same embryo. **G**: a stage 42 embryo (dorsal) showing distribution of *Noelin* isoforms in the cranial nerves (e.g., arrowheads) and eye (arrow). *Noelin* expression is also found in lateral line cells. **H**: boxed area in G is magnified. Arrows point to lateral line neuromasts. A lateral schematic view of a stage 42 embryo is drawn to the right of H. e, eye; olf, olfactory placodes; sc, spinal cord; trig, trigeminal ganglion; V, trigeminal ganglion; VII, geniculate ganglion.

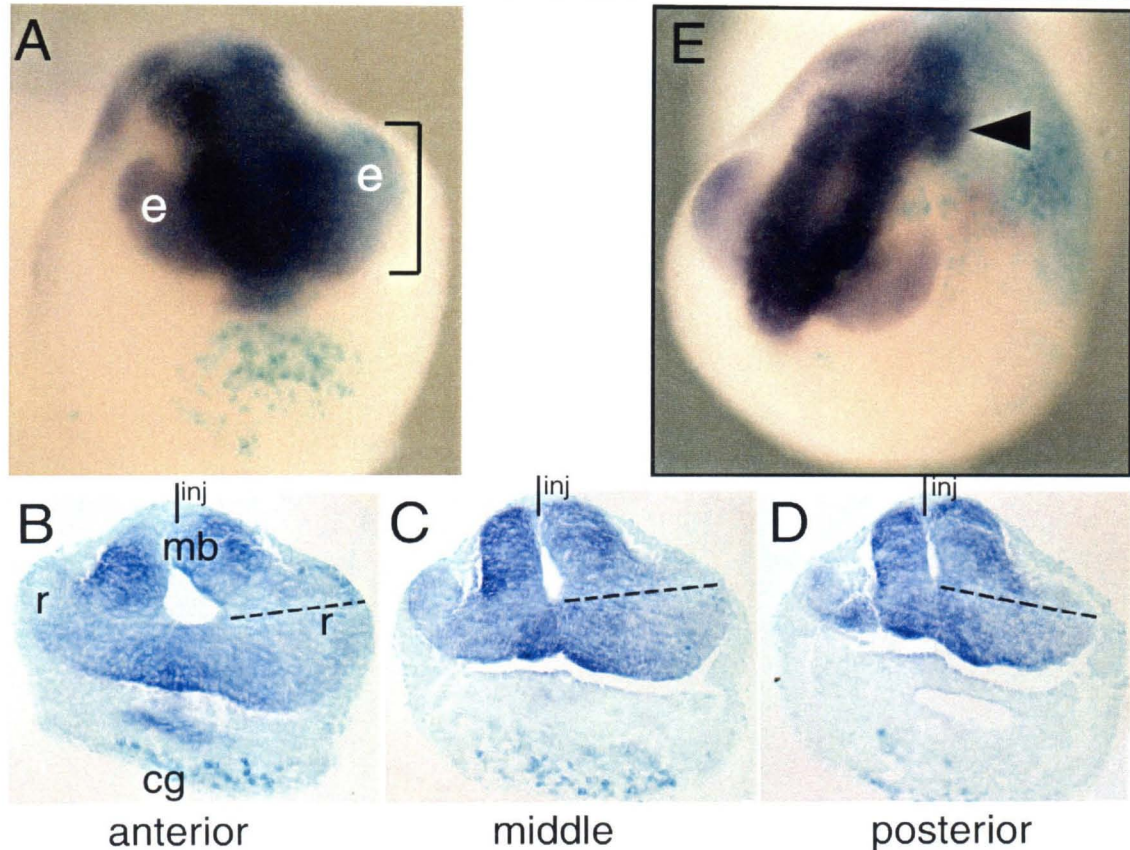
**Figure 5:** *Neurogenin* induces *Noelin-3* and *-4*



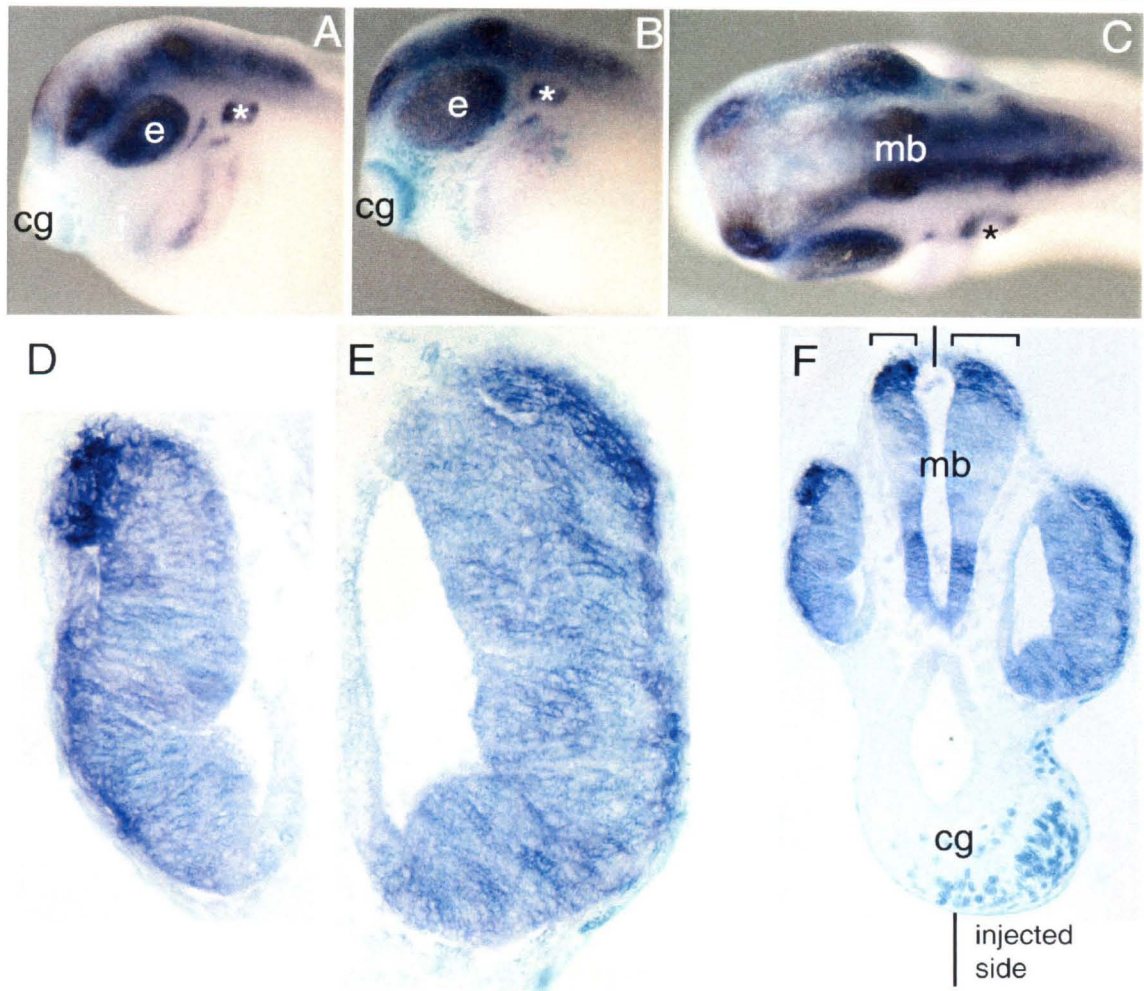
*Neurogenin* (*X-ngnr-1*) induces *Noelin-3* and *-4* expression in animal caps and in whole embryos. Embryos were injected at the 2-cell stage with 100pg *X-ngnr-1* or  $\beta$ -galactosidase mRNA in one blastomere (for whole embryo experiments) or both (for animal caps). Samples were processed for expression of the Y exon or *N-tubulin* at stage 24 or when siblings reached stage 24 (animal caps). The Y exon is representative of *Noelin-3* and *Noelin-4* expression. C-E show 10  $\mu$ m cross-sections through the animal caps. **A:** In whole embryos, Y exon expression is induced by overexpression of *X-ngnr-1* (arrows, anterior to the left). **B:** *N-tubulin* is strongly induced by *X-ngnr-1* (arrows, anterior to the left). **C:** *X-ngnr-1*-injected animal cap shows weak Y exon induction (e.g., arrowhead). **D:** Control animal cap injected with *X-ngnr-1* expresses *N-tubulin* strongly (arrowhead). **E:** Control animal cap injected with 100pg  $\beta$ -galactosidase mRNA and stained with *N-tubulin* shows no expression of the neuronal differentiation marker. Embryos in this experiment were derived from pigmented females; brown color is due to pigment granules. e, eye.

**Figure 6:** Neural plate expansion by over-expression of *Noelin-4*

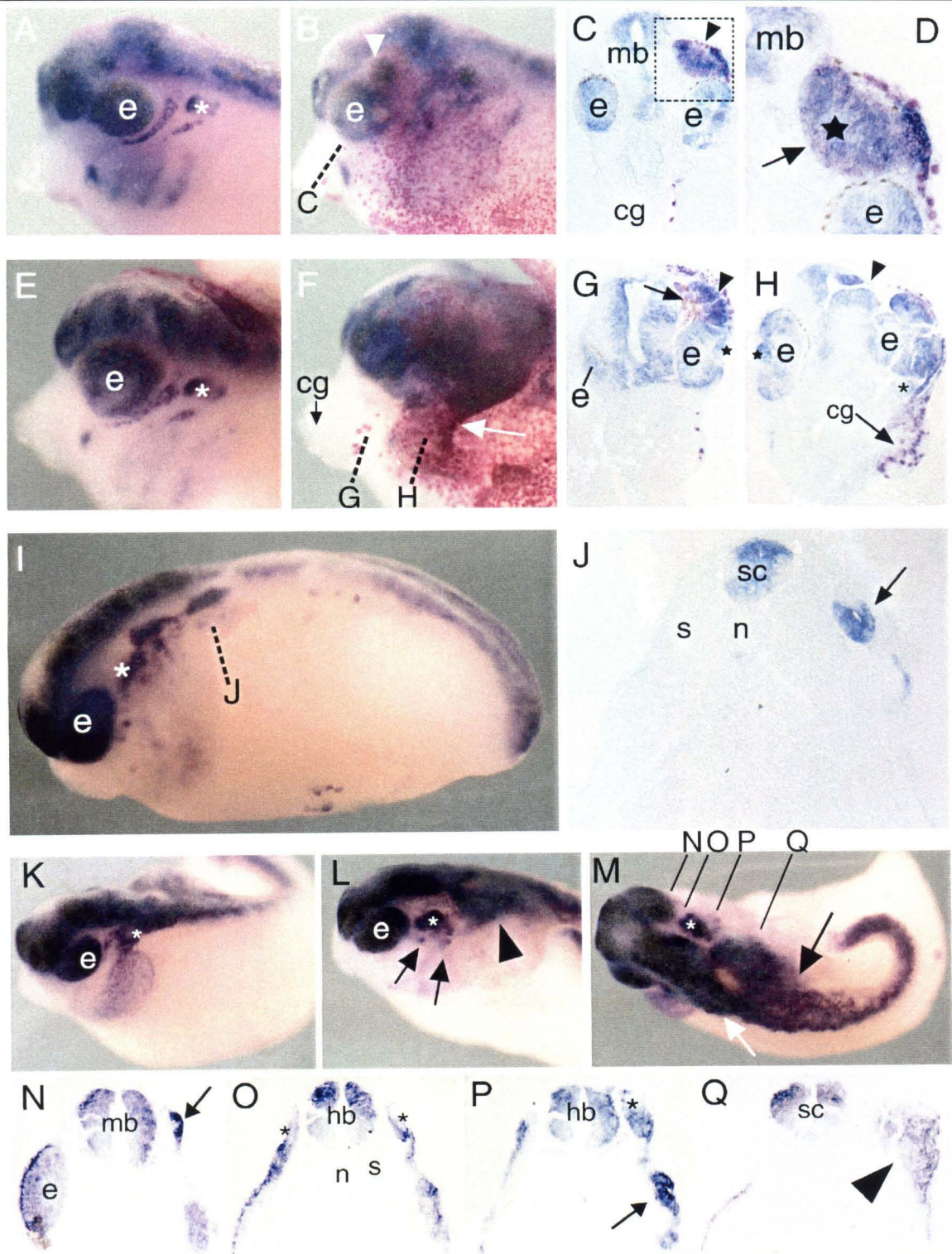
Over-expression of *Noelin-4* causes expansion of the neural plate. Embryos were injected with 500pg of *Noelin-4*, *Noelin-2*, or  $\beta$ -galactosidase and assayed by whole mount *in situ* hybridization against the pan-neural marker *Sox-2* at stage 16 (panel A) or stage 17 (panels C and D). Anterior is up in A, C, and D. **A:** *Noelin-4* causes expanded neural plate on the injected side. The neural plate is demarcated by purple *Sox-2* staining, the lineage tracer ( $\beta$ -galactosidase) is stained turquoise to indicate injected side of the embryo. Anterior neural plate regions are visibly enlarged in the whole mount view. Vertical line indicates embryo midline, bars above embryo indicate relative sizes of each side of the forebrain neural plate. The embryo has a faulty blastopore closure in the caudal region (forked *Sox-2* staining posteriorly). Dashed arrow indicates level of section in B. **B:** Cross-section through the forebrain region of the embryo in A. Section is counterstained with Light Green to visualize the morphology of unstained areas. Note the extent of the neural plate on the injected side (left of vertical bar) as compared to the uninjected side. Position of the neural folds is marked with arrowheads. **C:** Embryo injected with *Noelin-2* in a similar region does not display an expansion of the neural plate. **D:** Embryo injected with  $\beta$ -galactosidase also has a normal neural plate. Bars above embryo indicate relative sizes of left and right halves of the neural plate. nf, neural folds; np, neural plate.

**Figure 7: Enlarged retina by over-expression of *Noelin-4***

Overexpression of *Noelin-4* in the eye leads to a large-eye phenotype. Embryos were injected with 500 pg of *Noelin-4* mRNA in one blastomere at the 2-cell stage, along with 100 pg of  $\beta$ -galactosidase mRNA as a lineage tracer. Embryos were processed for  $\beta$ -gal staining and *in situ* hybridization against the neural marker *Sox-2* at stage 24. **A:** An embryo in which the injection primarily localized to the region of the developing eye and cement gland. On the injected side (right side of panel), the eye field is enlarged as compared with the uninjected side. Bracket indicates the injected side eye. **B-D:** Cross-sections through the embryo in A, counterstained with Light Green. Dashed line indicates long diameter of injected-side retina. **B:** A section at the anterior margin of the uninjected-side retina. On the injected side, the retina is enlarged and has already appeared in previous cross sections. Line indicates injected side, **C:** A section through the middle region of the uninjected-side retina. The injected side (right side of panel) is enlarged relative to the uninjected side. **D:** A section through the most posterior region of the retina on the injected side reveals a still-large retina while the uninjected-side retina is nearly out of the section. **E:** Another *Noelin-4*-injected embryo in which the injection localized to more caudal regions, largely excluding the eye field. In this embryo, the eyes are equal sizes; however the neural tube appears expanded on the injected side in the hindbrain region (arrowhead). cg, cement gland; e, eye; mb, midbrain; r, retina.

**Figure 8:** Retina expansion by over-expression of *Noelin-4*

Expansion of retina persists at stage 29. Embryo injected in one blastomere at the 2-cell stage with 500 pg *Noelin-4* and 100 pg  $\beta$ -galactosidase, and processed for  $\beta$ -gal staining (turquoise) and whole mount in situ hybridization for the neural marker *Sox-2* (dark blue) at stage 29. Anterior is to the left. **A:** Uninjected side of embryo shows normal morphology of head structures. **B:** Injected side of same embryo shows expanded eye. **C:** Dorsal view. **D:** Cross-section through the largest part of the retina on the uninjected side. The retina is beginning to evaginate into the optic cup. **E:** Cross-section through the largest part of the retina on the injected side, at the same magnification as in D. The retina is not evaginating. Retina is expanded both in circumferential size as well as in thickness. **F:** Complete cross-section through the midbrain region for orientation. Note that neural tube appears enlarged on injected side as well. e, eye; cg, cement gland; mb, midbrain; asterisks denote otic vesicles.

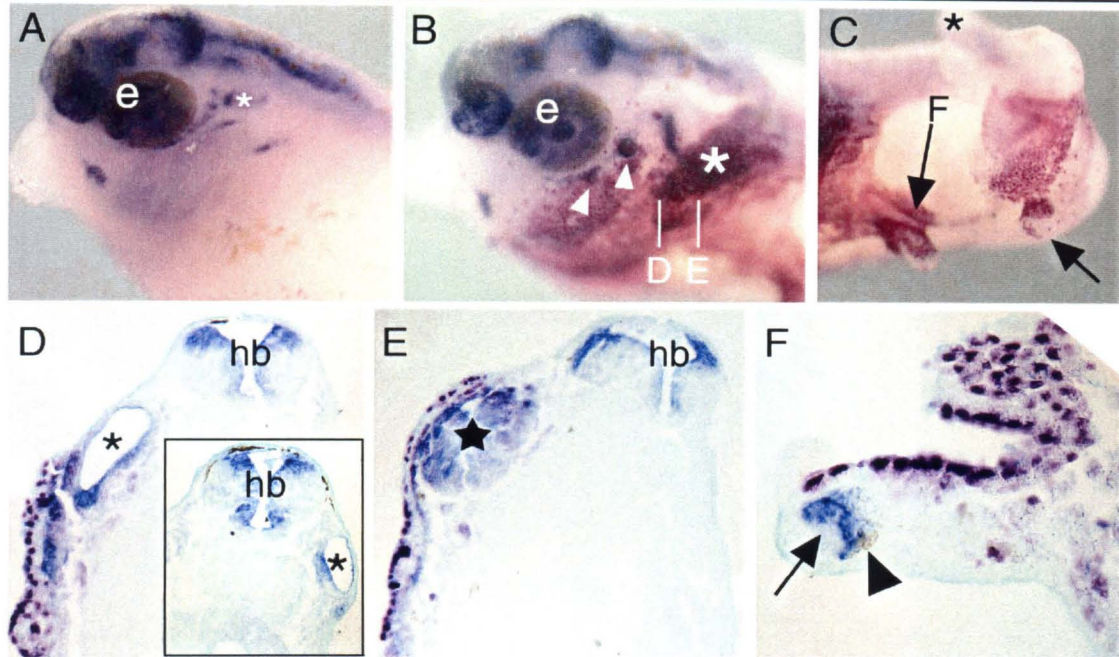
**Figure 9:** High dose overexpression of *Noelin-4*

## Figure 9: High-dose phenotypes of *Noelin-4* overexpression.

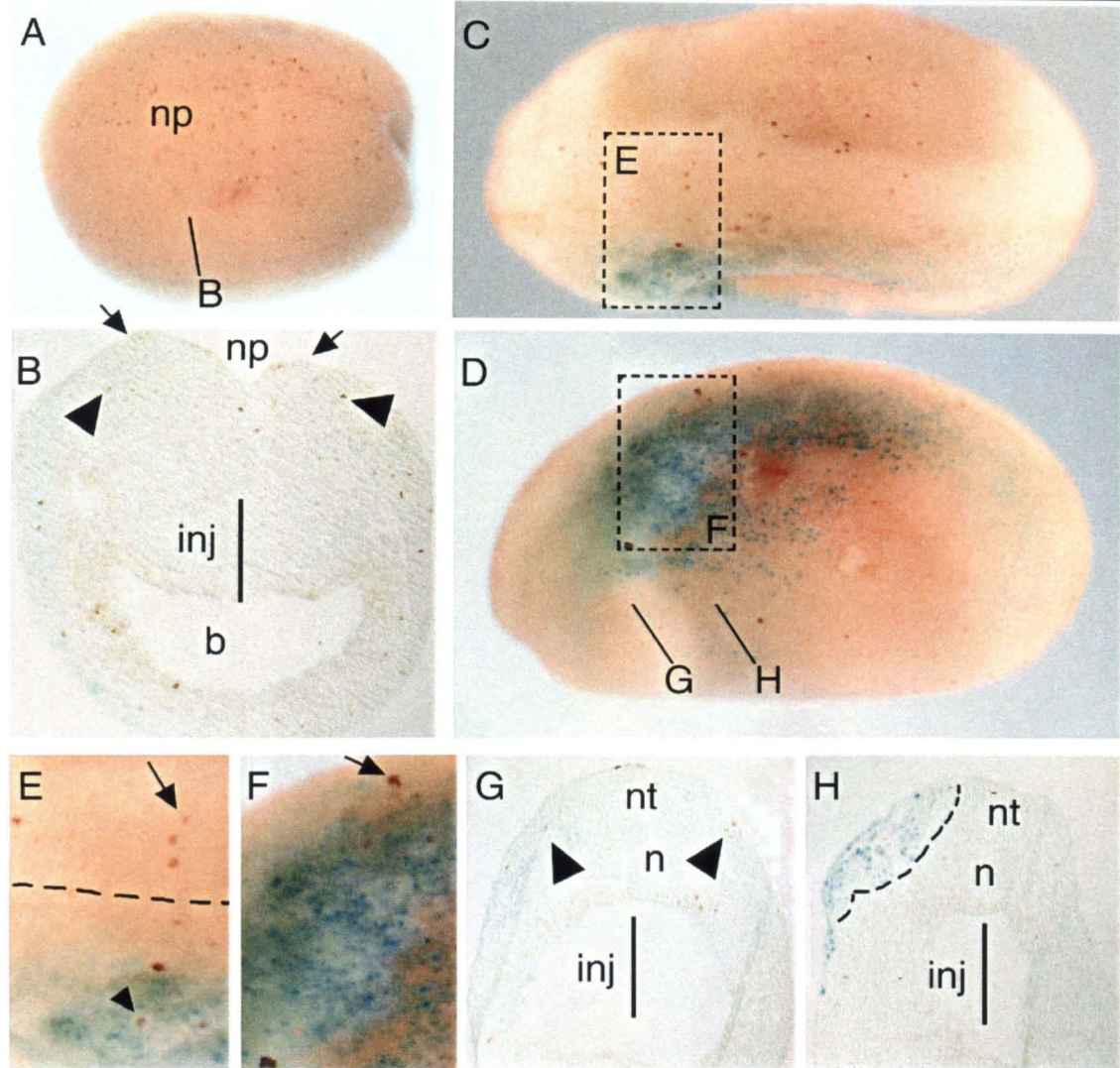
---

Embryos injected with 1 ng of *Noelin-4* and lineage tracer mRNAs [100 pg of  $\beta$ -galactosidase (A-H) or *green fluorescent protein (gfp)* (I-Q)] in one blastomere at the 2-cell stage and processed for in situ hybridization for *Sox-2* (purple) at stage 35 (A-H) or stage 29 (I-Q).  $\beta$ -galactosidase is stained magenta. High doses cause abnormal development of *Sox-2*-positive structures along the anterior-posterior axis (anterior is to the left). **A:** Uninjected side of a stage 35 embryo shows relatively normal development and *Sox-2* expression pattern. **B:** Injected side of the embryo shows bulge of ectopic *Sox-2*-positive tissue above the eye (arrowhead). Level of sections shown in C and D is indicated. **C:** Cross-section through the midbrain level shows large *Sox-2*-positive ectopic tissue dorsal to the normal eye (arrowhead). Boxed region is magnified in D. **D:** Magnification of the ectopic tissue (starred) shows that the tissue appears to have a basement membrane (arrow) around its proximal region, and is eye-shaped. **E:** Another stage 35 embryo with normal *Sox-2* staining on the uninjected side. **F:** On the injected side, no clear eye structure is discernible, but a mass of *Sox-2* staining is visible. Levels of sections in G and H are indicated. White arrow points to ectopic cement gland seen in cross-section in panel H, and normal cement gland is indicated (arrow, cg). **G:** Section through the midbrain and rostral eyes. On the injected side (right side of panel) an eye can be seen (e), although there is a group of pigmented cells that are not properly located (arrow). The retina appears continuous with the midbrain (arrowhead), which is not normal for this stage. There appears to be a lens formed next to the retina (starred, compare with normal lens on uninjected side in H, also starred). **H:** The overgrowth of the eye is visible in this caudal midbrain section. Below the overgrowth is a remnant of the eye in panel G (white asterisk). The midbrain vesicle is clearly continuous with the overgrown retina (arrowhead). Arrow points to an ectopic cement gland that has formed in this embryo. Compare locations of normal and ectopic glands in F and H. **I:** A stage 29 embryo shown from the injected side. Ectopic *Sox-2* cells are located along the axis in groups and are also scattered in the epidermis. Level of cross section in J is indicated. An ectopic vesicle has formed in the trunk (**J**, arrow) with a morphology and distribution of *Sox-2* transcripts similar to an otic vesicle (compare to panel O). **K:** Another stage 29 embryo. Uninjected side shows normal location of *Sox-2* staining. **L:** injected side shows an expanded *Sox-2*-positive otic vesicle (white asterisk, compare to white asterisk in (K), some small regions of *Sox-2*-positive cells (arrows) and a large ectopic structure (arrowhead). **M:** Dorsal view. White asterisk marks otic vesicle on injected side. Ectopic neural structure is continuous with the neural tube posteriorly (black arrow). White arrow marks neural tube. Embryo lacks complete tail structures. Lines indicate level of sections in N-Q. **N:** Cross-section through midbrain level (caudal portion of eye is visible on uninjected side, the left side of the panel). Arrow points to ectopic *Sox-2* staining in epidermal ectoderm. **O:** Section through the hindbrain at the level of the otic vesicles (asterisks). **P:** Enlarged otic vesicle on injected side extends posteriorly and is still visible in this section (asterisk), along with an ectopic vesicle structure (arrow). **Q:** Large, ectopic *Sox-2*-positive structure in cross section (arrowhead). e, eye; cg, cement gland; hb, hindbrain; mb, midbrain; n, notochord; s, somite; sc, spinal cord; asterisks mark otic vesicles except in H.

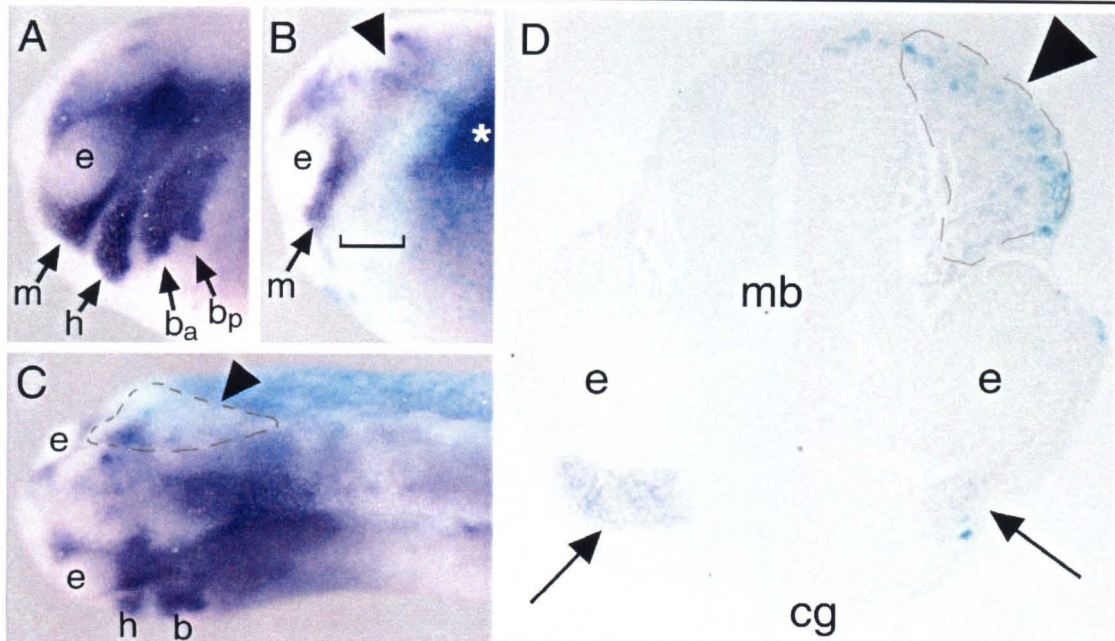
---

**Figure 10:** *Noelin-4* overexpression causes ectoderm conversion

Ectopic neural tissue and conversion of ectoderm is induced by *Noelin-4* at high levels of expression. An embryo injected with 1 ng *Noelin-4* mRNA and 100 pg  $\beta$ -galactosidase at the 2-cell stage and then stained with Magenta Gal (pink) and *Sox-2* (purple/blue) at stage 35. Sections are counterstained with Light Green. Anterior is to the left. **A:** Uninjected side of the embryo shows normal development of head structures. (Brown color is due to retinal pigmented epithelium in the eye and melanocytes in the skin.) **B:** Injected side displays atypical *Sox-2* staining (white arrowheads) and a large ectopic *Sox-2*-positive structure (white asterisk) that is continuous with the neural tube posteriorly. Level of sections in D and E are indicated with white lines. **C:** In the trunk, epidermal ectoderm fails to cover the embryo and tissue protrusions form (arrows). Central area that is unstained for the lineage tracer is bare mesoderm. Tip of the tail (out of focal plane) is marked with a black asterisk. **D:** Section through the hindbrain at the otic vesicle level: on the injected side (left side of panel) the otic vesicle (asterisk) is greatly enlarged as compared with that on the uninjected side (asterisk, boxed inset at same magnification). Each view in D represents the largest section of the otic vesicle on each side of the embryo. **E:** Section through the caudal hindbrain shows large ectopic *Sox-2*-positive structure (starred). **F:** Section through the protrusion indicated in panel C. At the distal portion of the protrusion is a *Sox-2*-positive group of cells with a visible basement membrane (arrow). Arrowhead marks pigmented cells adjacent to the *Sox-2* positive cells. e, eye; hb, hindbrain; asterisks mark otic vesicles or as indicated.

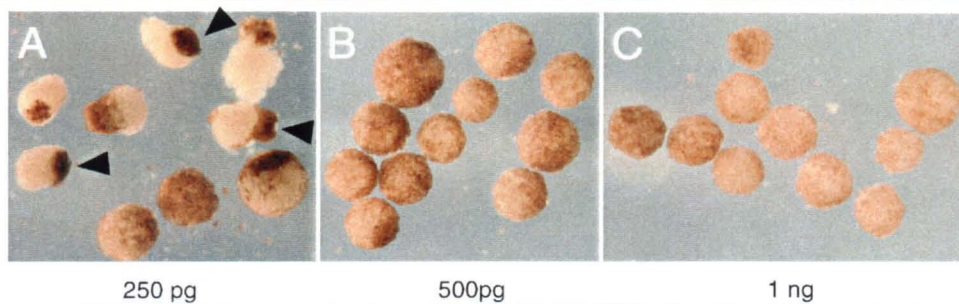
**Figure 11:** Extra proliferation is not the expansion mechanism

Overexpression of *Noelin-4* does not cause increased proliferation. Embryos were injected with 500 pg of *Noelin-4* and 100 pg of lineage tracer ( $\beta$ -galactosidase, turquoise) in one blastomere at the 2-cell stage and cultured until indicated. Embryos were stained with the anti-Histone H3 antibody (brown nuclei) which marks cells in metaphase. Anterior is to the left. **A:** A stage 14 embryo with uniform appearance of mitotic nuclei. Injected side is toward the bottom of the panel. Level of section in B is indicated. **B:** Section through the neural plate of the embryo in A. Injected side is to the left. Neural folds are indicated with arrows; mitotic nuclei on both sides are indicated with arrowheads. **C:** Dorsal view of a stage 23 embryo (injected side is towards the bottom of the panel). Area magnified in E is indicated. **D:** Lateral view of injected side. Within the  $\beta$ -galactosidase-positive area an expanded region of cells characteristic of *Noelin-4* overexpression is seen (partially boxed). Area magnified in F, as well as plane of sections in G and H are as shown. **E:** Close-up view of dorsal neural tube. Mitotic nuclei appear on both sides, arrow indicates a cell in metaphase on the uninjected side, arrowhead points to a mitotic cell on the injected side. Dashed line indicates embryo midline. **F:** Close-up view of expanded tissue on injected side. Some of the cells are mitotic (arrowhead) but not at numbers higher than on the uninjected side. **G:** Cross-section through rostral hindbrain level. Injected side is to the left. Mitotic cells are indicated with arrowheads on both sides of the embryo. There does not appear to be an increase in number on the injected side. **H:** A section through the expanded tissue region shows no unusual mitotic activity. Expanded region is indicated with dashed line. inj indicates injected side; n, notochord; np, neural plate; nt, neural tube.

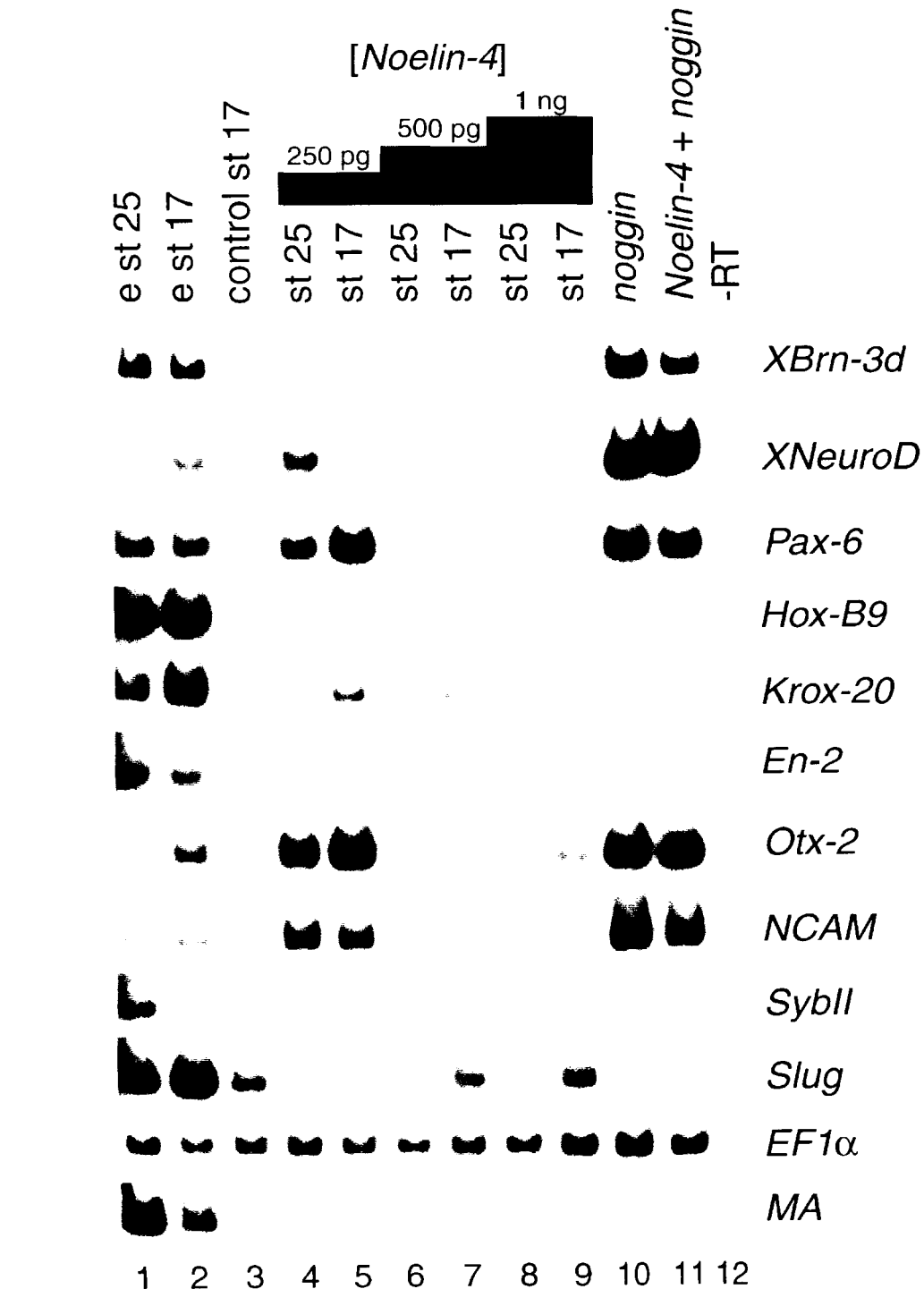
**Figure 12:** Neural crest formation is affected by *Noelin-4*

Neural crest formation is perturbed by *Noelin-4* overexpression. Embryos were injected with 1 ng *Noelin-4* mRNA in one blastomere at the 2-cell stage, along with 100 pg of  $\beta$ -galactosidase mRNA (turquoise stain) as a lineage tracer. Neural crest defects were assayed at stage 25 by *in situ* hybridization with *XTwist*, a neural crest cell marker. Anterior is to the left. **A:** Uninjected side of the embryo shows normal cranial neural crest migration. Mandibular (m), hyoid (h), and the anterior and posterior branchial (ba, bp) streams of migrating cells are visible. **B:** On the injected side, only mandibular crest appears (m, arrow), while the other streams are missing (bracket). Dark region posterior to bracketed area is due to shadow created by tissue bulge (asterisk), not *XTwist* staining (also see C). **C:** Dorsal view shows that a large mass of tissue (dashed outline) stained with the lineage tracer is in the region where the neural crest streams should be. **D:** A cross-section through a different embryo with a similar morphological phenotype to the one shown in A-C shows that ectopic tissue induced by *Noelin-4* does not express the neural crest marker (arrowhead marks outlined ectopic tissue). In addition, this embryo displays less *XTwist* expression in the mandibular neural crest on the injected side (right side arrow, compare to left side arrow). ba, anterior branchial neural crest; bp, posterior branchial neural crest; cg, cement gland; e, eye; h, hyoid neural crest; m, mandibular neural crest; mb, midbrain.

**Figure 13:** *Noelin-4* induces cement glands



Dose response for *Noelin-4* reveals that low dose induces cement gland formation in cultured animal caps. Embryos were injected in both blastomeres at the 2-cell stage with the indicated amount of *Noelin-4* mRNA, plus 60 pg *green fluorescent protein (gfp)* mRNA. Animal caps were cut at stage 8-9 and cultured until stage 25. **A:** Low dose (250 pg) *Noelin-4* injections. Cement gland formation is evident in seven animal caps (e.g., arrowheads). **B:** Middle dose injection (500 pg). Animal caps do not display cement glands and appear as epithelial balls. **C:** High dose injections (1 ng) also do not exhibit cement glands.

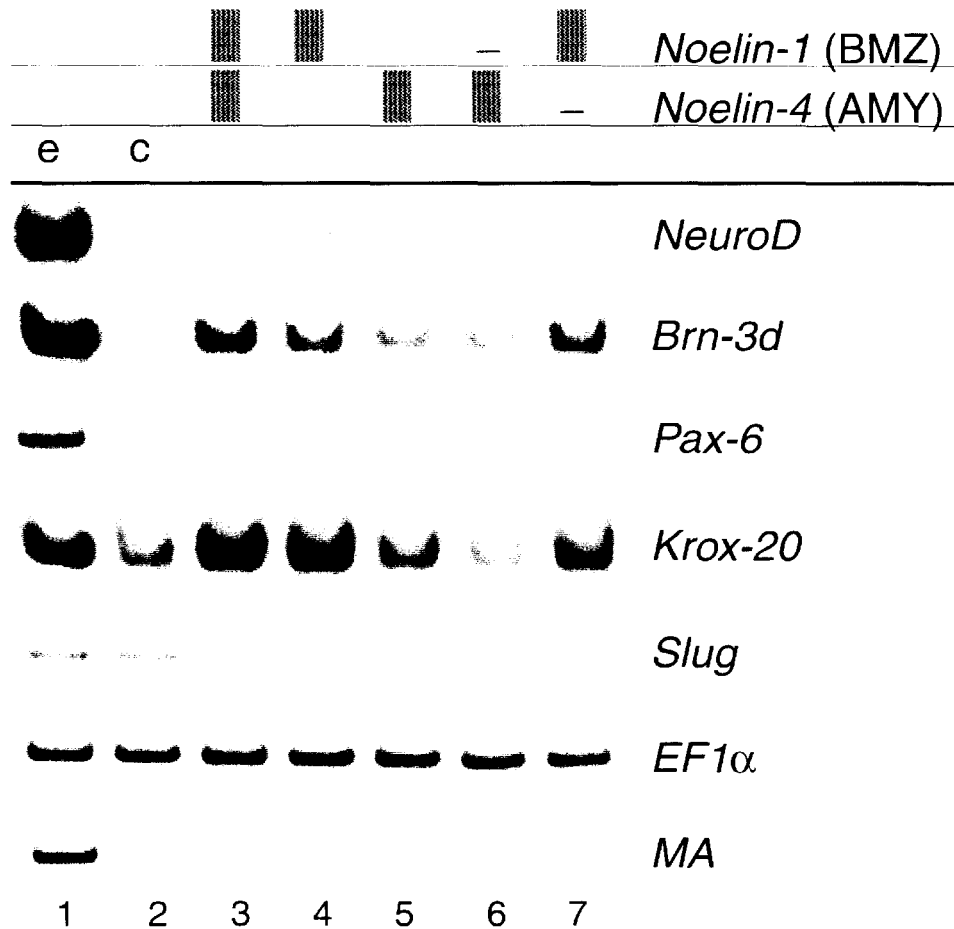
**Figure 14:** Neural induction by *Noelin-4*

## Figure 14: *Noelin-4* acts as a neural inducer

---

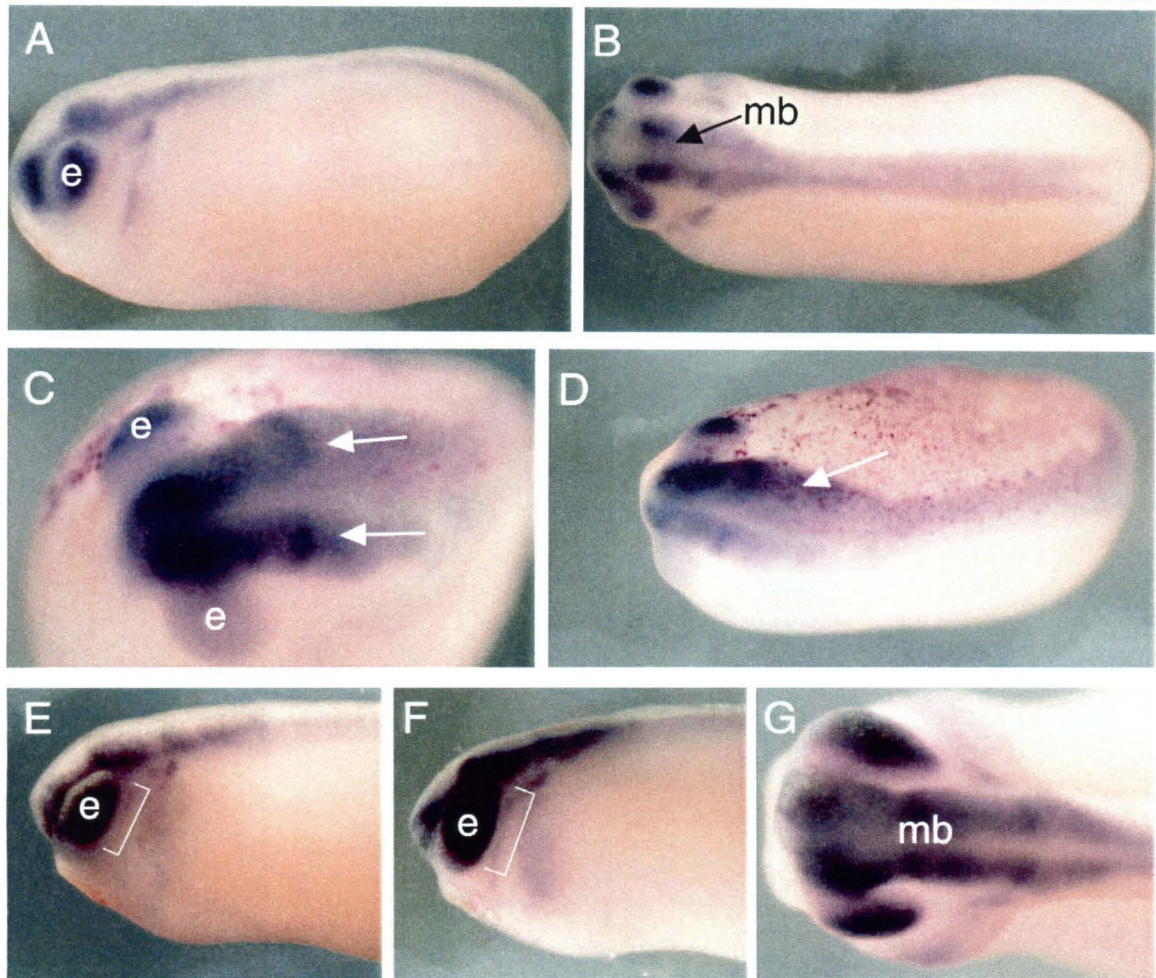
Animal cap explants as assayed by RT-PCR with a range of neural markers. Embryos were injected in two blastomeres at the 2-cell stage with the indicated amount of *Noelin-4* and/or *noggin* mRNA. Animal caps were isolated at stage 8-9 and were cultured until sibling-equivalent stages either 17 or 25 as noted. **Lane 1:** Whole embryo stage 25 control. **Lane 2:** Whole embryo stage 17 control. **Lane 3:** Control animal caps injected with 500 pg  $\beta$ -galactosidase, collected at stage 17. **Lane 4:** Injected with 250 pg *Noelin-4* and collected at stage 25. **Lane 5:** Injected with 250 pg *Noelin-4* and collected at stage 17. **Lane 6:** Injected with 500 pg *Noelin-4* and collected at stage 25. **Lane 7:** Injected with 500 pg *Noelin-4* and collected at stage 17. **Lane 8:** Injected with 1 ng *Noelin-4* and collected at stage 25. **Lane 9:** Injected with 1 ng *Noelin-4* and collected at stage 17. **Lane 10:** Injected with 100 pg *noggin* and collected at stage 25. **Lane 11:** Injected with 500 pg *Noelin-4* + 100 pg *noggin*, and collected at stage 25. **Lane 12:** All cDNAs were confirmed to be free of genomic DNA in -RT reactions; one is shown (PCR on total RNA from stage 25 embryos). cDNAs were normalized to EF1a levels and tested for mesoderm contamination with *Muscle Actin (MA)*. Whole embryos express all of the markers tested (lanes 1 and 2). Control animal caps express little to none of the markers (lane 3) as is characteristic for each primer set. Animal caps injected with 250 pg *Noelin-4* mRNA express *NCAM*, *Otx-2*, and *Pax-6* at stages 25 and 17 (lanes 4 and 5), and *NeuroD* at stage 25 (lane 4). This is similar to the profile of genes induced by *noggin* over-expression (see lane 10). Animal caps injected with 500 pg *Noelin-4* mRNA express low levels of *NeuroD* at stage 25 (lane 6), but do not express the other neural markers that the 250 pg dose animal caps express (lanes 6 and 7, compare to lanes 4 and 5). Animal caps expressing 1 ng of *Noelin-4* mRNA do not exhibit neural marker induction (lanes 8 and 9). *Noggin*-injected animal caps express the typical profile of neural induction, expressing *NCAM*, *Otx-2*, *Pax-6*, *NeuroD* and *XBrn-3d*. *Noelin-4* + *noggin* animal caps express the same neural markers as *noggin*-alone injections. *Slug* expression is not induced by *Noelin-4*; however, low dose injection eliminated background expression of *Slug* in animal caps in the same way that *noggin* injections do (compare lanes 4 and 5 with lanes 10 and 11). *Noelin-4* does not cause early neuronal differentiation as gauged by *Sybl1* expression, and *Noelin-4* + *noggin* also does not induce *Sybl1* expression. Posterior neural markers *En-2*, *Krox-20* and *HoxB9* are not induced by *Noelin-4*, whether alone or in conjunction with *noggin*.

---

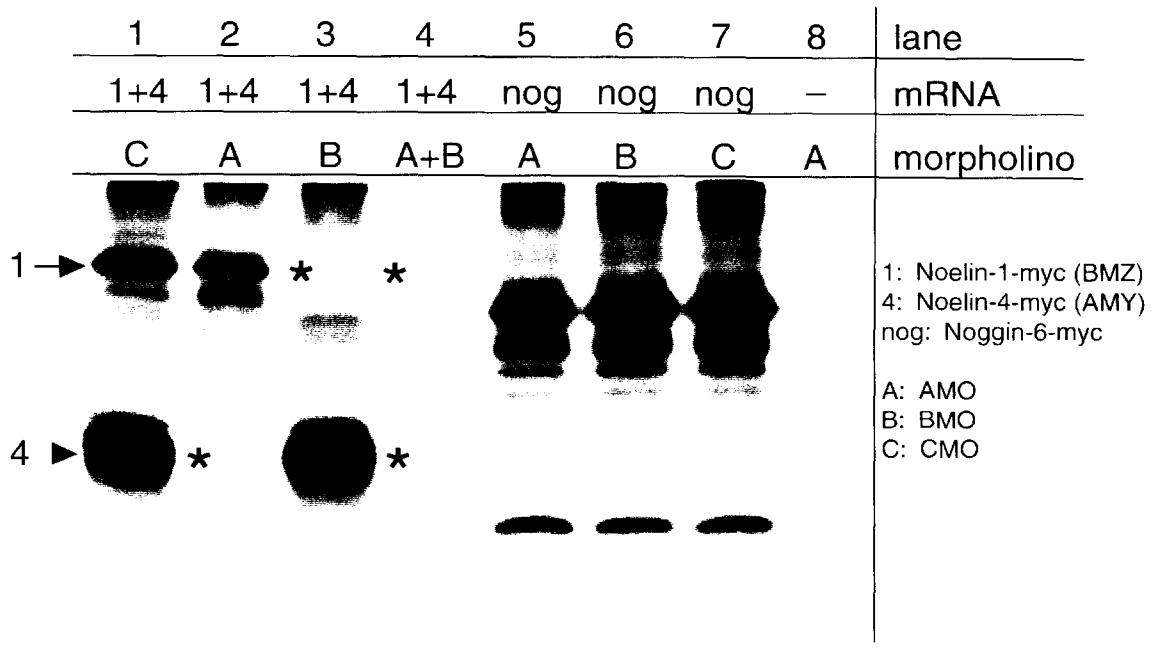
**Figure 15: *Noelins* functionally interact**

*Noelin* isoforms may cooperate in their endogenous functions. *Noelin-1* and *Noelin-4* were co-expressed at either equimolar levels (high/high dose) or at a four-fold excess (high/low dose). Animal caps were cut at stages 8-9, then cultured to stage 21. RT-PCR was performed to determine gene expression for a panel of neural markers. **Lane 1**, whole embryo control; **lane 2**, control animal caps; **lane 3**, 1 ng *Noelin-1* + 250 pg *Noelin-4*; **lane 4**, 1 ng *Noelin-1* + 62 pg *Noelin-4*; **lane 5**, 250 pg *Noelin-1* + 250 pg *Noelin-4*; **lane 6**, 250 pg *Noelin-4*; **lane 7**, 1 ng *Noelin-1*. Bars above gels indicate dose of injection: tall hatched bar for high, short gray bar for low; minus indicates no injection. Animal caps were tested for mesoderm contamination by *muscle actin* (*MA*) expression, and were normalized against *EF1α* levels. No significant changes in background expression of the neural crest marker *Slug* were found. *Krox-20*, a hindbrain marker, was induced by high doses of *Noelin-1* (lane 7). Co-expression of *Noelin-1* (high dose) with *Noelin-4* at both high and low doses (lanes 3 and 4) increased this induction. *Pax-6*, a marker of anterior neural tissue, was induced by *Noelin-4* alone (lane 6), and by high dose *Noelin-1* plus both high and low doses of *Noelin-4* (lanes 3 and 4). *Noelin-1* alone did not induce *Pax-6* (lane 7). *Brn-3d*, a sensory neural marker, was induced by high dose *Noelin-1* (lane 7) but not by *Noelin-4* (lane 6, compare to control in lane 2). When high dose *Noelin-1* was co-expressed with high dose *Noelin-4*, a higher level of *Brn-3d* was induced (lane 3), while co-expression of high *Noelin-1* plus low *Noelin-4* did not increase the induction. *NeuroD*, a neuronal determination marker, was induced by high doses of *Noelin-1* plus high or low doses of *Noelin-4* (lanes 3 and 4), but was not significantly induced by low *Noelin-1* plus high *Noelin-4* (lane 5), or by either isoform alone (lanes 6 and 7).

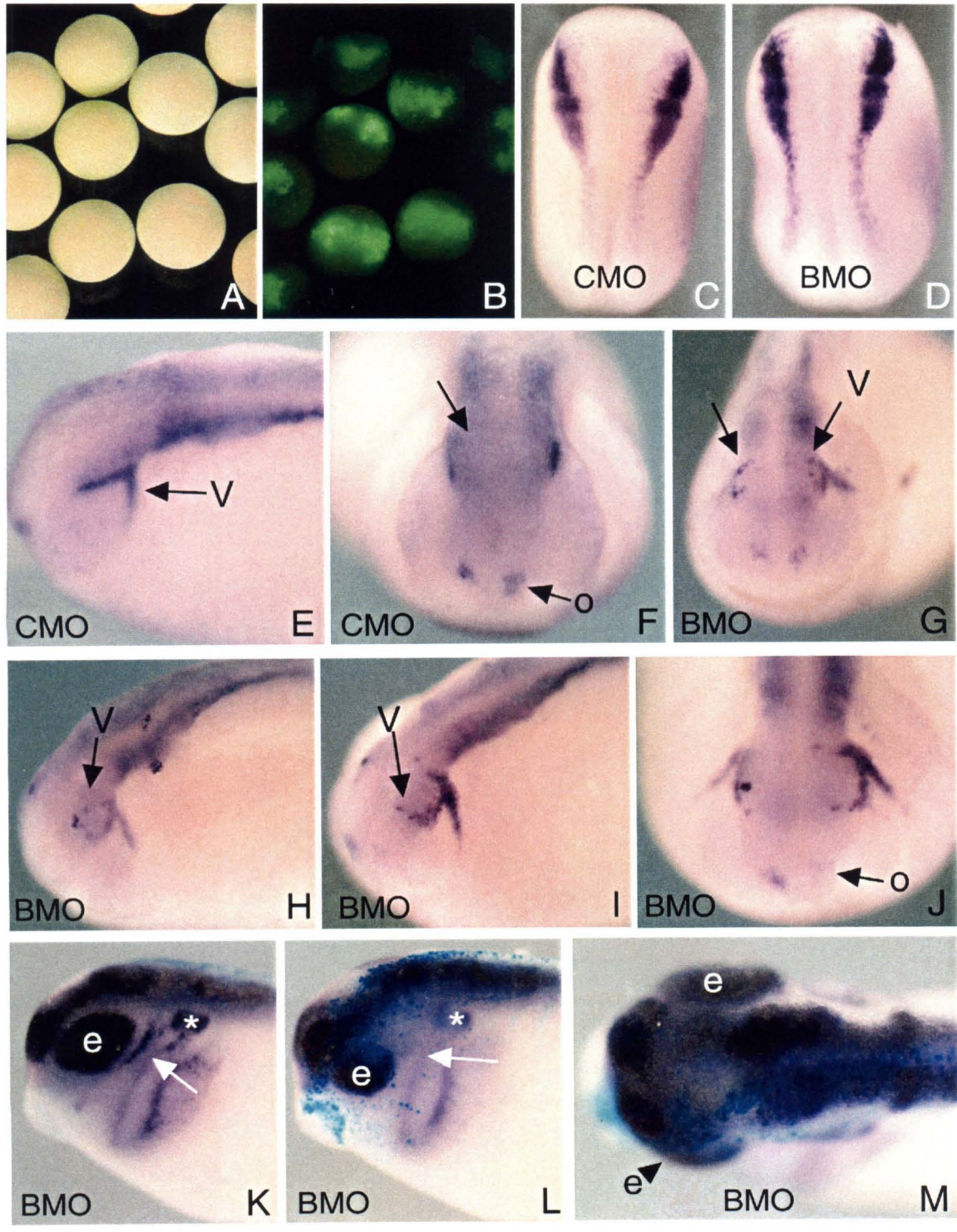
**Figure 16:** *Noelin-3* behaves like *Noelin-4* by overexpression



Embryos over-expressing *Noelin-3* also exhibit expanded neural tissue. *Noelin-3* mRNA (500 pg, plus 100 pg  $\beta$ -galactosidase) injections were in one blastomere at the 2-cell stage. Embryos were cultured until stage 24 and then processed for *in situ* hybridization against *Sox-2*. Anterior is to the left. **A:** Control embryo with normal *Sox-2* staining pattern. **B:** Dorsal view of same embryo, neural structures are symmetrical in size and shape. **C:** *Noelin-3*-injected embryo showing expanded neural tube on injected side (top of panel) arrows point to midbrain/hindbrain border on each side. **D:** Dorsal view of same embryo. Arrow indicates expanded neural tube. **E:** Side view of another embryo, uninjected side. Eye size (e) is indicated with bracket. **F:** Injected side shows expanded eye size (bracket). **G:** Dorsal view of the same embryo shows expanded eye on injected side (top of panel). All lineage tracer-positive cells are located in the retina of the injected side and are blocked by the dark *Sox-2* staining. e, eye; mb, midbrain.

**Figure 17:** Morpholinos inhibit translation of *Noelin* isoforms

Morpholino oligonucleotides (MO) directed against the first 25 coding nucleotides of *Noelin-1* and *Noelin-4* including the translation initiation site inhibit translation *in vitro*. Messenger RNA for *Noelin-1-myc* plus *Noelin-4-myc* together, or *Noggin-6-myc* alone, was incubated with MOs directed against the A and B exons of *Noelin* splice forms (AMO, BMO), or with a standard control MO (CMO) in an *in vitro* translation system. After translation incubation, the samples were immunoprecipitated with the myc antibody. Lane 1: *Noelin* isoforms plus CMO; lane 2: *Noelins* plus AMO (targets *Noelin-4*); lane 3: *Noelins* plus BMO (targets *Noelin-1*); lane 4: *Noelins* plus both A- and B-MOs; lane 5: *Noggin* plus AMO; lane 6: *Noggin* plus BMO; lane 7: *Noggin* plus CMO; lane 8: minus RNA control, plus AMO. In **lane 1**, CMO does not inhibit translation of either *Noelin* transcript. *Noelin-1* protein (arrow) and *Noelin-4* protein (arrowhead) are abundant in this sample. **Lane 2** shows that AMO specifically inhibits *Noelin-4* protein synthesis (asterisk) but not *Noelin-1*. **Lane 3** shows *Noelin-1* translation is specifically inhibited by BMO (asterisk). In **lane 4**, both *Noelin* transcripts are essentially untranslated when mixed with AMO and BMO. *Noggin* translation is not inhibited by AMO, BMO or CMO (**lanes 5-7**). **Lane 8** shows that AMO alone has no effect in the *in vitro* translation system. Asterisks mark gel location of proteins whose translation is inhibited by the MOs. 1, *Noelin-1*; 4, *noelin-4*; nog, *noggin*.

**Figure 18:** Morpholino injections perturb neural development

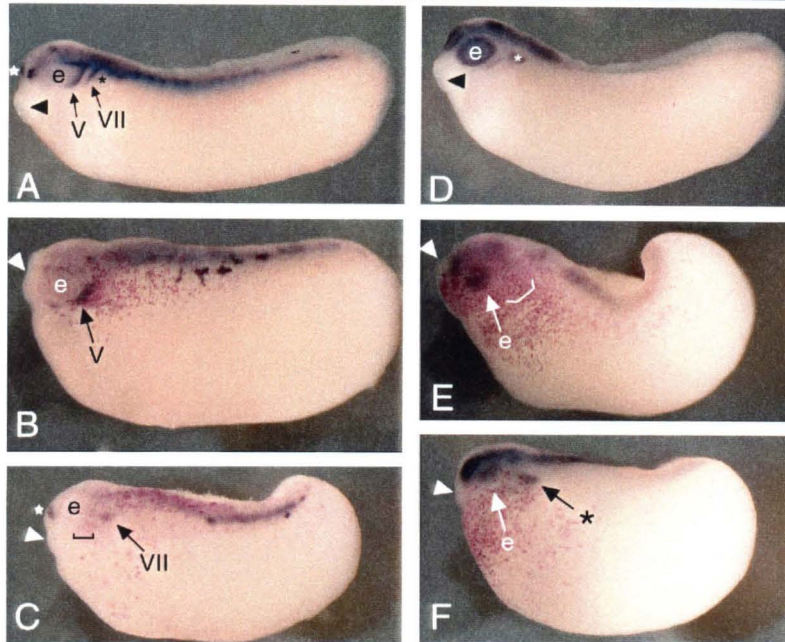
## Figure 18: MO injections cause neural defects

---

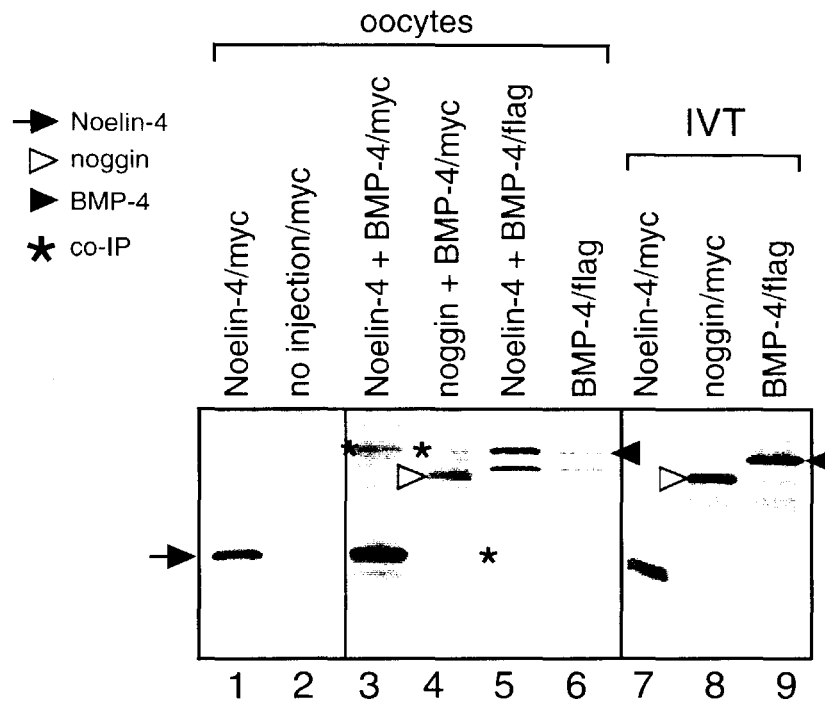
MOs designed against the first 25 coding nucleotides of the B exon (BMO, injected at 5-20 ng per embryo as indicated), which targets the B-containing isoforms *Noelin-1* and *Noelin-3*, or a control MO (CMO, injected at 20 ng per embryo) were injected in both blastomeres at the 2-cell stage (C-J) or in one blastomere (K-M) and then assayed for a variety of neural markers by whole mount *in situ* hybridization at the stage indicated. **A:** Embryos injected with the fluoresceinated CMO at stage 10 in bright field view. **B:** Same embryos under fluorescence show the CMO is present at this stage. **C:** Embryo injected with 20 ng CMO and stained for the neural crest marker, *Slug*, at stage 17. Normal expression pattern is observed (anterior is up). **D:** Stage 17 embryo injected with 20 ng BMO and stained for *Slug* also exhibits a normal expression pattern. Anterior is up. **E:** Stage 24 embryo (anterior to the left) injected with 20 ng CMO and stained for *N-tubulin*, a neuronal differentiation marker. Normal expression pattern is observed in the neural tube and trigeminal ganglia (arrow). **F:** Anterior view of same embryo. Midbrain area is indicated by arrow and shows no *N-tubulin* staining in the superficial tissue layers. The olfactory placodes are indicated. **G:** Embryo injected with 10 ng BMO and stained for *N-tubulin* at stage 24. Some *N-tubulin*-positive cells appear in unusual locations (arrows) outside of the trigeminal ganglia in this anterior view. **H:** Another stage 24 embryo (anterior to the left) injected with 10 ng BMO also exhibits *N-tubulin*-positive cells in more superficial layers (arrow). **I-J:** Another stage 24 embryo injected with 10 ng BMO, *N-tubulin* stain. Side view (I) arrow points to cells expressing *N-tubulin* outside of the ganglion. **J:** Arrow indicates olfactory placode with less staining than is usual for this stage (compare to olfactory placodes in F). **K:** Embryo injected with 10 ng BMO in one blastomere at the 2-cell stage, stained with the neural marker *Sox-2* at stage 30, uninjected side. **L:** Injected side shows a reduced eye (e) and cranial placode staining (arrow). **M:** Dorsal view for comparison of eye size (e with arrowhead on injected side). e, eye; o, olfactory placode; V, trigeminal ganglion region. Asterisks mark otic vesicles.

---

## Figure 19: Targeted A+B Morpholino injection



Embryos were injected with 5 pg AMO + BMO or CMO in 2 cells at the 32-cell stage. A- and B-tier cells were chosen to target prospective neural ectoderm. Embryos were cultured until stage 27 when they were fixed and processed for  $\beta$ -galactosidase staining (magenta, lineage tracer mRNA injected at 60 pg per embryo) and whole mount in situ hybridization against the neuronal differentiation marker *N-tubulin* (A-C) or the pan-neural marker *Sox-2* (D-F). Anterior is to the left, degree of magnification is not necessarily equivalent between panels. **A:** Control embryo injected with CMO and stained for *N-tubulin* displays normal expression pattern and morphology. Arrowhead indicates cement gland, asterisk indicates otic vesicle, olfactory placode indicated by star. Cranial ganglia are indicated (V, trigeminal; VII, geniculate). **B:** Embryo injected with A+B MOs appears ventralized, lacking anterior neural tube structures and with a displaced cement gland (arrowhead). V<sup>th</sup> ganglion is indicated, VII<sup>th</sup> appears to be missing, as is the olfactory placode. **C:** Another embryo injected with A+B MOs with a similar morphological phenotype, but with missing V<sup>th</sup> ganglion (bracket) and a reduced VII<sup>th</sup> (arrow). Cement gland and olfactory placode are indicated (arrowhead and star), compare to control in A. **D:** CMO-injected control embryo stained for *Sox-2*. Eye (e), otic vesicle (asterisk) and cement gland (arrowhead) are indicated. **E:** A+B MO injected embryo lacks normal head formation, eye size is reduced (arrow, e) and cement gland is displaced (arrowhead). Region where placode staining should be is bracketed. Embryo also has open spinal cord. **F:** Another embryo injected with A+B MOs, severely ventralized with reduced or missing anterior neural structures (see eye size and small cement gland). Embryo may have an otic vesicle (asterisk). e, eye.

**Figure 20:** Noelin-4 interacts with BMP-4 in oocytes

Co-immunoprecipitation assay. Oocytes were injected with mRNAs for Noelin-4-myc alone, Noelin-4-myc + BMP-4-flag, noggin-6myc + BMP-4-flag, or BMP-4-flag alone, and cultured for 24 hours in the presence of  $^{35}\text{S}$ -methionine. The same mRNAs were also used for *in vitro* translation (IVT). Oocyte and *in vitro* translated proteins were immunoprecipitated (IP) with anti-*myc* or anti-*flag* antibodies and electrophoresed on a 14% SDS-polyacrylamide gel. Images were captured on a PhosphorImager. Lanes 1 and 2 were run on a different gel from lanes 3-9. **Lane 1:** Noelin-4 protein immunoprecipitated from oocytes with anti-*myc* antibody (arrow). No other proteins are prominently immunoprecipitated. In **lane 2**, control uninjected oocytes do not immunoprecipitate any specific proteins with anti-*myc*. **Lane 3:** Oocytes injected with Noelin-4 + BMP-4 and immunoprecipitated with anti-*myc*, also bring down a larger band (asterisk). **Lane 4:** Oocytes injected with noggin + BMP-4 and immunoprecipitated with anti-*myc*, co-immunoprecipitate noggin (open arrowhead) and a band of the same size as in lane 3 (asterisk). **Lane 5:** Oocytes injected with Noelin-4 + BMP-4 and immunoprecipitated with anti-*flag*, co-immunoprecipitate a protein of the same size as Noelin-4 (asterisk). **Lane 6:** Oocytes injected with BMP-4 and immunoprecipitated with anti-*flag* bring down 2 bands for BMP-4 (arrowhead marks full-size protein). **Lane 7:** IVT Noelin-4, immunoprecipitated with anti-*myc*. **Lane 8:** IVT noggin, immunoprecipitated with anti-*myc* (open arrowhead). **Lane 9:** IVT BMP-4, immunoprecipitated with anti-*flag* (arrowhead). Asterisks denote co-immunoprecipitated proteins.

## **Chapter 4**

**Mouse *Noelin-1/2* expression pattern and comparison with  
*Noelin* homologs in other vertebrates**

## INTRODUCTION

Noelin proteins comprise an interesting family of isoforms with divergent roles in development across species. In the chick embryo, retroviral over-expression of *Noelin-1* causes prolonged and excessive neural crest migration from cranial neural tube (Barembaum *et al.*, 2000, Appendix Chapter 1). In the frog embryo, *Noelin-1* functions to promote neuronal differentiation in neuralized animal caps, but has no autonomous effect on neural crest development (Moreno and Bronner-Fraser, 2001; Chapter 2). These seemingly disparate functions can be related back to the expression patterns of the gene in each species.

Chick embryos express *Noelin-1* from the neural plate stage onward, with a striking pattern of expression in which *Noelin-1* expression correlates with cells that have the potential to give rise to neural crest cells. In the frog, *Noelin-1* cannot be detected in the neural crest by whole mount *in situ* hybridization, but it is expressed in post-mitotic neural cells in the neural tube, cranial ganglia, and eye. Thus the differentiation-promoting activity of frog *Noelin-1* is consistent with its expression pattern. The chick expression pattern in early cells with neural crest potential also correlates with its gain-of-function phenotype, in which cranial neural tube continues to produce neural crest long after it would normally have ended.

The rat *Noelin* homologs were the first to be isolated (Danielson *et al.*, 1994). They were cloned in a screen for brain-specific genes in post-natal rats, and found to be highly expressed in the cortex (Danielson *et al.*, 1994). There are no functional data regarding their roles in rat development. Later, Noelin

isoforms were isolated from mouse (called Pancortins 1-4, (Nagano et al., 1998), chick (Barembaum et al., 2000), and frog (Moreno and Bronner-Fraser, 2001).

Expression of each of the four *Noelin* isoforms may be specifically regulated, although they all are transcribed from two promoters. There is evidence of differential regulation of the *Noelin* gene promoters in some species: the B-containing isoforms (*Noelin-1* and *-3*, BMZ and BMY) have been shown to be expressed in kidney cells as well as in neural tissues in the rat, while the A-containing isoforms (*Noelin-2* and *-4*, AMZ and AMY) are only expressed in neural tissues (Kondo et al., 2000). In the frog, all isoforms are activated by over-expression of neurogenic genes, suggesting that *Noelin* expression may be controlled by these genes *in vivo* (Moreno and Bronner-Fraser, 2001). However, the frog B-containing isoforms appear to be expressed earlier than the A-containing isoforms (see Chapter 3). Moreover, differential regulation of splicing has been suggested by data from the chick system, where the Y-containing isoforms *Noelin-3* and *-4* (BMY and AMY) are first expressed several stages after the Z-containing isoforms *Noelin-1* and *-2* (BMZ and AMZ). Thus there appears to be a complex system of regulation of the isoforms across species; in some the promoters are differentially regulated, and in others, splice form formation is differentially regulated.

What is the general function of *Noelin-1*? It appears that between frog and chick, there is no consensus. The chick studies did not address whether neuronal differentiation was affected in the retroviral over-expression experiments; however, in the frog it is clear that *Noelin-1* over-expression had no effect on neural crest induction or migration. To investigate further the function of *Noelin-*

1 across species, I cloned mouse *Noelin-1* and examined its expression pattern. This is an important first step toward determining whether there could be a consensus function for the *Noelin* genes in vertebrates, or whether their divergent expression patterns reflect divergent mechanisms of function.

## METHODS

### **Cloning and sequencing a partial mouse *Noelin-1***

The Mouse *Noelin* Z exon was isolated by reverse transcriptase-polymerase chain reaction (RT-PCR). The subclone was generated using upstream primer 5'-CAG AAG GTG ATA ACC GG-3' and downstream primer 5'-CAG CGC GCG GTC TTT AG-3' to amplify a 616 base pair (bp) fragment of the Z exon from embryonic day 10 cDNA (Moreno and Bronner-Fraser, 2001). Total RNA was isolated using RNazol B (Tel-Test, Inc.) according to the manufacturer's instructions. cDNA was synthesized using random hexamers (Life Technologies) and MMLV Reverse Transcriptase (Roche). The fragment was subcloned into the pBluescript plasmid (Stratagene) and sequenced by dideoxy termination with [<sup>35</sup>S]-dATP (NEN) using the Sequenase kit according to manufacturer's instructions (USB).

DNA and protein analysis were performed using DNASTar Sequence Analysis software, and compared to sequences in the databases by Blast searching (Altschul et al., 1990).

## Embryo collection and whole mount *in situ* hybridization

Pregnant females from timed matings of c57/bl6J mice (Jackson Labs) were sacrificed with CO<sub>2</sub> gas at the appropriate number of days post conception (dpc). The uterus was removed through an abdominal incision and the embryos were dissected out in PBS. Embryos were fixed for 2 hours in 4% paraformaldehyde/0.25% glutaraldehyde at room temperature. Embryos were dehydrated into 100% ethanol and stored at -20°C until further processing.

Whole mount *in situ* hybridization was performed as described in Henrique *et al.* (1995). *Noelin Z* exon antisense probe was synthesized by *in vitro* transcription using digoxigenin-11-UTP (Roche) and T7 polymerase (Promega) according to the manufacturer's instructions, on pBS-m*Noelin-Z* cut with *Spe I* (Roche).

Embryos were embedded for cryosectioning by sinking in 5%, then 15% sucrose in PBS, then incubating for 3 hours in 7.5% gelatin/15% sucrose. Embryos were positioned in plastic molds and allowed to set at room temperature. Before sectioning, blocks were quick-frozen in liquid nitrogen and allowed to warm to -30°C before mounting on a chuck with OCT (Tissue Tek). Embryos were sectioned on a cryostat at 15 µm.

Embryos to be sectioned in wax were dehydrated to 100% ethanol, then incubated 2 x 20 minutes in HistoSol (National Diagnostics). HistoSol was removed and embryos were incubated overnight in Paraplast Plus at 60°C (Oxford), then changed to fresh wax for 1 hour at 60°C before embedding and sectioning on a Leitz microtome at 10 µm.

## RESULTS AND DISCUSSION

### **Cloning of mouse *Noelin***

A mouse *Noelin* cDNA was cloned by RT-PCR using the known rat genomic sequences (Danielson et al., 1994) to design primers. Embryonic day 10 RNA was isolated and reverse-transcribed, and then amplified with oligonucleotides specific to the Olfactomedin domain (Barembaum et al., 2000; Kulkarni et al., 2000) of the Z region. The PCR product was subcloned into the pBluescript vector for sequencing and *in situ* probe synthesis.

The sequence of the 616 base pair (bp) product was identical to the mouse *Noelin-1* and -2 sequences that were later submitted to GenBank (also known as *Pancortin-1* and -3, accession numbers BAA28765 and BAA28767, Nagano *et al.*, 1998).

### **Phylogeny of *Noelin* genes**

*Noelin* homologs across diverse vertebrate species are highly conserved, both at the nucleic acid and amino acid levels. Figure 1 shows an amino acid alignment of *Noelin-1* homologs from five species: chick, human, mouse, rat, and *Xenopus*. Each protein shares more than 93% identity with each other homolog, and many of the sequence substitutions are conservative in nature.

Phylogenetic analysis reveals that *Noelin* genes are related as expected (Fig. 2A). When compared with Olfactomedin, the founding member of the family of Olfactomedin-domain-containing proteins (Snyder et al., 1991), *Xenopus* and chick *Noelin-1* sequences are closer to each other than to mammalian

counterparts, and mouse and rat group together, with the human sequence being the closest relative (Fig. 2A).

A sequence distance table shows that all Noelin-1 homologs are highly related (Fig 2B). Mouse and rat are 99% identical, and mouse and human are 98% identical. In addition to the sequences shown here, GenBank contains Noelin-like sequences from pigeon, quail, medaka, zebrafish, bovine and pig. Thus, Noelin-1 is a highly conserved protein across many vertebrate species.

### **Mouse *Noelin* is expressed in neural plate and neural crest**

In order to determine the spatiotemporal expression pattern of *Noelin-1* (BMZ) and *-2* (AMZ) isoforms in the mouse, the Z exon of *Noelin-1* and *-2* (hereafter designated *Noelin-1/2*) was used to probe embryos from various stages by whole mount *in situ* hybridization. This analysis will reveal cells that express either *Noelin-1* or *Noelin-2* or both, but will not determine a distinction in expression pattern between the two.

Mouse cup-shaped embryos at embryonic day 7.5 (E7.5, advanced primitive streak stage) were probed with *Noelin-1/2* and then sectioned at 10  $\mu$ m in order to examine the expression pattern in detail. Sections shown in Figure 3 were made transversely across the anterior/posterior axis (a/p axis) starting from anterior head and posterior tail and moving down through the embryo, eventually reaching the middle of the a/p axis which is folded essentially in half at this stage. In the head region, *Noelin-1/2* was expressed in the developing cranial neural plate as well as weakly in the allantois and strongly in the amnion (Fig. 3A). Extra-embryonic membranes did not express *Noelin-1/2* (Fig. 3A).

Further caudally, *Noelin-1/2* was also found in the developing neuroepithelium where the neural folds will eventually form (arrows, Fig. 3B), as well as in the cranial neural plate. In a section midway through the embryo, *Noelin-1/2* was found in the rostral neural plate region as well as caudally in the neuroepithelium, and some expression was also observed in the lateral mesoderm (arrow, Fig. 3C).

Slightly later in development, *Noelin-1/2* had a more complex expression pattern. At E8 (unturned embryo with 6-8 somite pairs), the embryo proper is better visible in whole mount. Figure 4A shows an embryo at this stage from a cranial view. The neural plate contained stain for the *Noelin-1/2*. When the embryo was tilted to give a view of the posterior region, the caudal neural plate was also observed to contain *Noelin-1/2* signal (Fig. 4B). Ventral views of the same embryo revealed that extra-embryonic membranes and endoderm were unstained (Fig. 4C, D).

In cross-sections at cranial levels, the neural plate was clearly stained (arrows), as was some head mesenchyme (asterisks) and pharyngeal endoderm (arrowheads) in Figures 4E-H. A caudal section at the neural plate level revealed neural plate staining (arrows, Fig. 4I) and some staining in the mesoderm (asterisks, Fig. 4I). Interestingly, expression in the hindbrain was stronger than in the forebrain (e.g., compare fb and hb in Figs. 4G and H).

At E8.5 (turning embryo with 10-12 somite pairs), *Noelin-1/2* clearly stained some neural crest in the head region. Pre-otic neural crest was positive for the gene (Fig. 5A, arrow) and the ectoderm was not stained (arrowhead). Pharyngeal endoderm continued to stain for *Noelin-1/2* (asterisk). A slightly

more caudal section through the hindbrain and otic vesicle level revealed positive neural crest cells (Fig. 5B, arrow) and negative invaginating otic placode (Fig. 5B, arrowhead). The closing neural tube now appears to express *Noelin-1/2* at lower levels than at the earlier stages shown in Figures 3 and 4. Pharyngeal endoderm was also positive (asterisks, Fig. 5B), as was the adjacent ectoderm that is likely to be the epibranchial placode (blue arrowhead, Fig. 5B).

At embryonic day 10 (approximately 30-35 somite pairs), mouse embryos expressed *Noelin-1/2* in the distal cranial ganglia, which are placode-derived (Baker and Bronner-Fraser, 2001), and in the brain and limb. Figure 6 shows a series of whole mount views of an E10 embryo. The olfactory placode and trigeminal (V), geniculate (VII), petrosal (IX) and nodose (X) ganglia expressed *Noelin-1/2* (Fig. 6A). Dorsally, *Noelin-1/2* was found in the neural tube from the midbrain and extending caudally through the embryo (Fig. 6B). In the limb buds, *-1/2* expression was found in the posterior region known as the zone of polarizing activity (ZPA, Fig. 6C). In addition to the cranial ganglia and neural tube staining, *Noelin-1/2* expression was also observed in the vagal neural crest (Fig. 6E, arrow) and branchial arches (Fig. 6E, arrowheads).

Cross-sections of an E10 embryo stained with *Noelin-1/2* revealed transcripts in the marginal zone (outer layer of the neural tube) at varying rostro-caudal levels. In a dorsal midbrain section, the expression was intense at the margins of the neural tube (Fig. 7A). Further caudally in the midbrain, *-1/2* expression was found in discrete regions of the neural tube, but always at the marginal zone and not in the ventricular zone (Fig. 7B and C). In the hindbrain, *Noelin* expression was found in the trigeminal (V), geniculate (VII), petrosal (IX)

and nodose (X) ganglia (Fig. 7D-F, petrosal not shown). Staining was not observed in the otic vesicle (Fig. 7E). At specific hindbrain regions, ventral staining of the marginal zone was observed (Fig. 7E). The posterior limb bud was also found to express *Noelin-1/2* in the mesenchyme but not in the ectoderm (Fig. 7G).

### ***Noelin* genes are expressed divergently in vertebrate species**

In order to gain more insight into the role that *Noelin* isoforms may play during vertebrate development, I next compared the mouse *Noelin-1/2* expression pattern with those of the frog and chick homologs. Frog and chick expression patterns are quite different, thus comparison of these patterns with the mouse could give some insight into the possibilities of conserved functions for the gene based on its expression pattern.

The *in situ* shown in Figures 3-7 were performed on embryos at developmental stages comparable to the *in situ* shown for frog *Noelin-1* in Chapter 2, and for chick *Noelin-1* in Appendix Chapter 1 (Barembaum et al., 2000). Figure 8 illustrates the differences between the frog and chick *Noelin* distribution patterns. Frog *Noelin-1* is expressed in post-mitotic cells in the cranial ganglia, eye, and neural tube, and is not observed in the neural crest or neural plate by whole mount *in situ* hybridization at earlier stages (Fig. 8A). In contrast, chick *Noelin-1* is expressed in the early neural plate and neural crest (Fig. 8B and Appendix Chapter 1).

The mouse *Noelin-1/2* is expressed in the early neural plate and ectoderm, and as development proceeds, it is found in the some of the cranial placodes,

neural crest and pharyngeal endoderm. Later, mouse *Noelin* is found in marginal zone cells of the neural tube, and in the placode-derived cranial ganglia. In *Xenopus in situs*, only the later expression pattern is observed. As described in Chapter 3, however, frog *Noelin* isoforms are expressed from the neural plate stage onward, although it is not known which tissues express the genes as the early expression is only detectable by RT-PCR.

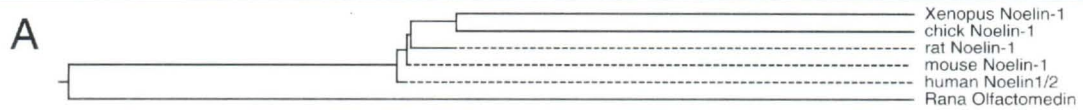
In the chick, the expression in the neural crest is more widespread than in the mouse. Expression is detected in migrating neural crest in the head and trunk, which was not the case in mouse embryos. Furthermore, chick *Noelin* is expressed in the dorsal root ganglia (trunk derivatives of neural crest cells), which I did not observe at the stages examined in the mouse. Thus, the expression pattern of this gene diverges between species, with the chick embryo revealing the greatest amount of neural crest staining, the mouse embryo with an intermediate level of neural crest staining, and the frog embryo with no neural crest staining. Mouse and chick also share *Noelin* expression in the cranial placodes, but frogs do not. All three species contain the later expression in differentiating neural tissues in the spinal cord, brain, and cranial ganglia.

The mouse *Noelin* expression pattern suggests that *Noelins* may play a role in neural crest formation in this species, since mouse embryos contain *Noelin* expression in the neural crest and early neural plate. This is similar to the chick pattern; moreover, chick neural crest production is affected by over-expression of *Noelin-1*. The observation that frog *Noelins* are expressed before they can be detected by whole mount *in situ* hybridization (Chapter 3) suggests that they too may have an earlier role in neural development. This is further

supported by the functional data presented in Chapter 3 for *Noelin-4*, the AMY isoform.

The *Noelin* isoforms are a dynamic group of proteins that play multiple roles in neural development. Further studies in the mouse where genetic ablation is possible will uncover fascinating information regarding the role of *Noelins* in mammalian neural development.



**Figure 2:** Sequence relationships between *Noelin* homologs

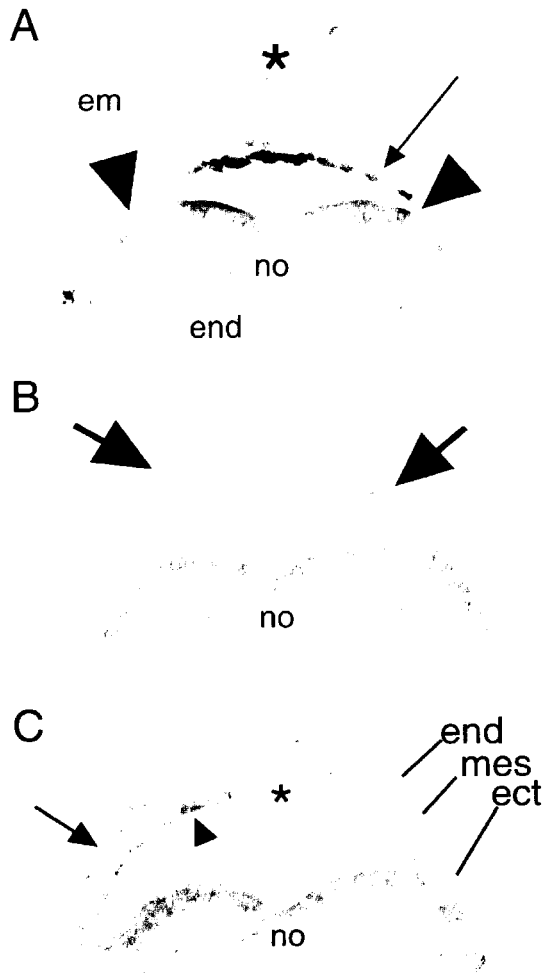
**B**

Percent Identity

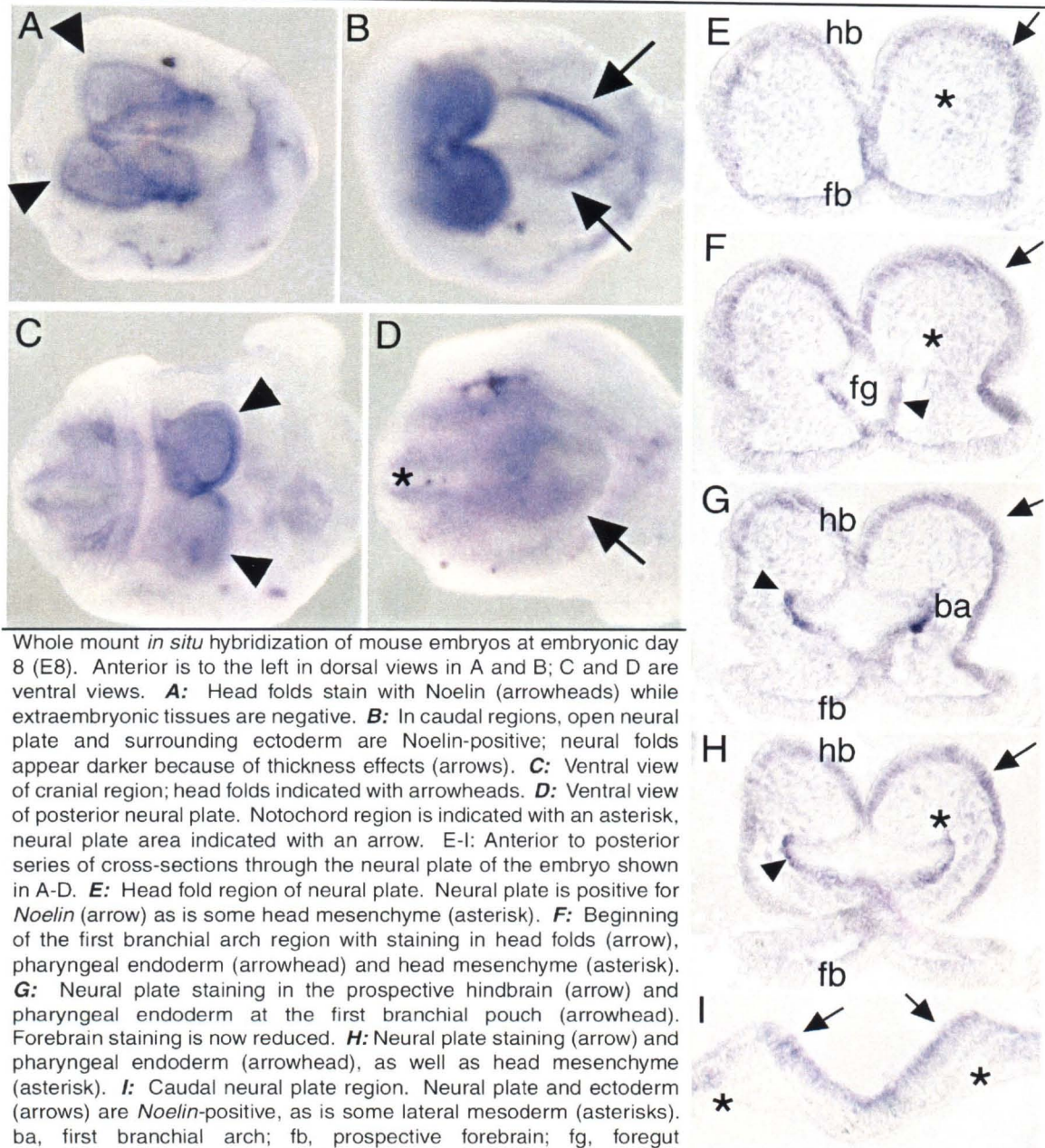
	1	2	3	4	5			
Divergence	1	█	95.9	96.1	96.3	93.6	1	chick Noelin-1
	2	4.3	█	98.2	98.4	93.1	2	human Noelin1/2
	3	4.0	1.9	█	99.4	93.2	3	mouse Noelin-1
	4	3.8	1.6	0.6	█	93.4	4	rat Noelin-1
	5	6.7	7.2	7.1	6.9	█	5	Xenopus Noelin-1
	1	2	3	4	5			

Phylogenetic relationships between Noelin-1 homologs. Noelin homolog accession numbers are as from Figure 6, Olfactomedin GenBank accession #L13595. **A:** Phylogenetic tree. *Xenopus* falls out as expected, closer to chick than to mouse, rat and human. All are compared to *Rana pipiens* Olfactomedin, a divergent family member. Mouse and rat are very close and fall out with human. Chick and *Xenopus* are closer to each other than to the mammalian proteins. **B:** Sequence distances table. Chick, human, mouse, rat and *Xenopus* are compared (without Olfactomedin). Each homolog exhibits greater than 93% identity to every other homolog.

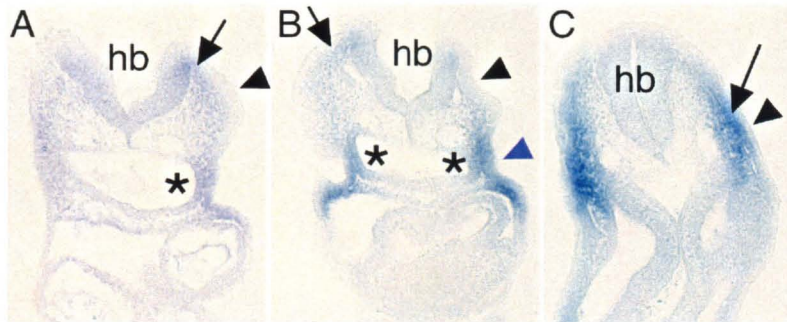
**Figure 3: *Noelin* is expressed in early neural ectoderm**



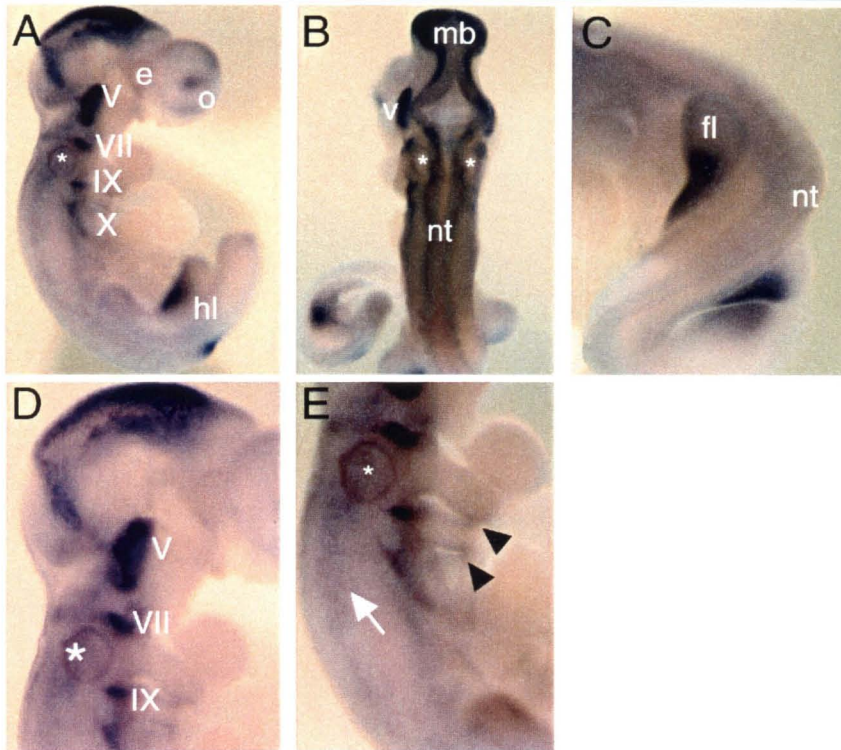
A cup-shaped embryo stained for the *Noelin* Z exon by whole mount *in situ* hybridization. Embryo was sectioned at 10 micrometers. Section in A comprises most anterior-region of embryo; successive panels show slightly more posterior sections. **A:** A cross-section through the rostral neural plate (arrowheads) and the allantois (asterisk). *Noelin* transcripts are detected in the neural plate and not in the endoderm under the neural plate or the extra-embryonic mesoderm surrounding the embryo. The amnion is positive (arrow). **B:** A cross-section through a more caudal region of the anterior neural plate (bottom half of panel) and the caudal neuroepithelium (top half of panel). *Noelin* transcripts are detected in the rostral neural plate. Some parts of the neuroepithelium at the primitive streak level where the neural folds will eventually form are also positive (arrows). **C:** A mid-level cross-section through the embryo. The neural plate is positive for *Noelin* transcripts, as is the ectoderm adjacent to it, extending to the caudal neuroepithelium (arrowhead) near the neural groove (asterisk). Some lateral mesoderm is stained (arrow). ect, ectoderm; em, extra-embryonic mesoderm; end, endoderm; mes, mesoderm; no, notochordal plate

**Figure 4: Mouse *Noelin* at E8**

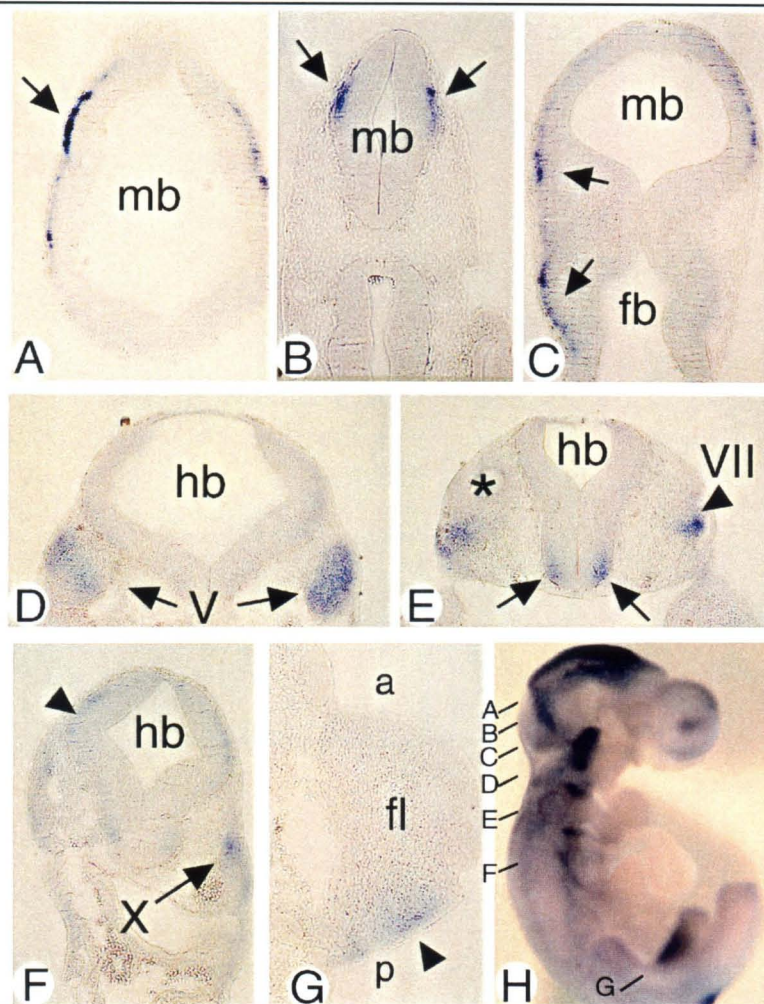
**Figure 5:** Mouse *Noelin* at E8.5



E8.5 embryo stained for the *Noelin* Z exon by whole mount *in situ* hybridization. 10 micrometer sections. **A:** Pre-otic level of the hindbrain at approximately rhombomere 4 shows neural crest staining (arrow) but no ectoderm stain (arrowhead). Pharyngeal endoderm is also positive (asterisk). **B:** Otic vesicle level. Otic vesicle is beginning to invaginate (arrowhead) and does not stain for *Noelin*. Epibranchial placode region is positive for *Noelin* (blue arrowhead), as is migrating neural crest (arrow). Asterisks mark pharyngeal endoderm that is positive for *Noelin*. **C:** Section through the post-otic level of the hindbrain. Neural crest is positive (arrow); ectoderm is negative (arrowhead). hb, hindbrain.

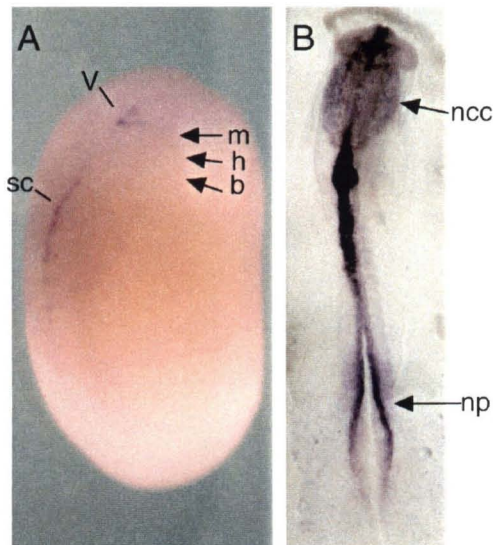
**Figure 6: *Noelin* expression at E10**

Embryonic day 10 embryo stained for *Noelin* Z exon by whole mount *in situ* hybridization. Anterior is up in all panels. **A:** Side view showing staining in cranial ganglia, neural tube, and hindlimb (posterior of embryo is looped forward showing the hindlimb, obscuring the forelimb). **B:** Dorsal view displaying neural tube and cranial ganglia expression. **C:** Close-up view of forelimb exhibiting *Noelin* staining in the posterior region. **D:** Close-up of head region showing cranial ganglia and brain staining. **E:** Close-up of branchial arches showing staining in arches (arrowheads), ganglia and neural crest (arrow). e, eye; fl, forelimb; hl, hindlimb; mb, midbrain; nt, neural tube; o, olfactory placode; V, trigeminal ganglion; VII, geniculate ganglion; IX, petrosal ganglion; X, nodose ganglion. Asterisks mark otic vesicles.

**Figure 7:** *Noelin* expression at E10

Mouse embryo at E10 stained for *Noelin* Z exon. Cross-sections cut at 10 micrometers. **A:** A dorsal midbrain section with *Noelin* expression in the marginal zone (arrow). **B:** A midbrain section with dark *Noelin* stain in the marginal zone (arrows). **C:** A midbrain section with forebrain also; staining is in marginal zone cells (arrows). **D:** A section through the hindbrain at the level of the trigeminal ganglia (V, arrows). **E:** A further caudal section through the hindbrain at the level of the otic vesicle (asterisk) and geniculate ganglia (arrowhead, VII). Staining is also present in marginal zone ventral hindbrain cells (arrows). **F:** Hindbrain section at the level of the nodose ganglion (arrow, X). Staining is also present in the marginal zone of the hindbrain (arrowhead). **G:** Forelimb section with *Noelin* staining in the posterior region (arrowhead; a and p indicate anterior/posterior axis of limb). **H:** Lateral view of whole embryo shows the level of each section. fb, forebrain; fl, forelimb; hb, hindbrain; mb, midbrain.

**Figure 8:** Cross-species comparison of *Noelin-1* expression pattern



*Noelin* Z exon is expressed in neural tissues but not in neural crest in the frog. A comparison between similar stages of embryos from frog and chick. **A:** Lateral view of a stage 21 frog embryo stained with *Noelin* Z exon reveals transcripts in the developing trigeminal ganglion and spinal cord (anterior is up). Cranial neural crest streams do not express *Noelin* (arrows point to streams: m, mandibular; h, hyoid; b, branchial). Neural crest in the trunk are also negative for *Noelin*. Staining is only found in post-mitotic neural tissues at this stage. **B:** Stage 9 chick embryo (anterior is up) stained with the Z exon reveals neural crest cells (ncc) in the midbrain region are positive for *Noelin* transcripts. *Noelin* expression is found throughout the antero-posterior axis in the dorsal neural tube from hindbrain through the open neural plate, where it stains the neural folds and neural plate (np). Photo in (B) is courtesy of M. Barembaum. V, trigeminal ganglion; sc, spinal cord.



## **Concluding Remarks**

## NON-CONSERVED EXPRESSION OF NOELINS IN VERTEBRATES

The expression patterns of *Noelin* genes in three vertebrate species have been characterized. Throughout, it is evident that their tissue distribution patterns are similar, but not the same. In frogs, detection of transcripts by whole mount *in situ* hybridization is not possible until after neural tube closure; however, in mouse and chick embryos, transcripts can be observed from gastrulation stages onward (Barenbaum et al., 2000, and Chapter 4). Later, mouse and chick embryos contain *Noelin* transcripts in the neural crest and neural tube, as well as in cranial placodes and ganglia. In frogs, though, only differentiating neurons express *Noelin* in the neural tube and ganglia. Although mouse and chick embryo patterns of expression are more similar, the degree to which each is expressed in certain tissues varies. In chick, migrating neural crest cells through all axial levels of the embryo express *Noelin-1* (Barenbaum et al., 2000); but in the mouse the trunk neural crest cells were not observed to express this gene (Chapter 4).

Is there a conserved set of functions for the *Noelin* genes? Or could each vertebrate have co-opted the isoforms for different purposes in neural development? These questions, raised by the similarities and contrasts between species, were the basis for examining the function of the *Xenopus* homolog.

## NOELIN FUNCTIONS VARY AMONG SPECIES

The *Noelin* isoforms in different species have apparently different functions. In avians, *Noelin-1* and -2 (the Z isoforms) promote neural crest induction, prolong the period during which they emigrate, and cause more cells

to emigrate than is normal (Barembaum et al., 2000). In frogs, *Noelin-1* and *-2* do not possess this activity. Neural crest formation and migration are normal in embryos over-expressing *Noelin-1* and *-2* (Moreno and Bronner-Fraser, 2001). However, *Noelin-1* promotes neuronal differentiation in neural tissue when over-expressed in naïve explants (Moreno and Bronner-Fraser, 2001). Moreover, the secretion of *Noelin-1* is important to some of its functions; it can only activate sensory neural and neuronal determination genes when it is secreted; when it is forced to remain inside the ER by a localization signal, it cannot induce expression of those markers. However, its neuronal differentiation promoting activity is not dependent on its localization; both ER-localized and secreted forms of the protein can induce expression of a differentiation marker.

Remarkably, the Y isoforms (*Noelin-3* and *-4*) have very different functions from the Z isoforms described above. *Noelin-3* and *-4* cause neural induction in naïve tissue explants and cause expansion of neural tissue and conversion of epidermal ectoderm and neural crest into neural tissue in whole embryos (Chapter 3). The overexpression phenotype of *Noelin-4* is similar to that of other neural inducers: it causes anterior neural tissue to form, induces cement gland formation, and increases the size of the neural tube and retina. It also induces ectopic neurogenesis in the epidermis. Furthermore, *Noelin-4* could co-immunoprecipitate from oocytes with BMP-4 protein and *vice versa*. This intriguing result suggests that perhaps *Noelin-4* and BMP-4 may interact *in vivo*. These observations, together with what is known about neural induction in amphibians, imply that *Noelin-4* could cause neural induction and neural expansion by inhibiting BMP signaling.

In antisense depletion experiments, Morpholino oligonucleotides (MOs) designed to target all four isoforms cause severe reduction in dorsoanterior tissues; forebrain, cement gland, and cranial ganglia are all affected. These results support an essential role for *Noelins* in neural induction. However, several important lines of evidence have yet to be established. First, the Morpholino phenotype must be rescued by co-injection of *in vitro*-transcribed *Noelin* isoforms to prove that the effects of the MOs are specific. Second, Noelin protein translation must be shown to be decreased when embryos are injected with the MOs. These experiments are necessary for making a determination about the necessity of *Noelins* in neural induction and subsequent development.

#### NOELINS INTERACT FUNCTIONALLY

I have also demonstrated that Noelins may functionally interact (Chapter 3). Noelin-1 makes large complexes when expressed in oocytes (Moreno and Bronner-Fraser, 2001, Chapter 2). When co-expressed in oocytes, Noelin-1 and Noelin-4 proteins each immunoprecipitate the other, suggesting that they may interact physically *in vivo*. I also tested whether these two isoforms could cooperate or antagonize each other's function in induction assays. The genes that I had previously shown to be activated by *Noelin-1* expression were up-regulated further when *Noelin-4* was co-expressed with *Noelin-1*. Surprisingly, this was the opposite for genes activated by *Noelin-4*: the presence of *Noelin-1* reduced the ability of *Noelin-4* to induce the anterior neural marker *Pax-6*.

Interaction of the two different isoforms and the differing functional activities that they possess in induction assays suggests some interesting

hypotheses for *Noelin* function *in vivo*. If Noelin-1 serves as a binding partner for Noelin-4, it could act to reduce its secretion (Noelin-1 is poorly secreted compared to Noelin-4 (Moreno and Bronner-Fraser, 2001); or it could act as an extracellular anchor for Noelin-4 (Noelin-1 is highly glycosylated and contains a domain which in another protein is involved in forming extracellular matrix of the olfactory epithelium; Yokoe and Anholt, 1993). Thus, Noelin interactions could compete for interactions with other proteins such as the BMPs.

The nature of the *Noelin* splice variants complicates the above-described scenario. When either promoter is active, it transcribes both a Y and a Z isoform; thus it would seem that the two would always be in balance. However, in some species, post-transcriptional regulation of transcripts has been observed: in chick, the Y-containing isoforms do not appear until later neural development after the Z-containing isoforms (Barembaum et al., 2000); in the mouse, the A-containing isoforms are not expressed in some tissues where the B-containing isoforms are expressed (Nagano et al., 2000; Nagano et al., 1998). This demonstrates that there could be varying levels of isoforms present due to both promoter-level regulation (to choose between A-containing and B-containing isoforms) and to splicing regulation (to choose between Y-containing and Z-containing isoforms).

*Xenopus* biochemical and functional data suggest an interesting explanation for the chick neural crest phenotype that is seen upon over-expression of *Noelin-1*. The postulation described below relies on several assumptions that are unproven; however, a reasonable mechanism can be proposed based on the available data. Noelin-4 may antagonize BMP signaling by binding to BMP molecules, but Noelin-4 binds with higher affinity to Noelin-

1. As mentioned previously, a balance between isoforms expressed in a particular area may be important for Noelin function. When Noelin-1 was over-expressed in chick embryo ectoderm, perhaps this imbalance served to sequester Noelin-4 that was present, thus relieving an inhibition of BMP signaling in the region. BMPs can induce neural crest from intermediate neural plate in culture (Liem et al., 1995). In this manner, perhaps the *Noelin-1* neural crest phenotype can be attributed to modulation of the BMP signaling pathway through inhibition or negative effects on Noelin-4.

The speculations detailed above require several lines of evidence to test their validity. First, avian Noelin-4 must be shown to be expressed in the embryonic ectoderm at primitive streak stages. Current data suggest that the Y isoforms are not expressed until later; however, as in the frog, very low levels may be present that are not detectable by the methods employed so far (Barembaum *et al.*, 2000). Most importantly, Noelin-4 must be shown to inhibit BMP signaling activity. Next, Noelin-4 must be shown to bind to Noelin-1 preferentially over BMP molecules. Further, Noelin-4 must be shown to inhibit avian neural crest generation when over-expressed. Preliminary data in the frog supports this last point: over-expression of Noelin-4 reduced expression of the neural crest marker *XTwist* in cranial neural crest.

## CONCLUSION

Noelin genes appear to play multiple roles at different stages in neural development. Early expression in the neural tissue of mammalian and avian embryos correlates with the gain of function of *Noelin-1* in which avian neural crest formation is prolonged in the cranial neural tube. In frogs, overexpression

of *Noelin-1* causes early differentiation of neurons in neuralized tissue, also correlating with its expression in post-mitotic neural tissues. *Noelin-4* physically interacts with *Noelin-1*, and acts as a neural inducer. This activity may be down-regulated by the presence of *Noelin-1*, and this negative effect may be due to competition for binding between *Noelin-1* and other proteins (e.g., BMP-4). *Noelin-4* itself can direct formation of ectopic neural tissue and cement gland in frog embryos, as well as cause perturbation in neural crest and epidermis, likely by conversion of the tissue to a neural fate

Together, the accumulation of data indicates that there may be several important roles for *Noelin* isoforms in neural development from induction through neurogenesis. There is much yet to be discovered about neural development in all species. *Noelin* genes may lead to some important insights into the links between neural induction and neurogenesis.



## **Appendix Chapter 1:**

# **Noelin-1 is a secreted glycoprotein involved in generation of the neural crest**

Meyer Barembaum, Tanya Moreno, Carole LaBonne, John Sechrist  
and Marianne Bronner-Fraser (2000)

Reprinted by permission from *Nature Cell Biology* Vol. 2 No. 4 pp 219-225

Copyright ©2000 Macmillan Magazines Limited

# Noelin-1 is a secreted glycoprotein involved in generation of the neural crest

Meyer Barembaum\*, Tanya A. Moreno\*, Carole LaBonne\*, John Sechrist\* and Marianne Bronner-Fraser\*†

\*Division of Biology, 139-74, California Institute of Technology, Pasadena, California 91125, USA  
†e-mail: MBronner@gg.caltech.edu

The vertebrate neural crest arises at the border of the neural plate during early stages of nervous system development; however, little is known about the molecular mechanisms underlying neural crest formation. Here we identify a secreted protein, Noelin-1, which has the ability to prolong neural crest production. Noelin-1 messenger RNA is expressed in a graded pattern in the closing neural tube. It subsequently becomes restricted to the dorsal neural folds and migrating neural crest. Over expression of Noelin-1 using recombinant retroviruses causes an excess of neural crest emigration and extends the time that the neural tube is competent to generate as well as regenerate neural crest cells. These results support an important role for Noelin-1 in regulating the production of neural crest cells by the neural tube.

The neural crest<sup>1</sup> represents one of the defining characteristics of vertebrates. This migratory cell population arises at the junction between the presumptive epidermis and the neural plate during neurulation. Initial formation of the neural crest probably occurs through an inductive interaction between the neural plate and non-neural ectoderm<sup>2,3</sup>. Following neural tube closure, presumptive neural crest cells undergo an epithelial-to-mesenchymal conversion and emigrate from the neural tube. They then migrate extensively within the embryo to form numerous and diverse derivatives including most of the craniofacial skeleton and peripheral nervous system.

Classically, the neural crest was viewed as a segregated population, separate from non-neural ectoderm (presumptive epidermis) and neural plate (presumptive central nervous system; CNS). Single-cell lineage analysis has, however, revealed that individual neural fold cells can give rise to neural crest, CNS and epidermal derivatives<sup>4</sup>. Furthermore, more ventral regions of the cranial neural tube have been found to regenerate neural crest cells when the endogenous neural crest has been surgically removed<sup>5-10</sup>.

Although in recent years some progress has been made in understanding how the neural tube is patterned along its dorsoventral axis<sup>11,12</sup>, little is known about the mechanisms by which a subset of dorsal neural tube cells ultimately gives rise to neural crest. To address the molecular basis of neural crest formation, we have screened for molecules expressed in the early developing nervous system. Here, we report the characterization of a secreted protein factor, chick Noelin-1, which may have a key role in conferring on neural tube cells the ability to form neural crest.

## Results

**Distribution of Noelin-1 transcripts.** Noelin-1 transcripts were isolated by screening a quail neural crest/neural tube complementary DNA library to identify novel genes involved in generation of the neural crest. Noelin-1 was selected for further study on the basis of its striking expression pattern within the closing neural tube (Fig. 1). Noelin-1 is the chicken homologue of a previously described rat gene *D25tulle/Noel* (neuronal olfactomedin-related endoplasmic reticulum localized<sup>13</sup>).

Because neurulation in the chick occurs in a rostrocaudal sequence, the neural tube can be closed in rostral regions while still open at caudal levels, thus reflecting multiple stages of neural tube closure within a single embryo. At the four-somite stage, Noelin-1 is expressed in a graded pattern within the open neural plate, with highest expression observed within the neural folds, gradually decreasing toward the ventral midline; more rostrally in the midbrain, it is restricted to the dorsal part of the closed neural tube (Fig. 1a-c) and

its expression precedes that of the zinc finger transcription factor Slug<sup>15</sup>. Following neural tube closure at the level of the midbrain and

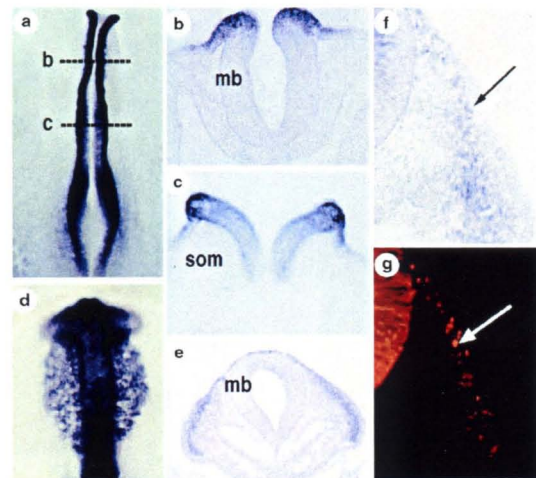


**Figure 1 Expression pattern of Noelin-1 in the early chick embryo revealed by *in situ* hybridization.** a-c, Whole-mount (a) *in situ* hybridization and transverse sections (b, c) at the levels indicated by the dashed lines in (a) of a four-somite stage chick embryo. Noelin-1 transcripts are present in the dorsal part of the neural tube at the level of the midbrain (b), in more caudal regions (c). Noelin-1 is expressed over most of the neural plate in a graded pattern, with high expression in the neural folds gradually decreasing toward the ventral midline. d-e, Whole-mount (d) and transverse section (e) through a 10-somite stage embryo show Noelin-1 expression restricted to the migrating neural crest cells adjacent to the midbrain. f-g, Dil labelling (red) of the premigratory neural crest cells within the neural tube at stage 9 followed by *in situ* hybridization 1 day later reveals that Noelin-1 is expressed by migrating neural crest cells. Arrows indicate Dil-positive cells (g) expressing Noelin-1 transcripts (f); mb, midbrain; som, somite.

hindbrain (stage 9+ to 11 embryos, according to the criteria of Hamburger and Hamilton (HH)<sup>14</sup>). Noelin-1 expression becomes largely restricted to the dorsal neural tube (from which neural crest cells will

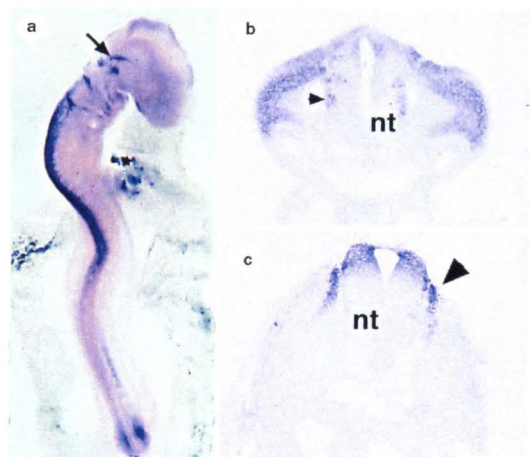


**Figure 2** Expression pattern of *Noelin-1* in stage 14–15 embryos. **a**, In whole mount embryos, *Noelin-1* transcripts are observed in the cranial ganglia, including the trigeminal (arrow) as well as in the dorsal neural tube and the forming dorsal root ganglia. **b**, A transverse section at the level of r4 shows *Noelin-1* staining in neural crest migratory streams as well as in interneurons (arrowhead) within the neural tube (nt). **c**, At trunk levels, *Noelin-1* is expressed in the dorsal neural tube as well as in the dorsomedial portion of the forming dorsal root ganglia (arrowhead).

arise) and then to migrating neural crest cells (Fig. 1d–f). Interestingly, centring at the level of rhombomere 4, which produces a large number of neural crest cells, *Noelin-1* expression extends further ventrally and persists for longer than at other axial levels (data not shown). Dil labelling of premigratory neural crest cells<sup>13</sup> confirmed that *Noelin-1* is expressed by migrating neural crest cells (Fig. 1f, g). Following neural crest migration, *Noelin-1* mRNA is detected in sensory ganglia, including the trigeminal ganglion (Fig. 2a), formed from both neural crest and placode-derived cells, and in interneurons within the neural tube (Fig. 2b).

In the trunk, *Noelin-1* is expressed first in the open neural plate, with a distribution similar to that observed at cranial levels. After neural tube closure, it becomes restricted to the dorsal neural tube (Fig. 2a) and is expressed in a subpopulation of migrating neural crest cells. *Noelin-1* transcripts are downregulated in the trunk neural tube by stage 12, but by stage 15 it is re-expressed in the dorsal neural tube as well as in the medial portion of the forming dorsal root ganglia (Fig. 2c). In addition to the neural crest, *Noelin-1* is expressed in a small number of other sites, including the wings of the head mesoderm during gastrulation, the ectoderm and mesoderm lateral to Hensen's node, and in the apical ectodermal ridge and anterior mesoderm region of the limb buds (data not shown).

**Molecular characterization of Noelin.** The largest open reading frame of the *Noelin-1* cDNA predicts a protein of 485 amino acids (Fig. 3a). The predicted protein has a signal sequence, but no apparent transmembrane domain. It is 96% similar at the amino-acid level to a splice variant of the rat gene *Noel<sup>2</sup>*, which encodes four alternatively spliced glycoproteins expressed in the brain of late embryonic and postnatal rats (referred to here as *Noelin-1* to 4; formerly designated BMZ, AMZ, BMY and AMY, respectively; Fig. 3b). The mouse homologues of this gene (pancortins<sup>10</sup>) are expressed at high levels in the adult cerebral cortex. A portion of *Noelin-1* displays amino-acid sequence similarity (49%) to olfactomedin, a glycoprotein found in the olfactory epithelium of the bullfrog<sup>17</sup>; this same region has 53% similarity to the TIGR protein

(trabecular-meshwork inducible glucocorticoid response protein), which has been implicated in some glaucomas<sup>18</sup>, and 54% similarity to the calcium-independent receptor of  $\alpha$ -latrotoxin (CIRL), a member of the G-protein-coupled receptor superfamily<sup>19</sup>. *Noelin-1* has eight consensus sites for N-glycosylation, two hyaluronic acid binding consensus sequences, as well as a glycosaminoglycan initiation site (also present in the olfactomedin and TIGR protein sequences<sup>17,19</sup>). Three conserved cysteine residues at positions 73, 75 and 410 have been implicated in intermolecular disulphide bond formation in olfactomedin<sup>17</sup>.

Northern blot analysis reveals a single 3.5 kilobase (kb) mRNA species present in the early embryo. *Noelin* mRNA levels, corresponding to *Noelin-1* and *Noelin-2* variants, are present throughout early embryonic stages (Fig. 3c). At later stages, higher levels of expression and additional bands (data not shown) corresponding to *Noelin-3* (BMY) and *Noelin-4* (AMY) (Fig. 3b) are detected in the brain, confirming the presence of numerous splice variants in birds.

Recent reports on the mouse and rat homologues of *Noelin-1* noted their presence in the endoplasmic reticulum but did not examine whether they were secreted<sup>10,11</sup>. To determine whether the largest *Noelin-1* open reading frame encodes a secreted protein, mRNA encoding a *Noelin-1* protein containing an internal Flag epitope (between residues 220 and 221) was overexpressed in *Xenopus* oocytes. Following metabolic labelling with [<sup>35</sup>S]methionine, oocyte and supernatant fractions were assayed for the presence of the tagged protein. Under non-reducing conditions, large complexes were immunoprecipitated using an anti-Flag antibody (data not shown). Under reducing conditions, multiple bands were specifically immunoprecipitated from oocyte samples (Fig. 3d). These are likely to be glycosylated forms of the protein as they collapse upon deglycosylation to a single band of relative molecular mass (*M*<sub>r</sub>) 55,000 (55 k), the predicted size of *Noelin-1* (Fig. 3d). The most highly glycosylated forms of *Noelin-1* were also precipitated from supernatant fractions, indicating that *Noelin-1* is a secreted protein.

**Excess Noelin-1 prolongs neural crest production.** In order to explore the function of *Noelin-1* during neural crest formation, we overexpressed it in early chick embryos using retrovirus-mediated gene transfer<sup>20</sup>. RCASBP (B) retrovirus expressing *Noelin-1* was applied to the surface ectoderm (including both non-neural ectoderm and open neural plate) of embryos of HH stages 7–8 (1–6-somite stage). Similar results were obtained from infections over this range of stages. Twenty four hours post-infection, retroviral gene products were observed in ectodermally derived cells (surface ectoderm, neural tube and neural crest cells), as assayed by viral p27 immunoreactivity (Fig. 4a). Interestingly, staining for the neural crest marker HNK-1 (ref. 21), revealed an increased number of neural crest cells over the dorsal neural tube in *Noelin-1*-infected embryos, suggesting an overproduction of cranial neural crest (Fig. 4b). This was not observed in embryos infected with control retrovirus.

To investigate the possible overproduction of neural crest cells following overexpression of *Noelin-1*, we infected embryos with retrovirus at the 1–6-somite stage and labelled their neural tubes with Dil at time points after which most neural crest cells should have emigrated (16–22 somite stage, HH stage 12–14). Normally, neural crest cells in the head emigrate from the neural tube for 8–16 hours, depending upon the exact axial level, with the last cells emigrating at midbrain levels by the 14–15 somite stage (ref. 22 and J.S. and M.B.F., unpublished observation). Accordingly, when embryos infected with control retrovirus were labelled with Dil at stage 12–14 (18–22 somite stage), most of the Dil label remained within the cranial neural tube (Fig. 4c, d; *n* = 14/14 embryos infected with empty vector; *n* = 14/15 infected with RCAS containing the alkaline phosphatase gene). No Dil-labelled neural crest cells were observed migrating at the level of the midbrain or rostral hindbrain, although emigration was observed at the level of r4. In contrast, embryos infected with retrovirus expressing *Noelin-1* produced numerous Dil-labelled

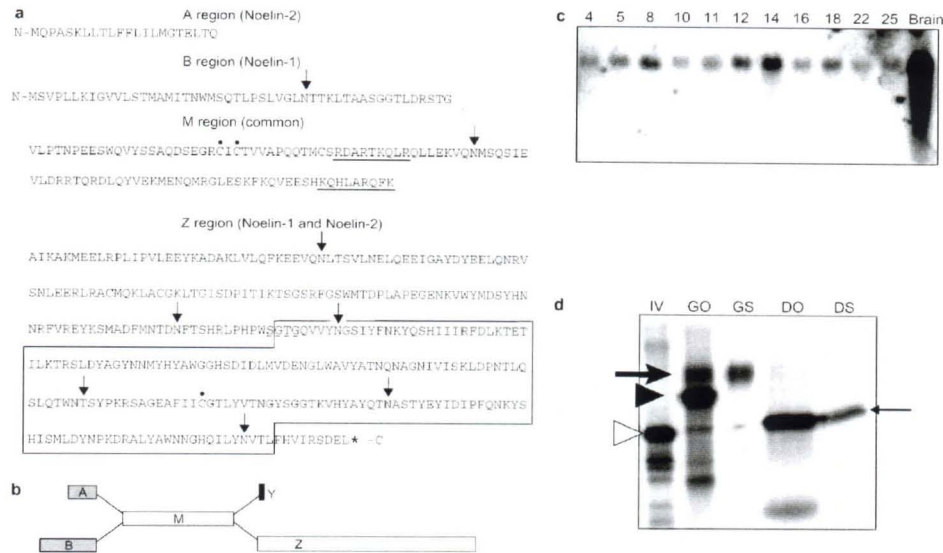


**Figure 3 Molecular characteristics of Noelin.** **a**, Deduced amino-acid sequence of the Noelin-1 and Noelin-2 open reading frames. The region with homology to olfactomedin is boxed. Cysteine residues conserved in olfactomedin have a dot above them, potential N-glycosylation sites are indicated by arrows; two potential hyaluronate binding sites have a solid underline and potential glycosaminoglycan initiation sites have dotted underlines. **b**, Schematic diagram showing the possible splice variants (based on ref. 12). **c**, The Z exon of the chicken cDNA was used to probe Northern blots containing total RNA isolated from chicken embryos from stages 4 to 25, and from 14-day embryonic chicken brains. Noelin RNA was present throughout early embryonic stages, with higher levels of expression in the brain. Noelin RNA expression was noted much earlier than reported for *D2 Sulf1e* in the rat<sup>12</sup>. **d**, To examine whether Noelin-1 was secreted, oocytes were injected with Flag-tagged Noelin-1 mRNA. Oocyte fractions were then immunoprecipitated with an anti-

Flag antibody and resolved on a 9% SDS gel. Deglycosylation was achieved by treating with peptide N-glycosidase F. Under deglycosylating and denaturing conditions, a single band corresponding to M, 55 k (the predicted size of Noelin-1; thin arrow) could be resolved in both the supernatant (DS) and oocyte (DO) fractions and its size correlated with that observed after *in vitro* translation of Noelin-1 (IV). GO, glycosylated oocyte fraction; GS, glycosylated supernatant fraction; DO, deglycosylated oocyte fraction; DS, deglycosylated supernatant. The thick arrow (left) indicates the highly glycosylated form of Noelin-1 that is present in the oocyte and supernatant fractions. The arrowhead (left) indicates a faster migrating glycosylated form that is present in the oocyte but not supernatant fraction. The thin arrow (right) indicates the deglycosylated form and the open arrowhead (left) the *in vitro* translated product.

migrating neural crest cells at the level of the caudal midbrain and rostral hindbrain (Fig. 4e–f;  $n = 12/14$  embryos). Thus, these embryos continued to produce cranial neural crest cells well beyond the time at which neural crest emigration had ceased in normal embryos, particularly at more rostral brain levels. Despite the large increase in the number of emigrating neural crest cells in Noelin-1-infected embryos, we noted no change in the overall range or size of derivatives produced by the neural crest, highlighting the remarkable ability of the embryo to regulate tissue size<sup>27</sup>. This is consistent with previous results showing that neural crest derivatives remain constant in size even after introduction of a large excess of exogenous neural crest cells<sup>27</sup>.

Neural crest cells migrating adjacent to the hindbrain follow three distinct streams adjacent to rhombomeres r1 and 2, r4 and r6 (ref. 22), leaving a neural crest-free zone lateral to r3 and r5 (refs 22, 25). DiI-labelled cells in both untreated and control-infected embryos exhibited this segmental pattern of migration at hindbrain levels (Fig. 5a, c). In contrast, analysis of DiI-labelling in serial sections along the rostrocaudal axis of several embryos overexpressing Noelin-1 revealed uniform generation of neural crest cells from the caudal forebrain to the otic vesicle, including the region adjacent to r3 (Fig. 5b, d). These results suggest that ectopic expression of Noelin-1 not only prolongs the duration of neural crest generation, but can also alter the migratory pattern of neural crest cells adjacent to

the hindbrain, such that they fill in the region lateral to r3. A possible mechanism for the increase in neural crest cell number in the hindbrain is by rescue from cell death<sup>28,29</sup>. To address this possibility, embryos infected with Noelin-1 retrovirus were labelled with the nuclear dye Topro, which only stains non-living cells. Despite considerable variability between embryos in the amount of Topro staining observed<sup>28</sup>, no consistent differences in cell death in the hindbrain were noted between experimental and control embryos (data not shown). This suggests that overexpression of Noelin-1 does not increase neural crest cell number by rescuing r3 cells from programmed cell death.

The Noelin-1 and Noelin-2 variants have distinct expression patterns. Noelin-1 is expressed in a dorsoventrally graded pattern in the neural tube (Fig. 6a), whereas Noelin-2, the only other splice variant expressed in the embryo, is expressed in placodes such as the otic (Fig. 6b), trigeminal, epibranchial and olfactory placodes, as well as in the presomitic mesoderm. Later, Noelin-1 and Noelin-2 transcripts have somewhat overlapping expression patterns in neural crest and placode-derived ganglia. To gain further insight into the important functional domains of Noelin, we compared the effects of overexpressing Noelin-2 and Noelin-1. When Noelin-2 retrovirus was injected into the neuroepithelium, infected embryos displayed a prolonged time of generation of neural crest cells (Fig. 6c–f) compared with control embryos. Because Noelin-1 and Noe-

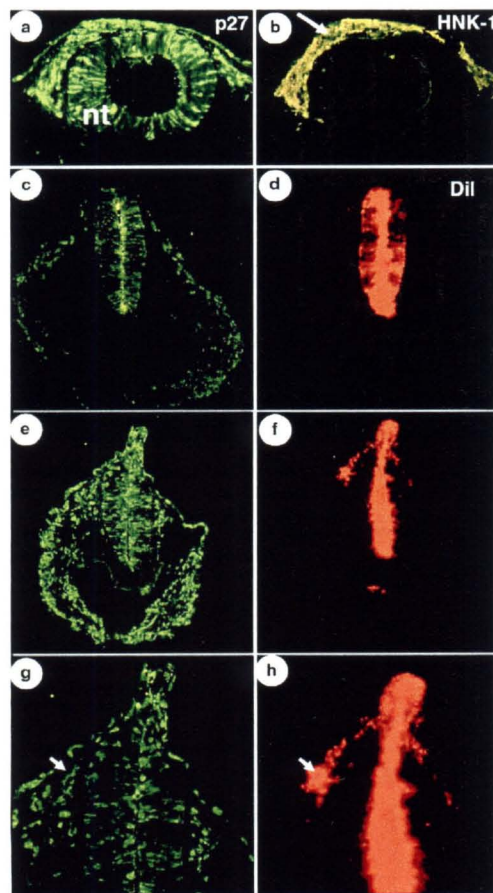


**Figure 4 Effects of *Noelin-1* overexpression on generation of neural crest cells.** **a**, Transverse section at the level of the rostral hindbrain through a chick embryo infected with *Noelin-1*-producing retrovirus. Retroviral gene products were detected by staining with antibodies against the viral protein p27 in the surface ectoderm, neural tube and neural crest cells. **b**, The same section as in **(a)** stained with anti-HNK-1 antibody to visualize migrating neural crest cells. Overproduction of neural crest cells (arrow) can be seen above the dorsal neural tube. **c**, Embryo infected with control (RCAS empty vector) retrovirus, stained 1 day after viral infection with the anti-p27 antibody (green) has infected cells in the ectoderm, neural tube and neural crest, shown here at the level of the rostral hindbrain. **d**, The same embryo as in **(c)** having received an injection of Dil (red) into the neural tube at the 18-somite stage and having been fixed at the 23-somite stage. Dil label was confined to the cranial neural tube. **e-h**, Low and high magnification views of an embryo infected with *Noelin-1*-producing retrovirus. The neural tube was labelled with Dil 1 day later, at the 21-somite stage, and then fixed at the 25-somite stage. p27 immunoreactivity (green; **e, g**) revealed infection in numerous ectodermal, neural crest and neural tube cells. Numerous Dil-labelled migrating neural crest cells (red; **f, h**) at the level of the rostral hindbrain were observed even when embryos were labelled with Dil at the 21–22 somite stage. This is well beyond the time of neural crest emigration in normal embryos. Prolonged emigration of Dil-labelled neural crest cells was observed in 12/14 *Noelin-1*-infected embryos but in 0/14 control embryos (RCAS empty vector) and 1/15 RCAS-alkaline phosphatase infected embryos. Some Dil-labelled cells lacked retroviral protein expression (arrows in **g, h**), suggesting that the effects of *Noelin-1* overexpression are not cell-autonomous. The 'dorsal fin-like' projection in the neural tube is a fixation artefact that occurs in a number of both experimental and control embryos.

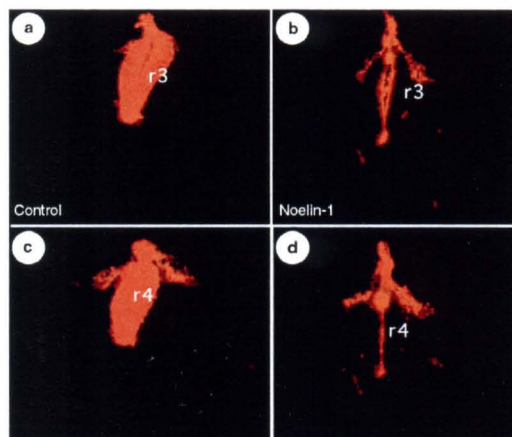


**Figure 5 Overexpression of *Noelin-1* increases neural crest production at the level of r3.** **a**, A Dil-labelled chick embryo infected with control retrovirus has no neural crest migration lateral to r3. **b**, A Dil-labelled embryo infected with *Noelin-1* retrovirus has labelled neural crest cells emigrating lateral to r3. **c, d**, Neural crest migration is observed at the level of r4 in both control **(c)** and *Noelin-1* infected **(d)** embryos.

lin-2 have different amino-terminal domains but similar biological activity, the results suggest that the functional domains of *Noelin* that are relevant to proper neural crest development lie in the M and/or Z domains (Fig. 3b).

***Noelin-1* prolongs neural crest regeneration and does not function cell-autonomously.** To examine further the functional role of *Noelin-1* in neural crest development, we tested whether its overexpression can prolong the ability of the cranial neural tube to regenerate neural crest cells. In previous experiments we have demonstrated that the cranial neural tube can regulate to form neural crest cells when the endogenous neural folds are removed. This regulative response is time-limited, declining by the 7–8 somite stage at the level of the caudal midbrain/rostral hindbrain. Embryos were infected with *Noelin-1* or control retrovirus at the 1–3-somite stage and reincubated for 12 h of development. At the 10–12-somite stage, their neural tubes were labelled with Dil and the dorsal third of the neural tube was subsequently removed. Under these conditions, *Noelin-1*-infected embryos retain the ability to regenerate neural crest cells (Fig. 7a;  $n = 14/14$  experimental versus 2/12 control embryos). In contrast, control infected embryos demonstrate little or no capacity to regenerate neural crest cells at this stage (Fig. 7b). Thus, *Noelin-1* overexpression can prolong the period during which the neural tube can regenerate neural crest cells.

It is interesting to note that some of the late-migrating neural crest cells in *Noelin-1* overexpressing embryos were not infected with retrovirus (see Fig. 4g, h). This, together with the finding that *Noelin-1* is secreted, suggests that it functions extracellularly and not cell-autonomously. To test this more directly, we implanted chick embryo fibroblast cells overexpressing *Noelin-1* within the cranial mesenchyme lateral to the neural tube. Emigration of neural crest cells was assayed by labelling the neural tube with Dil at the 18–22-somite stage, well past the time of normal neural crest emigration in the midbrain and rostral hindbrain. We find that this exogenous source of *Noelin-1* is sufficient to promote emigration of neural crest cells well after the time that they would normally leave the neural tube ( $n = 6/8$  embryos). Dil-labelled cells were

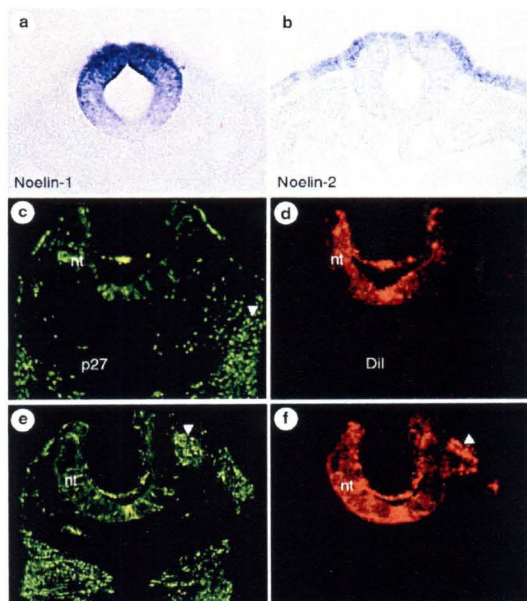


**Figure 6 Effects of overexpression of Noelin-2 on neural crest production by the neural tube.** **a**, Noelin-1 is expressed in the neural tube. **b**, Noelin-2 is expressed in placodes such as the otic placode. **c**, An embryo infected with control (RCAS-alkaline phosphatase) retrovirus shows infected cells labelled with the p27 antibody (green; arrowhead) in the ectoderm, neural tube and neural crest, shown here at the level of the rostral hindbrain. **d**, The same embryo as shown in **(c)** having received an injection of Dil (red) into the neural tube (nt) at the 19-somite stage and having been fixed at the 32-somite stage. Dil label was confined to the cranial neural tube. **e**, **f**, An embryo infected with Noelin-2-expressing retrovirus. The neural tube was labelled with Dil at the 18-somite stage, and then fixed at the 33-somite stage. p27 (green) immunoreactivity (arrowhead in **e**) reveals infection in numerous ectodermal, neural crest and neural tube cells. Numerous Dil-labelled migrating neural crest cells (arrow in **f**) at the level of the rostral hindbrain were observed. These results were similar to those observed with Noelin-1. Prolonged emigration of Dil-labelled neural crest cells was observed in 13/15 Noelin-2-infected embryos but in only 1/15 RCAS-alkaline phosphatase control embryos.

observed departing from r2 (Fig. 7c–f) and occasionally from the rostral midbrain. Although fibroblasts were injected unilaterally, it is interesting to note that neural crest emigration could occur either unilaterally (Fig. 7c) or bilaterally (Fig. 7e) in embryos injected with Noelin-1-expressing fibroblasts. Similarly, when fibroblasts overexpressing Noelin-2 were injected lateral to the rostral hindbrain, they provoked late emigration of neural crest cells (data not shown;  $n = 7/8$  embryos). In contrast, control fibroblasts had no effect on neural crest emigration (Fig. 7g, h;  $n = 0/9$  embryos injected with fibroblasts infected with RCAS empty vector and  $0/9$  embryos injected with fibroblasts infected with RCAS-alkaline phosphatase). No apparent changes were noted in the cranial mesenchyme cells, suggesting that the neural tube/neural crest is the primary target.

**Noelin-1 overexpression upregulates *Slug* transcription.** To investigate the mechanisms by which Noelin-1 regulates neural crest production, we asked whether its overexpression altered the pattern of dorsoventral gene expression within the neural tube. The neural crest marker, *Slug*, is expressed in the closing neural folds and dorsal neural tube as well as in early migrating neural crest

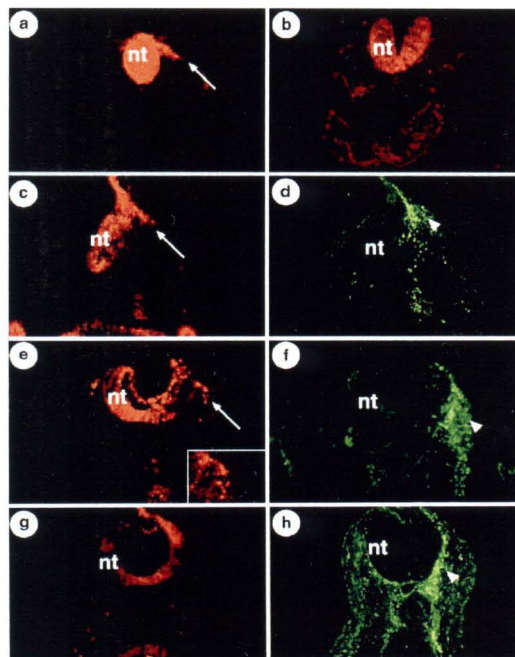


**Figure 7 Noelin-1 prolongs the ability of the neural tube to regenerate neural crest cells and functions non-cell-autonomously.** **a**, In an embryo infected with Noelin-1 retrovirus at the head-fold stage, Dil-labelled neural crest cells (arrow) have migrated out of the remaining neural tube 1 day after dorsal neural tube ablation at the 10-somite stage. **b**, In embryos infected with control retrovirus, by contrast, no migrating Dil-labelled cells were observed following dorsal neural tube ablation at the 10-somite stage. **c–f**, Noelin-1 extends neural crest emigration time in a non-cell-autonomous manner. Fibroblasts infected with Noelin-1 retrovirus were injected lateral to the neural tube of 18–22-somite embryos, well past the time that neural crest cells normally leave the neural tube (as assayed by Dil labelling). In embryos injected with Noelin-expressing fibroblasts, Dil-labelled neural crest cells emigrated from the neural tube either unilaterally (**c**) or bilaterally (**e** and inset). p27 staining (arrowheads in **d**, **f**) indicates the location of the injected fibroblasts. **g**, **h**, In contrast, embryos injected with control fibroblasts (arrowhead in **h**) had no Dil-labelled cells external to the neural tube. Embryos were fixed after 14 h to ensure insufficient time for secondary infection, as verified by lack of p27 in the neural tube.

cells<sup>10</sup>. Overexpression of Noelin-1 resulted in two interesting effects on *Slug* expression. First, there appeared to be a general upregulation of *Slug* transcripts in the dorsal neural tube and migrating neural crest population. Second, Noelin-1-infected embryos had an increased number of *Slug*-positive cells (neural crest cells) within the cranial mesenchyme compared with control embryos (Fig. 8a–d). In contrast, when we examined the expression pattern of the dorsal neural tube markers *Pax-3* (Fig. 8e, f), *Wnt-1* and *BMP-4*, and the floorplate marker *Sonic hedgehog* (data not shown), no changes in levels or distribution patterns were noted in experimental versus control embryos. These results suggest that Noelin-1 acts by modulating the ability of the dorsal neural tube to produce neural crest cells, but that it does not alter the pattern of the neural tube itself.

Previously, we found that the transcriptional regulator, *Id2*, was expressed in the cranial neural folds and that its overexpression affected cell fate decisions in the neural folds<sup>7</sup>. To examine the rela-

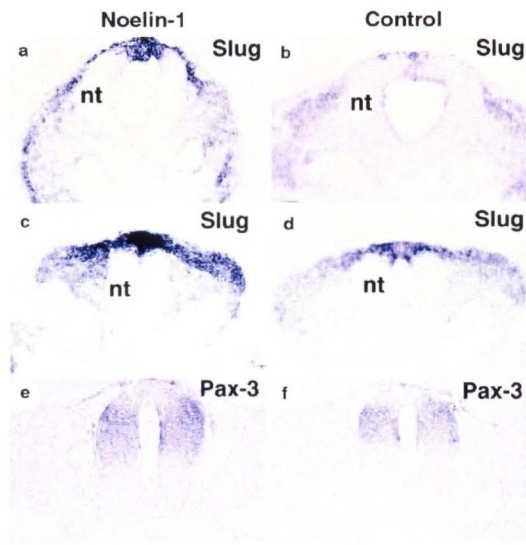


**Figure 8** Overexpression of Noelin-1 upregulates Slug expression but not other dorsoventral neural tube markers. **a-d**, Effect of Noelin-1 overexpression on Slug expression. Transverse sections through the r1/r2 (**a, b**) or r4 (**c, d**) level. There was a large upregulation of Slug transcripts in the dorsal neural tube and migrating neural crest cells 1 day after infection with Noelin-1 retrovirus (**a, c**) compared with controls (**b, d**). In addition, the number of Slug-positive cells migrating within the cranial mesenchyme appeared markedly higher in Noelin-1-infected embryos. **e, f**, In contrast to Slug, no apparent changes were observed in Pax-3 expression, shown here at the level of r4, in experimental (**e**) or control (**f**) embryos. Similarly, no changes were noted in expression of *Wnt-1*, *BMP-4* or *Sonic hedgehog* (data not shown).

relationship between *Noelin-1* and *Id2*, we overexpressed *Noelin-1* in the ectoderm/neuroectoderm and examined its effects on the expression of *Id2* and vice versa. No alterations in the expression pattern of either transcript were observed after overexpression of the other (data not shown), suggesting that their developmental functions are not interdependent.

## Discussion

In this study, we have identified a secreted glycoprotein, Noelin-1, that is involved in the generation of neural crest cells. In normal development Noelin-1 is expressed in a dorsoventrally graded pattern within the closing neural tube and its expression precedes that of the earliest known neural crest marker, *Slug*<sup>13</sup>. Noelin-1 expression becomes largely restricted to the dorsal neural tube, from which the neural crest arises, at the time of tube closure. The dorsoventral gradient of expression in the early neural tube may be due to repression of Noelin-1 expression by the notochord, as grafted notochords can downregulate Noelin-1 (M.B. and M.B.F., unpublished observation). Interactions between neural plate and non-neural ectoderm have been shown to generate neural crest cells<sup>47</sup>. Interestingly, Noelin-1 is expressed within the early neural plate at a time at which this tissue can respond to induction by the non-neural ectoderm<sup>48</sup> and is downregulated when the neural tube loses its ability to regenerate neural crest cells<sup>49</sup>.

Our overexpression experiments support an important functional role for Noelin-1 during neural crest formation. Embryos infected with Noelin-1 retrovirus produce an increased number of

neural crest cells and continue to generate cranial neural crest cells well past the time at which the last cells normally exit the neural tube. These results suggest that Noelin-1 has a key role in conferring on neural tube cells the ability to become neural crest. Consistent with this, Noelin-1 is expressed before *Slug* and can upregulate expression of *Slug*, a marker of cells with the potential to form neural crest. Noelin-1 may act by directly affecting cell fate decisions within the dorsal neural tube. Alternatively, it could act by prolonging the proliferation of a multipotent neural crest precursor<sup>50</sup>. Taken together, these results suggest that Noelin-1 has an important role in making the neural tube competent to form neural crest. □

## Methods

### cDNA libraries

Quail neural tube/neural crest cultures were prepared as described previously<sup>13</sup>, washed in PBS after 1 day of culture and extracted with RNazol. The cDNA library was constructed using a commercial kit (Promega) into pGEM-4.

### Isolation of Noelin

The library was screened according to standard procedures<sup>51</sup> using a degenerate oligonucleotide primer to the link region of the C2-H2 zinc finger domain<sup>52</sup>, GAA/C/G/G/C/C/A/T/G/C/A/G/G/A/C/T/G/T/G/A/C/G/G/G/A/G/G/G/A/G/C/C/T/C/A/C/A. Plasmids were sequenced using Sequenase 2.0 (United States Biochemical). Most cDNA clones contained zinc finger domains, although some non-zinc finger cDNAs, including *Noelin-1*, were also isolated. Reverse transcription and polymerase chain reaction (RT-PCR) were used to isolate chicken *Noelin-1* using the antisense oligo C ATG AGG TCC ATG T C C and the sense oligo C A C G G A A T T C A C A T G T C T G C T T A C T C, which overlaps with the initiation codon. The cDNA was cloned into pGEM-1 vector (Promega) and plasmid DNA was isolated. The RT-PCR clone was then used to probe a 2-4 day-old chicken embryo cDNA library (kindly provided by Sue Bryant) at high stringency. A 3.4 kb clone was isolated which included the entire coding region and 3' untranslated region (Fig. 3a). The nucleic acid sequence of the chicken cDNA was 95% identical to the quail. Additional 5' sequence was obtained by RACE-PCR (Boehringer Mannheim). Sequencing was done with Sequenase 2.0 and either oligos corresponding to known *Noelin-1* sequence or by generating nested exonuclease III deletions (Promega). In addition to the cDNA clones corresponding to the rat *BMZ* RNA, we isolated cDNAs corresponding to the rat A and Y exons<sup>13</sup>. Northern blots were performed according to standard procedures<sup>53</sup>.

### In situ hybridization, Dil labelling and immunocytochemistry

The complete chicken *Noelin-1* cDNA, as well as smaller fragments, were used as templates for antisense RNA probes labelled with digoxigenin, and *in situ* hybridization was performed according to the procedures of Wilkinson<sup>54</sup>. Similar results were obtained with full-length probe or smaller fragment probes covering only the Z region, whereas sense probes did not hybridize to any significant degree. Probes were also made covering only the A or B region. Dil labelling of the surface ectoderm and neural tube was performed as previously described<sup>13</sup>. Embryos were cross-sectioned at 20µm. For immunohistochemistry, embryos were fixed and sectioned as described<sup>13</sup>. Sections were stained with either the anti-p27 antibody (SPAFAAS), which recognizes the viron protein (M, 27,000) from avian myeloblastosis virus, or the anti-INK-1 antibody (American Tissue Culture), which recognizes migrating neural crest cells.

### Retroviral constructs

The coding regions of *Noelin-1* and *Noelin-2* were amplified by PCR, cloned into the shuttle vector Slax 15 and then cloned into the retrovirus vector RCAS BP B subtype<sup>55</sup>. Control viruses consisted of empty vector or retrovirus encoding alkaline phosphatase. Viruses were produced according to published procedures<sup>56</sup>.

### Embryo infection

Chick embryos (0-h-old; HH stage 7-8; 1-6-somite stage) were visualized by injecting ink beneath the blastoderm and were injected with retroviral supernatant (encoding Noelin-1, Noelin-2, alkaline phosphatase or empty vector) in polybrene (80µg/ml<sup>-1</sup>) under the vitelline membrane to cover the embryo. Eggs were incubated at 37°C overnight. In some cases the eggs were removed from the incubator after 15-20h and Dil was injected into the neural tube; embryos were incubated for a further 1h before fixation. For regeneration experiments, embryos were infected as described above at the 1-3-somite stage and incubated until the 10-12-somite stage, at which time the neural tube was labelled with Dil followed 1h later by ablation of the dorsal third of the neural tube as described elsewhere<sup>13</sup>. Embryos were fixed the next day and processed for sectioning.

### Chick embryo fibroblasts

Time 0 chick embryo fibroblasts<sup>57</sup> were infected with RCAS virus encoding Noelin-1, Noelin-2, or, as controls, RCAS empty vector or RCAS-alkaline phosphatase. After several passages to ensure complete infection, cells were removed from the dish, washed, centrifuged and resuspended in a small amount of culture medium (DMEM). The neural tubes of 18-22-somite stage embryos were labelled with Dil. Fibroblasts were back-filled into a micropipette and 200-1,000 cells were injected into the mesenchyme lateral to the neural tube at the level of rhombomere 2. Embryos were fixed and analysed after a further 14h incubation.

### Oocyte injections

Stage VI *Xenopus* oocytes were manually defolliculated and allowed to recover for 1 day before injection. Capped RNA was transcribed and up to 2µg was injected into oocytes<sup>58</sup>. After a 4h recovery period, up

to 4pCi of [<sup>35</sup>S]-methionine was injected in a volume that did not exceed 40 µl. After 24 h culture, ovocyte and supernatant fractions were collected and immunoprecipitated using the M2 anti-Flag antibody (Eastman Kodak) at 10 µg/ml. In vitro translated protein was synthesized using the same capped RNAs in a rabbit reticulocyte system (Promega). Samples were analysed on a 9% SDS-PAGE gel.

RECEIVED 4 JANUARY 2000; ACCEPTED 28 FEBRUARY 2000; PUBLISHED 8 MARCH 2000

1. Le Douarin, N. *The Neural Crest* (Cambridge University Press, Cambridge, 1982).
2. Baker, C.V.H. & Bronner-Fraser, M. The origins of the neural crest. Part I: Embryonic induction. *Mech. Dev.* **69**, 3–11 (1997).
3. Mouny, J.D. & Jacobson, A.G. The origins of neural crest cells in the axolotl. *Dev. Biol.* **141**, 243–253 (1990).
4. Selleck, M.A. J. & Bronner-Fraser, M. Origins of the avian neural crest: the role of neural plate-epidermal interactions. *Development* **121**, 525–538 (1995).
5. Dickinson, M.E., Selleck, M.A. J., McMahon, A.P. & Bronner-Fraser, M. Dorsalization of the neural tube by the non-neural ectoderm. *Development* **121**, 2099–2106 (1995).
6. Liem, K.F., Tremmi, G., Roelink, H. & Jessell, J.M. Dorsal differentiation of neural plate cells induced by BMP-mediated signals from epidermal ectoderm. *Cell* **82**, 969–979 (1995).
7. Scherson, I., Serbedzija, G., Fraser, S. & Bronner-Fraser, M. Regulative capacity of the cranial neural tube to form neural crest. *Development* **118**, 1049–1061 (1993).
8. Sechrist, J., Nieto, A., Zamanian, R. & Bronner-Fraser, M. Regulative response of the cranial neural tube after neural fold ablation: spatiotemporal nature of neural crest generation and up-regulation of *Shg*. *Development* **121**, 4103–4135 (1995).
9. Hunt, P., Ferretti, P., Kramilait, R., & Thorogood, P. Restoration of normal Hox code and branchial arch morphogenesis after extensive deletion of hindbrain neural crest. *Dev. Biol.* **168**, 584–597 (1995).
10. Suzuki, H. R. & Kirby, M.L. Absence of neural crest cell regeneration from the postotic neural tube. *Dev. Biol.* **184**, 222–233 (1997).
11. Tanabe, Y. & Jessell, J.M. Diversity and pattern in the developing spinal cord. *Science* **274**, 1115–1123 (1996).
12. Danielson, P.E., Forss-Petter, S., Battenberg, E.L.L., del'acqua, L., Bloom, F.L. & Sutcliffe, I.G. Four structurally distinct neuron-specific, olfactomedin-related glycoproteins produced by differential promoter utilization and alternative mRNA splicing from a single gene. *J. Neurosci. Res.* **38**, 468–478 (1994).
13. Nieto, M.A., Sargent, M.G., Wilkinson, D.G. & Cooke, J.C. Control of cell behavior during vertebrate development by *Shg*, a zinc finger gene. *Science* **264**, 835–839 (1994).
14. Hamburger, V., & Hamilton, H.L. A series of normal stages in the development of the chick embryo. *J. Morphol.* **88**, 49–92 (1951).
15. Serbedzija, G.N., Fraser, S.L. & Bronner-Fraser, M. A vital dye analysis of the timing and pathways of avian trunk neural crest cell migration. *Development* **106**, 809–816 (1989).
16. Nagano, T. et al. Differentially expressed olfactomedin-related glycoproteins (pancortins) in the brain. *Mol. Brain Res.* **53**, 13–23 (1998).
17. Yokoe, H., & Anholt, R.R.H. Molecular cloning of olfactomedin, an extracellular matrix protein specific to olfactory neuroepithelium. *Proc. Natl Acad. Sci. USA* **90**, 4655–4659 (1993).
18. Nguyen, L.D., Chen, P., Huang, W.D., Chen, H., Johnson, D. & Polansky, J.R. Gene structure and properties of TIGR, an olfactomedin-related glycoprotein cloned from glucocorticoid-induced trabecular meshwork cells. *J. Biol. Chem.* **273**, 6541–6550 (1998).
19. Krasnoperov, V.G. et al.  $\alpha$ -Latrotoxin stimulates exocytosis by the interaction with a neuronal G<sub>i</sub> protein-coupled receptor. *Neuron* **18**, 925–937 (1997).
20. Morgan, B.A. & Fekete, D.M. in *Methods in Avian Embryology* (ed. Bronner-Fraser, M.) 185–218 (Academic Press, San Diego, CA, 1996).
21. Vincent, M. & Thiery, J.P. A cell surface marker for neural crest and placodal cells: further evolution in peripheral and central nervous system. *Dev. Biol.* **103**, 468–481 (1984).
22. Lumsden, A., Sprawson, N. & Graham, A. (1991). Segmental origin and migration of neural crest cells in the hindbrain region of the chick embryo. *Development* **113**, 1281–1291 (1986).
23. Raff, M. Size control: the regulation of cell numbers in animal development. *Cell* **86**, 173–175 (1996).
24. Bronner-Fraser, M.E. & Cohen, A.M. Analysis of the neural crest ventral pathway using injected tracer cells. *Dev. Biol.* **77**, 130–141 (1980).
25. Sechrist, J., Serbedzija, G.N., Fraser, S.L., Scherson, I. & Bronner-Fraser, M. Segmental migration of the hindbrain neural crest does not arise from segmental generation. *Development* **118**, 691–703 (1993).
26. Farlie, P.G., Kerr, R., Thomas, P., Symes, L., Mimichello, L., Hearn, C. & Newgreen, D. A paraxial exclusion zone creates patterned cranial neural crest cell outgrowth adjacent to rhombomeres 3 and 5. *Dev. Biol.* **213**, 70–84 (1999).
27. Martensen, B. & Bronner-Fraser, M. Neural crest cell fate is regulated by the helix-loop-helix transcriptional regulator, *Id2*. *Science* **281**, 988–991 (1998).
28. Bronner-Fraser, M. & Fraser, S. Cell lineage analysis shows multipotentiality of some avian neural crest cells. *Nature* **335**, 161–164 (1988).
29. Lallier, T. & Bronner-Fraser, M. Avian neural crest cell attachment to laminin: involvement of divalent cation dependent and independent integrins. *Development* **113**, 1069–1084 (1991).
30. Sambrook, J., Fritsch, E.F. & Maniatis, T. *Molecular Cloning: A Laboratory Manual* (Cold Spring Harbor Press, NY, 1989).
31. Bray, P., Lichter, P., Thiesen, H.J., Ward, D.C. & Dawid, I.B. Characterization and mapping of human genes encoding zinc finger proteins. *Proc. Natl Acad. Sci. USA* **88**, 9563–9567 (1991).
32. Wilkinson, D.G. in *In Situ Hybridisation: A Practical Approach*, (ed. Wilkinson, D.G.) 75–83 (IRL Press, Oxford, 1992).
33. Hughes, S.H., Greenhouse, J.L., Petropoulos, C.L. & Sutcliffe, P. Adaptor plasmids simplify the insertion of foreign DNA into helper-independent retroviral vectors. *J. Virol.* **61**, 3004–3012 (1987).
34. Smith, W.C., Knecht, A.K., Wu, M., & Harland, R.M. Secreted noggin protein mimics the Spemann organizer in dorsalizing *Xenopus* mesoderm. *Nature* **361**, 547–549 (1993).

#### ACKNOWLEDGEMENTS

We thank C. Baker, S. Fraser, M. Dickinson, B. Murray and M. Selleck for helpful discussions and comments on the manuscript and J. Neri and R. Velasco for help with sectioning. This work was supported by NS 46585 and NS 34671.

Correspondence and requests for materials should be addressed to M.B.F.

Sequences for Noelin-1 and Noelin-2 have been deposited in GenBank (accession nos AF182815 and AF239804, respectively).

## Appendix Chapter 2

*Xenopus Ring3r*, a homolog of *Drosophila* female sterile  
homeotic protein

## INTRODUCTION

The Ring3 protein (really interesting new gene 3) is a homolog of a *Drosophila* female-sterile mutant known as *female sterile homeotic* (*fsh*, Gans et al., 1975; Digan et al., 1986; Beck et al., 1992). Mutations in the *fsh* locus in flies cause homeotic transformations of thoracic segments (Digan et al., 1986). The gene codes for a nuclear protein with two bromodomains. The bromodomain is a region of 110 amino acids that is highly conserved among regulatory proteins that contain it, and is thought in general to be involved in transcriptional activity by chromatin remodeling or by binding to acetylated lysine residues on histone proteins (reviewed in Haynes et al., 1992; Bannister and Miska, 2000; Dyson et al., 2001; Kouzarides, 2000; Nogales, 2000). In human cell lines, Ring3 may act as a nuclear kinase. Its *Drosophila* counterpart is known to genetically interact with *trithorax*, a gene that in humans is translocated in some leukemias. The linkage of developmental regulation by *Ring3* in *Drosophila* and the possible implications of a connection in leukemia makes *Ring3* an interesting gene to study further in vertebrate development.

Here I describe the cloning of *Xenopus Ring3r* and characterization of its expression pattern. The gene is highly conserved to the other vertebrate homologs, and its transcripts are distributed in neural tissue in early development.

### ***Drosophila* female sterile homeotic protein**

The *Drosophila female sterile homeotic* gene (*fsh*) was first discovered in a screen for X-linked female sterile mutations (Gans et al., 1975). Later both

maternal and zygotic phenotypes were observed: homozygous mutant females were sterile due to embryo lethality, and zygotic mutants displayed homeotic transformations of the third thoracic (T3) segment into the second (T2), similar to *bithorax* homeotic transformations (Digan et al., 1986). Furthermore, the *fsh* phenotype was exacerbated by certain mutant alleles of *trithorax* (*trx*) or *ultrabithorax* (*ubx*), suggesting that *fsh* may interact genetically with these embryonic patterning genes (Digan et al., 1986). In *Drosophila*, maternal *fsh* is expressed in nurse cells and oocytes, both derivatives of germline cells (Haynes et al., 1989). After fertilization, embryonic *fsh* is ubiquitously expressed at the syncytial blastoderm stage in the cortical cytoplasm and not in the yolk; at germ-band extension, *fsh* is expressed uniformly in the embryo (Haynes et al., 1989). In hemizygous embryos with conditional alleles of *fsh*, expression patterns of the homeotic gene *ubx*, the pair rule gene *even-skipped*, and the gap gene *Krüppel* were affected at the semi-permissive conditions (Huang and Dawid, 1990). These results suggested that *fsh* could play an important role in early patterning of the *Drosophila* embryo.

### **History of *Ring3***

The next appearance of an *fsh*-related gene in the literature came from a project to sequence the chromosomes containing the class II region of the major histocompatibility complex in humans (MHC II). A homolog to *Drosophila fsh* was sequenced and named *Ring3* (Beck et al., 1992). *Ring3* is not an MHC gene and appears to be unrelated to antigen processing, with no obvious relationship to the immune system. The *Ring3* cDNA was isolated from a human T-cell

library (Beck et al., 1992). *Ring3* genes in vertebrates human, mouse, chick and *Xenopus* are all conserved in location within the MHC II region, suggesting that selective pressure maintained this non-immune-related gene within the immune locus (Beck et al., 1992; Salter-Cid et al., 1996; Thorpe et al., 1997; Taniguchi et al., 1998); while in invertebrates (*Drosophila* and *C. elegans*), the gene is on the X chromosome (Thorpe et al., 1996).

### **Function of Ring3**

Subsequently, *Ring3* was isolated as a nuclear kinase activity which was then biochemically cloned and sequenced and found to be the same as the *Ring3* gene (Denis and Green, 1996). *Ring3* was not immediately suspected to be a kinase because its kinase domains are scrambled from the usual arrangement (Denis and Green, 1996). However, the observation that *Ring3* acted as a kinase could not be duplicated by two other groups; instead it was suggested that *Ring3* likely interacted with a separate protein which was responsible for the kinase activity originally attributed to *Ring3* (Platt et al., 1999; Rhee et al., 1998).

*Ring3* was found to be capable of transforming NIH/3T3 cells under certain conditions, and caused tumor formation in mice with implanted 3T3 cells expressing *Ring3*, but not when the kinase activity was rendered catalytically inactive by a K to A mutation (Denis et al., 2000). In addition, *Ring3* transactivates promoters of cell-cycle regulatory genes in a macromolecular complex with the E2F protein (Denis et al., 2000).

*Drosophila* *fsh* interacts genetically with *trithorax* (*trx*). Homeotic transformations in flies carrying alleles of both genes are synergistically

activated. these results are very interesting because of a connection with certain leukemias in which the human homolog of trithorax, *ALL-1*, is translocated (Cimino et al., 1991; Djabali et al., 1992; Ford et al., 1993; Gu et al., 1992; Tkachuk et al., 1992); a conservation of the *Drosophila* genetic interaction between *fsh* and *trx* suggests that *ALL-1* and *Ring3* may participate together in a signaling pathway that is de-regulated in leukemia. This hypothesis is further supported by the fact that phosphorylation activity is increased in leukaemic cells (Denis et al., 2000), and *Ring3* is able to transform cell lines (Denis et al., 2000).

### ***Ring3* protein domains**

The *Ring3* gene contains important functional domains (Beck et al., 1992; Denis and Green, 1996). A domain known as the bromodomain is found twice in *Ring3*. This highly conserved sequence is shared by other proteins, from yeast transcription activators *SNF2* (*SWI2*) and *SPT7* to the human cell cycle control gene *CCG-1* (Bannister and Miska, 2000; Dyson et al., 2001; Kouzarides, 2000; Nogales, 2000). It seems likely that bromodomain-containing proteins are a class of regulatory genes involved in transcriptional activation. At present there are over 150 different proteins that contain the bromodomain, and an understanding of the functional consequences of this domain is rapidly emerging. The bromodomain is known to interact with acetylated lysine residues, and may be involved in chromatin remodeling as well as being able to act as a transcriptional transactivator by binding to transcription factors (Dyson et al., 2001; Kouzarides, 2000).

## *Xenopus Ring3*

In this chapter, I discuss the cloning and characterization of a *Xenopus Ring3* homolog. *Ring3r* is highly conserved among *Xenopus*, chick, mouse and humans in sequence and structure. In *Xenopus* embryos, *Ring3r* is expressed in neural tissues from neural plate stages onward. Interestingly, the *Xenopus* probe also gave a specific expression pattern in chick embryos, in the same tissues. These results suggest that *Ring3r* could be an important gene that functions during neural development, and the accumulation of functional data in *Drosophila* mutants and human cell lines indicates that its developmental function could potentially be very interesting with respect to control of developmental processes.

## METHODS

### Library screening and cDNA isolation

A stage 28 phage cDNA library in Lambda ZapII made from *Xenopus* head tissues was kindly provided by Dr. R. Harland (Hemmati-Brivanlou et al., 1991).  $1 \times 10^6$  plaque-forming units were screened with chick *Noelin-1* and a PCR fragment of the mouse Z exon at low stringency (see Chapter 4). The mouse subclone was generated by RT-PCR using upstream primer 5'-CAG AAG GTG ATA ACC GG-3' and downstream primer 5'-CAG CGC GCG GTC TTT AG-3' to amplify a 616 base pair (bp) fragment of the Z exon from embryonic day 10 cDNA. Total RNA was isolated using RNazol B (Tel-Test, Inc.) according to

manufacturer's instructions. cDNA was synthesized using MMLV Reverse Transcriptase (Roche).

A partial clone of *Xenopus Ring3* was isolated as a weak duplicating signal from this library, encompassing 421 bases of 5' untranslated region and the first 1401 base pairs of the coding region. This clone was found to be a backwards insert in the library, perhaps as a result of some low-complexity regions in the DNA sequence that were picked up by the linkers used in the library construction. Sequencing was done by PCR using dye-terminators and run on an ABI Prism automated sequencer. Sequences were compiled and edited using the DNASTAR programs. Sequences were compared to others in GenBank using BLAST (Altschul et al., 1990).

### **Collection of embryos for *in situ* hybridization:**

#### *Xenopus laevis* fertilizations and collection of embryos

*Xenopus* embryos were obtained by *in vitro* fertilization using eggs from pigmented and albino females and testis from pigmented males, according to established methods (Sive et al., 2000). Embryos were staged according to the normal tables of Nieuwkoop and Faber (1967).

#### *Chick embryo isolation*

Fertile white leghorn chicken eggs were incubated for 30 hours (stage 8, 6 somite stage) or 36 hours (stage 10, 10 somite stage) and then collected in Howard's ringers and fixed in 4% paraformaldehyde in PBS for 2 hours at room

temperature. Embryos were dehydrated to 100% ethanol and stored at  $-20^{\circ}\text{C}$  until processed for whole mount *in situ* hybridization.

### **Whole mount *in situ* hybridization and sectioning**

*In situ* hybridization was performed as described for chick embryos (Henrique et al., 1995) and for *Xenopus* embryos (Knecht et al., 1995). Protocols are given in Appendix Chapter 3.

Embryos were sectioned in wax after *in situ* hybridization was complete. Samples were dehydrated to 100% ethanol with several changes over 1 hour, then washed 2 X 20 minutes in HistoSol (National Diagnostics), 1 X 1 hour Paraplast Plus wax (Oxford) at  $60^{\circ}\text{C}$ , followed by an overnight incubation in wax. Embryos were embedded in fresh wax and sectioned on a Leitz microtome at  $10\ \mu\text{m}$ . Sections were dewaxed by rinsing 3 X 5 minutes in HistoSol and coverslipped in Permount (Sigma). Sections were viewed on a Zeiss Axiophot microscope and photographed on Kodak 400 film.

## **RESULTS AND DISCUSSION**

### **Sequence and structure information for *Xenopus Ring3r***

During a screen for *Noelin* homologs in a *Xenopus* tailbud-stage cDNA library, a *Xenopus Ring3* homolog was isolated. The sequence did not exhibit any overt similarity to the *Noelin* probes used for the screen (as determined by low-stringency sequence alignments and Blast searching); however, the signal for this gene was a duplicating spot on the filters. It was sequenced from both ends and then primers were designed to give overlapping sequences on both top and

bottom strands. Upon sequencing, it was found that the insert was oriented in the backwards direction, likely a result of an internal *Eco* RI restriction site that may have been used as an alternate cloning site when the cDNA was processed for library construction.

The nucleotide sequence of the gene is given in Figure 1A. The clone consists of 421 base pairs of 5' untranslated region followed by the first 1401 bases of coding region. Blast searches revealed that the clone had a very high degree of similarity to several proteins; among the most related were the Ring3 homologs in mouse, chick and human.

Ring3 secondary structure had been previously characterized (Beck et al., 1992; Denis and Green, 1996). The *Xenopus* clone encoded a deduced amino acid sequence homologous to the first 467 amino acids of the human *Ring3* gene, including the domains that had been described: two bromodomains (red underlines, Fig. 1B), scrambled kinase domains (blue underlines, Fig. 1B), and nuclear localization signals (green underlines, Fig. 1B). The remainder of the protein is predicted to be 250 amino acids long, and was not isolated in the screen.

Similarity in the bromodomain was above 96% across species; elsewhere in the protein, there were observed to be inserted sequences that were not homologous to mouse or human Ring3, and among the Ring3 proteins there were some variants in the database. These results suggested that there may be multiple Ring3 genes, and phylogenetic analysis of several homologs supports this idea. Figure 2A shows a phylogenetic tree based on a multiple sequence alignment of 7 *Ring3* homologs: chick *Ring3* (accession number X96669); mouse

Ring3.1.1 (CAA15818); *Drosophila fsh* (AAA28541); a *Xenopus Ring3-like* gene that was not the same as the one described here (AAB18943); mouse *Fsrg-2*, a mouse *Ring3*-related gene (AF269193); and a human *Ring3-like* gene (NP031397).

These homologs were truncated to contain only the regions that were cloned in the *Xenopus Ring3* clone obtained in this study; carboxy terminal domains may also influence degree of similarity and this is not taken into account in this analysis. In any case, the *Ring3* homologs described here fell into three apparent groups: the first made up of chick *Ring3*, mouse *Ring3.1.1*, *Drosophila fsh*, and *Xenopus Ring3-like*; the second containing only the *Ring3* gene described here; and the third containing mouse *Fsrg-2* and human *Ring3-like*. These results may indicate that there are three different family members closely related to, but separate from the original *Ring3* gene. Thus I have named this clone *Xenopus Ring3r* for *Ring3*-related, to designate that it is not necessarily the direct homolog of human *Ring3* described by Beck *et al.*, (1992).

### **Expression pattern of *Xenopus Ring3r***

In order to determine the spatiotemporal expression pattern of *Xenopus Ring3r*, I performed whole mount *in situ* hybridization experiments with a range of developmental stages. No other *Ring3* homolog has been characterized during development, with the exception of the *Drosophila* homolog *fsh*. Early in neural development, *Ring3r* was expressed in the neural plate and non-neural ectoderm (stage 14, Fig. 3A). The expression in the neural plate was slightly stronger, suggesting a greater presence of the gene in neural ectoderm. During neurulation, expression is markedly greater in the neural crest area and the

neural folds and of the closing neural tube (stage 17, Fig. 3B) and also in the eye primordial (Fig. 3C). As development proceeds, this pattern of transcript distribution continued (stage 22 in Fig. 3D, stage 24 in 3F), and staining was also observed in the neural crest (Fig. 3E).

At tailbud stages, the time from which the library was made from which *Ring3* was isolated, expression was observed at high levels in the head. The eye, brain, and the three neural crest streams stained strongly for *Ring3r* (stage 28 in Fig. 3G and H). Furthermore, some cranial ganglia also revealed the presence of *Ring3r* transcripts: the olfactory placode, geniculate ganglion (VII) and epibranchial ganglion IX were all stained. Later in development, the same head regions were stained, as was the developing tailbud where neurulation takes place posteriorly (stage 33, Fig. 3I).

Thus, *Xenopus Ring3r* is expressed in developing neural ectoderm from early stages of neural development. It is difficult to attribute this pattern of expression solely to *Ring3r*, since by extension of the database search results and the phylogenetic analysis presented here, it is quite likely that other *Ring3* homologs exist in *Xenopus*, and in fact a partial sequence for a divergent *Xenopus Ring3* homolog was found (called *Ring3-like* in this Chapter; Salter-Cid et al., 1996). Furthermore, the probe used here contains the sequences for the highly conserved bromodomain that is likely to be able to hybridize to close relatives.

### **Pattern of *Ring3r* hybridization in chick embryos**

The nucleotide sequences of *Ring3* genes are highly conserved, with 82% identity overall and higher identity within the bromodomain. It was possible that the *Xenopus* gene could serve as a probe for whole mount *in situ*

hybridization in chick embryos. Chicken embryos were probed with the *Xenopus* clone at similar developmental stages. Indeed, I found that the expression pattern of the *Xenopus* gene was similar in chick embryos (Figure 4). At the 10 somite stage, (stage 10) *Ring3r* hybridized to the migrating cranial neural crest, the dorsal neural tube and the neural folds in the open neural plate (Fig. 4A-C). *Ring3r* staining was also found in the ectoderm surrounding the embryo, similar to the results in *Xenopus* (Fig. 4A). However, in chick embryos, hybridization was also found in the notochord rostral to and extending through the open neural plate. This was not observed in *Xenopus* embryos. At an earlier stage (6 somite stage), *Ring3r* hybridization was found in the neural folds (Fig. 4H, I). Overall, *Ring3r* staining in chick embryos resembles that of *Slug*, a zinc-finger transcription factor that is a widely used neural crest marker (Nieto et al., 1994) and is expressed in dorsal neural tube and migratory neural crest in the chick (Fig. 4J). Sense control probe did not reveal any non-specific staining due to reaction components (Fig. 4K).

## Discussion

The expression patterns of *Ring3r* in *Xenopus* and chick embryos were similar to each other. Both species contained staining in the neural ectoderm from early stages, as well as staining in non-neural ectoderm. In *Drosophila*, *fsh* is expressed ubiquitously and its function does not depend on its localization; this suggests that co-factors that are localized may be important for regulatory functions associated with *fsh/Ring3*. It is likely that the bromodomain is an important component of the function of this gene, and the list of interacting

partners is growing (Bannister and Miska, 2000; Dyson et al., 2001; Kouzarides, 2000; Nogales, 2000).

The possibilities for protein-protein interactions defining *Ring3* function in different embryonic tissues are vast. Already it is known that in culture, human *Ring3* genes functions as a transactivator for regulating cell cycle and that it binds to E2F proteins and can transform cultured cells (Denis et al., 2000). Furthermore, the ET domain in human Ring3 (function otherwise unknown; not part of the *Xenopus* clone described here) interacts with the latent nuclear antigen of Kaposi's sarcoma-associated herpesvirus (LANA) and that this interaction regulates the phosphorylation of LANA, although Ring3 itself is not the phosphorylating activity (Platt et al., 1999). *Drosophila fsh* acts as a developmental regulator by interacting with transcription factors like *trithorax* or *Krüppel* (Digan et al., 1986; Haynes et al., 1989; Huang and Dawid, 1990). Thus the information to date suggests that *Ring3* homologs may have multiple interactions *in vivo* and may be able to cause a variety of effects in cells. The implications for these interactions during vertebrate development are undiscovered as yet; however, this gene may play an important role in developmental regulation.

## ACKNOWLEDGEMENTS

I am grateful to Sara Ahlgren for critical reading of the manuscript.

## Figure 1: *Xenopus Ring-3r* sequence

**A** CGCAGACACGTAGCGGCCGCCCGCCCCCCCCCCCCCGACAAATCCCAGCAGGCCAGTGCGGTGA  
 GGGCGCATGCGCGCCGCGCAGTTGGAACCTCTATTATGCTGCTTGGCTGGGGATAAAA  
 AGAAGAGCAACTGGAGGCAGCGTACGGCAAACGTTCCGGGAGCCGCCGGGGGAACAATC  
 CCAAGGAAGAGGGTCCATTGTGCTGTTCCAGAACTGAAGAGGTTTTGCTGANAAATCTG  
 CCAGTCTGATCTTTTCCTTATGTTGGTGATGATGTCACAGAGAAAGATGGTTGACTCCTG  
 ACTCTGGAAGTGCTTTATGGTCAGACCCCTGAAATGGGATGTCTTTCCATTTGGGGACC  
 ATAAAGGAAGAGATTGTGTTGCTCAGCTGTCACAAAAGGAAGTGCTAGAGCGAACGGCGA  
 GATGCTCTGCTGTGACTGCAGGAGCTCAGGCTCCACAAGGGCCTTCAAACCTGCCGCCTCC  
 TGAAGTACCAACTCTAATAAACAGGTCGGAAGACCAACCAATTGCAGTACATGCAGAA  
 TGTAGTGGTGAAGACTCTTTGGAAGCACCAGTTTGCCTGGCCATTCTATCAACCTGTTGA  
 CTGTGTGAAGTTAAGCCTCCCTGACTATCACAAGATTATTAAGAACCAATGGACATGGG  
 GACAATAAAGAAGAGGTTGGAAAATACTACTACTGGAGTGCTAATGAGTGCATGCAGGA  
 TTTCAATACCATGTTTACAACTGTTATATCTATAATAAGTCTACCGATGATATTGTTTT  
 AATGGCACAAGCATTGGAGAAGATCTTCTGCAGAAGGTAGCACAGATGCCTCAGGAAGA  
 GGTGGAATTACTACCCCTGCCCAAAGGCAAAGGCCGAAAACCTCCCACAGCAACACC  
 CCAAGCACCAGTTGTTAGAGAAGTGGAGACACCTGTAGAAAACCGGCCACCACCACCCC  
 CCGGCTCCAGCCCCTGCCCGAAGCCTGCCGAAGTTGAACGTCCCCTACCAGACGGGGC  
 TGAGCCACCAGCGGAACCACGCAGGGAGCGTTACAAAGGAGCGACACAAGCATCAGCAGT  
 GTCCAGTGTGAACCCATCCATACCCATACTAATGCCACCCCGTGGCTTCTCAGACCCC  
 TGTCAATTGCCGTCACCTCTGTGCCAACTATAATGGCAAATGTCGCCCCAGCTTCTGCCCA  
 GCCGGCCTGTACCAGCTGCTTCTTCTCAAATGGTTCTGTGCTCCAGTCGTTAAGAGGAA  
 AGGGGTGAAACGAAAAGCCGACACCACCACCCACCCTTCAGCAATCACAGCCAGCCG  
 TAGTGAGTCTCCCGTTCTGTTTTGGAGCCCAAGCTTGCAAAGGTTTTCGAACCGGCGAGA  
 AAGCGGGGCGCGTCCATTAAACCACCAAAGAAGGACTTGGAAGATGGTGAGATTACCCA  
 GCAAGCAGGAAAAAAGGGCAAACCTGACCGAACATCTCAAGTACTGTGATAGCATCTTGAA  
 AGAGATGCTTTCCAAGAAGCACGCTGCCTATGCTTGGCCCTTTTACAAACCGGTGGATGC  
 GGCAGCCTTGGAAGTGCATGACTACCATGATATCATCAAGCACCCCTATGGACCTCAGTTC  
 TGTTAAAAGAAAAATGGACGCACGAGAGTATGCAGATGCACAGGCTTTTGCAGCCGATAT  
 CCGGTTAATGTTTTCTAACTGCTACAAGTATAATCCTCCTGACCATGAGGTGGTAGCCAT  
 GGCTAGGAAGCTCCAGGATGTTTTTGAGATGAGATTTGCAAAAATGCCAGACGAACCTGT  
 AGAGCCCCCAGCTCCTCCTACC

**B** MSAVTAGAQAPQGPSNLPPPEVTNSNKPGRKTNQLQYMQNVVVKTLWKHQFAWPFYQP 58  
 VDCVKLSLPDYHKI IKNPMDMGTIKKRENNYYWSANECMQDFNTMFTNCYIYNKSTD 116  
 DIVLMAQALEKIFLQKVAQMPQEEVELLPPAPKGKGRKLPTATPQAPVVREVETPVEK 174  
 PATTTPLRLQPLRSLPKLVPLPDGAEPPEPRRERYKGATQASAVSSVNPSPHPTNA 232  
 TPVASQTPVIAVTPVPTIMANVAPASAQPACTSCFFSNGSCAPVVKRKGVKRKADTTT 290  
 PTTSAITASRSESPVPVLEPKLAKVSNRRESGARPIKPPKDLEDGEITQQAGKKGKL 348  
 TEHLKYCDSILKEMLSKKAAYAWPFYKPVDAAALELHDYHDI I KHPMDLSSVVKRKM 406  
 AREYADAQAFAADIRLMSFCYKYNPPDHEVVAMARKLQDVFEMRFAKMPDEPVEPPA 464  
 PPT... 467

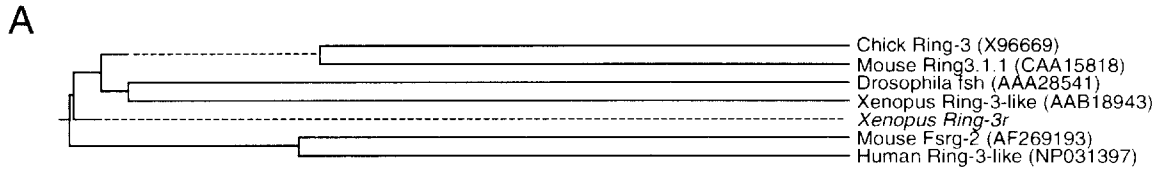
**Figure 1: *Xenopus Ring3r* sequence information**

---

Sequence and structural information for *Xenopus Ring-3r*. **A:** Nucleic acid sequence. cDNA subclone was inserted into the library in a backwards orientation, thus only 5' sequences were obtained. Black nucleotides indicate 5' untranslated sequences, red nucleotides indicate start codon, blue indicates coding region. Length of clone is 1822 base pairs. **B:** Deduced amino acid sequence from longest open reading frame. Ring-3r contains several important domains. Two bromodomain sequences are found in the coding region, from amino acid # 30-138 and from # 350-455 (red underlines). Also found are three nuclear localization signals (green underlines) at positions indicated. Scrambled Conserved sequences related to kinase domains are found, indicated by blue overlines and domain numbers. The domains are found in a scrambled order from the usual sequences. Identities within the consensi are shown as blue residues. The amino acid sequence likely extends for 250 residues more, as is the case for homologs of this gene in mouse, human and chick.

---

## Figure 2: *Ring-3* and related genes

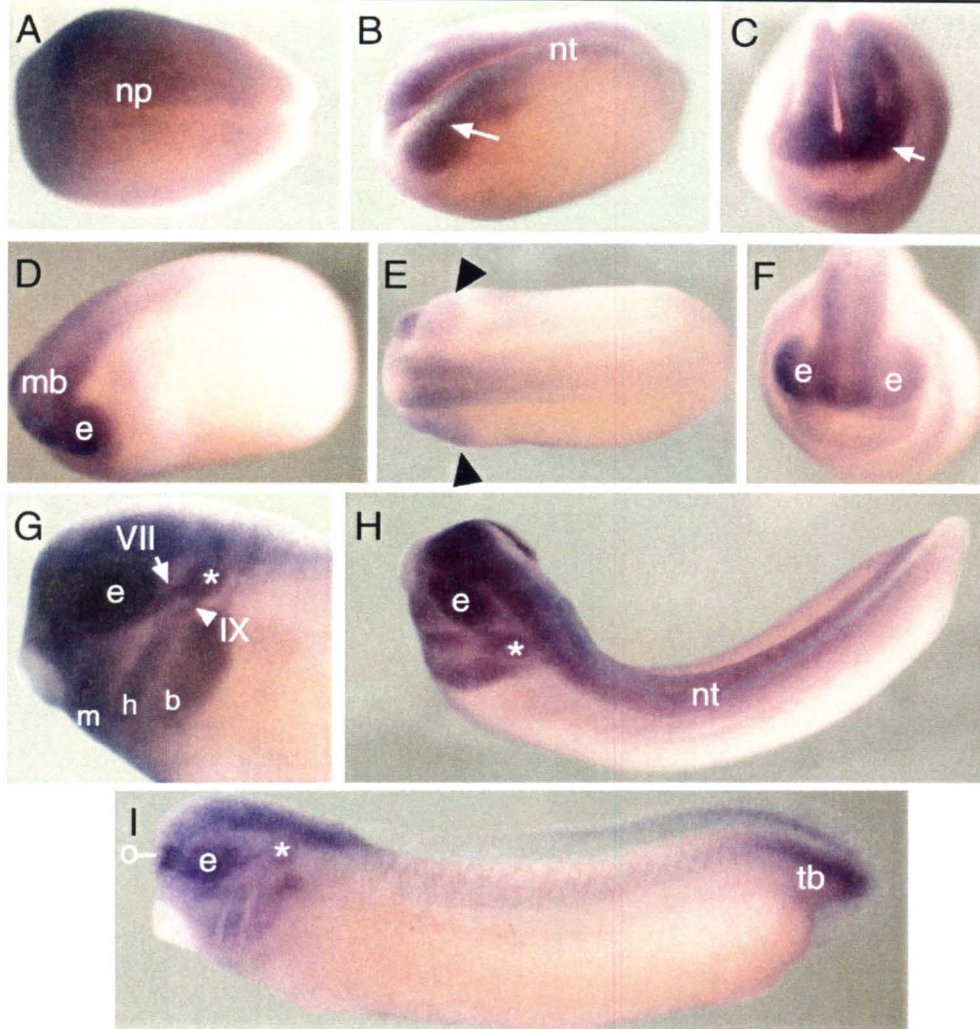


**B**

		Percent Identity								
		1	2	3	4	5	6	7		
Divergence	1	■	54.5	36.2	32.5	56.9	45.5	51.5	1	Drosophila fsh
	2	68.5	■	42.6	38.0	85.6	61.8	65.0	2	Chick Ring-3
	3	100.0	100.0	■	96.5	44.0	35.0	49.8	3	Human Ring-3-like
	4	100.0	100.0	3.6	■	39.0	35.4	43.9	4	Mouse Fsrq-2
	5	63.2	16.0	97.4	100.0	■	62.7	65.5	5	Mouse Ring-3
	6	92.8	52.9	100.0	100.0	51.2	■	48.6	6	Xenopus Ring-3-like
	7	75.9	46.9	80.3	97.7	46.0	83.8	■	7	<i>Xenopus Ring-3r</i>
		1	2	3	4	5	6	7		

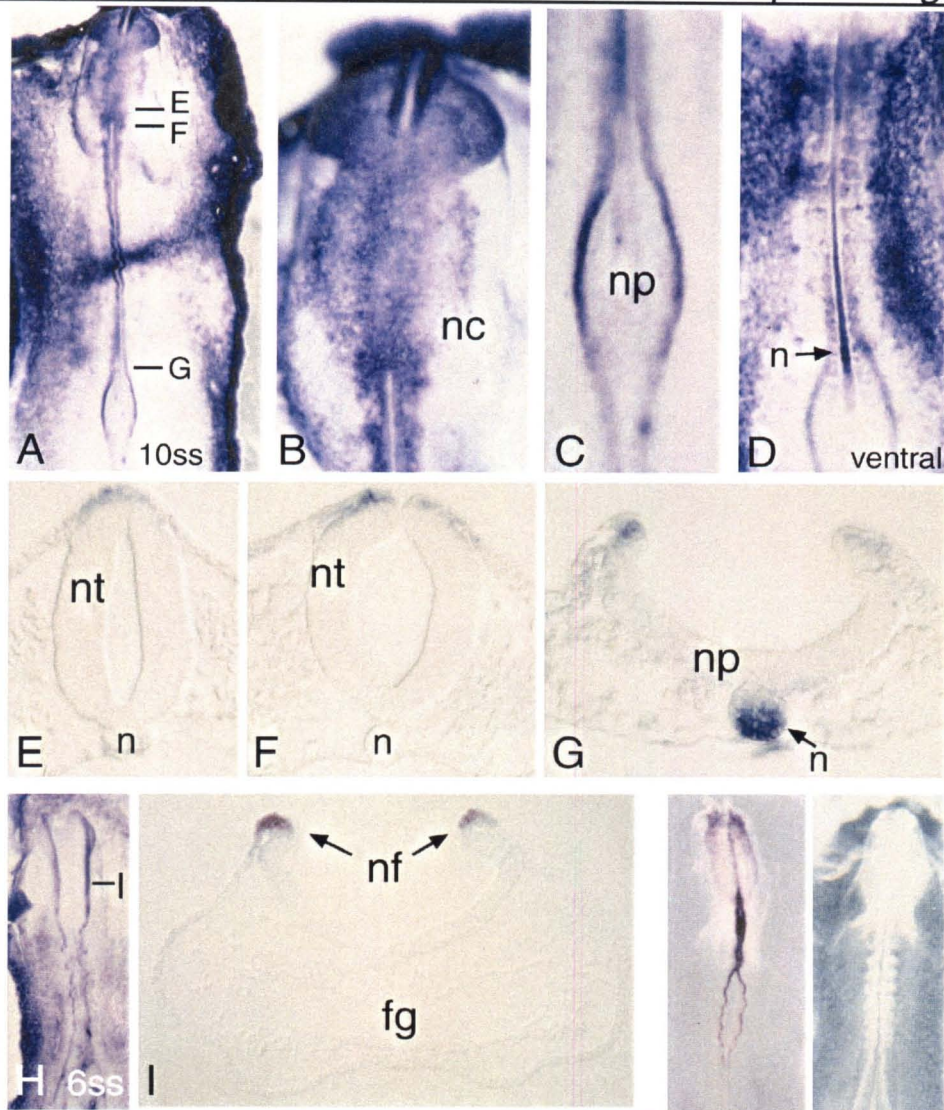
Homologs to Ring-3 are found across vertebrate species. Protein sequences (only the regions homologous to those that were cloned for *Xenopus Ring-3r*) were compared by multiple sequences alignment and analyzed for similarity. **A**: Phylogenetic tree analysis for chick *Ring-3* (accession # X96669), Mouse *Ring3.1.1* (CAA15818), *Drosophila female sterile homeotic* (AAA28541), *Xenopus Ring-3-like* (AAB18943), *Xenopus Ring-3r*, Mouse *Fsrq-2* (AF269193) and Human *Ring-3-like* (NP031397). Chick *Ring-3* and Mouse *Ring 3.1.1* form one subgroup, as do *Xenopus Ring-3-like* and *Drosophila fsh*. *Xenopus Ring-3r* falls out as a distant relative of this branch of the phylogenetic tree. On a separate branch, related *Ring-3* genes from mouse (*Fsrq-2*) and Human (*Ring-3-like*) were found. This tree implies that there may be 3 related orthologs in vertebrates, with the chick *Ring-3*, mouse *Ring3.1.1* and *Drosophila fsh* in one group, mouse *Fsrq-2* and human *Ring-3-like* on another, and on a third, the *Xenopus Ring-3r* described in this Chapter. **B**: Sequence Identity table shows sequence relationships among *Ring-3* genes at the amino acid level.

### Figure 3: *Xenopus Ring-3r* expression pattern



Expression pattern of *Xenopus Ring-3r*. Embryos were stained with the entire cDNA clone as a probe for whole mount in situ hybridization; the probe was hydrolyzed for better penetration. Developmental series of embryos, with anterior to the left except where noted. **A:** Stage 14 embryo showing diffuse *Ring-3r* staining in the ectoderm, at slightly higher levels in the neural ectoderm. **B:** Stage 17 embryo lateral view shows neural plate (closing neural tube) and neural crest staining (arrow). **C:** Anterior view of the same embryo shows *Ring-3r* staining in the head region and developing retina (arrow). **D:** Dorso-anterior view of a stage 22 embryo with staining in the eye and neural tube. **E:** Dorsal view of a stage 24 embryo with staining in the neural tube, eyes, and developing branchial arches (arrowheads). **F:** Anterior view of the same embryo showing continued staining in the eye and brain regions. **G:** Side view of a stage 28 embryo with extensive staining in the head. Eye and brain continue to be stained, as well as neural crest streams in the mandibular, hyoid and branchial streams, as well as in the cranial ganglia (geniculate, VII; and epibranchial IX). The last neural crest migrating into the branchial stream can be seen dorsal to the main branchial mass, coming from the neural tube. **H:** dorsal view of the same embryo shows extent of staining along the rostro-caudal axis. **I:** Stage 33 embryo with staining in the eye, brain, branchial arches, cranial ganglia and also in the tailbud. Olfactory placode staining is indicated. e, eye; b, branchial neural crest; h, hyoid neural crest; m, mandibular neural crest; mb, midbrain; np, neural plate; nt, neural tube; tb, tailbud; asterisks mark otic vesicle location.

## Figure 4: Chick embryos stained with *Xenopus Ring-3r*



Chick embryos stained by whole mount *in situ* hybridization using the *Xenopus Ring-3r* cDNA as a probe. Anterior is up in all panels. **A:** Stage 10 embryo (10 somite stage, ss) with staining in the neural crest and dorsal neural tube, also in the neural folds in the open neural plate. Darker staining appears in the ectoderm outlying the embryo.

Levels of cross-sections in E-G are shown. **B:** Head region of embryo in (A) shows a close up on the migrating cranial neural crest cells that contain *Ring-3r* signal. **C:** Close-up of the neural plate shows staining in the neural folds. **D:** Ventral view shows the notochord also staining for *Ring-3r*. **E:** Cross section through the head region shows neural crest cells staining with *Xenopus Ring-3r* (arrow). **F:** Dorsal staining at a slightly more caudal brain level. **G:** Open neural plate region reveals *Ring-3r* staining in the neural folds and notochord. **H:** A 6-ss embryo displays *Ring-3r* staining in the neural folds along the length of the axis. Level of cross-section in I is indicated. **I:** Cross-section of the 6ss embryo in H shows strong staining in the neural folds in the head. **J:** 10-ss embryo stained with chick *Slug* for comparison. Cranial neural crest and dorsal neural tube are stained for *Slug*. **K:** Negative control sense probe of *Xenopus Ring-3r* is free of staining. fg, foregut; n, notochord; nc, neural crest; nt, neural tube.

## **Appendix Chapter 3**

### **Methods and Miscellaneous Information**

*Appendix 3.1:***Table 1: Clones sequenced in screen for *Noelin* homologs**

<b>CLONE NAME</b>	<b>SIGNAL STRENGTH</b>	<b>INSERT SIZE (kb)</b>	<b>HOMOLOGY TO GENES</b>	<b>PRIMERS FOR SEQUENCING</b>
XHL 1	**	3	<b>Thaumatococcus-like</b>	M13r, T7
XHL 2	****	0.8	<b>unknown</b>	M13r
XHL 3	**	1.6	<b>Cytochrome Oxidase subunit 1</b>	M13r
XHL 4	***	0.9	<b>unknown</b>	M13r
XHL 5	**	1.4	<b>unknown</b>	M13r
XHL 6	*	0		
XHL 7	***	1.4		
XHL 8	**	2	<b>GMP Reductase (domain)</b>	M13r, T7
XHL 9	****	?		
XHL 10	***	0		
XHL 11	**	0	<b>vector sequence</b>	T3
XHL 12	*	1	<b>Arginine N-Methyl Transferase</b>	T3
XHL 13	***	0		
XHL 14	***	1.4		
XHL 15	***	1.3		
XHL 16-3	*****	2	<b>Transposase, Lens Epith. GF</b>	M13r, T7
XHL 16-4	*****	2.2	<b>PLIC-2</b>	
XHL 18	***	2.9	<b>Armadillo Repeat protein</b>	M13r, T7
XHL 19	*****	3	<b>Noelin (AMZ splice variant)</b>	complete
XHL 20	**	?		
XHL 21	****	0.6	<b>unknown</b>	M13r, T7
XHL 22	***	?		
XHL 23	****	1.4	<b>lost insert!!</b>	M13r, T7
XHL 24	***	1	<b>lost insert!!</b>	M13r, T7
XHL 25-2	***	1	<b>domain: Zn finger, Peripilin</b>	M13r, T7
XHL 25-4	***	0.5	<b>short regions: Lunatic Fringe</b>	M13r, T7
XHL 26	****	2.2	<b>human cgi-55 90% ID</b>	M13r, T7
XHL 27	**	2.1		
XHL 28	**	2		
XHL 30	*	1.4		
XHL 31	**	0.8		
XHL 32	****	1		
XHL 33	**	?		
XHL 34	**	1.5		
XHL 35	***	0		
XHL 36	**	1.8		

Number of asterisks indicates strength of hybridization signal.

*Appendix 3.2:***Protocols for in situ hybridization****Xenopus whole mount in situ hybridization protocol**

Modified from Knecht et al. (1995). Use new, clean 1 dram glass vials for up to several dozens of embryos; if many separate samples are to be processed, it is best to use mesh-bottom tubes (baskets) for batch solution changes. For hybridization, embryos in mesh-bottom tubes can be transferred to snap-cap culture tubes.

Xenopus embryos to be processed for in situs should be fixed in MEMFA and stored in 100% ethanol at  $-20^{\circ}\text{C}$ .

**Day 1:**

Rehydrate embryos:

Wash 1 X 5 minutes each:	100% EtOH
	75% EtOH/water
	50% EtOH/water
	25% EtOH/75 % PTw
Wash 3 X 5 minutes:	100% PTw

Proteinase K treatment:

- 1 X 5 minutes in 10  $\mu\text{g}/\text{ml}$  PK (Roche) in PTw
- Titrate time to embryo stage: 5 minutes is sufficient for stages 12-30. Increase time for older/larger embryos.
- Wash 2 X 5 minutes in 0.1 M TEA
- Add 2.5  $\mu\text{l}$  acetic anhydride per ml of TEA, incubate 5 minutes
- Add another 12.5  $\mu\text{l}$  acetic anhydride to TEA, 5 minutes
- Rinse 2 X 5 minutes PTw

Post-fix:

- Re-fix in 4% formaldehyde in PTw, 20 minutes

- Rinse 3 X 5 minutes PTw

Pre-hybridization and Hybridization:

- Draw off most of the PTw, add 250  $\mu$ l hyb buffer and let embryos settle
- Replace with 0.5 ml hyb buffer incubate with rocking for 10 minutes at 60°C
- Prehyb for 1-6 hours at 60°C
- Hybridize in 0.5 ml hyb buffer containing 0.1- 1 $\mu$ g/ml probe overnight at 60°C

**DAY 2:**

Post hybridization washes and RNase treatment:

- Replace probe with fresh hyb buffer (or 5 X SSC, 50% formamide, 0.1% Tween-20) incubate for 10 minutes @ 60°C
- Wash in 2X SSC 3 X 20 minutes @ 60°C

RNase treatment: (not necessary for most probes—can skip to 0.2 X SSC step):

- 20  $\mu$ g/ml RNase A + 10 units/ml RNase T1 in 2 X SSC for 30 minutes @ 37°C
  - Important that this is done in 2 X SSC! At lower salt concentrations RNases cleave double-stranded RNA.
- Wash 2 X SSC 10 minutes @ room temperature
- Wash 2 X 30 minutes in 0.2X SSC @ 60°C

Blocking and antibody incubation:

- 2 X 10 minutes in MAB @ R.T.
- Block for 1 hour in MAB + 2% BM Blocking Reagent (Roche) + 20% Heat treated sheep serum
- Replace with same solution containing 1:2500 dilution of  $\alpha$ -digoxigenin FAb fragments O/N @ 4°C , or 4 hours @ R.T.

**DAY 3:**

Post-antibody washes and color development:

- Wash in MAB, 5 X 1 hour @ R.T (minimum wash time is 3 hours with at least 6 changes, or one wash can be O/N @ 4°C).
- Wash 2 X 5 minutes NTMT

develop color in BMPurple:

- Add 5mM levamisole to BMPurple and incubate at room temp or 4°C( not for fast-developing or intensely staining probes)

or in NBT/BCIP:

- 4.5  $\mu$ l NBT (75 mg/ml in 70% DMF; can be reduced to 0.45  $\mu$ l per ml)
- 3.5  $\mu$ l BCIP (50 mg/ml in 100% DMF) per ml of NTMT

Stop chromogenic reaction when satisfied. Incubate in MEMFA for 1 hour at room temperature to overnight at 4°C, then change to 100% ethanol for reduction of non-specific staining and storage at -20°C.

**Xenopus in situ protocol solution recipes:**

PTw: PBS + 0.1% Tween-20 (Sigma)

0.1M TEA pH 7.8:

make up with liquid Triethanolamine (7.5 M)  
pH with concentrated HCl  
autoclave. Fresher is better; can keep for 6 months.

HYBRIDIZATION SOLUTION: (100 mls)

50% formamide	50 ml
5X SSC pH 7.0 (important!)	25 ml of 20X
1 mg/ml Torula RNA	2 ml of 50 mg/ml
100 $\mu$ g/ml heparin	10 mg (can make 100 mg/ml & freeze)
1 X Denhardt's	1 ml of 100 X
0.1% Tween-20	0.1 g or 100 $\mu$ l
0.1% CHAPS	0.1 g

5 mM EDTA

1 ml of 0.5 M EDTA

## MALEIC ACID BUFFER (MAB):

100 mM Maleic acid

11.6 g Maleic acid

150 mM NaCl

30 ml of 5 M

7.8 g NaOH

check that pH is 7.5, adjust with 10 N NaOH

## ANTIBODY INCUBATION BUFFER:

MAB

+2% Boehringer Mannheim Blocking Reagent (BMB)

melt 10% BMB in MAB in the microwave until clear; store at -20°C.

+20% heat treated lamb serum (30 minutes @ 55°C)

## ALKALINE PHOSPHATASE BUFFER:

100 mM Tris, pH 9.5 5 ml 1 M Tris

50 mM MgCl<sub>2</sub> 5 ml 0.5 M MgCl<sub>2</sub>

100 mM NaCl 5 ml 1 M NaCl

0.1% Tween-20 5 ml 1% Tween-20

+5 mM Levamisole (0.24 mg/ml; add fresh)

## 10 X MEM salts:

1 M MOPS, pH 7.4

20 mM EDTA

10 mM MgSO<sub>4</sub>

autoclave and store at room temp

## MEMFA:

1 X MEM

4% formaldehyde

**Chick and mouse whole mount *in situ* hybridization protocol**

Modified from Henrique *et al.*, (1995).

Dissections:

1. Dissect embryos in PBS (chick, mouse)
2. Fix in 4% paraformaldehyde in PBS for 1-2 hours at room temperature or 4° O/N
3. Wash 2 X 5 minutes PTw
4. Wash 2 X 5 minutes in 50% etoh/PTw, then 2 X 100% etoh. Store at -20°C

Pretreatments and Hybridization:

1. Rehydrate embryos in glass vials: in 75/25 etoh/PTw, then 50/50, then 25/75, then wash 2 X 5 minutes PTw
2. Treat with Proteinase K at 10  $\gamma$ /ml for 15 minutes
3. Rinse briefly in PTw, then postfix for 20 minutes in 4% paraformaldehyde + 0.1% glutaraldehyde in PTw
4. Rinse once and then wash 2 X 5 minutes in PTw. Leave about 300  $\lambda$  in the vial after wash
5. Add 300  $\lambda$  hybridization buffer, let embryos settle
6. Rinse in hyb buffer, then replace with fresh hyb buffer and incubate at 60° for 4-6 hours
7. Add probe to 0.5 ml pre-warmed hyb buffer at 0.1-1 $\gamma$ /ml and incubate O/N at 60°C

Post-Hybridization Washes:

1. Rinse 2 X 5 minutes with pre-warmed hyb buffer at 60°C
2. Wash 2 X 30 minutes at 60°C with 1.5 ml in pre-warmed hyb buffer
3. Wash 10 minutes at 60°C with pre-warmed 1:1 hyb:MABT
4. Rinse 2 X 5 minutes with MABT
5. Wash 15 minutes in MABT
6. Incubate 1 hour in MABT+2% BMB
7. Incubate > 1 hour in MABT + 2% BMB + 20% heat-treated sheep serum

8. Incubate O/N at 4°C (or 4 hours at room temperature) in fresh MABT + 2% BMB + 20% serum + 1:2000 Anti-dig AP antibody.

Post-Antibody Washes and Histochemistry:

1. Rinse 3 X MABT
2. Wash 3 X 1 hour in 10-20 ml MABT
3. Wash 2 X 10 minutes with NTMT
4. Develop color with BMPurple (Roche) color substrate (bring to room temperature before use)
5. When color has developed, rinse 1 X and wash 2 X with PTw. Refix with 4% Paraformaldehyde, 0.1% Glutaraldehyde in PTw (40  $\lambda$  for 10 ml), for 2 hours at room temperature. Store at 4°C in PTw.

**Henrique *in situ* protocol solution recipes:**

PTw: 1 X PBS + 0.1% Tween 20

Hyb Buffer:

<u>Recipe</u>	<u>Final Conc.</u>	<u>Volume</u>
Formamide	50%	25 ml
20 X SSC, pH 4.5 (w/ citric acid)	1.3 X SSC	3.25 ml
0.5M EDTA, pH 8.0	5 mM	500 $\lambda$
10mg/ml Yeast tRNA	50 $\gamma$ /ml	250 $\lambda$
Tween-20	0.2%	100 $\lambda$
CHAPS	0.5%	250 mg
Heparin	100 $\gamma$ /ml	5 mg
<u>H<sub>2</sub>O</u>	<u>to 50 ml</u>	<u>21 ml</u>
Total volume		50 ml

Store at -20°C.

## MABT:

100 mM Maleic Acid	11.6 g
150 mM NaCl	30 ml of 5 M
pH 7.5	7.8 g NaOH
+0.1% Tween-20	1 ml
<hr/>	
total volume =	1000 ml, pH 7.5

## NTMT (Make fresh before each use.):

1 ml	5 M NaCl
2.5 ml	2 M Tris-HCl pH 9.5
2.5 ml	1 M MgCl <sub>2</sub>
43.5 ml	H <sub>2</sub> O
<hr/>	
total volume	50 ml

## 10 X MEM:

20.93 g	MOPS
to 80 ml	dep'c H <sub>2</sub> O
	pH to 7.4 with 10 N NaOH
then add:	
0.761 g	EGTA
0.247 g	MgSO <sub>4</sub> ·7H <sub>2</sub> O
to 100 ml	dep'c H <sub>2</sub> O
<hr/>	

Filter with a 0.2 $\mu$  filter and store at 4°C in the dark.

## MEMFA:

1X MEM
4% Formaldehyde

**DiI neural crest labeling injections**

Embryos were staged according to the developmental tables of Neuwkoop and Faber (Neuwkoop and Faber, 1967). Vitelline membranes of

early neurula stages (13-15) were removed with fine forceps and embryos were allowed to recover in 1 X MMR before injection at stage 17 with Cell Tracker CM DiI (Molecular Probes).

CM DiI was prepared by dissolving one tube in 10  $\mu$ l of 100% ethanol, to which 90  $\mu$ l of fresh, pre-warmed (37°C) 10% sucrose was added. The mixture was centrifuged prior to loading in the needle to minimize needle clogging. Less than 3 nl was injected into several positions along the neural folds, usually in three locations on each side of the embryo. Embryos were cultured until approximately stage 33 in 0.1 X MMR. Embryos were fixed in MEMPFA for 3-4 hours to assure that the DiI was well fixed. This resulted in lower signal for in situ hybridization, but fix time could be reduced although with some loss of DiI signal. Quality of DiI fixation varied between experiments.

### ***Appendix 3.3:***

#### **X-Gal Histochemistry**

Fix:

For tissue culture cells:

4% Paraformaldehyde

0.4% Glutaraldehyde

1X PBS

For *Xenopus* embryos:

MEMFA (4% formaldehyde in MEM salts (see in situ protocol))

Staining solution:

10 mM Potassium Ferrocyanide

10 mM Potassium Ferricyanide

2 mM MgCl<sub>2</sub>

in PBS, pH 7.4

then add 10  $\lambda$  of 10% X-Gal (100 mg/ml in DMF) when ready to use.

## Staining tissue culture cells:

- Remove media and wash 1 X 5 minutes in PBS
- Fix for 20 minutes at room temperature
- Wash 3 X 5 minutes in PBS
- Add X-Gal solution at 1 mg/ml and incubate at 37°C
  - pCMX- $\beta$ gal stain in COS-7 cells comes up after 10 minutes and is optimal after 1.5 hours
- Wash in 3X in PBS when staining is complete, store in PBS or coverslip with aqueous gel mount and photograph

Staining *Xenopus* embryos:

- Remove fix and wash 3 X 5 minutes in PBS
- Rinse once and then wash 1 X 5 minutes in staining solution
- Add new stain solution + 1 mg/ml X-Gal or other  $\beta$ -galactosidase substrate
- Incubate at 37°C until staining is optimal
- Rinse 2 x 5 minutes in PBS
- Dehydrate to 100% ethanol for indefinite storage at -20°C

## Hints and notes:

- Staining is less at higher pH such as 7.5-7.6 than at 7.2-7.3
- Potassium Ferri/Ferro-cyanide concentrations can be modified to suit specific purposes:
  - use 4mM for maximum sensitivity in cultured cells
  - use 16mM to minimize diffusion of stain in tissues; slight but acceptable loss of sensitivity results, but decreased diffusion results in better labeling
- If crystals form during incubation, use a bit less X-Gal; and/or be sure that PBS is at room temperature before adding X-Gal to it. (If X-Gal is dissolved in DMSO, refrigerator temperature causes it to freeze.)
- Gradual increase in background will result from storage in PBS. To avoid this, stained samples can be stored in fix or in ethanol.

## *Appendix 3.4:*

### **Cell transfections**

#### **COS-7 cell Lipofection Protocol**

1. Plate  $1.5 \times 10^5$  cells per well of a 6-well plate or 35 mm dish the day before transfection. Cells should grow to about 50-80% confluence before transfecting.
2. Prepare DNA and Lipofectamine (Gibco BRL):
  - + 8  $\lambda$  lipofectamine (optimal for COS-7 cells in this format)
  - + 92  $\lambda$  OptiMem (Gibco, reduced-serum media) in a sterile tube per sample to be transfected
  - + 1-2  $\gamma$  DNA in 100  $\lambda$  OptiMem (total volume) in a sterile tube per sample to be transfected.
1. Mix together the DNA and Lipofectamine dilutions and let sit at room temperature for 15 to 45 minutes to form liposomes.
2. During this time, rinse the cells to be transfected with 2 ml OptiMem solution (to get rid of serum).
3. Add 800  $\lambda$  OptiMem to each mixture to bring volume up to 1 ml (lower volume = better kinetics of formation).
4. Add the 1 ml of lipofection mixture to the cells and incubate at 37°C with 5% CO<sub>2</sub> for approximately 5 hours. (No antibiotics should be in this media.)
5. After the incubation period, add 1 ml DMEM with double strength serum (20% for COS-7) and let incubate at 37°C with 5% CO<sub>2</sub>.
6. Replace with fresh media (DMEM+10% fetal bovine serum+pen/strep) the next day.
7. Assay 24 to 48 hours after transfection.

## Appendix 3.5:

### Protein methods:

#### Immunoprecipitation

For oocyte-generated and in vitro translated proteins:

1. Collect oocyte and supernatant fractions separately.
2. Rinse oocytes with 200  $\mu$ l of OR2 (Sive *et al.*, 2000 ) to remove any secreted material that might have adhered to the cell surface; add this wash to the supernatant fraction. (Samples can be quick-frozen at  $-80^{\circ}\text{C}$  until further processing.)
3. Synthesize *in vitro* translated protein using the same capped mRNAs in Nuclease-treated Rabbit Reticulocyte Lysate (Promega) according to the manufacturer's instructions. (See also MO IVT methods.)
4. Prepare the oocyte fraction for immunoprecipitation by pipet trituration of 5 oocytes in 300  $\mu$ l PBS + 1% NP40 + inhibitors (PBSNI; inhibitors: Aprotinin, Leupeptin, Pepstatin, PMSF; Sigma), then adding fresh 1  $\mu$ l PMSF.
5. Centrifuge for 3 minutes at  $4^{\circ}\text{C}$  and then collect the aqueous phase, bringing it up to 750  $\mu$ l with PBSNI. Add fresh 1  $\mu$ l PMSF.
6. Prepare the supernatant fraction for immunoprecipitation by bringing it up to 750  $\mu$ l with PBSNI.
7. *Myc-tagged proteins*: Add anti-myc antibody (mouse monoclonal antibody 9E10, Santa Cruz Biotechnology) to the samples at a 1:500 dilution and incubated with rocking for 2 hours at  $4^{\circ}\text{C}$ .

*Flag-tagged proteins*: Either use Flag-conjugated Sepharose (Eastman Kodak) with the samples at  $4^{\circ}\text{C}$  with rocking for 1 hour, and skip to step 9, or add anti-Flag antibody M2 (best for internal and external flag insertions) at 10  $\mu\text{g}/\text{ml}$ .

8. Protein A Sepharose (Sigma) is incubated with the antibody-treated samples for 1 hour at  $4^{\circ}\text{C}$  with rocking. (Prepare new PAS by swelling at least 1h in PBS (prefer overnight), then wash 3 times with large volumes PBS. Store in PBS + 0.02% thimerosal up to 6 months.)

9. Wash the sepharose beads washed three times in PBSNI and resuspend in 1 X SDS loading buffer.
10. Boil samples for 5 minutes prior to loading on SDS-polyacrylamide gels (Laemmli, 1970).
11. Fix gels for 15 minutes in 40% methanol, 20% glacial acetic acid, rinse in H<sub>2</sub>O then amplify for 10 minutes in 1M Na-Salicylate (Sigma), rinse in H<sub>2</sub>O, and dry at no higher than 80°C. Expose overnight at -80°C with an intensifying screen.
12. If desired, deglycosylation of samples can be performed with Peptide-N-Glycosidase (Promega) according to the manufacturer's instructions. The enzyme is active in SDS sample buffer, so the reactions can be done on samples that have already been prepared for loading.

### **Deglycosylation of glycoproteins**

Deglycosylation was achieved with Peptide-N-Glycosidase (PNGase F, Promega) following the manufacturer's instructions. The enzyme is active in SDS sample buffer, so the reaction can be done on samples already prepared for loading. Briefly: 10 µl of sample protein was denatured by boiling for 10 minutes in 1 X Denaturing Buffer (supplied with the enzyme). The enzyme reaction volume was 50 µl with 2 µl of Peptide-N-Glycosidase in the supplied reaction buffer and detergent, with a reaction time of 1 hour at 37°C. After completion of the reaction, 10 µl of SDS sample loading buffer was added and samples were boiled again before loading on the gel.

### **Morpholino (MO) Translation Inhibition**

*In vitro* translation (IVT):

1 µl RNA (higher concentration seems to work better)

2 µl MO at 10 mg/ml

0.5 µl aa mix minus Methionine

0.5 µl RNAsin

3 µl lysate (nuclease-treated Rabbit Reticulocyte Lysate, Promega)

15' RT

Then add:

14 $\mu$ l	lysate
1 $\mu$ l	aa mix minus Methionine
1 $\mu$ l	<sup>35</sup> S-Methionine

---

90' 30°C

Immunoprecipitation is the *very best* way to visualize the knock-down of translation, so it's best to use epitope-tagged constructs. Crude lysate preps are very difficult to judge because you get a lot of degradation products in the lanes. This is based on what Summerton did in this paper describing cell-free assays (Summerton et al., 1997), but with several variations in time and temp of annealing the oligo to the RNA.

#### **Preparation and storage of Morpholino oligos:**

I dissolve the MO in dep'c water at 10mg/ml for later RNA co-injections. Store in aliquots of reasonable sizes at -20°C. The oligos are very stable and can be stored at 4°C or repeatedly freeze-thawed without damage, but it is always better to treat them nicely. For electroporation of the oligos, they should be altered to 0.1X MMR.

#### **For Morpholino oligo injections into embryos:**

Heasman used between 3-20 ng and found a good effective concentration at around 5-10 ng for  $\beta$ -catenin MOs (Heasman et al., 2000 #788]. I make dilutions of 1 in 5, 1 in 10 and 1 in 20 (= 2, 1 and 0.5 ng/nl respectively) and I inject 10 nl. I have been using  $\beta$ -galactosidase mRNA to trace since the fluoresceinated control MO is not visible after fixation and in situ hybridization. Perhaps it could be visualized by anti-fluorescein immunohistochemistry. However, I have found that the RNA, the MO, or both, precipitate if mixed and then freeze-thawed. It is best to prepare lineage tracer + MO fresh for each injection experiment. The standard control MO has not been toxic at the highest dose, so that is the only dose that I use for the control injections. I have injected

up to 40 ng without too many gastrulation defects, embryonic lethality or mutations.

### **SDS-Polyacrylamide gel electrophoresis**

Protein samples were stacked in a 4% polyacrylamide stacking gel and separated in 9-14% polyacrylamide gels, depending upon expected protein sizes and according to the method of (Laemmli, 1970). Samples were run until the bromophenol blue in the loading buffer was approximately 1/2" from the bottom of the gel in a BioRad Mini-Protean II vertical gel apparatus.

Fixing gels: Gels were rinsed once in water, then fixed for 20' in 40% Methanol/20% glacial acetic acid. After fixing, gels were rinsed in water and then enhanced in 1 M sodium salicylate for 10 minutes. Gels were rinsed in water before drying at 80°C under a vacuum for 30 minutes. Dried gels containing [<sup>35</sup>S]-Methionine-labeled proteins were exposed at -80°C with an intensifying screen.

**Table 2: SDS-PAGE Recipes**

<b>15%</b>										
<b>Gel Volume (mL)</b>	<b>5</b>	<b>10</b>	<b>15</b>	<b>20</b>	<b>25</b>	<b>30</b>	<b>35</b>	<b>40</b>	<b>45</b>	<b>50</b>
<b>5 X LGS (mL)</b>	1	2	3	4	5	6	7	8	9	10
<b>30% Acrylamide (mL)</b>	2.5	5.0	7.5	10.0	12.5	15.0	17.5	20.0	22.5	25.0
<b>H<sub>2</sub>O (mL)</b>	1.5	3.0	4.5	6.0	7.5	9.0	10.5	12.0	13.5	15.0
<b>10% APS (mL)</b>	50	100	150	200	250	300	350	400	450	500
<b>TEMED (mL)</b>	10	20	30	40	50	60	70	80	90	100

<b>14%</b>										
<b>Gel Volume (mL)</b>	<b>5</b>	<b>10</b>	<b>15</b>	<b>20</b>	<b>25</b>	<b>30</b>	<b>35</b>	<b>40</b>	<b>45</b>	<b>50</b>
<b>5 X LGS (mL)</b>	1	2	3	4	5	6	7	8	9	10
<b>30% Acrylamide (mL)</b>	2.3	4.7	7.0	9.3	11.7	14.0	16.3	18.7	21.0	23.3
<b>H<sub>2</sub>O (mL)</b>	1.7	3.3	5.0	6.7	8.3	10.0	11.7	13.3	15.0	16.7
<b>10% APS (mL)</b>	50	100	150	200	250	300	350	400	450	500
<b>TEMED (mL)</b>	10	20	30	40	50	60	70	80	90	100

<b>10%</b>										
<b>Gel Volume (mL)</b>	<b>5</b>	<b>10</b>	<b>15</b>	<b>20</b>	<b>25</b>	<b>30</b>	<b>35</b>	<b>40</b>	<b>45</b>	<b>50</b>
<b>5 X LGS (mL)</b>	1	2	3	4	5	6	7	8	9	10
<b>30% Acrylamide (mL)</b>	1.7	3.3	5.0	6.7	8.3	10.0	11.7	13.3	15.0	16.7
<b>H<sub>2</sub>O (mL)</b>	2.3	4.7	7.0	9.3	11.7	14.0	16.3	18.7	21.0	23.3
<b>10% APS (mL)</b>	42	83	125	167	208	250	292	333	375	417
<b>TEMED (mL)</b>	8	17	25	33	42	50	58	67	75	83

<b>9%</b>										
<b>Gel Volume (mL)</b>	<b>5</b>	<b>10</b>	<b>15</b>	<b>20</b>	<b>25</b>	<b>30</b>	<b>35</b>	<b>40</b>	<b>45</b>	<b>50</b>
<b>5 X LGS (mL)</b>	1	2	3	4	5	6	7	8	9	10
<b>30% Acrylamide (mL)</b>	1.5	3	4.5	6	7.5	9	10.5	12	13.5	15
<b>H<sub>2</sub>O (mL)</b>	2.5	5	7.5	10	12.5	15	17.5	20	22.5	25
<b>10% APS (mL)</b>	42	83	125	167	208	250	292	333	375	417
<b>TEMED (mL)</b>	8	17	25	33	42	50	58	67	75	83

## Appendix 3.6

### RT-PCR

#### Optimization of primer sets

For each new primer set:

Optimize cycle number for amplification within the linear range by doing four different cycle numbers (e.g., 21, 24, 27, 30 cycles) on whole embryo cDNA from the appropriate stage, using a standard amount of RNA→cDNA per reaction.

E.g., for stage 25 embryos:

2 embryos' worth of RNA dissolved in 40  $\mu$ l dep'c H<sub>2</sub>O  
 ↓  
 2  $\mu$ l RNA for cDNA synthesis in f.v. 80  $\mu$ l  
 ↓  
 4  $\mu$ l cDNA per PCR reaction.

#### Normalization of cDNA amounts

For each new experiment, equalize cDNA amounts per experimental condition by normalizing to EF1 $\alpha$  or ODC, etc. After quantification on the PhosphorImager on a trial reaction using 4  $\mu$ l of each cDNA, adjust volumes of cDNA samples to make 4  $\mu$ l of each one contain equivalent amounts of loading control cDNA (EF1 $\alpha$ , ODC, etc.) by adding water to dilute samples to a consistent concentration for the linear test primer set.

For -RT reactions: use 1  $\mu$ l RNA for each experimental sample in a one-half-size cDNA reaction mixture minus Reverse Transcriptase. Leave at 10  $\mu$ l and test 4  $\mu$ l in EF1 $\alpha$  (or other linear test set) PCR. If this is clean then it can be assumed that all primer sets will be clean for the cDNA sample and no further -RT reactions are necessary.

**Isolation of RNA from animal caps and whole embryos:**

Collect 10 caps per condition, or two whole embryos. Isolate total RNA with 0.3  $\mu\text{g}/\mu\text{l}$  Proteinase K (ICN Pharmaceuticals) in 100  $\mu\text{l}$  per 10 caps, or 200  $\mu\text{l}$  per 2 embryos, and incubate at 37°C for 1 hour. Phenol-chloroform extract and add 10  $\mu\text{g}$  RNase-free glycogen (Roche) before precipitation with 2 volumes 100% ethanol and 1/10 volume 7.5M ammonium acetate. Wash once in 70% ethanol, slightly air dry, and then resuspend in 50  $\mu\text{l}$  of DNase I reaction mix: 5  $\mu\text{l}$  any 10 X restriction buffer with sufficient magnesium levels (I use NEB buffer 4), 2  $\mu\text{l}$  20 mM DTT, 0.5  $\mu\text{l}$  RNase inhibitor (Promega), and 1  $\mu\text{l}$  DNase I (RNase-free, Roche). Incubate at 37°C for 45 minutes. Phenol-chloroform extract and add 10  $\mu\text{g}$  RNase-free glycogen (Roche), before precipitation with 2 volumes 100% ethanol and 1/10 volume 7.5M ammonium acetate. Wash once in 70% ethanol, slightly air dry, and then resuspend in 22  $\mu\text{l}$  dep'c H<sub>2</sub>O (2.2  $\mu\text{l}$  per cap), or 40  $\mu\text{l}$  (per two embryos). Use 11  $\mu\text{l}$  caps RNA or 2  $\mu\text{l}$  embryo RNA for cDNA synthesis:

**cDNA synthesis**

11  $\mu\text{l}$  RNA (or water + RNA)  
 1 $\mu\text{l}$  random hexamers at 20  $\mu\text{M}$   
 heat to 70°C for 10 minutes, then ice for 2 minutes

Add 7.5  $\mu\text{l}$  reaction mix:

4  $\mu\text{l}$  5 X First strand buffer (Life Technologies)  
 2  $\mu\text{l}$  100mM DTT  
 1  $\mu\text{l}$  dNTPs at 10mM each (Roche)  
 0.5  $\mu\text{l}$  RNase inhibitor (Promega)  
 1  $\mu\text{l}$  SuperScript II reverse transcriptase (Life Technologies)

for 20  $\mu\text{l}$  final volume.

Incubate at 42°C for 1 hour (for random hexamer priming) and then heat-kill the enzyme at 95°C for 10 minutes, then ice 5 minutes. Resuspend the cDNA in 80  $\mu\text{l}$  final volume and use 4  $\mu\text{l}$  per PCR reaction for the linear test, then dilute with PCR-sterile water to normalize for the linear test primer set.

**PCR reactions**

Mix together in a PCR tube:

4  $\mu$ l cDNA  
 1  $\mu$ l primers (0.5  $\mu$ l of each forward and reverse)  
 1  $\mu$ l H<sub>2</sub>O

Make a PCR cocktail:

15.65  $\mu$ l H<sub>2</sub>O  
 2.5  $\mu$ l 10 X PCR buffer + Magnesium (Roche)  
 0.5  $\mu$ l dNTPs at 10 mM each  
 0.05  $\mu$ l [ $\alpha$ -<sup>32</sup>P]-dCTP (NEN)  
 0.3  $\mu$ l Taq Polymerase (Roche)

Add 19  $\mu$ l to each cDNA/primer sample.

Standard PCR conditions are: 30 seconds at 94°C, 1 minute at 55°C, 1 minute at 72°C for the pre-determined number of cycles; preceded by 5 minutes at 94°C and followed by 5 minutes at 72°C. Run samples on a 5% Acrylamide gel in 1 X TBE.

**Table 3: PCR gel recipes**

volume 5% PCR gel (ml)	10	15	20	25	27	30	35	40	50
10XTBE (ml)	1	1.5	2	2.5	2.7	3	3.5	4	5
30% Acrylamide (ml)	1.7	2.5	3.3	4.2	4.5	5.0	5.8	6.7	8.3
H <sub>2</sub> O (ml)	7.3	11.0	14.7	18.3	19.8	22.0	25.7	29.3	36.7
10% APS ( $\mu$ l)	50	75	100	125	135	150	175	200	250
TEMED ( $\mu$ l)	10	15	20	25	27	30	35	40	50

**Table 4: PCR primer sets**

Gene	upstream/downstream	product	# cyc	citation
$\beta$ -crystallin	TGC CTG GAG TGG AAC AAT GC TGT TGA ACC ATC CCA TAG CC	200	28	Altmann 1997
Brn-3d	CAT CAC CCT TCT GTT TTA GGG TCT GTT TCA CTT TCA	277	30	Hutcheson and Vetter, 2001
EF1 $\alpha$	CCT GAA CCA CCC AGG CCA GAT TGG TG GAG GGT AGT CAG AGA AGC TCT CCA CG	221	20	Agius et al. (2000)
En-2	cgg aat tca tca ggt cgg aga tc gcg gat cct ttg aag tgg tgg cg	303	28	Hemmati-Brivanlou et al. 1994
Hox-B9	TAC TTA CGG GCT TGG CTG GA AGC GTG TAA CCA GTT GGC TG	236	28	Harland lab (6/00)
Krox20	ATT CAG ATG AGC GGA GTG ATG TGC TCC AGG TCA CTT	323	30	Harland lab (6/00)
MA	GCT GAC AGA ATG CAG AAG TTG CTT GGA GGA GTG TGT	222	23	XMMR
NCAM	CAC AGT TCC ACC AAA TGC GGA ATC AAG CGG TAC AGA	342	25	Kintner & Melton 1987
NeuroD	GTG AAA TCC CAA TAG ACA CC TTC CCC ATA TCT AAA GGC AG	238	30	Lee et al., 1995
NF-M	GAA CAG TAC GCC AAG CTG ACT GCA GCA ATT TCT ATA TCC AGA G	321	30	Sasai et al (1995)
ngn	CAA GAG CGG AGA AAC TGT GT GAA GGA GCA ACA AGA GGA AG		28	Ma 1996
Otx2	GGA TGG ATT TGT TGC ACC AGT C CAC TCT CCG AGC TCA CTT CTC	314	25	XMMR
Pax-2	gga tat gca ctg caa gg tca ttg tgg cag att cc	377	26	Heller & Brandli 1997
Pax-6	CAG AAC ATC TTT TAC CCA GGA ACT ACT GCT AAT GGG AAT GTG	232	25	
Slug	CAA TGC AAG AAC TGT TCC TCT AGG CAA GAA TTG CTC		26	C LaBonne's 1998 paper
Sox2	GAG GAT GGA CAC TTA TGC CCA C GGA CAT GCT GTA GGT AGG CGA	214		De Robertis, et al. (1997)
Syb II	ATT TGT CTG TGC GCA GGT TIT AAG CCA CTC CCT GCT	307	30	Harland lab (6/00)
Tanabin	gaa ggc aaa tgg aga gca c gca aag tct tag ggg cat cc		30	Hemmati-Brivanlou et al. 1994
Xbra	GGA TCG TTA TCA CCT CTG GTG TAG TCT GTA GCA GCA	188	30	Harland lab/XMMR
XCG-1	GGT TGA TGT TAC TTC CCC AGA GCA G GGG AAG TAA CAT CAA ACA AAG CAA CCA		21	Gammill 1998
XlhBox6	TAC TTA CGG GCT TGG CTG GA AGC GTG TAA CCA GTT GGC TG	217	25-27	XMMR

## Appendix 3.7

Table 5: Primary antibodies

Antibody	species	type	working conc	specimen type	fix/embe dding	notes
12/101	mouse monoclonal	IgG1	1 in 5	whole mount	memfa	stains somitic muscle; did primary incubation in whole mount, then sectioned in paraffin, then did secondary Alexa Red. Worked well. From Harland.
14h7	mouse monoclonal	IgG 1/2a	neat	sections	mempfa/ gelatin	didn't work yet; stains vimentin; sugg conc = 1 in 10 (Dent 1987); supposed to work in Dent's fix... see Messenger & Warner(?) paper about neurons & glia appearance from the late 80's
			neat	sections	mempfa/ paraffin	didn't work yet
			neat	whole mount	stored in etoh	didn't work yet
2G9	mouse monoclonal	IgG	1 in 5	whole mount	stored in etoh	E. Jones; stains neural, lateral lines
3A10	mouse monoclonal	IgG1	1 to 1, neat	sections	memfa/p araffin	DSHB, vfaint on st28, st35; used in Messenger 1999 to show neurite outgrowth in noggin-induced caps + noradrenaline
			1 to 4	whole mount	stored in etoh	stains neurites, differentiating neurons, sensory axons
40.2D6	mouse monoclonal	IgG1	1 in 10	sections	mempfa/ gelatin	works pretty well, stains RGC and INL. Islet-1 homeobox.
			1 in 10	sections	mempfa/ paraffin	
4d	mouse monoclonal	IgG1	1 to 1, neat	sections	memfa/p araffin	DSHB, vvvfaint on st28, st35
6F11 (NCAM)	mouse monoclonal	IgG	neat	sections	memfa/p araffin	from R. Harland; doesn't work in wax sections; made by W Harris; NCAM. Used in Lee neuroD paper, many others.
			1 to 1	sections	memfa/g elatin	works very well; stains neural tissues especially spinal cord. Lower signal in brain.
			1 to 4	whole mount	stored in etoh	
acetylated alpha tubulin	mouse monoclonal	IgG2b	1 in 5000	sections	memfa/p araffin	Sigma t-6793; stains neurites, ciliated epidermis; used in Schlosser 2000
$\beta$ -crystallin	rabbit polyclonal	IgG	1 in 500	whole mount	stored in etoh	from S. Zigler, used in AHB lens paper
BMP 2/4	goat polyclonal	IgG	1 in 300	western blot		Santa Cruz Biotech
			1 in 100	immuno- precipitation		works on chick, mouse, human

Antibody	species	type	working conc	specimen type	fix/embe dding	notes
BMP-4	mouse monoclonal	IgG2b	1 in 200	western blot		Chemicon
			1 in 100	immuno-precipitation		ref: Masuahara et al. Bone, 1995
Flag M2	mouse monoclonal	IgG	1 in 500??	immuno-precipitation	cell extracts from Xenopus and IVT	Eastman/Kodak (IBI) M2 version recognizes internal and external epitopes; best one for general use.
			1 in 500	western blot	cell extracts from Xenopus and IVT	too dilute. Use 1 in 100 for better results
GFAP (G-A-5)	mouse monoclonal	IgG1	1 in 400	sections	mempfa/gelatin	didn't work yet; from Sigma
			1 in 400		mempfa/parafin	didn't work yet
			1 in 400	whole mount	stored in etoh	didn't work yet
Glutamine Synthetase	rabbit polyclonal	IgG	1 to 50	sections	try memfa/whole mt	From Vardimon (Israel) Iris Ben Dror; stains Muller glia in the eye
			1 in 200	western blots		advice of Ben Dror
HNK1	mouse monoclonal	IgM	1 to 1	sections	memfa/p arafin	lab supernatant, works ok stains neurons in stages 20's. Not in neural crest in frogs
Hu	mouse monoclonal	IgG2b	1 in 1000	sections	memfa/p arafin	Molecular Probes anti HuC/D cat # A21271; do not dissolve per mfr instructions: do in 100ul and use at 1:400... much better results. Did not work when dissolved in 1ml and used at 1:500. Don't freeze/thaw.
			1 in 400	sections	memfa/g elatin	works very well on gelatin sections, at least from st36. Did not work in wax.
			1 in 400	whole mount	stored in etoh	does not work in etoh-stored embryos. Works on fresh-fixed.
myc (9E10)	mouse monoclonal	IgG	1 in 500	sections	memfa/p arafin	Santa Cruz Biotech
			1 in 500	western blot	cell extracts from Xenopus and IVT	too dilute. Use 1:250 for better results.
			1 in 500	immuno-precipitation	cell extracts from Xenopus and IVT	Works great, on single-myc versions of proteins, too.

Antibody	species	type	working conc	specimen type	fix/emb edding	notes
NCAM	rabbit polyclonal	IgG	1 in 200-1000	sections	memfa/ gelatin,	from Rutishauser; doesn't work in wax or etoh so far
			1.5 in 400	whole mount	memfa/ parafin	stored in etoh
NeuroD1	rabbit polyclonal	IgG	1 in 200-1000	sections	memfa/ gelatin, memfa/ parafin	from Cemines; doesn't work in wax or etoh. Or in Xenopus. Or in chick
NF-M	mouse monoclonal	IgG2a	1 in 300	sections	memfa/ parafin	from Virginia Lee; doesn't work in wax on frogs;
Pax6	mouse monoclonal	IgG1	neat	sections	mempfa/ gelatin	doesn't work on frog; DSHB supernatant
			neat	sections	mempfa/ parafin	doesn't work on frog
phospho Histone H3	rabbit polyclonal	IgG	1 in 200	sections	mempfa/ gelatin	works well; mitosis marker from Upstate Biotech. see DB paper on cell division in Xenopus Saka & Smith 2001
			1 in 200	sections	mempfa/ parafin	didn't work (but it's supposed to.)
			1 in 200	whole mount	stored in etoh	works well, fluorescence is better for pretty chromosome staining!
R2-12N	mouse monoclonal	IgG2b	1 to 50	sections	mempfa/ gelatin	from P Hargrave; works great! Stains photoreceptor layer (rod opsin)
			1 to 50	sections	mempfa/ parafin	works great!
R5	mouse monoclonal	IgM	1 to 1	sections	try memfa/ gelatin	Drager, 1984 supplied antibody. Used by Ohnuma et al 1999 (p27Xic paper). used extensively by Bill harris' group
rPax6	rabbit polyclonal	IgG	1 in 300	sections	mempfa/ gelatin	from BABCO; works if stored in etoh first!
			1 in 300	sections	mempfa/ parafin	vvv faint in parafin sections
			1 in 300	whole mount	fresh-fixed	works ok; should do HRP staining--not AP.
Tor 103	mouse monoclonal	IgG	1 to 1	sections	memfa/ gelatin	from R. Harland; works like tor 219
Tor 219	mouse monoclonal	IgG	1 to 1	sections	mempfa/ parafin	works at least at st 30
			1 to 1	sections	memfa/ gelatin	from R. Harland; stains sensory axons at least at st36
XAP-1	mouse monoclonal	IgG	neat	sections	mempfa/ gelatin	DSHB; labels photoreceptors (cones and rods)
			neat	sections	mempfa/ parafin	Sakaguchi

Antibody	species	type	working conc	specimen type	fix/embe dding	notes
XAP-2	mouse monoclonal	IgG	neat	sections	mempfa/gelatin	DSHB; rod photoreceptor outer segments; from Sakaguchi
XAR-1	mouse monoclonal	IgG1	1 in 20 to 1 in 100	sections		stains retinal pigmented epithel. From Don Sakaguchi

**Table 6: Secondary antibodies**

Secondary conjugate	species	against	working conc	special	Notes
Oregon Green	goat anti-mouse	IgG	1 in 1000	488nm	Molecular Probes
	goat anti-rabbit	IgG	1 in 1000		Molecular Probes
AP	goat anti-rabbit	IgG	1 in 1000		Zymed
	goat anti-mouse	IgG	1 in 1000		Zymed
HRP	goat anti-rabbit	IgG	1 in 400	whole mount	Zymed
	goat anti-mouse	IgG	1 in 400	whole mount	Zymed
Alexa green	goat anti-rabbit	IgG	1 in 1000		Molecular Probes; best for longevity & doesn't bleach better than Oregon green.
	goat anti-mouse	IgG	1 in 1000		
Hi-FITC	goat anti-mouse	IgG	1 in 300		

## Immunohistochemistry

### For sectioned samples

1. Block for 30 minutes in 5% goat serum in PBS + 1% BSA + 1% Triton-X-100 (PBT).
2. Incubate with 100  $\mu$ l primary antibody under a coverslip, in PBT for 3 hours at room temperature or overnight at 4°C.
3. Wash 3 X 5 minutes in a slide washer full of PBS.
4. Incubate with secondary antibody in 100  $\mu$ l under a coverslip for 1 hour at room temperature.
5. Wash as in step 3.

6. Coverslip with Fluormount G (Southern Biotechnology Associates, Inc).

### **For whole mounts**

1. Wash embryos for 15 minutes in PBT.
2. Block for 45 minutes in PBT + 5% goat serum.
3. Incubate with primary antibody in PBT + 5% goat serum overnight at 4°C.
4. Wash 5 X 2 hours in PBT.
5. Incubate with secondary antibody in PBT + 5% goat serum overnight at 4°C or for 4 hours at room temperature.
6. Wash as in 4.
7. Color development: for HRP secondaries:
  - a. Put embryos in 500 µl PBS.
  - b. Add 500 µl of filtered 1 mg/ml 3', 3'-diaminobenzidine (DAB) in PBS (can be kept frozen in aliquots at -80°C).
  - c. Add 1 µl 1:1 H<sub>2</sub>O<sub>2</sub> in H<sub>2</sub>O.
  - d. Develop color with rocking, usually about 20 minutes at room temperature for a slow reaction.
  - e. When color is developed, rinse twice in water, then PBS, then dehydrate to ethanol for indefinite storage at -20°C.

## Appendix 3.8:

Table 7: Expression constructs, *Noelin* subclones and *in situ* probes

Name	Insert	Vector, cloning sites	lin/pol	Notes
873	Xenopus Idx		EcoRI, T7	xIdx in situ probe, from T Mohun
1192	Xenopus Id2		XbaI, SP6	xId2 in situ probe, from T Mohun
1257	xenopus Idx $\Delta$ D mutation	pSP64T	XbaI, SP6	expression construct; from T Mohun
1475	xenopus Idx wild type	pSP64T	XbaI, SP6	expression construct; from T Mohun
10A	7A2 x EcoRI, XbaI	pCDG-1 x EcoRI, XbaI		expression of tagged np1
10B	7 E2 x EcoRI, XbaI	pCDG-1 x EcoRI, XbaI		expression of tagged np1
10C	7B4 x EcoRI, XbaI	pCDG-1 x EcoRI, XbaI		backwards control Bam FLAG
10D	7D5 x EcoRI, XbaI	pCDG-1 x EcoRI, XbaI		backwards control Nsi FLAG
10E	z18 x EcoRI, XbaI	pCDG-1 x EcoRI, XbaI		untagged version in exp vector
11A	XHC 6 x NotI, BamHI	PBS KS x NotI, BamHI		Zexon + 3' UTR in situ probe
12A	XHC 6 x EcoRI, BamHI	pBS KS x EcoRI, BamHI	EcoRI/T3	short Z exon in situ probe
13A	cNP1 x EcoRI-bl, XbaI	pCDG-1 x EcoRI-bl		expression clone of cnp1 w/o 5'UTR
14A	7A2 x EcoRI, XbaI	pCI-neo x EcoRI, XbaI		Bam FLAG exp clone w/neo resistance
14B	7 E2 x EcoRI, XbaI	pCI-neo x EcoRI, XbaI		Nsi FLAG exp clone w/neo resistance
14C	7B4 x EcoRI, XbaI	pCI-neo x EcoRI, XbaI		exp clone w/neo resistance; backwards Bam FLAG
14D	7D5 x EcoRI, XbaI	pCI-neo x EcoRI, XbaI		exp clone w/neo resistance; backwards Nsi FLAG
15A	10A x NcoI (800bp frag)	10A x NcoI 6.1kb frag		cuts off 5'UTR and signal sequence
15B	10B x NcoI (800bp frag)	10E x NcoI 6.1kb frag		cuts off 5'UTR and signal sequence
15C	7B4 x NcoI, XbaI (700 & 800bp frags)	pCDG-1 x NcoI, XbaI		cuts off 5'UTR and signal sequence
15D	7D5 x NcoI (800bp frag)	10E x NcoI 6.1kb frag		cuts off 5'UTR and signal sequence
15E	10A x NcoI (800bp frag)	10E x NcoI 6.1kb frag		cuts off 5'UTR and signal sequence
16A	z18 pcr:z18-1-4xb, xEcoRI, PfIMI	14A x EcoRI, PfIMI		pCI neo construct w/o 5' UTR
16B	z18 pcr:z18-1-4xb, xEcoRI, PfIMI	14B x EcoRI, PfIMI		pCI neo construct w/o 5' UTR
16C	z18 pcr:z18-1-4xb, xEcoRI, PfIMI	14C x EcoRI, PfIMI		pCI neo construct w/o 5' UTR
16D	z18 pcr:z18-1-4xb, xEcoRI, PfIMI	14D x EcoRI, PfIMI		pCI neo construct w/o 5' UTR
16E	z18 pcr:z18-1-4xb, xEcoRI, PfIMI	14E x EcoRI, PfIMI		pCI neo construct w/o 5' UTR
1A	z18 x NcoI	pGEX KG x NcoI		GST fusion protein
1B	z18 x PvuII, EcoRI	pGEX KG/EcoRI, NcoI-bl		GST fusion protein
1C	z18 x BclI-bl, EcoRI	pGEX KG/EcoRI, NcoI-bl		GST fusion protein
21A	7A2 x EcoRI, XbaI	pCS2p x EcoRI, XbaI	NotI, SP6	xenopus expression construct
21B	7 E2 x EcoRI, XbaI	pCS2p x EcoRI, XbaI	NotI, SP6	xenopus expression construct
21C	7B4 x EcoRI, XbaI	pCS2p x EcoRI, XbaI	NotI, SP6	xenopus expression construct
21D	7D5 x EcoRI, XbaI	pCS2p x EcoRI, XbaI	NotI, SP6	xenopus expression construct

Name	Insert	Vector, cloning sites	lin/pol	Notes
21E	14E x EcoRI, XbaI	pCS2p x EcoRI, XbaI	NotI, SP6	xenopus expression construct
22A	16A x EcoRI, XbaI	pTracer x EcoRI, XbaI		dual cassette vector; GFP in position #2
22B	16B x EcoRI, XbaI	pTracer x EcoRI, XbaI		dual cassette vector; GFP in position #2
22E	16E x EcoRI, XbaI	pTracer x EcoRI, XbaI		dual cassette vector; GFP in position #2
23A	16A x EcoRI, XbaI	pCS2p x EcoRI, XbaI	NotI, SP6	xenopus expression construct
23B	16B x EcoRI, XbaI	pCS2p x EcoRI, XbaI	NotI, SP6	xenopus expression construct
23E	16E x EcoRI, XbaI	pCS2p x EcoRI, XbaI	NotI, SP6	xenopus expression construct
24A	pCS2-ngal x BglII-bl, SmaI	22A1 x BbrPI, CIP		puts nuclear $\beta$ gal in place of GFP Zeo in pTracer
24B	pCS2-ngal x BglII-bl, SmaI	22B1 x BbrPI, CIP		puts nuclear $\beta$ gal in place of GFP Zeo in pTracer
24E	pCS2-ngal x BglII-bl, SmaI	22E2 x BbrPI, CIP		puts nuclear $\beta$ gal in place of GFP Zeo in pTracer
25A	pCS2-ngal x NotI-bl, SmaI	pCI-neo x BamHI-bl, StuI		puts n bgal in place of neo in pCI-neo
26A	XHC1 pcr:TM10-TM23 (3'UTR)	pGEM-T	SpeI, T7	Z exon 3' UTR in situ probe
27A3	XHC1 pcr:TM28-TM31 (coding only), x ClaI, EcoRV	pCS2mt x (ClaI, NcoI)-bl, CIP	NotI, SP6	puts one myc-tag at the end of XHC1, cuts off first 5 myc tags of pCS2mt.
28A3	XHC1 x HpaI, SstI	pBS KS x EcoRV, SstI	SstII, T3	xenopus B exon in situ probe
29A	XHC1 pcr:TM28-TM32, x ClaI, XhoI	pCS2p x ClaI, XhoI	NotI, SP6	xenopus BMZ cdr in exp vector
2A	z18 x PvuII, EcoRI	pBS ksII, EcoRI, EcoRV		for subclone to pGEX
30A	XHC1 pcr:TM28-TM33, x ClaI, XhoI	pCS2p x ClaI, XhoI	NotI, SP6	xenopus BMZ cdr in exp vector, w/o DEL
31A3	XHC1 pcr:TM29-TM30	pGEM-T	NcoI, SP6	xenopus M exon in situ probe
33B9	SDEL oligos annealed, XhoI ends	27A3 x XhoI, CIP	NotI, SP6	xenopus BMZ-myc-SDEL
33D2	KDEL oligos annealed, XhoI ends	27A3 x XhoI, CIP	NotI, SP6	xenopus BMZ-myc-KDEL
38A13	cNP1 pcr:TM28-cNP1-4, x (EcoRV, ClaI)-bl	pCS2mt x (NcoI, ClaI)-bl	NotI, SP6	chick np1-myc
40D3	SDEL oligos annealed, XhoI ends	38A13 x XhoI, CIP	NotI, SP6	chick np1-myc-SDEL
42A1	XHL19-1 pcr: T3-TM44	pGEM-T easy	SalI, T7	xenopus A exon probe
43A4	XHL19-1 pcr: TM49-TM32	pCS2p x ClaI, XhoI	NotI, SP6	xenopus AMZ expression construct
45A2	XHC5 pcr: TM49-TM50	pCS2p x ClaI, XhoI	NotI, SP6	xenopus AMY expression construct
46A1	XHC5 pcr: TM51-T7	pBS ks x BamHI, EcoRI	BamHI, T3	xenopus Y exon probe
47A	AMZ; pcr XHL19-1 TM 49/31	CS2+mt		
48A2	AMY; pcr XHC5 TM53/52	CS2+mt	NotI, SP6	CS2+AMY-mt expression construct
49A1	MY; pcr XHC5 TM54/52	CS2+mt	NotI, SP6	CS2+MY-mt expression const.
50A1	AMY; pcr XHC5 TM53/55	CS2p	NotI, SP6	CS2p+AMY expres.constr.
51A	MY; pcr XHC5 TM 54/55	CS2p		

Name	Insert	Vector, cloning sites	lin/pol	Notes
52A2	zebrafish np1 #2602426	pBS KS x XhoI		sequenced 3/01 IMAGE clone
53A2	zebrafish np1 #2599775	pBS KS x XhoI		sequenced 3/01 IMAGE clone
56A1	Xenopus Noelin-3	pCS2p x ClaI, XhoI	NotI, SP6	Noelin-3 expr construct --PCR from Noelin-1 B-M + gly-stop
72-x-Delta-1 H/R	Xenopus Delta-1 HindIII/EcoRV	pSP72 x HindIII/SmaI	XhoI, T7	Kintner in situ probe
7A	BamHI FLAG annealed oliqos	z18 KS x BamHI		for subcloning into exp vector
7B	BamHI FLAG annealed oliqos	z18 KS x BamHI		for subcloning into exp vector
7D	NsiI FLAG annealed oliqos	z18 KS x NsiI		for subcloning into exp vector
7E	NsiI FLAG annealed oliqos	z18 KS x NsiI		for subcloning into exp vector
9A2	mouse np1 Z exon byRT-PCR	pGEM-T	SpeI, T7	mouse Z exon probe, used to screen for frog
CS2+ +dn-Pax6-flag	dnPax6 (Singh et al 1998)	pCS2++	SacII, SP6	A. H. Brivanlou expression construct
CS2+ +xPax6-flag	xPax6 coding region	pCS2++	SacII, SP6	A. H. Brivanlou expression construct
CS2+Pax6-mt	XPax6 coding region	pCS2+	NotI, SP6	W. Harris expression construct
CS2-X-Delta-1	Xenopus Delta-1coding region	CS2	NotI, SP6	Kintner
ET-BSSK	xenopus ET	pBS SK	NotI, T7	Y. Rao (Laura)
myc-nog	xenopus noggin	pCS2mt	NotI, SP6	from K Wunnenberg (K Cho)
NCAM	xenopus NCAM	pSP70-N1	EcoRV, SP6	Kintner in situ probe
nrp-1	xenopus nrp-1 (pNPG152)	pBS KS	BamHI, T3	Harland, Good, in situ probe (Laura)
Ntub	xenopus neural specific class II $\beta$ -tubulin		BamHI, T3	from C Kintner; also Blumberg
p27XicI	xenopus p27XicI		NotI, SP6	expression construct by J Maller
p27XicI	xenopus p27XicI		BamHI, T7	for making in situ probe. From Papalopulu
Pax2a(1)	xenopus pax2	pBS SK	EcoRI, T3	Andre Brandli; in situ probe
pBS-xPax6	xPax6 cDNA	pBS SK	XbaI, T7	W. Harris in situ probe
pCS2mt-x12A	xenopus NeuroD full length	pCS2	NotI, SP6	expression construct from Jackie Lee
pND12b	xenopus NeuroD	T/A cloning vector	SpeI, T7	in situ probe from Jackie Lee
pSP6-En2	xenopus big En-2	pSP65 x EcoRI	XbaI, SP6	Hemmati-Brivanlou (Laura)
pXKrox20	xenopus Krox20	pGEM4	EcoRI, T7	Wilkinson, D (Laura)
pXotch	xenopus Notch	pSP72	ClaI, SP6	Kintner in situ probe
SybII	xenopus Synaptobrevin	pBS KS-, EcoRI	BamHI, T3	Harland (Richter & Good)
tBR-64T	dominant neg. BMP receptor	p64T	EcoRI, SP6	Melton

<b>Name</b>	<b>Insert</b>	<b>Vector, cloning sites</b>	<b>lin/pol</b>	<b>Notes</b>
x3.15	xenopus Xash-3	pBS	NotI, T3	in situ probe from Kathy Zimmerman
xBF-1	xenopus BF-1 (winged helix)	pCS2, EcoRI, XhoI	NotI, SP6	Papalopolu. Cdr only, 1.3kb
xbm-BMP7-flag	xenopus BMP7-flag	pxβm	XhoI, SP6	from K Wunnenberg; expression construct
xBrn3	xenopus brn3 probe	pCS107	SalI, T7	LaBonne
XHC 1	xenopus BMZ, full length	pBS sk, EcoRI, NotI	BamHI, T7	Harland library clone, Z exon probe when cut BamHI, T7 pol
XHC 5	xenopus AMY, full length	pBS sk, EcoRI, NotI		Harland library clone
XHC 6	xenopus MZ starts @ quail #574	pBS sk, EcoRI, NotI		Harland library clone
XHC 7	RING3/fsh related	pBS sk, EcoRI, NotI	EcoRI, T3	Harland library clone; insert is backwards
XHL19-1	xenopus AMZ, full length	pBS sk, EcoRI, NotI		Harland library clone
xLim-3	xenopus Lim-3 cDNA	pBS KS+	BamHI, T3	M Taira; in situ probe
x-ngnr-1	xenopus neurogenin	pCS2mt, EcoRI	NotI, SP6	from DJAnderson
Xotch ICD	xenopus Notch ICD (activated Notch)	pCS2+	NotI, SP6	Kintner expression construct
XOtx2	xenopus Otx2	pBS	XhoI, T3	Laura Gammill; in situ probe
xSlug	xenopus Slug		BglII, SP6	R. Mayor in situ probe 3' utr, small.
xSox10	xenopus Sox10 probe	pGEM-T		LaBonne
xSox2	xenopus Sox2 in situ probe	pBS KS+, EcoRI	XbaI, T7	from R Grainger
xSox3	xenopus Sox3 in situ probe	pBS KS+, EcoRI	SmaI, T7	from R Grainger
xTwist	xenopus Twist probe	?	KpnI, T7	Vize
z18KS	quail np1 (BMZ)	pBS ks, EcoRI, XbaI	EcoRI, T3	from M Barembaum

## **Appendix Chapter 4**

### **Cited Literature**

## REFERENCES

- Agius, E., Oelgeschlager, M., Wessely, O., Kemp, C. and De Robertis, E. M.** (2000). Endodermal Nodal-related signals and mesoderm induction in *Xenopus*. *Development* **127**, 1173-83.
- Altmann, C. R., Chow, R. L., Lang, R. A. and Hemmati-Brivanlou, A.** (1997). Lens induction by Pax-6 in *Xenopus laevis*. *Dev Biol* **185**, 119-23.
- Altschul, S. F., Gish, W., Miller, W., Myers, E. W. and Lipman, D. J.** (1990). Basic local alignment search tool. *J Mol Biol* **215**, 403-10.
- Anderson, D. J.** (1993). Molecular control of cell fate in the neural crest: the sympathoadrenal lineage. *Annu. Rev. Neurosci.* **16**, 129-158.
- Anderson, D. J.** (1995). Neural development. Spinning skin into neurons. *Curr Biol* **5**, 1235-8.
- Anderson, D. J.** (1999). Lineages and transcription factors in the specification of vertebrate primary sensory neurons. *Curr. Op. Neurobiol.* **9**, 517-524.
- Artinger, K. B. and Bronner-Fraser, M.** (1992). Partial restriction in the developmental potential of late emigrating avian neural crest cells. *Dev. Biol.* **149**, 149-157.
- Artinger, K. B., Chitnis, A. B., Mercola, M. and Driever, W.** (1999). Zebrafish *narrowminded* suggests a genetic link between formation of neural crest and primary sensory neurons. *Development* **126**, 3969-3979.
- Baker, C. V. and Bronner-Fraser, M.** (1997). The origins of the neural crest. Part I: embryonic induction. *Mech Dev* **69**, 3-11.
- Baker, C. V. and Bronner-Fraser, M.** (2001). Vertebrate cranial placodes I. Embryonic Induction. *Dev Biol* **232**, 1-61.
- Baker, C. V., Bronner-Fraser, M., Le Douarin, N. M. and Teillet, M. A.** (1997). Early- and late-migrating cranial neural crest cell populations have equivalent developmental potential in vivo. *Development* **124**, 3077-87.
- Baker, J. C., Beddington, R. S. P. and Harland, R. M.** (1999). Wnt signaling in *Xenopus* embryos inhibits BMP4 expression and activates neural development. *Genes Dev.* **13**, 3149-3159.

- Bal, R. S. and Anholt, R. R.** (1993). Formation of the extracellular mucous matrix of olfactory neuroepithelium: identification of partially glycosylated and nonglycosylated precursors of olfactomedin. *Biochemistry* **32**, 1047-53.
- Bang, A. G., Papalopulu, N., Kintner, C. and Goulding, M. D.** (1997). Expression of Pax-3 is initiated in the early neural plate by posteriorizing signals produced by the organizer and by posterior non-axial mesoderm. *Development* **124**, 2075-2085.
- Bannister, A. J. and Miska, E. A.** (2000). Regulation of gene expression by transcription factor acetylation. *Cell Mol Life Sci* **57**, 1184-92.
- Barembaum, M., Moreno, T. A., LaBonne, C., Sechrist, J. and Bronner-Fraser, M.** (2000). Noelin-1 is a secreted glycoprotein involved in generation of the neural crest. *Nat Cell Biol* **2**, 219-225.
- Bartelmez, G. W.** (1922). The origin of the otic and optic primordia. *J. Comp. Neurol.* **34**, 201-232.
- Basler, K., Edlund, T., Jessell, T. and Yamada, T.** (1993). Control of cell pattern in the neural tube: regulation of cell differentiation by *dorsalin-1*, a novel TGF $\beta$  family member. *Cell* **73**, 687-702.
- Beck, S., Hanson, I., Kelly, A., Pappin, D. J. and Trowsdale, J.** (1992). A homologue of the *Drosophila* female sterile homeotic (*fsh*) gene in the class II region of the human MHC. *DNA Seq* **2**, 203-10.
- Bitgood, M. J. and McMahon, A. P.** (1995). *Hedgehog* and *Bmp* genes are coexpressed at many diverse sites of cell-cell interaction in the mouse embryo. *Dev. Biol.* **172**, 126-138.
- Blitz, I. L. and Cho, K. W.** (1995). Anterior neurectoderm is progressively induced during gastrulation: the role of the *Xenopus* homeobox gene *orthodenticle*. *Development* **121**, 993-1004.
- Bonstein, L., Elias, S. and Frank, D.** (1998). Paraxial-fated mesoderm is required for neural crest induction in *Xenopus* embryos. *Dev Biol* **193**, 156-168.
- Bourguignon, C., Li, J. and Papalopulu, N.** (1998). XBF-1, a winged helix transcription factor with dual activity, has a role in positioning neurogenesis in *Xenopus* competent ectoderm. *Development* **125**, 4889-900.

- Bradley, L. C., Snape, A., Bhatt, S. and Wilkinson, D. G.** (1993). The structure and expression of the *Xenopus* Krox-20 gene: conserved and divergent patterns of expression in rhombomeres and neural crest. *Mech Dev* **40**, 73-84.
- Bronner-Fraser, M.** (1986). Analysis of the early stages of trunk neural crest migration in avian embryos using monoclonal antibody HNK-1. *Dev. Biol.* **115**, 44-55.
- Bronner-Fraser, M.** (1993). Mechanisms of neural crest cell migration. *BioEssays* **15**, 221-230.
- Bronner-Fraser, M. and Fraser, S.** (1989). Developmental potential of avian trunk neural crest cells *in situ*. *Neuron* **3**, 755-766.
- Bronner-Fraser, M. and Fraser, S. E.** (1988). Cell lineage analysis reveals multipotency of some avian neural crest cells. *Nature* **335**, 161-164.
- Bueno, D., Skinner, J., Abud, H. and Heath, J. K.** (1996). Spatial and temporal relationships between Shh, Fgf4, and Fgf8 gene expression at diverse signalling centers during mouse development. *Dev Dyn* **207**, 291-299.
- Carr, V. M. and Simpson Jr., S. B.** (1978). Proliferative and degenerative events in the early development of chick dorsal root ganglia. *J. Comp. Neuro.* **182**, 727-740.
- Chang, C. and Hemmati-Brivanlou, A.** (1998a). Cell fate determination in embryonic ectoderm. *J. Neurobiol.* **36**, 128-151.
- Chang, C. and Hemmati-Brivanlou, A.** (1998b). Neural crest induction by Xwnt7B in *Xenopus*. *Dev. Biol.* **194**, 129-134.
- Chitnis, A., Henrique, D., Lewis, J., Ish-Horowicz, D. and Kintner, C.** (1995). Primary neurogenesis in *Xenopus* embryos regulated by a homologue of the *Drosophila* neurogenic gene *Delta*. *Nature* **375**, 761-766.
- Chitnis, A. B.** (1999). Control of neurogenesis--lessons from frogs, fish and flies. *Curr Opin Neurobiol* **9**, 18-25.
- Chow, R. L., Altmann, C. R., Lang, R. A. and Hemmati-Brivanlou, A.** (1999). Pax6 induces ectopic eyes in a vertebrate. *Development* **126**, 4213-22.
- Christian, J. L., McMahon, J. A., McMahon, A. P. and Moon, R. T.** (1991). Xwnt-8, a *Xenopus* Wnt-1/int-1-related gene responsive to mesoderm-inducing growth factors, may play a role in ventral mesodermal patterning during embryogenesis. *Development* **111**, 1045-1055.

- Cimino, G., Moir, D. T., Canaani, O., Williams, K., Crist, W. M., Katzav, S., Cannizzaro, L., Lange, B., Nowell, P. C., Croce, C. M. et al.** (1991). Cloning of ALL-1, the locus involved in leukemias with the t(4;11)(q21;q23), t(9;11)(p22;q23), and t(11;19)(q23;p13) chromosome translocations. *Cancer Res* **51**, 6712-4.
- Collazo, A., Bronner-Fraser, M. and Fraser, S. E.** (1993). Vital dye labeling of *Xenopus-laevis* trunk neural crest reveals multipotency and novel pathways of migration. *Development* **118**, 363-376.
- Connolly, D. J., Patel, K. and Cooke, J.** (1997). Chick noggin is expressed in the organizer and neural plate during axial development, but offers no evidence of involvement in primary axis formation. *Int J Dev Biol* **41**, 389-396.
- Couly, G., Grapin-Botton, A., Coltey, P. and Le Douarin, N. M.** (1996). The regeneration of the cephalic neural crest, a problem revisited: the regenerating cells originate from the contralateral or from the anterior and posterior neural fold. *Development* **122**, 3393-407.
- Cox, W. G. and Hemmati-Brivanlou, A.** (1995). Caudalization of neural fate by tissue recombination and bFGF. *Development* **121**, 4349-4358.
- Dale, L., Howes, G., Price, B. M. J. and Smith, J. C.** (1992). Bone Morphogenetic Protein 4: a ventralizing factor in *Xenopus* development. *Development* **115**, 573-585.
- Dale, L. and Slack, J. M.** (1987). Fate map for the 32-cell stage of *Xenopus laevis*. *Development* **99**, 527-51.
- Danielson, P. E., Forss-Petter, S., Battenberg, E. L., deLecea, L., Bloom, F. E. and Sutcliffe, J. G.** (1994). Four structurally distinct neuron-specific olfactomedin-related glycoproteins produced by differential promoter utilization and alternative mRNA splicing from a single gene. *J Neurosci Res* **38**, 468-78.
- Davletov, B. A., Shamotienko, O. G., Lelianova, V. G., Grishin, E. V. and Ushkaryov, Y. A.** (1996). Isolation and biochemical characterization of a Ca<sup>2+</sup>-independent alpha-latrotoxin-binding protein. *J Biol Chem* **271**, 23239-45.
- De Robertis, E. M., Larrain, J., Oelgeschlager, M. and Wessely, O.** (2000). The establishment of Spemann's organizer and patterning of the vertebrate embryo. *Nat Rev Genet* **1**, 171-81.

- Deblandre, G. A., Wettstein, D. A., Koyano-Nakagawa, N. and Kintner, C.** (1999). A two-step mechanism generates the spacing pattern of the ciliated cells in the skin of *Xenopus* embryos. *Development* **126**, 4715-28.
- Delot, E., Kataoka, H., Goutel, C., Yan, Y.-L., Postlethwait, J., Wittbrodt, J. and Rosa, F. M.** (1999). The BMP-related protein Radar: a maintenance factor for dorsal neuroectoderm cells? *Mech. Dev.* **85**.
- Denis, G. V. and Green, M. R.** (1996). A novel, mitogen-activated nuclear kinase is related to a *Drosophila* developmental regulator. *Genes Dev* **10**, 261-71.
- Denis, G. V., Vaziri, C., Guo, N. and Faller, D. V.** (2000). RING3 kinase transactivates promoters of cell cycle regulatory genes through E2F. *Cell Growth Differ* **11**, 417-24.
- Dickinson, M. E., Selleck, M. A., McMahon, A. P. and Bronner-Fraser, M.** (1995). Dorsalization of the neural tube by the non-neural ectoderm. *Development* **121**, 2099-106.
- Digan, M. E., Haynes, S. R., Mozer, B. A., Dawid, I. B., Forquignon, F. and Gans, M.** (1986). Genetic and molecular analysis of *fs(1)h*, a maternal effect homeotic gene in *Drosophila*. *Dev Biol* **114**, 161-9.
- Djabali, M., Selleri, L., Parry, P., Bower, M., Young, B. D. and Evans, G. A.** (1992). A trithorax-like gene is interrupted by chromosome 11q23 translocations in acute leukaemias. *Nat Genet* **2**, 113-8.
- Dorsky, R. I., Moon, R. T. and Raible, D. W.** (1998). Control of neural crest cell fate by the Wnt signalling pathway. *Nature* **396**, 370-373.
- Doupe, A. J., Landis, S. C. and Patterson, P. H.** (1985a). Environmental influences in the development of neural crest derivatives: Glucocorticoids, growth factors and chromaffin cell plasticity. *J. Neurosci.* **5**, 2119-2142.
- Doupe, A. J., Patterson, P. H. and Landis, S. C.** (1985b). Small intensely fluorescent (SIF) cells in culture: Role of glucocorticoids and growth factors in their development and phenotypic interconversions with other neural crest derivatives. *J. Neurosci.* **5**, 2143-2160.
- Dudley, A. T., Lyons, K. M. and Robertson, E. J.** (1995). A requirement for bone morphogenetic protein-7 during development of the mammalian kidney and eye. *Genes Dev.* **9**, 2795-2807.

- Dyson, M. H., Rose, S. and Mahadevan, L. C.** (2001). Acetyllysine-binding and function of bromodomain-containing proteins in chromatin. *Front Biosci* **6**, D853-65.
- Eickholt, B. J., Graham, A., Lumsden, A. and Wizenmann, A.** (2001). Rhombomere interactions control the segmental differentiation of hindbrain neurons. *Mol Cell Neurosci* **18**, 141-8.
- Ekker, S. C. and Larson, J. D.** (2001). Morphant technology in model developmental systems. *Genesis* **30**, 89-93.
- Erickson, C. A. and Perris, R.** (1993). The role of cell-cell and cell-matrix interactions in the morphogenesis of the neural crest. *Dev. Biol.* **159**, 60-74.
- Fainsod, A., Deissler, K., Yelin, R., Marom, K., Epstein, M., Pillemer, G., Steinbeisser, H. and Blum, M.** (1997). The dorsalizing and neural inducing gene follistatin is an antagonist of BMP4. *Mech. Dev.* **63**, 39-50.
- Fainsod, A., Steinbeisser, H. and De Robertis, E. M.** (1994). On the function of *BMP-4* in patterning the marginal zone of the *Xenopus* embryo. *EMBO J.* **13**, 5015-5025.
- Ferreiro, B., Kintner, C., Zimmerman, K., Anderson, D. and Harris, W. A.** (1994). XASH genes promote neurogenesis in *Xenopus* embryos. *Development* **120**, 3649-55.
- Fode, C., Gradwohl, G., Morin, X., Dierich, A., LeMeur, M., Goridis, C. and Guillemot, F.** (1998). The bHLH protein NEUROGENIN 2 is a determination factor for epibranchial placode-derived sensory neurons. *Neuron* **20**, 483-94.
- Ford, A. M., Ridge, S. A., Cabrera, M. E., Mahmoud, H., Steel, C. M., Chan, L. C. and Greaves, M.** (1993). In utero rearrangements in the trithorax-related oncogene in infant leukaemias. *Nature* **363**, 358-60.
- Frank, E. and Sanes, J. R.** (1991). Lineage of neurons and glia in chick dorsal root ganglia: Analysis in vivo with a recombinant retrovirus. *Development* **111**, 895-908.
- Furuta, Y., Piston, D. W. and Hogan, B. L.** (1997). Bone morphogenetic proteins (BMPs) as regulators of dorsal forebrain development. *Development* **124**, 2203-12.
- Gallera, J. and Nicolet, G.** (1969). [The inductive capacity of the presumptive endoblast located in the young primitive streak of the chick embryo]. *J Embryol Exp Morphol* **21**, 105-18.

- Gammill, L. S. and Sive, H.** (2001). *otx2* Expression in the Ectoderm Activates Anterior Neural Determination and Is Required for *Xenopus* Cement Gland Formation. *Dev Biol* doi:10.1006/dbio.2001.0470, 1-14.
- Gans, M., Audit, C. and Masson, M.** (1975). Isolation and characterization of sex-linked female-sterile mutants in *Drosophila melanogaster*. *Genetics* **81**, 683-704.
- George-Weinstein, M., Gerhart, J., Reed, R., Flynn, J., Callihan, B., Mattiacci, M., Miehle, C., Foti, G., Lash, J. W. and Weintraub, H.** (1996). Skeletal myogenesis: the preferred pathway of chick embryo epiblast cells in vitro. *Dev Biol* **173**, 279-91.
- Godsave, S. F. and Slack, J. M.** (1989). Clonal analysis of mesoderm induction in *Xenopus laevis*. *Dev Biol* **134**, 486-90.
- Golden, J. A., Bracilovic, A., McFadden, K. A., Beesley, J. S., JL, R. R. and Grinspan, J. B.** (1999). Ectopic bone morphogenetic proteins 5 and 4 in the chicken forebrain lead to cyclopia and holoprosencephaly. *Proc Natl Acad Sci U S A* **96**, 2439-44.
- Groves, A. K. and Bronner-Fraser, M.** (1999). Neural crest diversification. *Curr Top Dev Biol* **43**, 221-58.
- Grunz, H. and Tacke, L.** (1989). Neural differentiation of *Xenopus laevis* ectoderm takes place after disaggregation and delayed reaggregation without inducer. *Cell Differ. Dev.* **28**, 211-218.
- Gu, Y., Nakamura, T., Alder, H., Prasad, R., Canaani, O., Cimino, G., Croce, C. M. and Canaani, E.** (1992). The t(4;11) chromosome translocation of human acute leukemias fuses the ALL-1 gene, related to *Drosophila trithorax*, to the AF-4 gene. *Cell* **71**, 701-8.
- Gurdon, J. B., Harger, P., Mitchell, A. and Lemaire, P.** (1994). Activin signalling and response to a morphogen gradient. *Nature* **371**, 487-92.
- Hagedorn, L., Suter, U. and Sommer, L.** (1999). P0 and PMP22 mark a multipotent neural crest-derived cell type that displays community effects in response to TGF $\beta$  family factors. *Development* **126**, 3781-3794.
- Hall, B. K. and Hörstadius, S.** (1988). *The Neural Crest*. Oxford: Oxford University Press.

- Hammerschmidt, M., Serbedzija, G. N. and McMahon, A. P.** (1996). Genetic analysis of dorsoventral pattern formation in the zebrafish: requirement of a BMP-like ventralizing activity and its dorsal repressor. *Genes Dev* **10**, 2452-2461.
- Hansen, C. S., Marion, C. D., Steele, K., George, S. and Smith, W. C.** (1997). Direct neural induction and selective inhibition of mesoderm and epidermis inducers by Xnr3. *Development* **124**, 483-492.
- Hardcastle, Z. and Papalopulu, N.** (2000). Distinct effects of XBF-1 in regulating the cell cycle inhibitor p27(XIC1) and imparting a neural fate. *Development* **127**, 1303-14.
- Harland, R.** (2000). Neural induction. *Curr Opin Genet Dev* **10**, 357-62.
- Harrison, R. G.** (1938). Die Neuralleiste Ergänzheft. *Anat. Anz.* **85**, 3-30.
- Hartenstein, V.** (1993). Early pattern of neuronal differentiation in the *Xenopus* embryonic brainstem and spinal cord. *J Comp Neurol* **328**, 213-31.
- Hartley, K., Hardcastle, Z., Friday, R., Amaya, E. and Papalopulu, N.** (2001). Transgenic *Xenopus* Embryos Reveal That Anterior Neural Development Requires Continued Suppression of BMP Signaling after Gastrulation. *Dev Biol* **238**, 168-184.
- Hata, A., Lagna, G., Massague, J. and Hemmati-Brivanlou, A.** (1998). Smad6 inhibits BMP/Smad1 signaling by specifically competing with the Smad4 tumor suppressor. *Genes Dev* **12**, 186-97.
- Hawley, S. H., Wunnenberg-Stapleton, K., Hashimoto, C., Laurent, M. N., Watabe, T., Blumberg, B. W. and Cho, K. W.** (1995). Disruption of BMP signals in embryonic *Xenopus* ectoderm leads to direct neural induction. *Genes Dev* **9**, 2923-35.
- Haynes, S. R., Mozer, B. A., Bhatia-Dey, N. and Dawid, I. B.** (1989). The *Drosophila* fsh locus, a maternal effect homeotic gene, encodes apparent membrane proteins. *Dev Biol* **134**, 246-57.
- Heasman, J.** (1997). Patterning the *Xenopus* blastula. *Development* **124**, 4179-91.
- Heasman, J., Kofron, M. and Wylie, C.** (2000). Beta-catenin signaling activity dissected in the early *Xenopus* embryo: a novel antisense approach. *Dev Biol* **222**, 124-34.
- Heller, N. and Brandli, A. W.** (1997). *Xenopus* Pax-2 displays multiple splice forms during embryogenesis and pronephric kidney development. *Mech Dev* **69**, 83-104.

- Hemmati-Brivanlou, A., de la Torre, J. R., Holt, C. and Harland, R. M.** (1991). Cephalic expression and molecular characterization of *Xenopus* En-2. *Development* **111**, 715-24.
- Hemmati-Brivanlou, A., Kelly, O. G. and Melton, D. A.** (1994). Follistatin, an antagonist of activin is expressed in the Spemann organizer and displays direct neuralizing activity. *Cell* **77**, 283-295.
- Hemmati-Brivanlou, A. and Melton, D. A.** (1994). Inhibition of activin receptor signaling promotes neuralization in *Xenopus*. *Cell* **77**, 273-81.
- Hemmati-Brivanlou, A. and Thomsen, G. H.** (1995). Ventral mesodermal patterning in *Xenopus* embryos: expression patterns and activities of BMP-2 and BMP-4. *Dev Genet* **17**, 78-89.
- Henrique, D., Adam, J., Myat, A., Chitnis, A., Lewis, J. and Ish-Horowicz, D.** (1995). Expression of a Delta homologue in prospective neurons in the chick. *Nature* **375**, 787-90.
- Hirsch, N. and Harris, W. A.** (1997). *Xenopus* Pax-6 and retinal development. *J Neurobiol* **32**, 45-61.
- His, W.** (1868). Untersuchungen über die erste Anlage des Wirbeltierleibes. Die erste Entwicklung des Hühnchens im Ei. Leipzig: F. C. W. Vogel.
- Hogan, B. L. M.** (1996). Bone morphogenetic proteins: multifunctional regulators of vertebrate development. *Genes Dev.* **10**, 1580-1594.
- Hollyday, M., McMahon, J. A. and McMahon, A. P.** (1995). *Wnt* expression patterns in the chick embryo nervous system. *Mech. Dev.* **52**, 9-25.
- Holmdahl, D. E.** (1928). Die Entstehung und weitere Entwicklung der Neuralleiste (Ganglienleiste) bei Vögeln und Säugetieren. *Z. Mikrosk.-anat. Forsch.* **14**, 99-298.
- Hoodless, P. A. and Hemmati-Brivanlou, A.** (1997). Inhibitory control of neural differentiation in mammalian cells. *Dev Genes Evol* **107**, 19-28.
- Hopwood, N. D., Pluck, A. and Gurdon, J. B.** (1989). A *Xenopus* mRNA related to *Drosophila* twist is expressed in response to induction in the mesoderm and the neural crest. *Cell* **59**, 893-903.
- Hörstadius, S.** (1950). The Neural Crest. Oxford: Oxford University Press.

- Hsu, D. R., Economides, A. N., Wang, X., Eimon, P. M. and Harland, R. M.** (1998). The *Xenopus* dorsalizing factor Gremlin identifies a novel family of secreted proteins that antagonize BMP activities. *Mol Cell* **1**, 673-83.
- Huang, D. H. and Dawid, I. B.** (1990). The maternal-effect gene *fsh* is essential for the specification of the central region of the *Drosophila* embryo. *New Biol* **2**, 163-70.
- Hume, C. R. and Dodd, J.** (1993). *Cwnt-8C*: a novel Wnt gene with a potential role in primitive streak formation and hindbrain organization. *Development* **119**, 1147-1160.
- Hunt, P., Ferretti, P., Krumlauf, R. and Thorogood, P.** (1995). Restoration of normal Hox code and branchial arch morphogenesis after extensive deletion of hindbrain neural crest. *Dev. Biol.* **168**, 584-597.
- Hutcheson, D. A. and Vetter, M. L.** (2001). The bHLH Factors *Xath5* and *XNeuroD* Can Upregulate the Expression of *XBrn3d*, a POU-Homeodomain Transcription Factor. *Dev Biol* **232**, 327-338.
- Ikeya, M., Lee, S. M., Johnson, J. E., McMahon, A. P. and Takada, S.** (1997). Wnt signalling required for expansion of neural crest and CNS progenitors. *Nature* **389**, 966-70.
- Isaacs, H. V., Tannahill, D. and Slack, J. M. W.** (1992). Expression of a novel FGF in the *Xenopus* embryo. A new candidate inducing factor for mesoderm formation and anteroposterior specification. *Development* **114**, 711-720.
- Ito, K. and Sieber-Blum, M.** (1993). Pluripotent and developmentally restricted neural crest-derived cells in posterior visceral arches. *Dev. Biol.* **156**, 191-200.
- Kengaku, M. and Okamoto, H.** (1993). Basic fibroblast growth factor induces differentiation of neural tube and neural crest lineages of cultured ectoderm cells from *Xenopus* gastrula. *Development* **119**, 1067-1078.
- Kintner, C. R. and Melton, D. A.** (1987). Expression of *Xenopus* N-CAM RNA in ectoderm is an early response to neural induction. *Development* **99**, 311-25.
- Kishimoto, Y., Lee, K. H., Zon, L., Hammerschmidt, M. and Schulte-Merker, S.** (1997). The molecular nature of zebrafish *swirl*: BMP2 function is essential during early dorsoventral patterning. *Development* **124**, 4457-66.

- Knecht, A. K., Good, P. J., Dawid, I. B. and Harland, R. M.** (1995). Dorsal-ventral patterning and differentiation of noggin-induced neural tissue in the absence of mesoderm. *Development* **121**, 1927-35.
- Kondo, D., Yamamoto, T., Yaoita, E., Danielson, P. E., Kobayashi, H., Ohshiro, K., Funaki, H., Koyama, Y., Fujinaka, H., Kawasaki, K. et al.** (2000). Localization of Olfactomedin-Related Glycoprotein Isoform (BMZ) in the Golgi Apparatus of Glomerular Podocytes in Rat Kidneys. *J Am Soc Nephrol* **11**, 803-813.
- Korade, Z. and Frank, E.** (1996). Restriction in cell fates of developing spinal cord cells transplanted to neural crest pathways. *J. Neurosci.* **16**, 7638-7648.
- Kouzarides, T.** (2000). Acetylation: a regulatory modification to rival phosphorylation? *Embo J* **19**, 1176-9.
- Krasnoperov, V. G., Bittner, M. A., Beavis, R., Kuang, Y., Salnikow, K. V., Chepurny, O. G., Little, A. R., Plotnikov, A. N., Wu, D., Holz, R. W. et al.** (1997). alpha-Latrotoxin stimulates exocytosis by the interaction with a neuronal G-protein-coupled receptor. *Neuron* **18**, 925-37.
- Kroll, K. L. and Amaya, E.** (1996). Transgenic *Xenopus* embryos from sperm nuclear transplantations reveal FGF signaling requirements during gastrulation. *Development* **122**, 3173-3183.
- Kroll, K. L., Salic, A. N., Evans, L. M. and Kirschner, M. W.** (1998). Geminin, a neuralizing molecule that demarcates the future neural plate at the onset of gastrulation. *Development* **125**, 3247-58.
- Kubota, R., Noda, S., Wang, Y., Minoshima, S., Asakawa, S., Kudoh, J., Mashima, Y., Oguchi, Y. and Shimizu, N.** (1997). A novel myosin-like protein (myocilin) expressed in the connecting cilium of the photoreceptor: molecular cloning, tissue expression, and chromosomal mapping. *Genomics* **41**, 360-9.
- Kulkarni, N. H., Karavanich, C. A., Atchley, W. R. and Anholt, R. R.** (2000). Characterization and differential expression of a human gene family of olfactomedin-related proteins. *Genet Res* **76**, 41-50.

- LaBonne, C. and Bronner-Fraser, M.** (1998a). Induction and patterning of the neural crest, a stem cell-like precursor population. *J. Neurobiol.* **36**, 175-189.
- LaBonne, C. and Bronner-Fraser, M.** (1998b). Neural crest induction in *Xenopus*: evidence for a two-signal model. *Development* **125**, 2403-2414.
- LaBonne, C. and Bronner-Fraser, M.** (1999). Molecular mechanisms of neural crest formation. *Annu. Rev. Cell Dev. Biol.* **15**, 81-112.
- Laemmli, U. K.** (1970). Cleavage of structural proteins during the assembly of the head of bacteriophage T4. *Nature* **227**, 680-5.
- Lallier, T. E. and DeSimone, D. W.** (2000). Separation of neural induction and neurulation in *Xenopus*. *Dev Biol* **225**, 135-50.
- Lamar, E., Kintner, C. and Goulding, M.** (2001). Identification of NKL, a novel Gli-Kruppel zinc-finger protein that promotes neuronal differentiation. *Development* **128**, 1335-46.
- Lamb, T. M. and Harland, R. M.** (1995). Fibroblast growth factor is a direct neural inducer, which combined with noggin generates anterior-posterior neural pattern. *Development* **121**, 3627-3636.
- Lamb, T. M., Knecht, A. K., Smith, W. C., Stachel, S. E., Economides, A. N., Stahl, N., Yancopoulos, G. D. and Harland, R. M.** (1993). Neural induction by the secreted peptide noggin. *Science* **262**, 713-718.
- Landacre, F. L.** (1921). The fate of the neural crest in the head of the Urodeles. *J. Comp. Neurol.* **33**, 1-43.
- Launay, C., Fromentoux, V., Shi, D. L. and Boucaut, J. C.** (1996). A truncated FGF receptor blocks neural induction by endogenous *Xenopus* inducers. *Development* **122**, 869-80.
- Le Douarin, N.** (1982). *The Neural Crest*. Cambridge: Cambridge University Press.
- Le Douarin, N. M.** (1986). Cell lineage segregation during peripheral nervous system ontogeny. *Science* **231**, 1515-1522.
- Le Douarin, N. M., Fontaine-Perus, J. and Couly, G.** (1986). Cephalic ectodermal placodes and neurogenesis. *Trends Neurosci.* **9**, 175-180.

- Lee, J. E., Hollenberg, S. M., Snider, L., Turner, D. L., Lipnick, N. and Weintraub, H.** (1995). Conversion of *Xenopus* ectoderm into neurons by NeuroD, a basic helix-loop-helix protein. *Science* **268**, 836-844.
- Lee, K. J. and Jessell, T. M.** (1999). The specification of dorsal cell fates in the vertebrate central nervous system. *Annu. Rev. Neurosci.* **22**, 261-294.
- Lemke, G.** (1996). Neuregulins in development. *Mol. Cell. Neurosci.* **7**, 247-262.
- Liem, K. F., Jr., Tremml, G., Roelink, H. and Jessell, T. M.** (1995). Dorsal differentiation of neural plate cells induced by BMP-mediated signals from epidermal ectoderm. *Cell* **82**, 969-79.
- Liem, K. F., Tremml, G. and Jessell, T. M.** (1997). A role for the roof plate and its resident TGFbeta-related proteins in neuronal patterning in the dorsal spinal cord. *Cell* **91**, 127-138.
- Lyons, K. M., Hogan, B. L. M. and Robertson, E. J.** (1995). Colocalization of BMP2 and BMP7 RNAs suggests that these factors cooperatively mediate tissue interaction during murine development. *Mech. Dev.* **50**, 71-83.
- Ma, Q., Chen, Z., del Barco Barrantes, I., de la Pompa, J. L. and Anderson, D. J.** (1998). neurogenin1 is essential for the determination of neuronal precursors for proximal cranial sensory ganglia. *Neuron* **20**, 469-82.
- Ma, Q., Kintner, C. and Anderson, D. J.** (1996). Identification of neurogenin, a vertebrate neuronal determination gene. *Cell* **87**, 43-52.
- Mahmood, R., Kiefer, P., Guthrie, S., Dickson, C. and Mason, I.** (1995). Multiple roles for FGF-3 during cranial neural development in the chicken. *Development* **121**, 1399-1410.
- Mancilla, A. and Mayor, R.** (1996). Neural crest formation in *Xenopus laevis*: mechanisms of *Xslug* induction. *Dev. Biol.* **177**, 580-589.
- Marchant, L., Linker, C., Ruiz, P., Guerrero, N. and Mayor, R.** (1998). The inductive properties of mesoderm suggest that the neural crest cells are specified by a BMP gradient. *Dev Biol* **198**, 319-329.
- Marchionni, M. A., Goodearl, A. D., Chen, M. S., Bermingham-McDonogh, O., Kirk, C., Hendricks, M., Danehy, F., Misumi, D., Sudhalter, J., Kobayashi, K. et al.** (1993). Glial

- growth factors are alternatively spliced erbB2 ligands expressed in the nervous system. *Nature* **362**, 312-318.
- Mariani, F. V. and Harland, R. M.** (1998). XBF-2 is a transcriptional repressor that converts ectoderm into neural tissue. *Development* **125**, 5019-31.
- Martinsen, B. J. and Bronner-Fraser, M.** (1998). Neural crest specification regulated by the helix-loop-helix repressor Id2. *Science* **281**, 988-91.
- Massagué, J., Hata, A. and Liu, F.** (1997). TGF- $\beta$  signalling through the Smad pathway. *Trends Cell Biol.* **7**, 187-192.
- Matzuk, M. M., Lu, N., Vogel, H., Sellheyer, K., Roop, D. R. and Bradley, A.** (1995). Multiple defects and perinatal death in mice deficient in follistatin. *Nature* **374**, 360-363.
- Mayor, R., Guerrero, N. and Martínez, C.** (1997). Role of FGF and noggin in neural crest induction. *Dev. Biol.* **189**, 1-12.
- Mayor, R., Morgan, R. and Sargent, M. G.** (1995). Induction of the prospective neural crest of *Xenopus*. *Development* **121**, 767-777.
- McGrew, L. L., Hoppler, S. and Moon, R. T.** (1997). Wnt and FGF pathways cooperatively pattern anteroposterior neural ectoderm in *Xenopus*. *Mech Dev* **69**, 105-114.
- McMahon, J. A., Takada, S., Zimmerman, L. B., Fan, C. M., Harland, R. M. and McMahon, A. P.** (1998). Noggin-mediated antagonism of BMP signaling is required for growth and patterning of the neural tube and somite. *Genes Dev* **12**, 1438-1452.
- Messenger, N. J., Rowe, S. J. and Warner, A. E.** (1999). The neurotransmitter noradrenaline drives noggin-expressing ectoderm cells to activate N-tubulin and become neurons. *Dev Biol* **205**, 224-32.
- Meyer, D. and Birchmeier, C.** (1995). Multiple essential functions of neuregulin in development. *Nature* **378**, 386-390.
- Meyer, D., Yamaai, T., Garratt, A., Riethmacher-Sonnenberg, E., Kane, D., Theill, L. E. and Birchmeier, C.** (1997). Isoform-specific expression and function of neuregulin. *Development* **124**, 3575-3586.

- Mishina, Y., Suzuki, A., Ueno, N. and Behringer, R. R.** (1995). Bmpr encodes a type I bone morphogenetic protein receptor that is essential for gastrulation during mouse embryogenesis. *Genes Dev* **9**, 3027-37.
- Mitani, S. and Okamoto, H.** (1991). Inductive differentiation of two neural lineages reconstituted in a microculture system from *Xenopus* early gastrula cells. *Development* **112**, 21-31.
- Mizuseki, K., Kishi, M., Matsui, M., Nakanishi, S. and Sasai, Y.** (1998a). *Xenopus* Zic-related-1 and Sox-2, two factors induced by chordin, have distinct activities in the initiation of neural induction. *Development* **125**, 579-87.
- Mizuseki, K., Kishi, M., Shiota, K., Nakanishi, S. and Sasai, Y.** (1998b). SoxD: an essential mediator of induction of anterior neural tissues in *Xenopus* embryos. *Neuron* **21**, 77-85.
- Moody, S. A.** (1987). Fates of the blastomeres of the 32-cell-stage *Xenopus* embryo. *Dev Biol* **122**, 300-19.
- Moreno, T. A. and Bronner-Fraser, M.** (2001). The secreted glycoprotein Noelin-1 promotes neurogenesis in *Xenopus*. *Dev Biol* **240**, 340-360.
- Moreno, T. A. and Bronner-Fraser, M.** (2001). PNS Precursor Cells. In *Stem Cells and CNS Development*, (ed. M. S. Rao), pp. 153-177. Totowa: Humana Press.
- Morrison, S. J., White, P. M., Zock, C. and Anderson, D. J.** (1999). Prospective identification, isolation by flow cytometry, and in vivo self-renewal of multipotent mammalian neural crest stem cells. *Cell* **96**, 737-49.
- Moury, J. D. and Jacobson, A. G.** (1990). The origins of neural crest cells in the axolotl. *Dev. Biol.* **141**, 243-253.
- Mujtaba, T., Mayer-Proschel, M. and Rao, M. S.** (1998). A common neural progenitor for the CNS and PNS. *Dev Biol* **200**, 1-15.
- Munro, S. and Pelham, H. R.** (1987). A C-terminal signal prevents secretion of luminal ER proteins. *Cell* **48**, 899-907.
- Nagano, T., Nakamura, A., Konno, D., Kurata, M., Yagi, H. and Sato, M.** (2000). A2-Pancortins (Pancortin-3 and -4) are the dominant pancortins during neocortical development. *J Neurochem* **75**, 1-8.

- Nagano, T., Nakamura, A., Mori, Y., Maeda, M., Takami, T., Shiosaka, S., Takagi, H. and Sato, M.** (1998). Differentially expressed olfactomedin-related glycoproteins (Pancortins) in the brain. *Mol Brain Res* **53**, 13-23.
- Nakayama, T., Gardner, H., Berg, L. K. and Christian, J. L.** (1998). Smad6 functions as an intracellular antagonist of some TGF-beta family members during *Xenopus* embryogenesis. *Genes Cells* **3**, 387-94.
- Nguyen, T. D., Chen, P., Huang, W. D., Chen, H., Johnson, D. and Polansky, J. R.** (1998a). Gene structure and properties of TIGR, an olfactomedin-related glycoprotein cloned from glucocorticoid-induced trabecular meshwork cells. *J Biol Chem* **273**, 6341-50.
- Nguyen, V. H., Schmid, B., Trout, J., Connors, S. A., Ekker, M. and Mullins, M. C.** (1998b). Ventral and lateral regions of the zebrafish gastrula, including the neural crest progenitors, are established by a *bmp2b*/swirl pathway of genes. *Dev Biol* **199**, 93-110.
- Nguyen, V. H., Trout, J., Connors, S. A., Andermann, P., Weinberg, E. and Mullins, M. C.** (2000). Dorsal and intermediate neuronal cell types of the spinal cord are established by a BMP signaling pathway. *Development* **127**, 1209-20.
- Nichols, D. H.** (1981). Neural crest formation in the head of the mouse embryo as observed using a new histological technique. *J. Embryol. Exp. Morph.* **64**, 105-120.
- Nielsen, H., Engelbrecht, J., Brunak, S. and von Heijne, G.** (1997). Identification of prokaryotic and eukaryotic signal peptides and prediction of their cleavage sites. *Protein Eng* **10**, 1-6.
- Nieto, M. A., Sargent, M. G., Wilkinson, D. G. and Cooke, J.** (1994). Control of cell behavior during vertebrate development by *Slug*, a zinc finger gene. *Science* **264**, 835-9.
- Nieuwkoop, P. D.** (1952a). Activation and organization of the central nervous system in Amphibians. Part I. Induction and activation. *J. Exp. Zool.* **120**, 1-31.
- Nieuwkoop, P. D.** (1952b). Activation and organization of the central nervous system in Amphibians. Part II. Differentiation and organization. *J. Exp. Zool.* **120**, 33-81.
- Nieuwkoop, P. D. and Faber, J.** (1967). Normal Table of *Xenopus laevis* (Daudin). Amsterdam: North-Holland.
- Nogales, E.** (2000). Recent structural insights into transcription preinitiation complexes. *J Cell Sci* **113 Pt 24**, 4391-7.

- Nordlander, R. H.** (1989). HNK-1 marks earliest axonal outgrowth in *Xenopus*. *Brain Res Dev Brain Res* **50**, 147-53.
- Oakley, R. A., Lasky, C. J., Erickson, C. A. and Tosney, K. W.** (1994). Glycoconjugates mark a transient barrier to neural crest migration in the chicken embryo. *Development* **120**, 103-114.
- Olson, E. C., Schinder, A. F., Dantzker, J. L., Marcus, E. A., Spitzer, N. C. and Harris, W. A.** (1998). Properties of ectopic neurons induced by *Xenopus* neurogenin1 misexpression. *Mol Cell Neurosci* **12**, 281-99.
- Olsson, L. and Hanken, J.** (1996). Cranial neural-crest migration and chondrogenic fate in the Oriental fire-bellied toad *Bombina orientalis*: defining the ancestral pattern of head development in anuran amphibians. *J. Morph.* **229**, 105-120.
- Orr-Urtreger, A., Trakhtenbrot, L., Ben-Levy, R., Wen, D., Rechavi, G., Lonai, P. and Yarden, Y.** (1993). Neural expression and chromosomal mapping of Neu differentiation factor to 8p12-p21. *Proc Nat Acad Sci* **90**, 1867-1871.
- Oschwald, R., Richter, K. and Grunz, H.** (1991). Localization of a nervous system-specific class II beta-tubulin gene in *Xenopus laevis* embryos by whole-mount in situ hybridization. *Int J Dev Biol* **35**, 399-405.
- Pannese, M., Polo, C., Andreazzoli, M., Vignali, R., Kablar, B., Barsacchi, G. and Boncinelli, E.** (1995). The *Xenopus* homologue of Otx2 is a maternal homeobox gene that demarcates and specifies anterior body regions. *Development* **121**, 707-20.
- Papalopulu, N. and Kintner, C.** (1996). A posteriorising factor, retinoic acid, reveals that anteroposterior patterning controls the timing of neuronal differentiation in *Xenopus* neuroectoderm. *Development* **122**, 3409-18.
- Parr, B. A., Shea, M. J., Vassileva, G. and McMahon, A. P.** (1993). Mouse *Wnt* genes exhibit discrete domains of expression in the early embryonic CNS and limb buds. *Development* **119**, 247-261.
- Pera, E., Stein, S. and Kessel, M.** (1999). Ectodermal patterning in the avian embryo: epidermis versus neural plate. *Development* **126**, 63-73.

- Perez, S. E., Rebelo, S. and Anderson, D. J.** (1999). Early specification of sensory neuron fate revealed by expression and function of neurogenins in the chick embryo. *Development* **126**, 1715-1728.
- Perris, R., von Boxberg, Y. and Lofberg, J.** (1988). Local embryonic matrices determine region-specific phenotypes in neural crest cells. *Science* **241**, 86-89.
- Perron, M., Opdecamp, K., Butler, K., Harris, W. A. and Bellefroid, E. J.** (1999). X-ngnr-1 and Xath3 promote ectopic expression of sensory neuron markers in the neurula ectoderm and have distinct inducing properties in the retina. *Proc Natl Acad Sci U S A* **96**, 14996-5001.
- Piccolo, S., Agius, E., Leyns, L., Bhattacharyya, S., Grunz, H., Bouwmeester, T. and De Robertis, E. M.** (1999). The head inducer Cerberus is a multifunctional antagonist of Nodal, BMP and Wnt signals. *Nature* **397**, 707-10.
- Piccolo, S., Sasai, Y., Lu, B. and De Robertis, E. M.** (1996). Dorsoventral patterning in *Xenopus*: inhibition of ventral signals by direct binding of chordin to BMP-4. *Cell* **86**, 589-598.
- Platt, G. M., Simpson, G. R., Mittnacht, S. and Schulz, T. F.** (1999). Latent nuclear antigen of Kaposi's sarcoma-associated herpesvirus interacts with RING3, a homolog of the *Drosophila* female sterile homeotic (fsh) gene. *J Virol* **73**, 9789-95.
- Raven, C. P. and Kloos, J.** (1945). Induction by medial and lateral pieces of the archenteron roof with special reference to the determination of the neural crest. *Acta. néerl. Morph.* **5**, 348-362.
- Rhee, K., Brunori, M., Besset, V., Trousdale, R. and Wolgemuth, D. J.** (1998). Expression and potential role of *Fsrg1*, a murine bromodomain-containing homologue of the *Drosophila* gene female sterile homeotic. *J Cell Sci* **111**, 3541-50.
- Richardson, M. K. and Sieber-Blum, M.** (1993). Pluripotent neural crest cells in the developing skin of the quail embryo. *Dev. Biol.* **157**, 348-358.
- Riese, J., Zeller, R. and Dono, R.** (1995). Nucleo-cytoplasmic translocation and secretion of fibroblast growth factor-2 during avian gastrulation. *Mech Dev* **49**, 13-22.
- Roelink, H. and Nusse, R.** (1991). Expression of two members of the Wnt family during mouse development-restricted temporal and spational pattern in the neural tube. *Genes Dev.* **5**, 381-388.

- Rollhäuser-ter Horst, J.** (1980). Neural crest replaced by gastrula ectoderm in Amphibia. *Anat. Embryol.* **160**, 203-211.
- Ruffins, S., Artinger, K. B. and Bronner-Fraser, M.** (1998). Early migrating neural crest cells can form ventral neural tube derivatives when challenged by transplantation. *Dev Biol* **203**, 295-304.
- Rupp, R. A., Snider, L. and Weintraub, H.** (1994). *Xenopus* embryos regulate the nuclear localization of XMyoD. *Genes Dev* **8**, 1311-23.
- Sadaghiani, B. and Thiebaud, C. H.** (1987). Neural crest development in the *Xenopus laevis* embryo, studied by interspecific transplantation and scanning electron microscopy. *Dev Biol* **124**, 91-110.
- Saint-Jeannet, J. P., He, X., Varmus, H. E. and Dawid, I. B.** (1997). Regulation of dorsal fate in the neuraxis by Wnt-1 and Wnt-3a. *Proc Natl Acad Sci U S A* **94**, 13713-8.
- Saka, Y. and Smith, J. C.** (2001). Spatial and temporal patterns of cell division during early *Xenopus* embryogenesis. *Dev Biol* **229**, 307-18.
- Salter-Cid, L., Du Pasquier, L. and Flajnik, M.** (1996). RING3 is linked to the *Xenopus* major histocompatibility complex. *Immunogenetics* **44**, 397-9.
- Sasai, Y.** (1998). Identifying the missing links: genes that connect neural induction and primary neurogenesis in vertebrate embryos. *Neuron* **21**, 455-8.
- Sasai, Y. and De Robertis, E. M.** (1997). Ectodermal patterning in vertebrate embryos. *Dev. Biol.* **182**, 5-20.
- Sasai, Y., Lu, B., Steinbeisser, H. and De Robertis, E. M.** (1995). Regulation of neural induction by the Chd and Bmp-4 antagonistic patterning signals in *Xenopus*. *Nature* **376**, 333-336.
- Sasai, Y., Lu, B., Steinbesser, H., Geissert, D., Gont, L. K. and De Robertis, E. M.** (1994). *Xenopus chordin*: a novel dorsalizing factor activated by organizer-specific homeobox genes. *Cell* **79**, 779-790.
- Sato, S. M. and Sargent, T. M.** (1989). Development of neural inducing capacity in dissociated *Xenopus* embryos. *Dev. Biol.* **134**, 263-266.
- Scherson, T., Serbedzija, G., Fraser, S. and Bronner-Fraser, M.** (1993). Regulative capacity of the cranial neural tube to form neural crest. *Development* **118**, 1049-1061.

- Schlosser, G. and Northcutt, R. G.** (2000). Development of neurogenic placodes in *Xenopus laevis*. *J Comp Neurol* **418**, 121-46.
- Schneider, C., Wicht, H., Enderich, J., Wegner, M. and Rohrer, H.** (1999). Bone morphogenetic proteins are required in vivo for generation of sympathetic neurons. *Neuron* **24**, 861-870.
- Schulte-Merker, S., Lee, K. J., McMahon, A. P. and Hammerschmidt, M.** (1997). The zebrafish organizer requires chordino. *Nature* **387**, 862-3.
- Schultheiss, T. M., Burch, J. B. and Lassar, A. B.** (1997). A role for bone morphogenetic proteins in the induction of cardiac myogenesis. *Genes Dev.* **11**, 451-462.
- Sechrist, J., Nieto, M. A., Zamanian, R. T. and Bronner-Fraser, M.** (1995). Regulative response of the cranial neural tube after neural fold ablation: spatiotemporal nature of neural crest regeneration and upregulation of *Slug*. *Development* **121**, 4103-4115.
- Seiber-Blum, M.** (1998). Growth factor synergism and antagonism in early neural crest development. *Biochem. Cell Biol.* **76**, 1039-1050.
- Selleck, M. A. and Bronner-Fraser, M.** (1995). Origins of the avian neural crest: the role of neural plate-epidermal interactions. *Development* **121**, 525-38.
- Selleck, M. A., Garcia-Castro, M. I., Artinger, K. B. and Bronner-Fraser, M.** (1998). Effects of *shh* and *noggin* on neural crest formation demonstrate that BMP is required in the neural tube but not ectoderm. *Development* **125**, 4919-4930.
- Serbedzija, G., Bronner-Fraser, M. and Fraser, S. E.** (1989). Vital dye analysis of the timing and pathways of avian trunk neural crest cell migration. *Development* **106**, 806-816.
- Serbedzija, G. N., Bronner-Fraser, M. and Fraser, S. E.** (1992). Vital dye analysis of cranial neural crest cell migration in the mouse embryo. *Development* **116**, 297-307.
- Serbedzija, G. N., Bronner-Fraser, M. and Fraser, S. E.** (1994). Developmental potential of trunk neural crest cells in the mouse. *Development* **120**, 1709-1718.
- Shah, N. M. and Anderson, D. J.** (1997). Integration of multiple instructive cues by neural crest stem cells reveals cell-intrinsic biases in relative growth factor responsiveness. *Proc Natl Acad Sci U S A* **94**, 11369-74.
- Shah, N. M., Groves, A. K. and Anderson, D. J.** (1996). Alternative neural crest cell fates are instructively promoted by TGFbeta superfamily members. *Cell* **85**, 331-43.

- Shah, N. M., Marchionni, M. A., Isaacs, I., Stroobant, P. and Anderson, D. J.** (1994). Glial growth factor restricts mammalian neural crest stem cells to a glial fate. *Cell* **77**, 349-360.
- Sharma, K., Korade, Z. and Frank, E.** (1995). Late-migrating neuroepithelial cells from the spinal cord differentiate into sensory ganglion cells and melanocytes. *Neuron* **14**, 143-152.
- Shen, H., Wilke, T., Ashique, A. M., Narvey, M., Zerucha, T., Savino, E., Williams, T. and Richman, J. M.** (1997). Chicken transcription factor AP-2: cloning, expression and its role in outgrowth of facial prominences and limb buds. *Dev Biol* **188**, 248-66.
- Sive, H. and Bradley, L.** (1996). A sticky problem: the *Xenopus* cement gland as a paradigm for anteroposterior patterning. *Dev Dyn* **205**, 265-80.
- Sive, H. L., Grainger, R. M. and Harland, R. M.** (2000). Early Development of *Xenopus laevis*: A Laboratory Manual. Plainview, New York: Cold Spring Harbor Laboratory Press.
- Slack, J. M. and Forman, D.** (1980). An interaction between dorsal and ventral regions of the marginal zone in early amphibian embryos. *J Embryol Exp Morphol* **56**, 283-99.
- Smith, J. C., Price, B. M., Van Nimmen, K. and Huylebroeck, D.** (1990). Identification of a potent *Xenopus* mesoderm-inducing factor as a homologue of activin A. *Nature* **345**, 729-31.
- Snyder, D. A., Rivers, A. M., Yokoe, H., Menco, B. P. and Anholt, R. R.** (1991). Olfactomedin: purification, characterization, and localization of a novel olfactory glycoprotein. *Biochemistry* **30**, 9143-53.
- Spemann, H. and Mangold, H.** (1924). Über Induktion von Embryonanlagen durch Implantation artfremder Organisatoren. *Arch. mikr. Anat. EntwMech.* **100**, 599-638.
- Stemple, D. L. and Anderson, D. J.** (1992). Isolation of a stem cell for neurons and glia derived from the mammalian neural crest. *Cell* **71**, 973-985.
- Stemple, D. L. and Anderson, D. J.** (1993). Lineage diversification of the neural crest: *in vitro* investigations. *Dev. Biol.* **159**, 12-23.
- Stone, E. M., Fingert, J. H., Alward, W. L. M., Nguyen, T. D., Polansky, J. R., Sunden, S. L. F., Nishimura, D., Clark, A. F., Nystuen, A., Nichols, B. E. et al.** (1997). Identification of a gene that causes primary open angle glaucoma. *Science* **275**, 668-70.
- Stone, L. S.** (1922). Experiments on the development of the cranial ganglia and the lateral line sense organs in *Amblystoma punctatum*. *J. Exp. Zool.* **35**, 421-496.

- Storey, K. G., Goriely, A., Sargent, C. M., Brown, J. M., Burns, H. D., Abud, H. M. and Heath, J. K.** (1998). Early posterior neural tissue is induced by FGF in the chick embryo. *Development* **125**, 473-484.
- Streit, A., Lee, K. J., Woo, I., Roberts, C., Jessell, T. M. and Stern, C. D.** (1998). Chordin regulates primitive streak development and the stability of induced neural cells, but is not sufficient for neural induction in the chick embryo. *Development* **125**, 507-519.
- Streit, A. and Stern, C. D.** (1999). Neural induction. A bird's eye view. *Trends Genet* **15**, 20-4.
- Summerton, J., Stein, D., Huang, S. B., Matthews, P., Weller, D. and Partridge, M.** (1997). Morpholino and phosphorothioate antisense oligomers compared in cell-free and in-cell systems. *Antisense Nucleic Acid Drug Dev* **7**, 63-70.
- Summerton, J. and Weller, D.** (1997). Morpholino antisense oligomers: design, preparation, and properties. *Antisense Nucleic Acid Drug Dev* **7**, 187-95.
- Suzuki, A., Kaneko, E., Ueno, N. and Hemmati-Brivanlou, A.** (1997). Regulation of epidermal induction by BMP2 and BMP7 signaling. *Dev Biol* **189**, 112-22.
- Suzuki, H. R. and Kirby, M. L.** (1997). Absence of neural crest cell regeneration from the postotic neural tube. *Dev. Biol.* **184**, 222-233.
- Taniguchi, Y., Matsuzaka, Y., Fujimoto, H., Miyado, K., Kohda, A., Okumura, K., Kimura, M. and Inoko, H.** (1998). Nucleotide sequence of the ring3 gene in the class II region of the mouse MHC and its abundant expression in testicular germ cells. *Genomics* **51**, 114-23.
- Tannahill, D., Isaacs, H. V., Close, M. J., Peters, G. and Slack, J. M. W.** (1992). Developmental expression of the *Xenopus int-2* (FGF-3) gene: activation by mesodermal and neural induction. *Development* **115**, 695-702.
- Thorpe, K. L., Abdulla, S., Kaufman, J., Trowsdale, J. and Beck, S.** (1996). Phylogeny and structure of the RING3 gene. *Immunogenetics* **44**, 391-6.
- Thorpe, K. L., Gorman, P., Thomas, C., Sheer, D., Trowsdale, J. and Beck, S.** (1997). Chromosomal localization, gene structure and transcription pattern of the ORFX gene, a homologue of the MHC-linked RING3 gene. *Gene* **200**, 177-83.
- Tkachuk, D. C., Kohler, S. and Cleary, M. L.** (1992). Involvement of a homolog of *Drosophila* trithorax by 11q23 chromosomal translocations in acute leukemias. *Cell* **71**, 691-700.

- Turner, D. L. and Weintraub, H.** (1994). Expression of achaete-scute homolog 3 in *Xenopus* embryos converts ectodermal cells to a neural fate. *Genes Dev* **8**, 1434-47.
- Vaccarino, F. M., Schwartz, M. L., Raballo, R., Rhee, J. and Lyn-Cook, R.** (1999). Fibroblast growth factor signaling regulates growth and morphogenesis at multiple steps during brain development. *Curr. Top. Dev. Biol.* **46**, 179-200.
- Varley, J. E., McPherson, C. E., Zou, H., Niswander, L. and Maxwell, G. D.** (1998). Expression of a constitutively active type I BMP receptor using a retroviral vector promotes the development of adrenergic cells in neural crest cultures. *Dev. Biol.* **196**, 107-118.
- Verwoerd, C. D. A. and van Oostrom, C. G.** (1979). Cephalic neural crest and placodes. *Adv. Anat. Embryol. Cell Biol.* **58**, 1-75.
- Watanabe, Y. and Le Douarin, N. M.** (1996). A role for BMP-4 in the development of subcutaneous cartilage. *Mech Dev* **57**, 69-78.
- Webb, J. F. and Noden, D. M.** (1993). Ectodermal placodes: contributions to the development of the vertebrate head. *Amer. Zool.* **33**, 434-447.
- Weinstein, D. C. and Hemmati-Brivanlou, A.** (1997). Neural induction in *Xenopus laevis*: evidence for the default model. *Curr. Op. Neurobiol.* **7**, 7-12.
- Weinstein, D. C. and Hemmati-Brivanlou, A.** (1999). Neural induction. *Annu Rev Cell Dev Biol* **15**, 411-33.
- Weston, J. A. and Butler, S. L.** (1966). Temporal factors affecting localization of neural crest cells in the chicken embryo. *Dev. Biol.* **14**, 246-266.
- Wilson, P. A. and Hemmati-Brivanlou, A.** (1995). Induction of epidermis and inhibition of neural fate by Bmp-4. *Nature* **376**, 331-333.
- Wilson, P. A. and Hemmati-Brivanlou, A.** (1997). Vertebrate neural induction: inducers, inhibitors, and a new synthesis. *Neuron* **18**, 699-710.
- Wilson, P. A., Lagna, G., Suzuki, A. and Hemmati-Brivanlou, A.** (1997). Concentration-dependent patterning of the *Xenopus* ectoderm by BMP4 and its signal transducer Smad1. *Development* **124**, 3177-3184.

- Wilson, S. I., Graziano, E., Harland, R., Jessell, T. M. and Edlund, T.** (2000). An early requirement for FGF signalling in the acquisition of neural cell fate in the chick embryo. *Curr Biol* **10**, 421-9.
- Winnier, G., Blessing, M., Labosky, P. A. and Hogan, B. L.** (1995). Bone morphogenetic protein-4 is required for mesoderm formation and patterning in the mouse. *Genes Dev* **9**, 2105-2116.
- Wodarz, A. and Nusse, R.** (1998). Mechanisms of Wnt signaling in development. *Annu. Rev. Cell Dev. Biol.* **14**, 59-88.
- Wolda, S. L., Moody, C. J. and Moon, R. T.** (1993). Overlapping expression of *Xwnt-3a* and *Xwnt-1* in neural tissue of *Xenopus laevis* embryos. *Dev. Biol.* **155**, 46-57.
- Wright, C. V., Morita, E. A., Wilkin, D. J. and De Robertis, E. M.** (1990). The *Xenopus* XlHbox 6 homeo protein, a marker of posterior neural induction, is expressed in proliferating neurons. *Development* **109**, 225-34.
- Xu, R. H., Kim, J., Taira, M., Sredni, D. and Kung, H.** (1997). Studies on the role of fibroblast growth factor signaling in neurogenesis using conjugated/aged animal caps and dorsal ectoderm-grafted embryos. *J Neurosci* **17**, 6892-6898.
- Xu, R. H., Kim, J., Taira, M., Zhan, S., Sredni, D. and Kung, H. F.** (1995). A dominant negative bone morphogenetic protein 4 receptor causes neuralization in *Xenopus* ectoderm. *Biochem Biophys Res Commun* **212**, 212-219.
- Yokoe, H. and Anholt, R. R.** (1993). Molecular cloning of olfactomedin, an extracellular matrix protein specific to olfactory neuroepithelium. *Proc Natl Acad Sci U S A* **90**, 4655-9.
- Zhang, H. and Bradley, A.** (1996). Mice deficient for BMP2 are nonviable and have defects in amnion/chorion and cardiac development. *Development* **122**, 2977-2986.
- Zimmerman, K., Shih, J., Bars, J., Collazo, A. and Anderson, D. J.** (1993). *XASH-3*, a novel *Xenopus achaete-scute* homolog, provides an early marker of planar neural induction and position along the mediolateral axis of the neural plate. *Development* **119**, 221-232.
- Zimmerman, L. B., De Jesus-Escobar, J. M. and Harland, R. M.** (1996). The Spemann organizer signal noggin binds and inactivates bone morphogenetic protein 4. *Cell* **86**, 599-606.